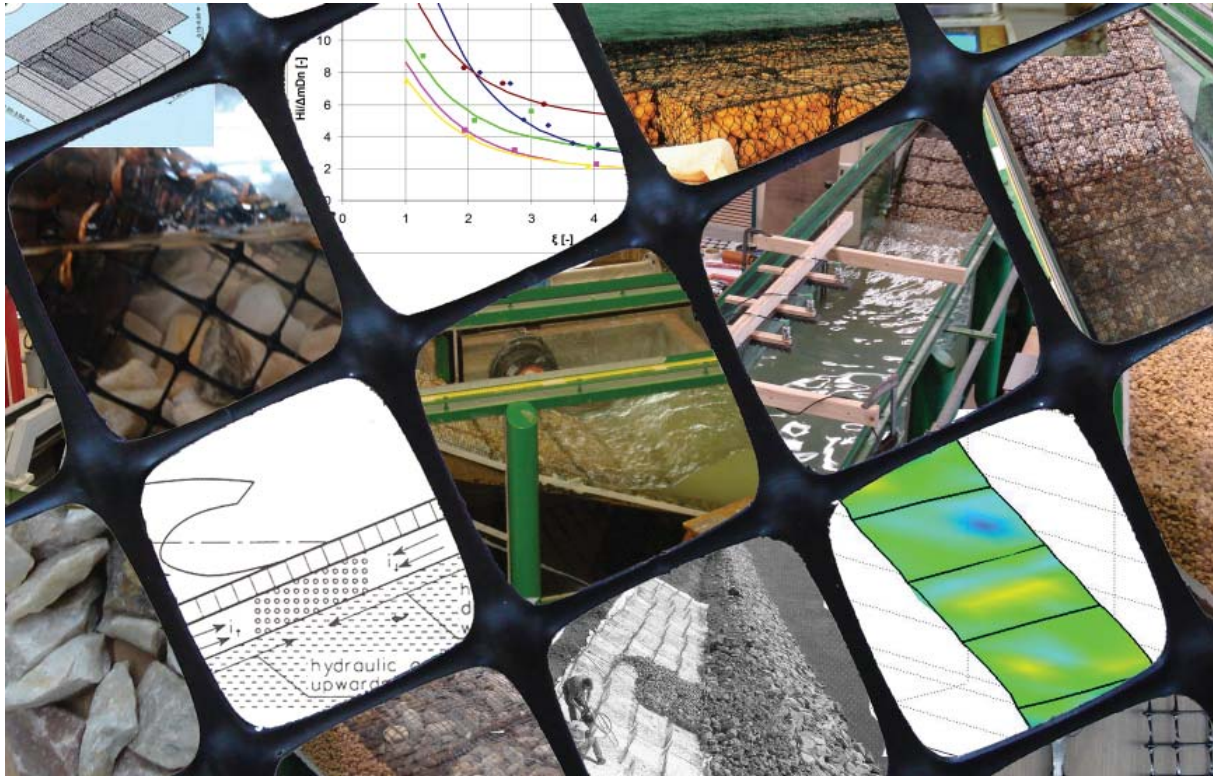


The Stability of Synthetic Gabions in Waves



Master of Science Thesis on the Application of Synthetic Grids in
Mattress Gabion Constructions and the Stability in Waves

J. Oosthoek
Delft, June 2008
Faculty of Civil Engineering and Geosciences
Section of Hydraulic Engineering



The Stability of Synthetic Gabions in Waves

Master of Science Thesis on the Application of Synthetic Gabions in Waves

Master of Science Thesis of J. Oosthoek

Graduation Committee:

Prof. Dr. Ir. M.J.F. Stive	Delft University of Technology, Section of Hydraulic Engineering, Chairman of the Graduation Committee.
Dr. Ir. W.S.J. Uijtewaal	Delft University of Technology, Section of Environmental Fluid Mechanics, Supervisor from the Fluid Mechanics Section.
Ir. H.J. Verhagen	Delft University of Technology, Section of Hydraulic Engineering, Supervisor of the Thesis Work.
Ing. F. de Meerleer	Texion Geosynthetics B.V. Supervisor from the Participating Company.



Delft University of Technology
Faculty of Civil Engineering and Geosciences
Section Hydraulic Engineering
Stevinweg 1
2628 CN Delft



Texion Geosynthetics N.V.
Esmoreitlaan 47 box 42
2050 Antwerp
Belgium

Jorg Oosthoek
Korvezeestraat 555
2628 CZ Delft
jorgoosthoek@hotmail.com

The use of trademarks in any publication of Delft University of Technology does not imply any endorsement or disapproval of this product by the University.

- Armorflex is a registered trademark of Armourtec, USA
- E'grid is a registered trademark of Newgrids Limited, United Kingdom
- Galfan is a registered trademark of International Lead Zinc Research Organization, USA
- Reno Mattress is a registered trademark of Maccaferri, Italy
- Terrafix is a registered trademark of Risi Stone Systems, Canada

Preface

This report is the final part of my master of science work at the University of Technology in Delft for the section of Hydraulic Engineering. The main subject of this thesis is the application of a synthetic geogrid in gabion constructions, instead of the more common steel wire grid. The report includes a general description of steel wire gabion constructions, including the advantages of and the possibilities for a synthetic variant. The application of a synthetic grid is focused on mattress constructions used in a environment with wave attack. Most benefit can be gained in these situations, compared to regular steel wire grid variant.

Physical model tests have been performed in a flume of the fluid mechanics laboratory. During these tests the process and sensitivity to mattress deformation and failure due to sliding are examined. Based on the test results recommendations and a first start of a improved design formula is given.

During the project help and assistance is provided by a number of people who I would like to thank. The co-workers of the fluid mechanics laboratory, for the assistance during the experiments. Texion Geosynthetics for providing the prototype material. The company Afcon for providing the model material. Nigel Wrigley for his assistance during the thesis work. My parents for their unconditional support during the total length of my education. And naturally the graduation committee with the members:

Prof. Dr. Ir. M.J.F. Stive
Dr. Ir. W.S.J. Uijtewaal
Ir. H.J. Verhagen
Ing. F. de Meerleer

*Jorg Oosthoek
June 2008*

Summary

Introduction

Revetment protections are found in all sorts of forms and shapes and are applied in different sorts of hydraulic environments. Gabions form one of these many alternatives. These so called composite structure consists out of a wire mesh in which stones are retained. In a revetment construction the gabion is applied in a mattress shape, which consists out of several compartments that are interconnected. The environment in which gabions can be applied is until 1.5 - 2 m waves.

Compared to a more conventional rip-rap protection, gabions spread the load over the entire length of the construction, since all compartments are interconnected. The retaining grid results in the effect that the particles inside a compartment function as group. Individual particle stability is of less importance. A gabion revetment protection can therefore be constructed out of smaller stones, because the general stability is of importance. This results in the advantage that gabion revetment protections can be made thinner, compared to a rip-rap construction. Less material is necessary to create the same result.

Facing these good qualities, some disadvantages of the current gabion mattress constructions are also present. The grid from which the construction is made consists out of zinc protected steel wire grid. This is the weakest link of the structure. Fill material movement or other damage of the zinc protective layer which results in corrosion of the grid. The life-time expectancy is therefore relatively uncertain. Besides this disadvantage, zinc also dissolves slowly in the water, which gives environmental objection. For these reasons the use of gabions is unpopular especially in a wave climate and salt water where these disadvantages can develop even faster.

Material

A solution for the disadvantages of the steel wire grid, is the application of a synthetic material. These days several strong synthetic materials are available that are not sensitive to corrosion or dissolving of harmful particles. The application of geogrids is suitable for the retaining function of gabions. A geogrid is a synthetic material consisting of parallel sets of intersection ribs with apertures of a certain size (2-8 cm). This material is normally used as a reinforcement in asphalt road constructions to absorb axis stresses. It results in a thinner and therefore cheaper road construction.

Synthetic materials need to satisfy certain demands which are present in the steel wire grid, but are also characteristic synthetic materials. A certain tension strength is needed to prevent rupture. Degradation due to ultra violet radiation should be prevented. Creep should be of a low degree, to prevent increasing compartment space or loss of strength. Leaching of particles, which can be a quality of synthetic materials, should not occur. The solution for a suitable material, that satisfies the demands, is found in the form of E'grid geogrid. Based on this material an alternative gabion construction is developed.

The general hesitation of applying synthetics in gabion constructions is that the construction will show deformation and fail due to this effect. The argument is that the flexural rigidity of synthetics is insufficient. Besides this there is hardly any experience of applying gabion mattresses in wave climates.

Deformation

Scale model tests have been performed to study the process of deformation. In these experiments the influence of grid rigidity, fill material size, angularity and filling degree have been investigated. From these tests it came forward that deformation depends for the greatest part on the filling degree of the compartment. Fill material will always settle itself in a bulging shape due to the flexural behaviour of the grid. The result is a tension on the grid that results in a pressure on the fill material. The pressure improves the group behaviour of the grid and further prevents the development of deformation as a result of the mutual blocking of the particles.

Some degree of deformation will always develop in a mattress, but a great part can be prevented by anticipation of the compartment shape that can develop. This can be done by filling the compartment into the bulging deformed shape until it is closed under tension. The particles are retained under pressure and deformation will be limited. Due to this process there is no influence of particles size or shape. More or less the same deformed shape will always develop independent of the fill material.

There is a difference in the amount of fill material that is applied to fill the gabion under tension. Smaller fill material is better able to follow the shape of especially the deformed compartment lid. Less extra fill material is needed of a larger size to create the same effect. The disadvantage of too large fill material is the sublayer that can erode through the mattress due to the more intense turbulence. The recommendation from literature to have a maximum D_{50} of half the mattress thickness is justified. This is also important for the functioning of the geometrical closed filter.

Run-up, Run-down, Reflection

During the experiment the run-up, run-down and reflection are measured. When the test data is compared with data from literature it shows a wider variation. This can be explained by the fact that the data from literature is based on rip-rap experiments. Gabion mattresses are relatively thinner and the influence of the filter will be larger, since less turbulence can be created by the thinner outer layer. The data is splitted in different groups dependent of the mattress thickness and filter. The experiments on the granular filter showed a more consistent relation compared to the other less permeable constructions.

Stability

The most suitable design formula for gabion mattresses in waves is from Pilarczyk. This formula is an adapted form of Hudson’s particle stability in waves, in which the Iribarren parameter is taken into account. The advantage of the Iribarren parameter is the indirect influence of run-down that is taken is implemented. The criticism on this formula is that it is based on individual particle stability. The functioning of gabion mattresses are not based on individual stability, but on overall stability.

The length of a mattress has therefore influence on the stability of the construction. The filter construction can also influence the stability. A granular filter has a better friction factor compared to a more smooth geotextile. A third shortcoming in the formula is the absence the permeability influence. Mattresses fail due to the uplift pressure created by the water level difference between the body and wave run-down. The amount of uplift pressure is dependent on the ability of the water to flow out. Permeability should therefore be taken into account.

Pilarczyk’s graph consists of one stability relation. Based on extra parameters as mattress length, friction and permeability the stability relation should be not restricted to one line. Depending on the design, the stability relation will have a certain position in the graph. The stability relation is on a relative higher position if the friction is higher of mattress is longer. Figure i represents the theory.

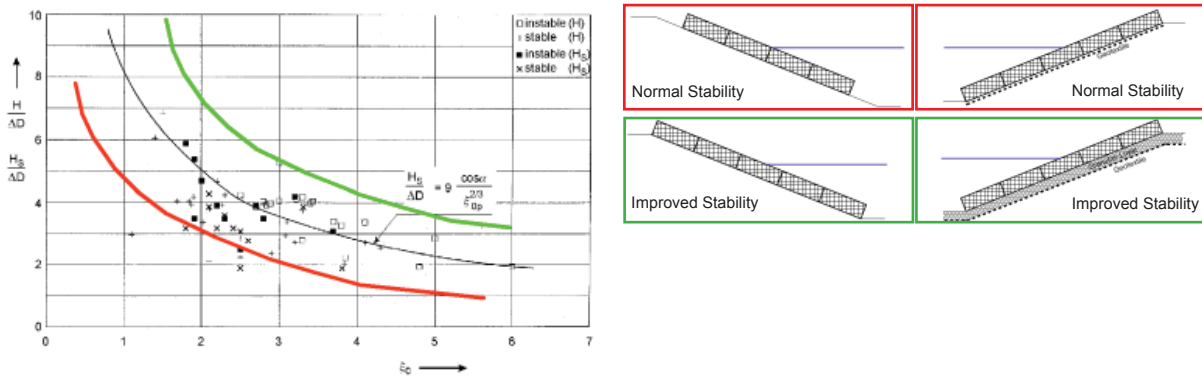


Figure i: Pilarczyk's improved stability relation

Model experiments are also performed to study the stability relations of different gabion mattress designs. The stability is tested based on varying mattress thickness, slope, filter permeability, friction and Iribarren parameter. The experimental results form a base to improve Pilarczyk's design formula and to implement the missing parameters.

Results

Figure ii shows the different results for different revetment designs that are made. Curves are drawn through these results. What should be noticed is that all experimental runs show more or less the same course for the stability relation. The only difference is the position in the graph. Run 1 is the only serie of experiments in which a horizontal crown and toe compartment is applied. This run shows a steeper and different course of the stability relation.

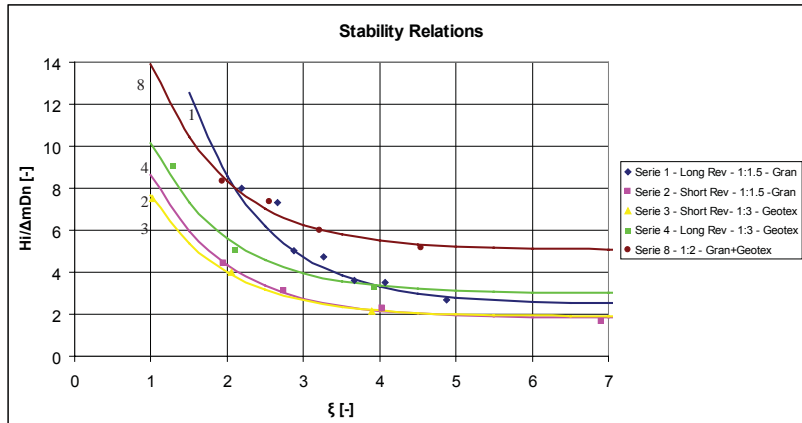


Figure ii: Sliding test results

A formula for the stability relation is described with two parts. The first part is the position of the stability relation. The second part is the course of the stability relation described by an exponential function which is dependent of the Iribarren parameter. In the formula three parameters are present to relate the different components. The shift factor c_1 which represents the position of the curve. The parameter c_2 which relates course of the stability relation to the factor c_1 . The sensitivity to the Iribarren parameter can be corrected by a constant c_3 . From the analysis it comes forward that this constant has a value 1.

The parameter c_1 depends on the amount of tension force that can be absorbed before the mattress slides down. The mattress length, friction and slope angle influence this parameter. Next to that the permeability of a revetment influences the amount of uplift that is generated. The uplift results in a decreased amount of tension force absorption. The permeability influences the stability relation. The value c_2 depends on the shape on the design of the mattress. If all compartments are placed on a slope, than the c_2 value is of the order 20.

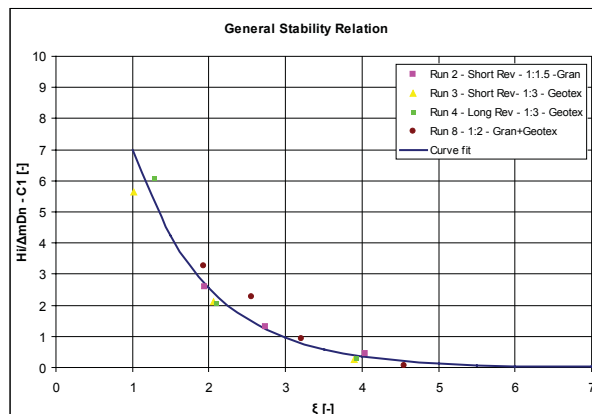
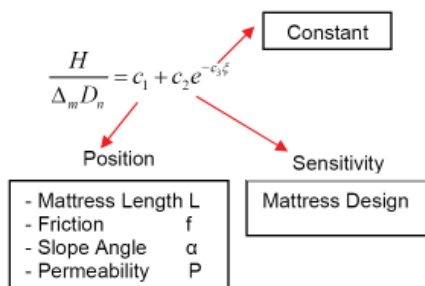


Figure iii: General stability relation

The stability relation of all runs, except run 1 can be written in one relation if the c_1 value is subtracted from the stability parameter. This results in the graph of Figure iii.

The stability depends on the amount of tension force that can be absorbed by an element and by the total length of this element. Two parameters are introduced. The R-value is a ratio of the capacity of an elements to absorb a certain amount of tension force. This value is independent of length or thickness. A longer mattress on the same slope will still have the same R-value. The distinction in capacity is made by the length of the mattress. Compartments placed under water will absorb less tension force. The length is expressed in a relative length corrected for the position of the mattress with respect to the water level. The relative length is made dimensionless by dividing the value through the wave length.

$$R = \frac{F_r}{F_d} = \frac{f}{\tan(\alpha)} \qquad \frac{L_{rel}}{L} = \frac{X + \frac{(L_m - X)}{\Delta}}{L}$$

The only aspect that is not implemented with these parameters is the influence of the permeability. The experiment program contained three types of filters with a different permeability: fully granular, granular + geotextile and geotextile. The test results are divided in three different groups. The amount of test data is rather limited for each revetment type only one R-value is available. By expressing the increase of tension force absorption different relations are developed for other R-values. A result for a granular geotextile combination is presented in Figure iv. Based on the stability parameter it is possible to determine the relative length of the mattress.

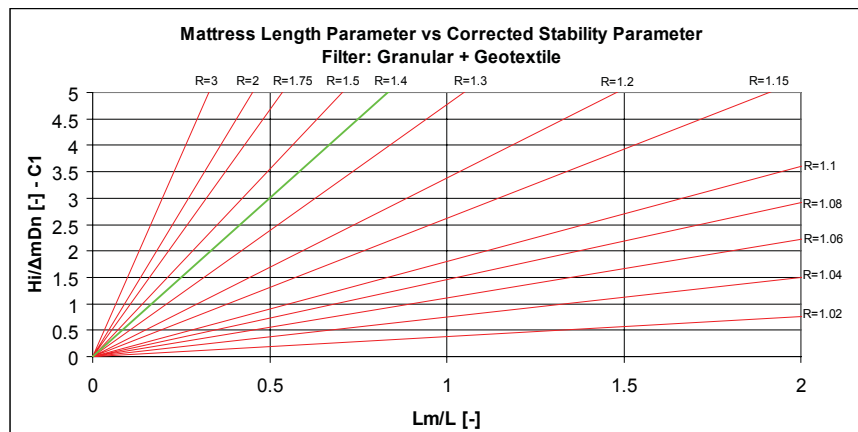


Figure iv: Stability relation for granular + geotextile filter

Conclusions & Recommendations

A first start is made for the improvement of the stability relation. A method is developed based on a limited amount of test data. The linear transformation of the R-value based in a increase or decrease of the tension force, might not be fully correct. Especially for the higher R-values the relation is questionable, because the aspect of uplift implemented. More extensive research in which this aspect is taken into account would result in a improved relation.

The influence of horizontal compartments is expressed by a different course of the stability relation (run 1). This is mainly ascribed to the interference of the subsoil bearing capacity under the crown compartment and the increased relative length. It is also possible to create a relation for the influence of these compartment on the total stability. Experiments devoted to this aspect are necessary for the development and further improvement of the stability relation.

During the experiments is became clear that there is a wider variation in the test data for run-up, run-down and reflection compared to results from literature that are based on rip-rap revetments. The relative thinner gabion mattress results in more interference of the filter construction. A clear relation could not be set up. Extra research in which the factors as mattress thickness and filter permeability are emphasized could result in a more clear distinction and relation for these processes.

In view of the material it might be useful to perform extra tests in which the geogrid is subjected to load repetitions that represent the tension force which is created by waves. The expectation is that the material will function properly according to its current application in roads, though experiments will take away the uncertainty that it could become a problem.

Table of Contents

Preface	vii
Summary	viii
Table of Contents	xii
1 Introduction	1
1.1 Gabion Elements	1
1.2 Hydraulic Properties of Gabions	2
1.3 Problem Analysis	3
1.4 Problem Definition	4
1.5 Objectives	5
1.6 Report Structure	5
2 Gabion Stability	7
2.1 Gabion Structures	7
2.2 Environmental Contribution	10
2.2.1 Environmental Friendly Banks	10
2.2.2 Vegetated Gabions	11
2.3 Introduction Stability Theory	13
2.3.1 Introduction	13
2.3.2 Definitions	13
2.3.3 Equilibrium of Forces of Particles in a Water Flow	15
2.3.4 Izbash Formula for Critical Velocity	15
2.3.5 Shields Formula for Critical Velocity	16
2.4 Gabion Mattress Design Formula's in Water Flows	18
2.4.1 Pilarczyk's Gabion Mattress Design Formula for Critical Velocity	18
2.4.2 Simons' Gabion Stability Formula in Waterflows	19
2.4.3 The Difference Between Simons and Pilarczyk	21
2.4.4 Deformation Effects	22
2.5 Gabion Mattress Design Formula's in Waves	24
2.5.1 Definitions with Respect to the Stability in Waves	24
2.5.2 Equilibrium of Forces of an Element	25
2.5.3 Anchor Length	28
2.5.4 Failure of the Revetment	29
2.5.5 Gabion Design Rules in Waves	30
2.5.6 Maccaferri's Gabion Stability Formula in Waves	30
2.5.7 Pilarczyk's Gabion Stability Formula in Waves	30
2.5.8 Pilarczyk's Improved Gabion Stability Formula in Waves	31
2.5.9 Motion of Fill Material	33
2.6 Comparison Between Gabions and Rip-Rap Protection	34
2.7 Filter Layers	35
2.7.1 Function of a Filter Layer	35
2.7.2 Filter Layers for Current Exposed Gabions	35
2.7.3 Filter Layers for Gabions Exposed to Waves	37
2.7.4 Klein Breteler Filter Design Method.	38
2.7.5 Requirements due to Blocking and Clogging of a Geotextile	45
2.8 Review on the Pilarczyk's Design Formula's for Gabions in Waves	46
3. Synthetic Materials for Gabions	49
3.1 Introduction	49
3.2 Material Properties	50
3.2.1 Material Requirements With Respect to Gabion Functioning	50
3.2.2 Material Requirements With Respect to Synthetic Properties	51
3.3 Geosynthetics	53
3.4 Geogrid Properties	55
3.4.1 Types of Geogrid	55
3.4.2 Reduction Factors	57
3.5 Construction of a Gabion	65
3.5.1 Creating a Volume	65
3.5.2 External Connections	66

Chapter 4. Experiment Description	67
4.1 Introduction	67
4.2 Scale Experiments	68
4.2.1 Scaling of Parameters	68
4.2.2 Scaling Method	69
4.3 Material Properties	70
4.3.1 Elasticity	70
4.3.2 Flexural Rigidity	71
4.4 Scaling	73
4.4.1 Scaling of the Geometrics	73
4.4.2 Scaling of the Elasticity	73
4.4.3 Scaling of the Flexural Rigidity	74
4.4.4 Scaling the EI Parameter	75
4.4.5 Determination of the Scale Factor.	76
4.5 Expected Failure Process	79
4.6 Experiment Program	81
4.6.1 Experiment Objectives	81
4.6.2 Altering Parameters	82
4.6.3 Experiment Program	84
4.7 Experiment Set-up	86
4.7.1 Wave Flume	86
4.7.2 Construction of the Gabion Model Mattress	87
4.7.3 Measurements	88
4.7.4 Work Method	90
Chapter 5. Observations, Test Results and Data Analysis	91
5.1 Deformation Observations	91
5.1.1 Fill Material Behaviour and Grid Interaction	91
5.1.2 Increased Compaction	92
5.1.3 Influence of the Mutual Connections	94
5.2 Sliding Observations	95
5.3 Deformation Test Results	99
5.4 Sliding Test Results	101
5.5 Run-up, Run-down and Reflection	105
5.5.1 Run-up Test Results	105
5.5.2 Run-down Test Results	108
5.5.3 Reflection Test Results	109
5.6 Analysis Deformation	110
5.7 Analysis Sliding Test Results	112
5.7.1 Parameter Analysis of Factor c_1	112
5.7.2 Parameter Analysis of Factor c_2	121
Chapter 6. Conclusions and Recommendations	123
6.1 Conclusions	123
6.1.1 Objectives	123
6.1.2 Material	124
6.1.3 Deformation	124
6.1.4 Run-up, Run-down and Reflection	125
6.1.5 Design Formula	126
6.2 Recommendations	128
6.2.1 Confirmation of Material Application	128
6.2.3 Run-up, Run-down and Reflection	128
6.2.3 Stability Relation	128
List of Symbols	129
Definitions	132
References	133
Internet	134
List of Figures	135
List of Tables	137
Appendix A: Soil Parameter Information	I
Appendix B: Fill Material Information	III
Appendix C: Wave Data Filter	VIII
Appendix D: Experiment Results	XI

Chapter 1. Introduction

1.1 Gabion Elements

The term gabion is defined as: a container made of wire mesh filled with rock, stone or crushed concrete, that is used for structural purposes. In hydraulic engineering gabions are used to protect banks, dikes, slopes and other structures against erosive forces of currents and waves. Gabions are used in a wide field of structures and can be found in many forms and sizes. Different gabion forms are: box, mattress, cylindrical or sack gabions. The first two are the most common applied shapes. Figure 1.1 shows the different alternatives.

Box gabions are containers uniformly partitioned into internal cells. The wire mesh that is placed for partitioning the element are the so-called diaphragms. This interior separation avoids displacement of fill material within the gabion. Typical dimensions of the box gabion are: $2 \times 1 \times 1$ m.

Gabion mattresses are thinner compared to their length and width. Typical dimensions are $6 \times 2 \times 0.15$ m. The thickness can be larger, but does rarely exceed 0.5 m, because of practical reasons.

Cylindrical or sack gabions are best described as sausage-like gabions that are mainly used for toe protection of banks. This type of structure is not common. Due to the rare application of this type, no further attention will be given to this alternative.

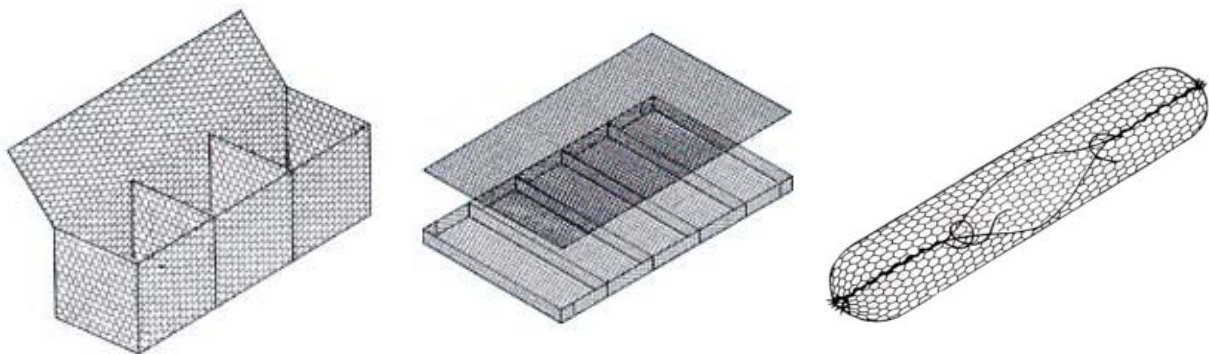


Figure 1.1: Box, mattress and cylindrical gabion

When high flow velocities or wave-attack is present, many different solutions are available to protect the bank or bed against erosion. Well-known solutions are for example riprap and concrete elements. The idea of the gabion protection system is to hold stones together that would normally wash away when they are individually subjected to a hydraulic load. The containing function of the grid results in a situation where the load can be divided over a larger area than the individual particle only. The particles are functioning as a group, this gives the ability to absorb a higher degree of hydraulic load.

The application of gabions is one of the many alternatives that can be used against erosion. Factors as the intensity of the hydraulic load, the availability of materials, the execution method and costs, are important for the choice of a protection.

The main field of gabion applications can be found in inland waters, like: canals, rivers and lakes. It is for example not common to apply gabions in situations with severe wave-attack from open sea. The use of gabions is therefore limited to a certain level of attack. Above this level the application of heavy riprap or concrete elements becomes more justified.

1.2 Hydraulic Properties of Gabions

Gabions consists of three elements that all together form the construction: the basket, fill material and the filter construction that is present beneath the structure. The open grid and relatively large diameter of the fill material, usually between 75-200 mm, results in a very open structure and enables water to flow through. The flow of water between the pores of the fill material generates a great amount of turbulence. This property results in the dissipation of energy, which is needed to decrease the ability of the current to pick up the particles underneath the protection and to prevent erosion.

Gabions that experience wave attack have the advantage of good energy dissipation, caused by the flow through the voids of the fill material. Next to that the compression of air between the fill-material contributes a little to the dissipation of energy. Gabions resist waves to a certain level. The maximum recommended wave height is estimated at 1.5 to 2 meter [CUR/RWS 2000].

Besides the good dissipation qualities, the open structure is also advantageous to prevent pressure build-up. The draw-down of waves creates a internal pressure on the protection caused by the water level difference between the inside of the revetment and wave run-down at that very moment. This mechanism can cause uplifting of the protection from the inside of the structure. The open structure of gabions gives the ability for the internal water pressure to flow out easily. This process will be explained in chapter 2, which describes the stability of gabions.

For gabions the critical velocity is defined as the velocity to initiate movement of stones in the gabion. Gabions under current attack have a higher critical flow velocity than rip-rap protections for the same diameter of fill material, since they function as a group. The ability to resist against a certain flow velocity depends on the thickness of the mattress and the size of the fill material. Mattress gabions with a thickness of 300 mm can resist a velocity to about 4 - 5.5 m/s. Box gabions are even capable of sustaining higher velocities of 5 - 6 m/s or more. This depends on the quality of construction and assembly [CIRIA, CUR, CETMEF 2007]. What should be kept in mind is that at the interface between subsoil and gabion the velocity can still be of a level that gives the ability to wash out material through the protection. A filter-construction is necessary to create a transition between these layers. Without a proper designed filter, erosion through the gabion construction could still be possible.

Flexible behaviour of a construction is important for a good quality protection. During time soil deformations and settlements can develop. Gabions possess a certain flexibility so a tight transition between subsoil and gabion is guaranteed. This quality is for example used to prevent the further development of a scour hole at the toe of a revetment (Figure 1.2).

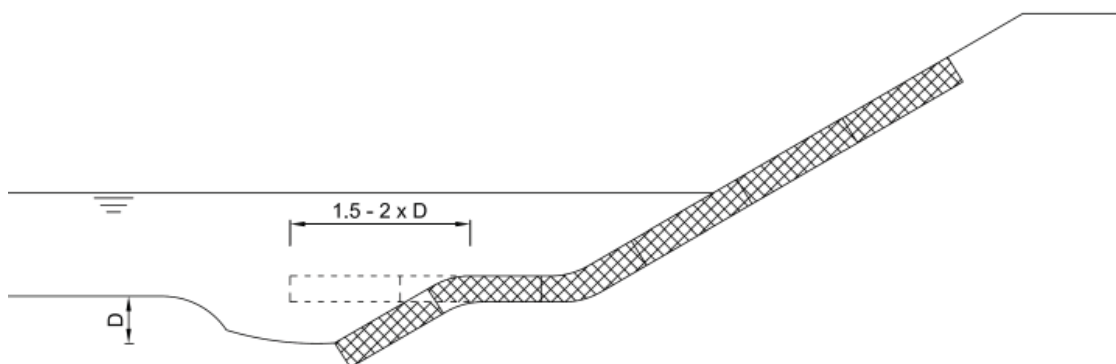


Figure 1.2: Scour hole coverage

1.3 Problem Analysis

Gabion containers are made from steel wire grid, from which three different types are available: double-twisted wire mesh, chain linked mesh and welded mesh. Most of the gabions are manufactured with the hexagonal double-twisted wire mesh. The advantage of this variant above the other two is that a structure can deform significantly without failing. A welded frame is less able to do this without failure of the weld. Chain linked mesh is also inferior, because if a wire breaks the grid will start to unravel. Twisted wire mesh does not have this problem. Figure 1.3 shows the principle of a failed wire and the potential effects.

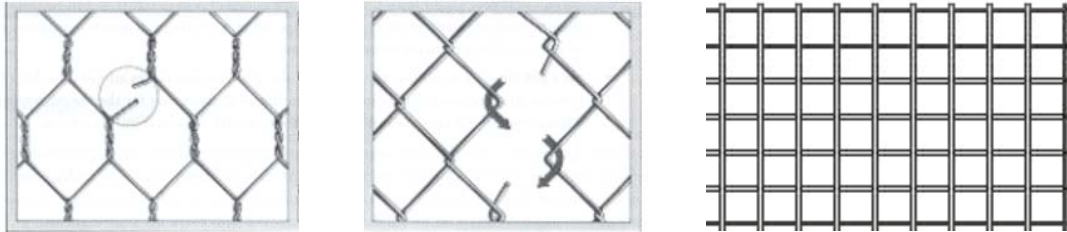


Figure 1.3: Double-twisted wire mesh, chain linked mesh and welded mesh

To protect the steel wire from corrosion the material is galvanized. Disadvantage of this zinc protection is that when the layer is damaged, the steel gets exposed and corrosion can originate. After some time the wires will break and the stones are washed out the container.

Damage to the coating can occur for several reasons. Frequent wave-, or current-attack can lead to a failure of the wire mesh, because of the movement of the grains along the wire. The vibration of particles can lead to scratching on the wire. The design formulas for gabion constructions are therefore based on no-, or little fill material movement. For a synthetic gabion the design could allow more fill material movement. A second initiator of corrosion can be material that is floating in the water. Waves can throw this material against the wires, which causes damage to the protective layer. Thirdly, also during the construction phase first damage can occur. When filling the containers care should be taken into account, because the filling material can damage the wire. Due to this reason many suppliers give the recommendation to use round stones, like gravel, as a filling material. The price of this filling material is higher than crushed rock or other coarse material.

Another disadvantage of zinc protection is the pollution of water on the long-term. Zinc is found naturally in water, although an excess of zinc is harmful for the environment. The galvanized layer slowly dissolves and zinc enters the water. Zinc particles will bind themselves with silt and pollute the soil where these particles accumulate. For animals and vegetation an excess of zinc gives problems. In these days the development of environmental friendly banks, that form an ecological transition between land and water, is important. For this reason the presence of zinc protective layer can be an argument not to install steel wire gabions.

A more innovative protection layer is the Galfan protection. A zinc-aluminum coating protects the wire and has the ability to recover itself to a certain level. Scratches not deeper than the protection layer will restore themselves. Aluminium is a more noble metal than zinc and will remain on the surface after the corrosion of zinc. This results in a more solid protection layer. Still the probability of corrosion exists in case of severe damage. Under normal conditions this protection can hold three to four times longer than regular galvanized protections, particularly in aggressive saline conditions [CIRIA, CUR, CETMEF 2007].

To give even further protection against scratching and damaging the protection can be covered with an extra PVC coating. This coating gives extra protection and results in a higher durability. This system is less suitable when grains also experience intensive movement. The relative softness of PVC will wear out because of the grain movement. The combination of a Galfan protection and a PVC layer will provide the firmest protection (Figure 1.4). Conventional galvanized zinc PVC coated gabion mattresses have been in place and shown to be durable in chemically aggressive hydraulic environments for more than 40 years to date, according to the manufacturer Maccaferri. The locations where problems occurred was the result of physical attrition from stones thrown up by waves or caused by poor construction. The internal abrasion of wire as stones move within the gabion is a weak point of the structure. According to the more independent *CUR/RWS*, the life time expectancy is estimated between 5 and 20 years

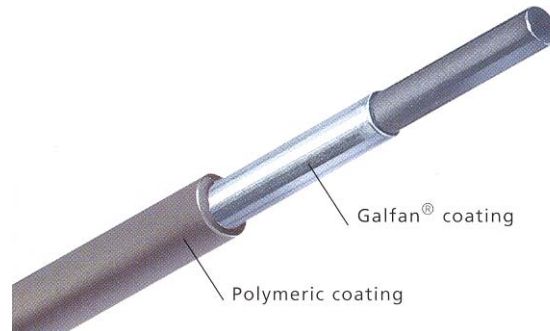


Figure 1.4: PVC - Galfan protection

The use of steel wire protected grid brings a certain number of problems with respect to the environment, but also the life-time expectancy is relative uncertain, due to possible sudden occurrence of corrosion. By replacing the steel wire grid with another material, these problems and uncertainties could be solved.

The application of a synthetic grid material will not have the problem of corrosion and dissolving of harmful particles. It will need the ability to be resistant against wearing due to the movement of stones. Because synthetics are generally softer, they can experience wearing. Excessive wearing can reduce the strength of the material, but a corrosion process is not started or accelerated when little wearing is initiated. The application of a synthetic grid therefore seems useful from a first point of view. Especially in conditions with salt water, a synthetic grid could make the gabion construction more suitable, because the steel wire variant is unpopular and not considered as an option. Next to that a synthetic alternative is better able to resist wave action. The steel wire variant is not applied in these conditions, since the sensitivity for damaging the protective layer is too large.

The general fear of applying synthetic materials is that deformation and material strength influence the gabion functioning on such a level that failure originates rather quickly. The lack of experience holds engineers back from developing and applying a synthetic alternative. In view of the application in waves is the gabions construction rather rare. The design formulas are therefore of a more or less basic form which results in a faster choice for a more conventional solution, that has proven itself, as for example rip-rap.

1.4 Problem Definition

A synthetic gabion, would be a serious alternative for the current steel wire variant. Not only for the current design situations, but also in situations with wave attack and salt water conditions. The problem definition of this project consists of three elements.

In the first place the properties of a synthetic material should be formulated, followed by a product description that fits these properties. Secondly, the process and sensitivity to deformation is unknown, including the influence of grid rigidity. Thirdly the design formula's for gabions in waves have the possibility for further improvement.

1.5 Objectives

From the problem definition it comes forward that there are three main aspects of interest. Each aspect brings a number of objectives that are subjects in this report. The first main objective of this thesis is to confirm the use of a synthetic material in the application of gabion revetment constructions. Certain demands are formulated which are necessary for the proper functioning of synthetic gabions. The material is checked on these demands.

The second objective is to study the deformation behaviour of the construction under wave attack. Since deformation is a feared mechanism for synthetic gabion failure, this aspect is investigated by performing a scale experiment inside a wave flume. To create a representative model it is of importance that the properties of the prototype material are scaled down by the correct scale factor. Based on a scale model, parameters are varied to study the deformation related to fill material size, shape and compaction. The type of wave attack and filter have also been altered. Based on the results recommendation are made.

Besides the deformation that is studied also the stability of the mattress construction in waves will be studied. The application of gabions in wave conditions is not that common and the available design formulas are of a rather simple form. A third main objective is therefore to improve the current design formula.

Summarizing for each main objective:

1) Material

- Formulating the demands of a synthetic material
- Confirmation of the application of a synthetic material

2) Deformation

- Determination of the grid material influence on the deformation
- Determination of the influence of fill material shape, size and compaction
- Recommendations for the construction of gabions

3) Design Formula

- Improvement of the current design formula

1.6 Report Structure

Chapter 1 presented the introduction of gabion structures and the potential advantages of a synthetic alternative. The lack of experience and general coarse design formulas for the application in waves results in an underestimated appreciation of this construction.

In chapter 2 the mechanisms and theory that is available from literature is presented. This chapter concludes with comments on the current design formula for the stability of gabions in waves. The possibility to improve the current design formula is described.

In the succeeding chapter 3, the requirements for the synthetic material are stated followed by the description of a material that is suitable for a synthetic gabion grid.

Chapter 4 describes the research program in which the scaling of the materials, the test program and the experiment set-up is presented.

The test results are presented in chapter 5. The observations are described followed by the analysis of the results. Based on the results a data analysis is performed, giving a first start of an improved design formula.

Conclusions and recommendations are presented in chapter 6. To keep the report legible, several graphs and additional information is placed in the appendixes.

Chapter 2. Gabion Stability

2.1 Gabion Structures

Gabions can be found in all sorts of hydraulic structures. In the overview below the situations are presented in which a gabion construction can be applied within the perspective of hydraulic engineering. Gabions have several qualities that are used in these structures, depending on the type of application. The qualities are:

- | | | |
|----|------------------------|---|
| 1. | Erosion | Ability to dissipate energy. |
| 2. | Drainage | Permeability results in good drainage capacities. |
| 3. | Stability | Ability to increase the stability of the soil or structure. |
| 4. | Flexibility | Ability to follow soil deformations. |
| 5. | Safety | Possibility to climb on the structure. |
| 6. | Environmental Friendly | Vegetation can grow on and through the structure. |

Bed Protection

- Function: Protection against erosion caused by high current velocities.
- Application: River constrictions, abutments culverts, constructions for the dissipation of high velocity streaming water.
- Gabion Type: For applications in these circumstances mattress gabions are used.
- Qualities: Erosion, Stability, Flexibility



Figure 2.1: Bed protection

Bank Protection

- Function: Protection against erosion caused by wave-, and current attack
- Application: Revetments that are subjected to wave-, and current attack
- Gabion Type: Box-, mattress-, and cylindric gabions
- Qualities: Erosion, Drainage, Flexibility, Safety, Environmental Friendly



Figure 2.2: Bank protection

Pre-bank Protection

- Function: Protection of the bank against wave attack and guidance of currents.
- Application: Protection of the bank behind it and creating a environment for the development of nature.
- Gabion Type: Box-, or cylindrical gabions.
- Qualities: Erosion, Stability, Flexibility, Environmental Friendly



Figure 2.3: Pre bank protection

Channel Lining

Function: Protection against high flow velocities that cause erosion and to prevent meandering of the river.
 Application: River training works.
 Gabion Type: Box-, or mattress gabions.
 Qualities: Erosion, Flexibility, Safety, Environmental Friendly



Figure 2.4: Channel lining

Pipeline Protection

Function: Protection against flow velocities that can cause free spans of the pipe. Protection against trawler fishnets.
 Application: Underwater pipelines.
 Gabion Type: Mattress gabions.
 Qualities: Erosion, Flexibility

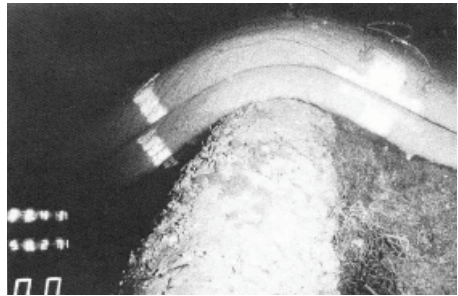


Figure 2.5: Pipeline protection

Drainage for Dikes and Levees

Function: Forming a stable sublayer and to lower the freatic level in the core.
 Application: In dikes and levees.
 Gabion Type: Box-, and mattress gabions.
 Qualities: Drainage, Stability, Flexibility



Figure 2.6: Toe-construction

Groynes

Function: The guidance of currents and to prevent meandering.
 Application: In rivers.
 Gabion Type: Box-, and Mattress gabions.
 Qualities: Erosion, Stability



Figure 2.7: Groyne

Weir

Function: To guide the water and influence the water level.
 Application: Increasing water level and controlling the ground water level.
 Gabion Type: Box gabions and sometimes mattress gabions.
 Qualities: Erosion, Environmental Friendly



Figure 2.8: Weir

Soil Retaining Wall

Function: Retaining soil and sometimes as a combined application for river guidance works.

Application: Steep transitions between water and land. Applied if there is a shortage of space

Gabion Type: Box gabions

Qualities: Erosion, Stability



Figure 2.9: Soil retaining wall

Furthermore gabions can also be found in different constructions that are not related to hydraulic engineering. Examples are: Gabions for degassing of a rubbish dump, scenery element, fence, noise barrier, etc.

Compared to other materials that are used in hydraulic structures, gabions have several advantages.

- There is no direct requirement for heavy equipment or machinery. In areas where labour is cheap a construction can be made without heavy equipment. This can reduce costs and create possibilities to construct in remote areas or where a plant is difficult to obtain.
- Local labour can rapidly be trained to construct high quality structures. The ensemble procedure and handling of the tools is simple.
- Construction makes use of low cost locally available stone.
- Structures may be added at a later moment.
- Rapid construction makes them ideal for emergency works. This can be done with help of lifting equipment. Prefabricated gabions, or gabions assembled on site can be lifted rapidly on its location. Only the mutual connection has to be made afterwards by hand.

It can be stated that gabions can be applied in a wide variety of structures. The combination of relatively cheap material and the flexibility in design, makes gabions a proper solution for the application in different hydraulic structures, but they also find their application in other fields of construction.

This report is focused on the development of a synthetic mattress gabions in a wave climate. The synthetic grid can give the greatest contribution in view of life-time expectancy and potential good alternative with respect to wave attack.

2.2 Environmental Contribution

2.2.1 Environmental Friendly Banks

In the Netherlands there is a pursuit to create banks, along rivers and canals, that offer the possibility for the development of vegetation. Shallow waters with a large variety of vegetation provides sources of food, a place for growth and shelter for animals. Besides a place of living ecological friendly banks also perform as an easy location for the crossing of animals between water and land. An example of ecological unfriendly banks are sheet piles. Animals which fall into the water and cannot get out, with possible drowning as a result. Ecological friendly banks form a gentle transition between water and land and provide a good place for crossing and development of vegetation.

One of the general advantages of gabions is that they have the ability for vegetation to grow through the protection. Vegetation in its own way is also able to absorb wave-energy. So called bioengineering solutions, based on only vegetation, are not the most reliable protection. Plants are subjected to growing seasons, diseases and are sometimes simply mowed off. Bioengineering products are difficult to establish, although dependent on the situation. A combination of gabions with vegetation provides a more certain solution against erosion. It provides a base for the vegetation to develop and can function as an environmentally friendly bank.

In CUR 202, Bank Protection Materials, an appendix is present in which an overview is given of all sorts of bank-protection materials. These materials are evaluated about their constructive and ecological properties. Briefly, how good they perform and how well the ecological contribution is. A shortened version of this appendix is stated in table 2.1.

Material	Aspect	Watertype							
		Small Watercourse	City Water	Creek	Large River	Channel	Fresh Lake	Brackish Lake	Tidal Salt Waters
Gabions	Constructive	+/o	+/o	+/o	+	+	+	+	+
	Ecology	o/-	o/-	o	o	o	o	+/o	+/o
Rip-rap	Constructive	+	+	+	+	+	+	+	+
	Ecology	-	-	o	o	o	o	+	+
Concrete Elements	Constructive	o	o	+/o	+	+	+	+	+
	Ecology	-	o/-	o/-	o	o	o	+	+

Code Tabel	Constructive	Ecology
+	good, suitable, material has proven itself	good possibilities looks like natural situation
+/o	good to average	reasonable possibilities
o	average	few possibilities natural situation is not achieved
o/-	average to worse	hardly any possibilities
-	worse	no possibilities, technical solution dominates

Table 2.1: Constructive and ecological evaluation of hydraulic bank protections

From a hydraulic point of view gabions are a good and suitable solution for the relative larger waters. For smaller waters the use of gabions is, from a constructive point of view, not necessary. Over-dimensioning is always more expensive and will not give a satisfying result. Compared with rip-rap and concrete elements there is no difference in view of hydraulic functioning.

From an ecological point of view steel wire gabions provide a moderate contribution to the environment. Rip-rap and concrete elements give even a slightly better contribution. The lower ecological appreciation is mainly ascribed to the zinc contamination and the fill material that can contain polluted elements. Rip-rap and concrete elements are valued slightly better, because vegetation can grow on the elements. What is not taken into account, in this table, is the possibility that vegetation is able to grow through the gabions. In combination with a synthetic material for the basket, the ecological appreciation might improve considerably.

2.2.2 Vegetated Gabions

Compared to concrete elements and rip-rap, the possibility for the development of vegetation on gabions is better. In 1984 an experiment was performed along the Princes Margriet Channel in the Netherlands [CUR 200]. It was tested how well vegetation would develop on different bank protection systems. The tested protection systems were: rip-rap, gravel, gabion mattresses and three types of blockmats (Armorflex open / closed and Terrafix). These systems were placed on a synthetic geotextile on peaty soil. Behind these constructions, on the land side at 0,25 m above the water level a 2 meter wide reed berm was placed. In 1992 this reed berm was fully developed and results were acquired. The block mats were subsided as a result of wash out of particles. The gabions did not remain unaffected, some of the fill material was washed out. The baskets were not strong enough, and the steel wire failed. Reason for this was the intensive marine traffic that caused quite some wave attack. As a result of this particles moved too intense and caused damage to the wire coating.

Apart from failure of the construction the development of vegetation through the gabion mattress was quite good compared to the other constructions that were applied. From the materials, the smooth gravel was covered with only 3% of vegetation, followed by the rip-rap 70% and the gabions and blockmats had a coverage of 82-92%.

Vegetation will only develop along banks if it is possible that silt and organic material is captured in holes and cracks or the roots are interfered with the subsoil. Gabions are very well capable of catching material if it is supplied enough and the hydraulic conditions do not wash out the material. Especially in the area where there is a lot of water movement around the waterline and just under it is hard for plants to place their roots, because the silt and organic material does not settle.

To successfully develop plants in these conditions a mild slope is needed. On rough and open structures under the waterline a number of macro fauna species is able to settle. To help and fasten the development of vegetation it is possible to place cuttings of plants or root stakes. For the upper part of the revetment the placing of stakes from willows or alders is quite common. The end is cut at an angle, for easy insertion, and hammered through the construction into the soil. A positive contribution is the improved interference with the subsoil that is created by the roots. This improves the stability against sliding.

On the lower parts of the revetment, in the so called aquatic zone, reeds are placed. Reeds can be used to create fringes in the regular inundated zones. The barrier of reed stalks that is formed, creates a very good protection against wave attack. The flexible behaviour of the stalks absorbs a certain amount of energy. This works till a certain wave height. Waves of 30 cm or more bend the reed and cause damage. There will be no development of the plantation and the vegetation fails [MORGAN & RICKSON 1995]. The intensity and amount of waves have influence on the success of vegetation development.

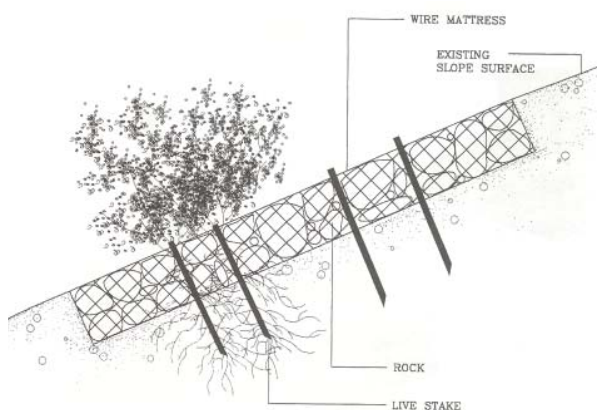


Figure 2.10: Illustration of an established gabion mattress

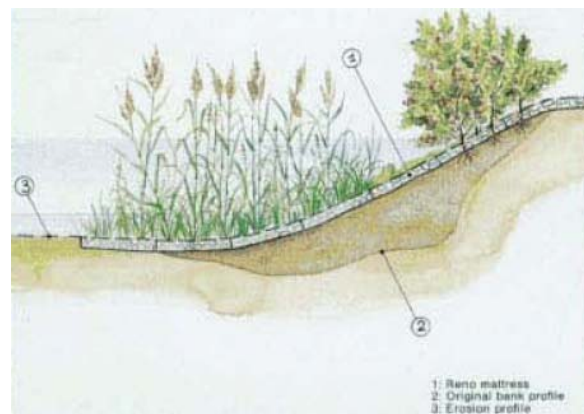


Figure 2.11: Vegetated mattress gabion, desired result

In the section above the accent of vegetation development lies mainly on locations with fresh water conditions. The sensitivity to corrosion is one of the main reasons why there is not much experience and literature about the combination of gabions and vegetation in salt water. Some experiments with soil-vegetation interaction in salt water vegetation has been performed. *Van Eerd*, 1986 [MORGAN & RICKSON 1995] performed a study in the Oosterschelde where the tensile strength of soft clay improved from 2.5 kPa to 5-6 kPa by applying vegetation. A increasing network of fine roots increases the tensile strength linearly. The specie common cordgrass (In Dutch: Engels slijkgras) with robust rhizomes and extensive root networks showed good resistance against waves and ability to hold the soil. Cordgrass seems a useful specie to apply in the same manner as other aquatic plants. Certain seaweeds could also perform a similar function, since they posses some resistance against tidal variation.

In combination with the synthetic grid the gabion mattress can result in a durable and environmental friendly bank protection. It should be noticed that vegetation can contribute to the stability of a gabion mattress construction. During the design this contribution cannot be taken into account, since the development and existence of vegetation is uncertain. Diseases, sudden pollution or water saltinity can have a great and fast influence on the condition and viability of the vegetation.

2.3 Introduction Stability Theory

2.3.1 Introduction

A slope protected by gabions has to be able to sustain a certain amount of load. The construction will succeed in fulfilling this function when the active forces are smaller than the strength of the construction. The load is present in the form of flow velocity or waves. The strength of the structure itself is obtained by the size, weight, thickness and slope of the protection. To provide enough strength for a certain level of load a number of design rules have been developed.

In this chapter an overview is given of the different design rules with respect to the stability of gabion protections in currents and waves. The most important and widely used methods will be described. This mainly includes the work of Pilarczyk and Simons. Pilarczyk did a lot of research with respect to the stability of composite revetment protections, including gabions. This work is of a relative recent date. Simons executed several experiments and developed a design method for the company Maccaferri. This company is one of the main producers and developers in the development and application of gabions. Maccaferri came as first with a gabion protection system as still can be found today. The research from *Simons 1984* [MACCAFERRI 1985] is still used today and is therefore included in this report. There are many more producers of gabions, which mainly apply the same sort of formula's in which only some coefficients differ. It is therefore not very useful to present all these design rules.

The most applied and founded rules will be described and compared. Most of these rules are based on the design rules of rip-rap protections. For the understanding of the general stability formulas the background and adaptation to gabion stability formulas is included. First the stability in water flow will be treated and then the stability in waves will be described.

2.3.2 Definitions

Before an explanation can be given about the theoretical design rules for gabion protections, some definitions, that are presented in the list of symbols, are explained. These definitions are important elements in the stability design rules.

Characteristic Thickness of the Element

For stability it is important what the characteristic size of the stones, sand or protection element is. This size is dependent on the shape of the material. In *Schiereck 2001* the nominal diameter of a stone or sand particle is represented by formula [1]:

$$d_n = \left(\frac{m_s}{\rho_s} \right)^{1/3} \quad [1]$$

The value d_n represents the length of a rib from a cube and is used as a nominal diameter for the particles. This approach is based on the mass of the element. There is no influence of any voids. This formula can be applied for gabions, but the mass of the gabion has to be corrected for the pores that are present between the stones. The result is that the formula is based on volume instead of mass. This is done by taking the percentage of pores into account. If this is done, then the nominal thickness can be assumed as the thickness of the gabion mattress (D_n).

Relative Density

Objects that are in or under water experience uplifting force, which results in relatively less weight in water. Mass based approaches correct this by taking the relative density in water into account. This is done by formula [2]:

$$\Delta = \frac{\rho_s - \rho_w}{\rho_w} \quad [2]$$

By taking the voids into account, the nominal thickness can be corrected and transferred to a volume based approach. This is achieved by adding an extra term in the formula for the relative density. It is corrected with the percentage of voids (n) in the filling material. Formula [3] represents this:

$$\Delta_m = \frac{(1-n)\rho_s - \rho_w}{\rho_w} \quad [3]$$

To give an example of the results from formula [2] and [3], values are filled in that are representative for particles and respectively gabion constructions.

Porosity fill material:	n	= 0.40 -
Density of stone:	ρ_s	= 2650 kg/m ³
Density of water:	ρ_w	= 1000 kg/m ³

$$\Delta = \frac{\rho_s - \rho_w}{\rho_w} = \frac{2650 - 1000}{1000} = 1.65 \quad \Delta_m = \frac{(1-n)\rho_s - \rho_w}{\rho_w} = \frac{(1-0.4)2650 - 1000}{1000} = 0.99$$

Reynolds Number

The Reynolds number (Re) informs about the stream condition of a flow. This condition is turbulent or laminar. The Reynolds number is equal to the ratio between velocity, length and the kinematic viscosity. During the laminar case the viscous forces are dominant. This occurs at low Reynolds numbers (Re<2300). In this situation a fluid is able to follow the geometry of a body and a linear smooth flow situation is present. In the situation with turbulent flow the inertial forces are dominant. Turbulent flow is characterized by the fact that the streamlines will come loose from the volume. This leads to eddies, vortices and other irregular flow fluctuations (Re>3000). In civil engineering there is almost always a turbulent situation.

$$Re = \frac{uL}{\nu} \quad [4]$$

Froude Number

For the classification of a current the ratio between the flow velocity and the propagation speed of waves is used. This ratio is called the Froude number. If the flow velocity is higher than the wave velocity, the waves cannot propagate against the water flow. For example if a pebble is thrown into the water. If the flow exceeds the wave celerity than it is not possible that the waves propagates upstream. This is called supercritical flow.

$$F_r = \frac{u}{\sqrt{gh}} \quad [5]$$

For gabion constructions the gradient is almost always fairly flat. This indicates that for rivers and channels the flow is subcritical. In civil engineering it is the most common type of flow, although in relatively steep channels or over culverts it is possible that the flow is supercritical. In mountainous areas this can be found.

2.3.3 Equilibrium of Forces of Particles in a Water Flow

The theory based on stability of stones with respect to current velocity is based on an equilibrium. Stones, which are present in a flow, experience a drag force (F_D), a lift force (F_L) and a shear force (F_S). These are the driving forces. The counter forces are the friction force (F_F) and the mass of the element (W). Figure 2.12 gives an overview of the different forces. The flow velocity which causes distortion of the equilibrium and starts motion of the particle is called the critical flow velocity u_c .

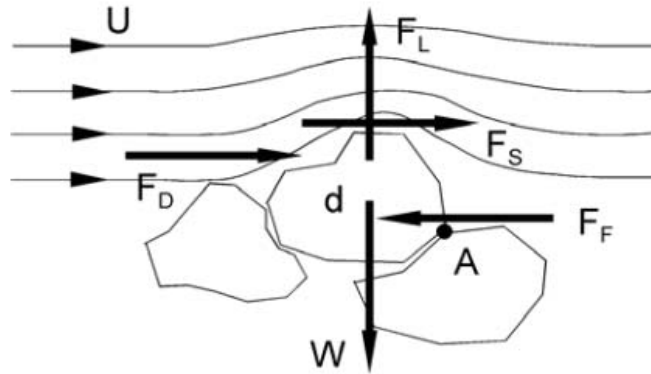


Figure 2.12: Forces on a particle as a result of flow

In reality it is not possible to judge the stability with an equilibrium presented in Figure 2.12. In the following sections the theory of stability is described.

2.3.4 Izbash Formula for Critical Velocity

One of the first relations between critical velocity and stone diameter was made by Izbash. Presented by formula [6] Schiereck 2001:

$$u_c = 1.2\sqrt{2\Delta gd} \quad \text{or} \quad \Delta d = 0.7\frac{u_c^2}{2g} \quad [6]$$

The constants in this formula are based on several experiments. It should be noticed that a water flow does not have the same velocity everywhere in the cross-section, but has a certain cross-section velocity profile. Near the bottom the velocity is lower than at the surface. This aspect is not taken into account in the formula of Izbash, it is more or less a tool for a first approximation in cases where a velocity near the bottom is known but the relation with the water depth is not clear.

2.3.5 Shields Formula for Critical Velocity

An improved approximation for the relation between velocity and stone diameter is the formula of *Shields 1936* [SCHIERECK 2001]. This formula gives a relation between a dimensionless shear stress and the particle Reynolds number (Re_*). Shields developed a stability parameter (Ψ_c) which is defined using a critical value of the velocity. Formula [7] represents Shields formula.

$$\Psi_c = \frac{\tau_c}{(\rho_s - \rho_w)gd} = \frac{u_{*c}^2}{\Delta g d} = f(Re_*) \quad [7]$$

With:

- τ_c = critical shear stress
- d = grain diameter
- u_{*c} = critical shear stress velocity

The particle Reynolds number (Re_*) gives information about the grain size in relation to the protrusion of the particles in the different flow layers. Between the bed ($u=0$) and the boundary of a turbulent layer, there is a layer that forms the transition. This is the so-called viscous sub-layer. The particle Reynolds number gives a dimensionless indication about the protrusion into these layers. This particle Reynolds number is calculated by formula [8].

$$Re_* = \frac{u_{*c} d}{\nu} \quad [8]$$

The dimensionless shear stress velocity u_{*c} is calculated by iteration (formula 7). *Van Rijn 1984* [SCHIERECK 2001] adapted the Shields relation by replacing the particle Reynolds number (Re_*) by a dimensionless particle diameter d_* . The advantage is that iteration is no longer required. This dimensionless particle diameter is calculated with formula [9].

$$d_* = d \left(\frac{\Delta g}{\nu^2} \right)^{1/3} \quad [9]$$

The relation between the critical shear stress and dimensionless particle diameter, according to *Shields – van Rijn 1984* [SCHIERECK 2001], is represented in Figure 2.13:

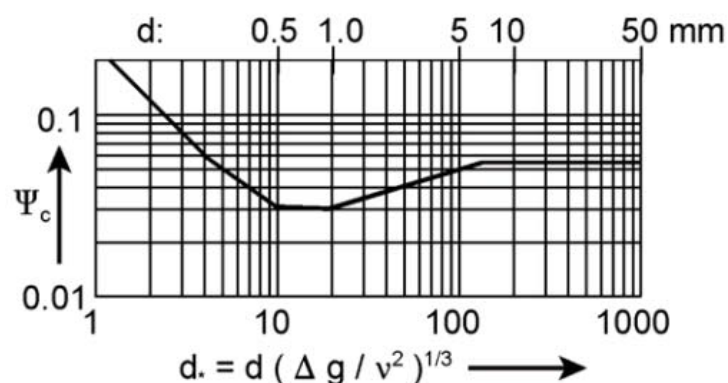


Figure 2.13: Critical shear stress relation by Shields and van Rijn

For the large particles, that protrude through the viscous layer, a turbulent flow is present. In this situation the dimensionless diameter has no longer influence and the stability parameter (Ψ_c) is constant, as can be seen on the right part of the graph. The lower stability parameters, indicating lower stability, are explained by the fact that the shear stress is dominating and creating a larger arm for the moment, leading to a more unstable situation. Small particles, that are only present in the viscous sub-layer, gain stability because the square of the velocity is no longer valid in the viscous sub-layer.

In reality it is not possible to calculate a critical velocity that indicates instability of particles. There exists a certain bandwidth around the critical shear stress, indicated by the Shields relationship. It differs from occasional movement of particles at some locations (line 1, Figure 2.14) to general transport of the bed protection (line 7, Figure 2.14). Between these lines several classes of motion can be observed. An actual threshold of motion cannot be defined. There will always be some transport. The choice of a certain Ψ_c depends on the amount of transport that is acceptable.

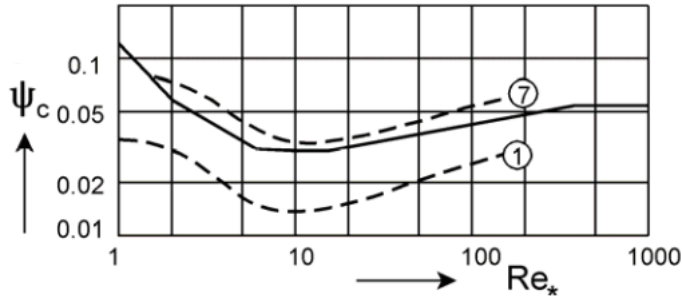


Figure 2.14: Shields graph for different stages of transport

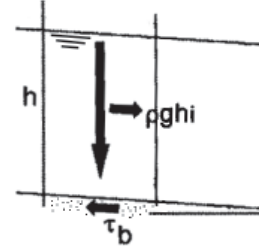


Figure 2.15: Equilibrium driving force and resistance

If a uniform flow is considered, than an equilibrium exists between the driving force, gravity force and the flow resistance expressed as the shear stress. Figure 2.15 shows the equilibrium of forces. The gradient (i) of a channel is small, therefore influence of the tangent of the slope is negligible and is left out of the equation. The shear stress depends on the velocity (quadratic in a turbulent flow), water density and a dimensionless friction factor.

The equilibrium of forces is:

$$\tau = \rho g h i = c_f \rho u^2 \quad [10]$$

The dimensionless friction coefficient c_f is expressed with empirical relations such as Chezy. The Chezy parameter (C) is a value for the hydraulic roughness of the stream profile. The formula for this roughness parameter is:

$$c_f = \frac{g}{C^2} \quad C = 18 \log \left(\frac{12h}{2d} \right) \quad [11-12]$$

The shear stress velocity u_* can now be expressed as a relation between the uniform flow velocity (u) and roughness of the channel. If uniform flow conditions are considered, Shields formula [7] can be rewritten in the same format as developed by Izbash. The shear stress velocity u_* can be calculated with formula [13] which is derived as follows:

$$\tau = c_f \rho u^2 \quad \rightarrow \quad u_*^2 \rho = \frac{g}{C^2} \rho u^2 \quad \rightarrow \quad u_* = u \frac{\sqrt{g}}{C} \quad [13]$$

If formula [13] is used in formula [7] than it can be rewritten and presented in the same format as the Izbash formula. The result shows that the water depth is implicitly present in the formula because the Chezy parameter is used. With this formula the particle diameter for stability can be derived.

$$\sqrt{\psi_c} = \frac{C}{\sqrt{\Delta g d}} \quad \rightarrow \quad \psi_c = \frac{u_*^2}{\Delta g d} \quad \rightarrow \quad \Delta d = \frac{u^2}{C^2 \psi_c} \quad [14]$$

2.4 Gabion Mattress Design Formula's in Water Flows

2.4.1 Pilarczyk's Gabion Mattress Design Formula for Critical Velocity

The Shields formula is used for loose stone protections. *Pilarczyk 1990* [CUR 201 1999] added some extra factors to the formula of Shields so that it could be applied for different sorts of revetments and bottom protections including gabions. On the strength side of the formula the relative density is corrected for the porosity of the fill material and the thickness of the gabion. On the load side of the formula some extra parameters are added and left out. The Chezy parameter is for example left out and replaced by parameters that represents certain location specific conditions.

The amount of turbulence influences the thickness. High turbulence conditions will result in further protrusion of high flow velocity into the gabion mattress and therefore some extra thickness is demanded to prevent erosion. A coefficient for the influence of the water depth is added. Depending on the velocity profile and depth of the protection. The last factor that is added is the use of a gabion as a bed-, or revetment protection.

The formula can be applied for gabions on the bottom of gently sloping rivers, up to 1:20 and on banks with a steepness of maximum 1:2.

$$\Delta_m D_n = \phi K_T \frac{0.035 K_h u^2}{\psi_c K_s 2g} \quad [15]$$

With:

Φ	= Stability parameter	[-]
K_T	= Turbulence and shear stress adjustment factor	[-]
K_h	= Depth factor (dependent on velocity profile)	[-]
K_s	= Slope factor	[-]

For gabions it is recommended to use for the critical shear stress parameter $\Psi_c = 0.070$. The stability factor Φ is 1.2 for exposed edges like the outer bends of rivers and 0.6 for continuous slope protections.

Site dependent factors are developed to take the local conditions into account.

Turbulence factor K_T

- Normal turbulence (quiet river)	$K_T = 1.0$
- Non uniform flow (below stilling basin, outer bends with $r/B > 2$)	$K_T = 1.5$
- High turbulence (under hydraulic jump, at local disturbances in outer bends with $r/B < 2$)	$K_T = 2.0$
- Heavy turbulence (jet turbulence, screw race at small waterdepth)	$K_T = 2.5$

Depth factor K_h

The depth factor depends on the velocity profile that is present.

- Logarithmic profile	$K_h = 2/\log(10h/k_n))^2 = 628/C^2$
- Not fully developed velocity profile	$K_h = (h/D_f)^{-0.2}$
- Shallow water ($h/D_f < 5$)	$K_h = 1$

Slope factor K_s

- River banks	$K_s = \cos\alpha \sqrt{(1 - \tan^2\alpha / \tan^2\theta)}$
- Bottom protection	$K_s = \cos\alpha_b$

The size of the filling material is also taken into account (D_f) and should not be larger than: $D_n/1.8$.

A restriction to the minimum fill material size is not given, although larger than the mesh size is a logical choice. In Pilarczyk's design formula some new parameters are introduced. In the overview below most are explained.

r	= Centre line radius of the river bend	[m]
B	= Width of the river	[m]
k_n	= Roughness (between $2D_f$ and $5D_f$)	[m]
D_f	= Size of gabion filling material	[m]
α	= Slope angle (perpendicular to the flow direction)	[°]
θ	= Angle of internal friction	[°]
u_b	= Velocity at gabion surface	[m/s]
α_b	= Slope angle of river bottom (parallel to the flow direction)	[°]

By using different extra parameters it is possible to adapt the construction for the appropriate situation with accompanying conditions. The formula is based on a blackbox model in which the extra parameter approximates the curve fit of several experiments.

2.4.2 Simons' Gabion Stability Formula in Waterflows

Simons' performed several tests for Maccaferri to develop design rules for Maccaferri's gabion mattresses. The Shields relation is also used to determine the stability of the revetment under a current. To develop the design rules, several experimental tests have been done at Fort Collins (Colorado U.S.A). Basically a big flume was used, in which the different gabion aspects were tested. In particular each test registered the point at which flow caused the first movement of stones in the compartments. This condition was the first indication of critical stability. With help of these experiments the Shields parameter (Ψ) could be defined. This is useful for a comparison with other types of revetment protections.

Simons also included the hydraulic roughness of channels in the formula. The amount of resistance depends on the flow velocity, skin friction and the hydraulic radius of the channel. The flow velocity is calculated with Chezy's law for uniform flow [16]. The roughness coefficient (c_f) is also evaluated with empirical formula's. Manning-Strickler, which is a comparable to Chezy's relation for hydraulic roughness, is used [17].

$$u = c_f \sqrt{Ri} \quad [16]$$

$$c_f = \frac{1}{n_r} R^{1/6} \quad [17]$$

The formula of Manning Stickler [17] is also based on a roughness coefficient. The coefficient can be evaluated from the Meyer-Peter-Müller formula [18].

$$n_r = \frac{d_{90}^{1/6}}{26} \quad [18]$$

Bed protection

Simons split the design formula in two situations: The bed protection and the revetement protection. A bed protection is considered stable if there is no movement of individual stones. The limit of the revetment's stability occurs at the point at which the stones are about to move. The shear stress that is exerted on the protection is:

$$\tau_b = \rho_w h i \quad [19]$$

The Shields parameter indicates how much movement of stones is tolerated, given by formula [7]. As been explained, the Shields parameter has a relation with the critical shear stress condition at initial movement [20]

$$\tau_c = \psi_c (\rho_s - \rho_w) g D_f \quad [20]$$

The revetment is stable if the following condition is verified:

$$\tau_b \leq \tau_c \quad [21]$$

The Shields parameter for loose stones is about 0.047, but depends on the amount of transport that is accepted. Stones that are contained in a wire mesh, can sustain a higher Shields parameter. After analysing the initiation of stone movement, Simons found a Shields parameter of 0.10.

The effect of the higher allowable parameter can be explained with a comparison of a rip-rap revetment. With the same size of stones the gabions are able to withstand more than double of the shear stress than rip-rap. Figure 2.16 shows the difference in the critical shear stress. This difference in Shields parameter value implicates that for the same solution smaller stones could be used, if they are applied as fill material instead of rip-rap.

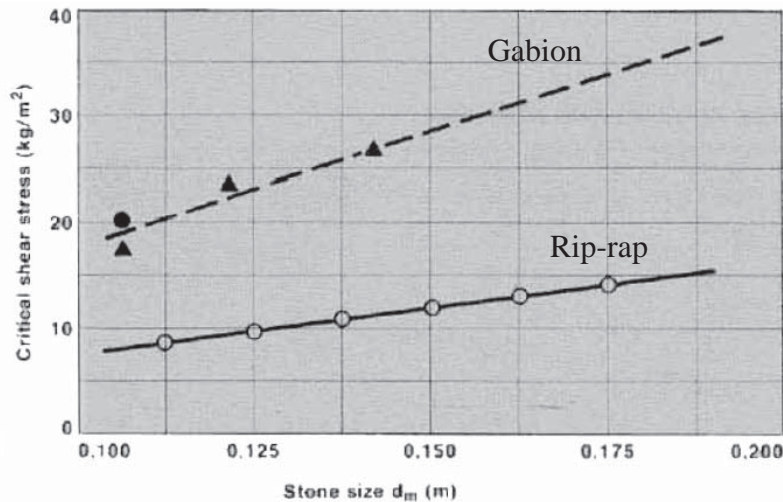


Figure 2.16: Difference in critical shear stress

Revetment protection

For the banks of a trapezium shape Simons gives a adapted form of the formulas for bed protections. The shear stress and critical shear stress is given by formula [22] and [23].

$$\tau_m = 0.75 \rho_w h i \quad [22]$$

$$\tau_s = \tau_c \sqrt{1 - \frac{\sin^2 \theta}{\sin^2 \varphi}} \quad [23]$$

For the angle of internal friction of the stone fill a value 41° is advised. The lining of this bank is stable when:

$$\tau_m \leq \tau_s \quad [24]$$

For curved sections the shear stress increases along the outer bank. For these situations an extra parameter is included in the formula for the shear stress. This parameter depends on the hydraulic radius of the river. The radius of the curvature and width of the water surface determines this coefficient. These expressions are not further included in this report.

In practice it is more easy to evaluate the stability of a revetment with the flow velocity as a reference. Pilarczyk's formula is based on the velocity as can be seen in formula [15]. Velocity and depth are related to the shear stress. It is possible to convert the shear stress approach to a velocity approach. Simons rewrote expression [19] by expressing the average shear stress (τ) as $\tau_b = \rho_w Ri$.

The combination of Manning's formula [16] and [17] is used to express the slope. This result is used to fill in the rewritten expression of Simons.

$$u = \frac{1}{n_r} R^{2/3} \sqrt{i}$$

$$u^2 = \frac{1}{n_r^2} R^{4/3} i$$

$$i = n_r^2 \frac{u^2}{R^{4/3}}$$

Filling in the result gives:

$$\tau_b = \rho_w Ri$$

$$\tau_b = \rho_w n_r^2 \frac{u^2}{R^{1/3}} \quad [25]$$

With this formula it is possible to use the velocity for the determination of stability. The critical velocity or critical shear stress only depends on the size of the fill material. Also in this approach the flow conditions, to which the gabion is exposed, is taken into account with the value of the Froude number [5]. If this ratio is close to one, than the flow will behave more like a supercritical flow. In practise this means that there is more turbulent behaviour.

For a certain type of rock size and mattress thickness a critical velocity can be determined. This is based on several tests carried out by *Simons 1983* [MACCAFERRI 1985]. The results from these tests are presented in the two graphs of Figure 2.17. As a condition for stability, the critical velocity should always be higher than the actual velocity, for a stable situation.

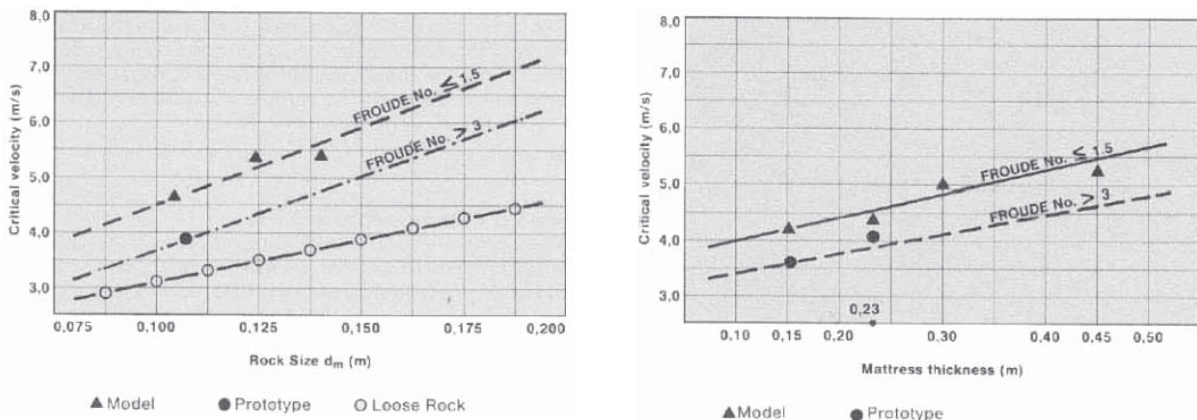


Figure 2.17: Rock size and mattress thickness versus critical velocity

2.4.3 The Difference Between Simons and Pilarczyk

The present gabion design guidance is based on either a shear stress or critical velocity approach. The critical velocity approach is preferred by most designers, because the shear stress is difficult to estimate. Therefore the shear stress approaches are converted to a velocity approach, like Simons method. It should be noticed that this method is only based on velocity with no dependence on depth. Pilarczyk's approach shows an equation with a depth effect using velocity (Chezy parameter). Disadvantage of this approach, compared to that of Simons, is that the cross section shape or alignment is not taken into account.

2.4.4 Deformation Effects

When the shear stress reaches the critical velocity some parts of the fill material can start to move inside the compartment of the mattress. If the vibrations increase two things can happen. First, the stones start moving into the downstream direction of the mattress. The revetment can lose its effectiveness, because the subsoil at the upstream part of the compartment gets exposed. Second, a new equilibrium will develop. In this situation it is important that the wire mesh is strong enough to fulfil its containment function. Figure 2.18 illustrates the movement of grains inside the compartment. The accumulation of stones downstream of the compartment will result in extra pressure on the wire mesh. To evaluate the amount of deformation a parameter is used ($\Delta z/D_f$). This parameter gives the relation between the height difference of the highest and lowest rock surface (Δz) and the size of the filling material (D_f).

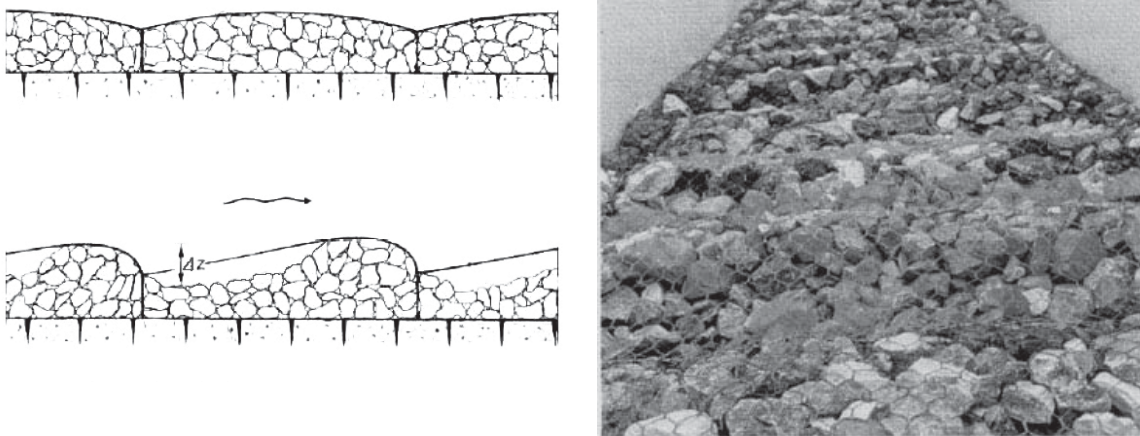


Figure 2.18: Deformation of a gabion mattress

A relation with the so called effective Shields parameter gives the difference between the shear stress and the critical shear stress with respect to the Shields parameter.

$$\psi_c^* = \frac{\tau_b - \tau_c}{(\rho_s - \rho_w)D_f} \quad [26]$$

The effective Shields parameter is used to develop a relationship with the deformation parameter and is expressed in Figure 2.19. These are the values of deformation for compartments of one meter wide. To insure that the soil is not getting exposed to the current, it is essential that deformation condition [27] is satisfied. It is therefore also proposed to have a thickness of at least two times the size of the fill material.

$$\frac{\Delta z}{D_f} \leq 2 \left(\frac{D_n}{D_f} - 1 \right) \quad [27]$$

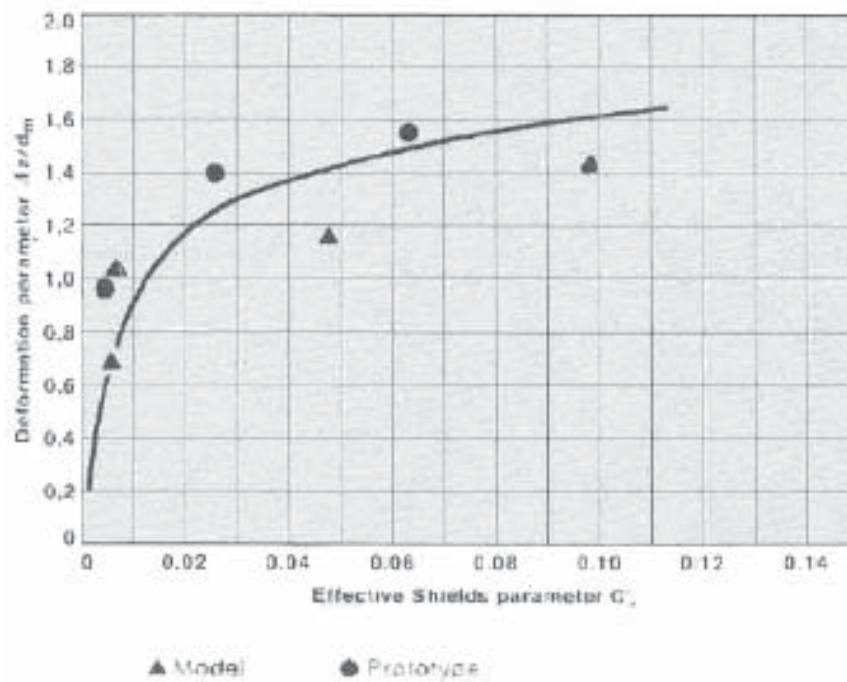


Figure 2.19: Mattress deformation as a function of the effective Shields parameter

In Figure 2.19 it can be seen that beyond certain values of the critical shear stress a mattress of 1.8-2.0 times the size of a stable stone can withstand more severe conditions than the initial design without losing effectiveness. Still it is important to control deformation.

It should be kept in mind that the amount of deformation also depends on the thickness of the revetment, the size of the compartments and the density of the stone fill. These properties must prevent movement caused by current and prevent erosion of the subsoil. The flow velocity between the interface of fill material and subsoil must therefore be of a level that no soil particles start to move through the gabion.

2.5 Gabion Mattress Design Formula's in Waves

2.5.1 Definitions with Respect to the Stability in Waves

In the previous section gabion design rules in currents have been treated. Along the banks of canals, rivers, but also along lakes and estuaries gabions can be subjected to wave attack. Waves initiated by wind or navigation can create severe erosion. Before the design rules for gabions in waves are given, some theoretical background about particle stability in waves is presented. Based on this theory the stability of gabions is derived.

Breaker parameter

When the load is in the form of waves, distinction is made in the condition present in front of the revetment. Not only the wave height, but also the shape of the wave can influence the loads on the revetment. This shape is determined with help of the wave breaker parameter also called the Iribarren number. This parameter is a relation between the angle of the revetment, wave height and wave length. Formula [28] represents the relation for this wave parameter [SCHIERECK 2001].

$$\xi = \frac{\tan \alpha}{\sqrt{H / 1.56 T_p^2}} \quad [28]$$

According to the value that follows from this parameter, a wave can be classified in a certain type of wave breaking. Figure 2.20 presents the different types of wave breaking and the accompanying parameter.

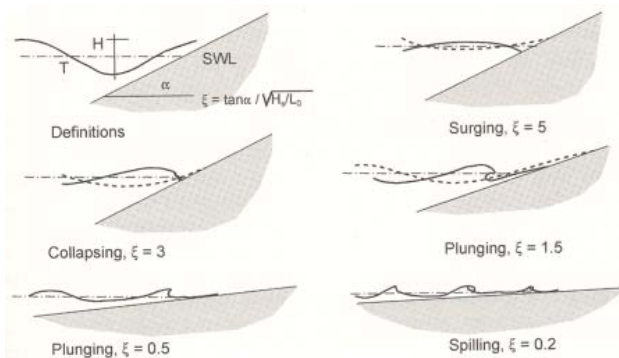


Figure 2.20: Iribarren number with breaker type

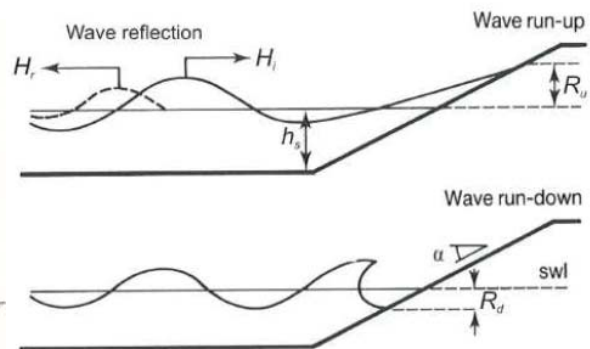


Figure 2.21: Wave run-up and wave run-down

Wave Run-up and Run-down

Wave attack on slopes will lead to a rise followed by a draw down of the water level. The terms run-up and run-down are defined as the maximum and respectively minimum waterlevel on a slope during a wave period. Figure 2.21 reflects the definition.

The amount of wave run-up and wave run-down can be expressed as a function of the Iribarren parameter. The graphs from Figure 2.22 show that there is a relation between the Iribarren parameter and the amount of run-up and run-down. For a higher breaker parameter the run-up and run-down increase, if the wave height is kept constant.

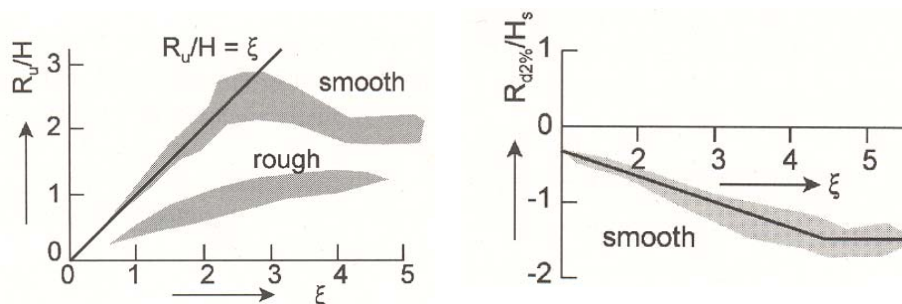


Figure 2.22: Relation between wave run-up and wave run-down

Wave Reflection

Incoming waves (H_i) that enter a slope will lose a part of the energy, which is absorbed by the revetment. The remaining part will be reflected in the form of the reflected wave (H_r). The amount of reflection is related to the breaker parameter. For a low breaker parameter the reflection will be small. A more gentle slope will therefore give less reflection than a more steep slope. In Figure 2.23 the reflection is expressed as a relation between the Iribarren number and reflection coefficient. The reflection coefficient (K_r) is the relation between the incoming and reflected wave H_r/H_i .

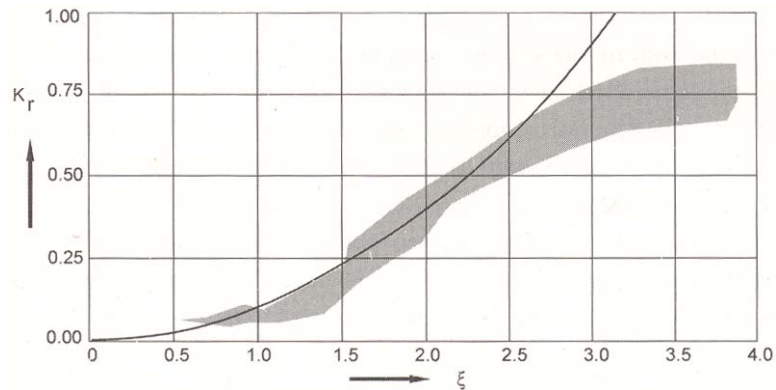


Figure 2.23: Wave reflection

2.5.2 Equilibrium of Forces of an Element

Driving Forces

Wave attack on gabions leads to a complex turbulent flow over the gabions and through the gabions. During the wave run-up the resulting forces by the waves will be directed opposite to the gravity force. Run-up is therefore less hazardous than wave run-down. Run-down will lead to two important load mechanisms.

First, the downward flowing water will exert a drag force on cover layer of gabions. This mechanism can be explained as a free flow through the gabion. The water will flow parallel to the angle of the slope. This can result in geotechnical instabilities such as subsoil erosion and sliding of the revetment due to distortion of the equilibrium.

Secondly, during the wave run-down there will be a difference between the waterlevel in front of the revetment and inside the revetment. Just before the impact of a wave there is a 'wall' of water giving a high pressure under the point of maximum run-down. Above the run-down point the surface of the gabions is almost dry and therefore there is a low pressure. The result is an upward flow and a maximum uplift pressure at the point of maximum wave run-down.

The uplift pressure depends on the steepness and height of the pressure front that reaches the cover layer, the thickness of the gabion protection and the level of the phreatic line in the structure. Because of the open structure of gabions the permeability does not influence the uplift pressure in a negative way. The permeability of the underlying filters can influence the stability.

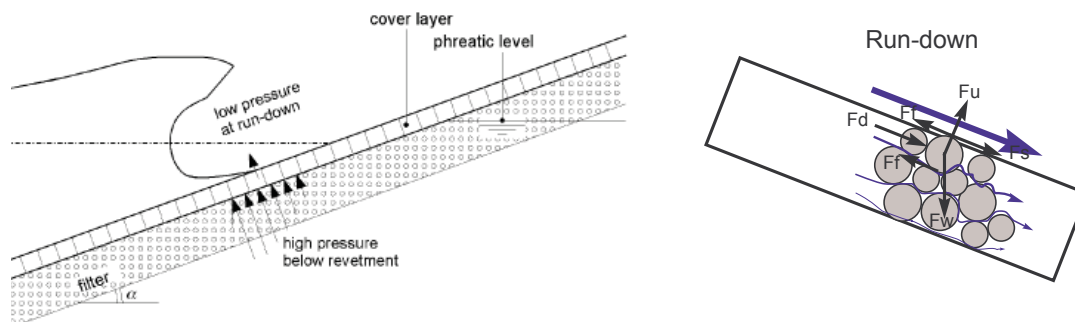
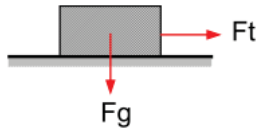


Figure 2.24: Uplift pressure and downrush force

Resistant Forces

Gabion revetment protections fail for several reasons. The most common failure mechanisms can be related to sliding of the construction. Sliding of the revetment is caused by the uplift pressure and drag force that is exerted on the gabions during run-down of the waves. The resistance to sliding is created by the friction between the mattress and subjected filter layer. The amount of friction plays an important role in the stability of the construction. The amount of friction between two layers is expressed by the friction factor f . This parameter is the relation between the gravity force on a horizontal element and the tension force that is needed to start moving the object.



$$f = \frac{F_t}{F_g} \quad [29]$$

Figure 2.25: Resistance to sliding of a horizontal element

Objects on a slope will have a component of the mass that works in downward direction parallel to the slope. The component perpendicular to the slope will generate the friction force. The equilibrium of forces, for a situation without waves, is illustrated in Figure 2.15. Sliding will take place if the parallel downward directed force (F_d), represented by $M \cdot dA \cdot \sin(\alpha)$ larger is than the resistance to sliding (W). The resistance to sliding in a still water situation depends on the friction between the layers. The friction between gabion and granular (f_1) layer, between the granular layer and geotextile (f_2). The situation with the lowest friction factor represents the normative situation.

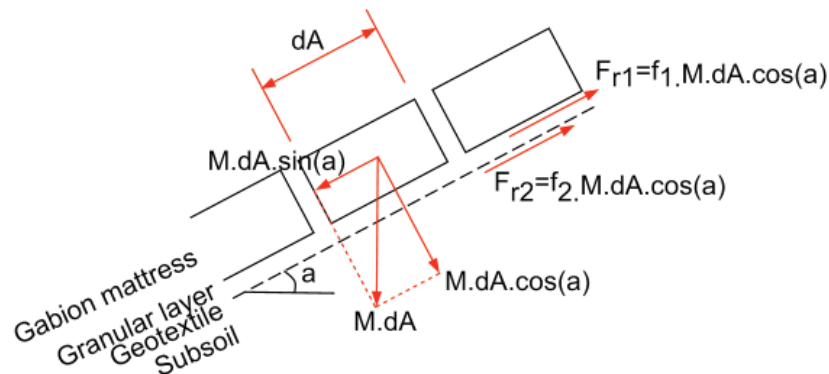


Figure 2.26: Resistance to sliding of a element on a slope

The amount of friction force is a result of the friction factor and the force that works perpendicular on the surface. In the situation of Figure 2.26 the weight of the construction represents this force. For steeper slopes the sinus term will increase and the situation will become less favourable. Increasing the thickness will not increase the stability of still water situation. In the following relation this is proven.

$$\begin{aligned} \text{Downward force } (F_p) &< \text{Resistant force } (F_r) \\ M \cdot dA \cdot \sin(\alpha) &< f \cdot M \cdot dA \cdot \cos(\alpha) \end{aligned} \quad [30]$$

The friction factor should therefore be higher than:

$$\begin{aligned} M \cdot dA \cdot \sin(\alpha) &< f \cdot M \cdot dA \cdot \cos(\alpha) \\ \sin(\alpha) &< f \cdot \cos(\alpha) \\ f &> \tan(\alpha) \end{aligned}$$

The friction and slope angle are the two most important parameters in the stability relation. The more close a construction is to the boundary of formula [30], the less possibility it has to absorb wave loads. Common values for the friction factor of a granular filter layer is 0.7, for the more smooth geotextiles this value is 0.4 [PILARCZYK 2000]. In Figure 2.27 the driving force and the resistant force are plotted in a graph.

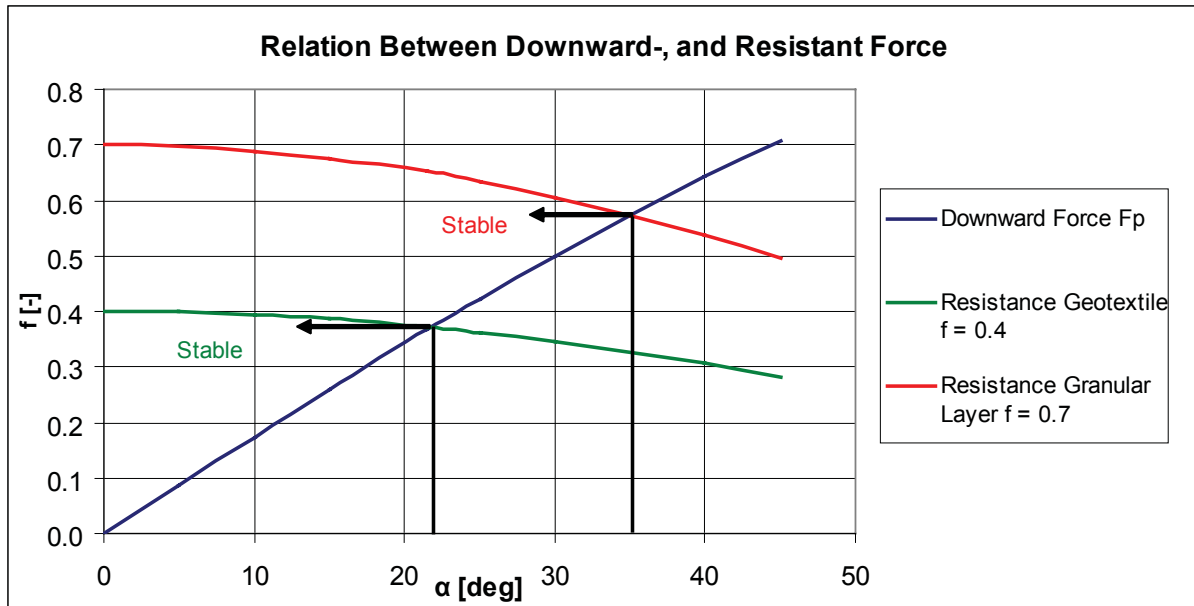


Figure 2.27: Relation between the driving-, and resistant forces for different filter layers

From Figure 2.27 it becomes clear that the application of only geotextile filter gives a restriction to the slope on which it can be applied. The relatively smooth surface of the geotextile creates a situation in which gabions can only be placed on the cloth if the slope angle is at least smaller than 21.5° . A construction based on a granular layer should have a slope angle with a maximum of 35° . It should be noticed that this graph represents a situation with a still water level situation. Wave action will result in extra forces that can disturb the equilibrium.

2.5.3 Anchor Length

The friction factor depends on the type of filter that is placed directly under the cover layer of the revetment. Steeper angles will create a situation where the construction cannot lay stable on the slope, based on its own friction. Below this level the element is stable depending on the wave forces that are present.

Gabion mattresses consist out of compartments that are mutual connected. The elements in the uplift-zone of the mattress could be unstable when there are no mutual connections between the compartments. The benefit of the connection is that the wave forces are spread over the total length of the mattress. The gabions that are in the upper part of the revetment can absorb a part of the downward directed tension force. The best method to prevent sliding is by increasing the friction or by adding some extra length above the revetment. This is the so called anchoring zone Figure 2.28.

The anchoring zone of the revetment will hold the uplift zone on its place when the equilibrium in this zone is not longer realized. The uplift zone is defined as the zone between the wave run-down and the still water level. This zone will hang on the anchoring zone during severe conditions. Supporting of the uplift zone is possible, but the risk of revetment failure caused by bulging or displacement is present.

For the anchoring function PILARCZYK 1998 proposed the following formula for the minimum length of the anchoring zone ($L_{a,min}$) [31].

$$L_{a,min} = 0.5 H (f \cdot \tan \alpha)^{-1} \quad [31]$$

This formula is more or less a estimating relation for the anchor length. It is rather simple relation since it does not take the Iribarren number into account. The influence of the uplift pressure has also not been implemented

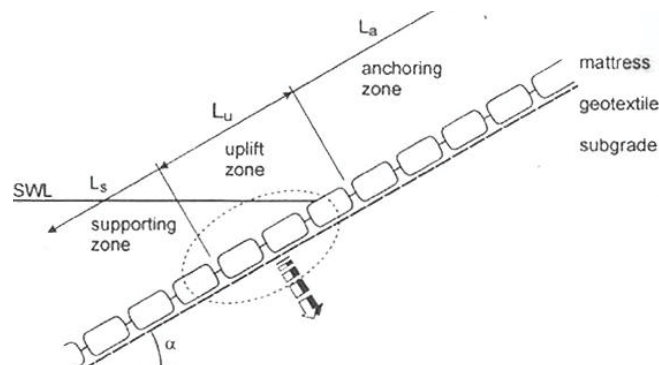


Figure 2.28: Anchor length

2.5.4 Failure of the Revetment

The first possible failure mechanism is continuing deformation with a loss of coverage of the sublayer. The filter layer will be damaged and potential start of erosion will be initiated. The second possibility of failure is sliding of the construction. The uplift forces generated by the waves, combined with the strong drag-, and shear forces can result in sliding of the whole construction or partly sliding. Figure 2.29 shows several failure modes due to sliding. From model experiments performed by Maccaferri, sliding is the predominant failure mode after fill material movement has started.

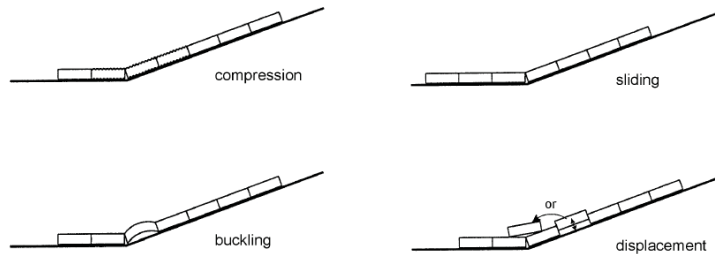


Figure 2.29: Gabion revetment failure

The resistance to sliding depends mainly on the friction between the mattress and slope. The advantage of gabions is that they are connected with each other and can share the load. Potential sliding can be absorbed by the friction that is present between the subsoil and mattress. The mattress that is present along the water level, will experience most of the uplift forces. If it will start to slide, it can transfer its forces on the mattress to which it is connected above.

A second option is the placement of a toe construction that gains extra stability. This can be done by building a extra long mattress on the bed or by placing a higher and thicker gabion at the toe. Though with this type of construction buckling and compression can still happen. It is therefore advised to use higher placed gabions as a resistance to sliding.

2.5.5 Gabion Design Rules in Waves

Like the design rules for gabions in water flow, the stability of gabions in waves is also based on a formula for particle stability. This base formula is Hudson's formula. Hudson performed tests and proposed the following formula for stability of elements in waves [CIRIA, CUR, CETMEF 2007]:

$$\frac{H_s}{\Delta d} = \sqrt[3]{K_D \cot \alpha} \quad [32]$$

This formula includes a so called dustbin factor (K_d). For various elements (natural rock, concrete elements) different K_d values are available. Further development of this formula for gabions is done by adaption of this right term based on experiments. It should be noticed that the amount of experimental verification is rather limited.

2.5.6 Maccaferri's Gabion Stability Formula in Waves

One of the first scale experiments was executed by *C.T. Brown 1979* for Maccaferri [MACCAFERRI 1985]. Gabions of 30 cm long and 20 cm wide and a varying thickness of 1.8 to 4.1 cm were used. The slope varied between 1:1.5 and 1:4 and the subsoil consisted out of sand. Failure of these constructions occurred in two ways. By uplifting at the less steep slopes. Or by downward sliding or buckling near the toe, for the steeper slopes. These experiments resulted in the following design criteria.

$$D_n = \frac{H_D}{3(1-n)(S_r - 1) \cot \alpha} = \frac{H_D}{3\Delta_m \cot \alpha} \quad \alpha > 1:3.5 \quad [33 \text{ a}]$$

$$D_n = \frac{H_D}{7(1-n)(S_r - 1) \cot^{1/3} \alpha} = \frac{H_D}{7\Delta_m \cot^{1/3} \alpha} \quad \alpha < 1:3.5 \quad [33 \text{ b}]$$

The results of the experiments were used to determine the dustbin factor K_d . Rewritten in the same style as Hudson's formula it gives:

$$\frac{H_D}{\Delta_m D_n} = 3 \cot \alpha \quad [34 \text{ a}]$$

$$\frac{H_D}{\Delta_m D_n} = 7 \cot^{1/3} \alpha \quad [34 \text{ b}]$$

2.5.7 Pilarczyk's Gabion Stability Formula in Waves

The experimental work that was executed by Brown was performed with regular waves. *Pilarczyk 1987* [PILARCZYK 1998] transformed these results into criteria for irregular waves, which results in heavier constructions compared to the Maccaferri relation. Based on Hudson's formula the result is as follows:

$$\frac{H_D}{\Delta_m D_n} = \frac{2}{\tan \alpha} \quad \alpha > 1:3 \quad [35 \text{ a}]$$

$$\frac{H_D}{\Delta_m D_n} = \frac{4}{(\tan \alpha)^{1/3}} \quad \alpha < 1:3 \quad [35 \text{ b}]$$

In the graph of Figure 2.30 the design rules are presented. Both of these formulas are based on scale experiments. The accuracy of these formulas is therefore questionable. In reality waves are irregular and therefore the Pilarczyk formula is preferred.

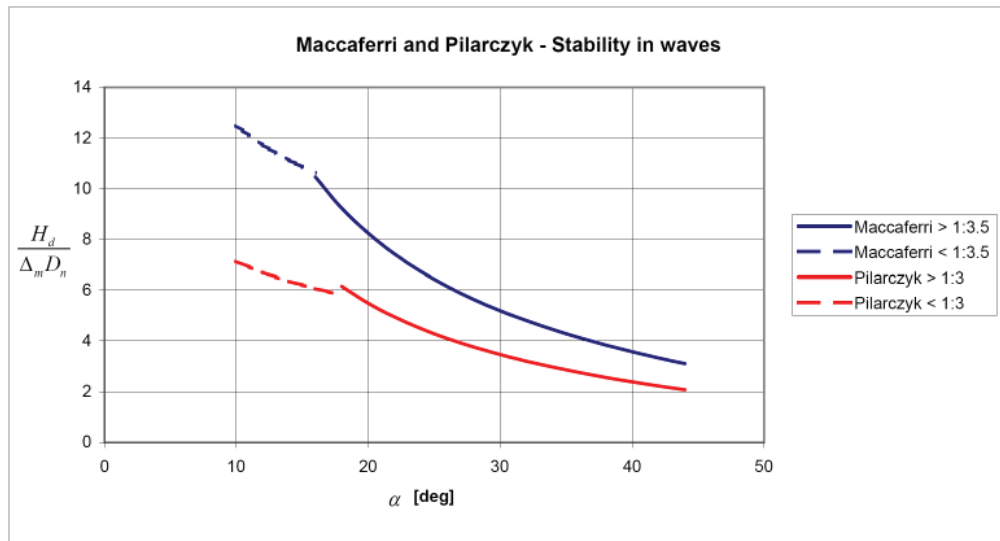


Figure 2.30: Maccaferri and Pilarczyk stability in waves

2.5.8 Pilarczyk's Improved Gabion Stability Formula in Waves

In section 2.5.1 it came forward that the wave forces are not only a result of the height, but also of the breaker parameter. Waves with higher Iribarren numbers will show more run-up, which increases the uplift pressure. A relation in which the Iribarren parameter is taken into account is therefore an improvement. This resulted in the following approximate design formula, from Pilarczyk for semi-permeable cover layers:

$$\frac{H_s}{\Delta_m D_n} = F \xi^{-2/3} \quad \text{with maximum} \quad \frac{H_s}{\Delta_m D_n} = 8.0 \quad [36]$$

With:

H_s = Significant wave height of incoming waves at the toe of the structure [m]
 F = Revetment stability factor $6 < F < 9$ [-]

This formula is also based on experiments, a so called black-box model. Disadvantage is that the stability factor (F) is known only very roughly. On the other hand the formula resembles with some experimental results. Pilarczyk used the performed scale test results and used these for the determination of the stability factor (F). In Figure 2.31 these results and the accompanying Pilarczyk formula are presented. The formula is represented by:

$$\frac{H_s}{\Delta_m D_n} = \frac{9 \cos \alpha}{\xi^{2/3}} \quad [37]$$

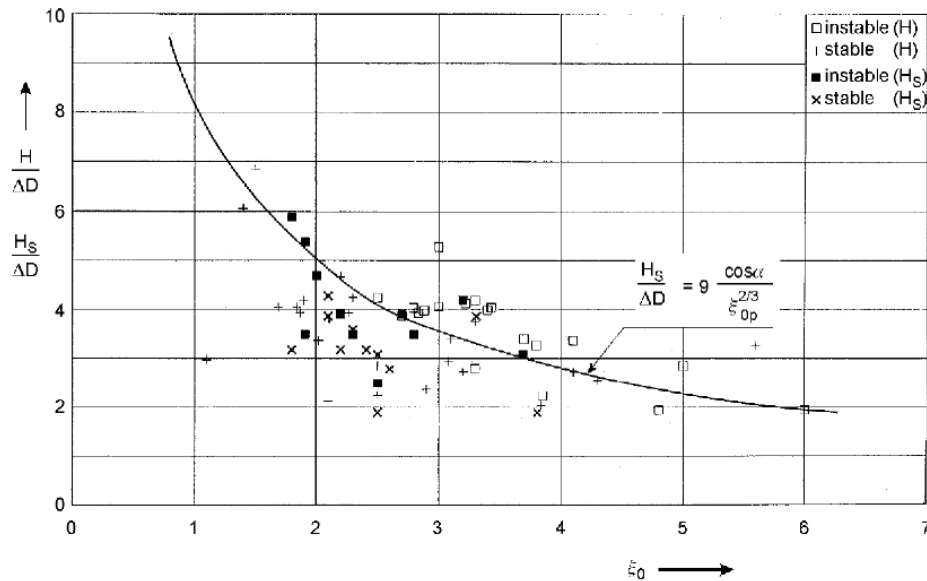


Figure 2.31: Test results with Pilarczyk design formula

To fit the test results, $F = 9 \cos(\alpha)$ is used. For revetments of 1:2 or milder the cosine term $\cos(\alpha) = 0.89 - 1.00$ so that $F \approx 8$. The proposed formula of Pilarczyk fits the scatter reasonably, although the experimental results do not show a consistent result. To be on the more safe side, $F = 8 \cos(\alpha)$ is recommended for the design.

The wide scatter is also caused by the inaccuracy of the test results, which were mostly on-scale experiments. Next to that the definition of failure is also quite flexible, especially for something like sliding and uplift. When is the movement of such a degree, that it is considered as failed. These boundaries can differ per experiment.

No unstable measuring results are found for Iribarren parameters smaller than two. This means that for breaker parameters smaller than two the stability relation is not supported by the measurement data. In these situations the lifting of the gabions determines the stability criterion. For higher Iribarren numbers the aspect of sliding of gabions increasingly starts to play a role.

Pilarczyk's improved formula, which includes the breaker parameter is preferable above the formula's that are based on only the wave height. The influence of the wave shape is logical, since increasing Iribarren numbers cause a increasing run-down and therefore higher internal pressure. The influence can best be shown with help of an example. The following values for several parameters are used in a example.

Initial values:

$$\begin{aligned} \Delta_m &= 0.95 \text{ [-]} \\ H &= 0.70 \text{ m} \\ \alpha &= 20^\circ \end{aligned}$$

If the mattress thickness is calculated for this situation than Maccaferri gives a thickness that is independent of the wave shape.

Maccaferri:

$$D_n = \frac{H_D}{3\Delta_m \cot \alpha} = \frac{0.7}{3 \cdot 0.95 \cdot \cot 20} = 0.09 \text{ m}$$

Pilarczyk gives an result that is dependent of the Iribarren parameter. The advised thickness of these gabions is calculated for two different Iribarren parameters 1.5 (plunging waves) and 4 (surging waves). It results in:

Situation 1, plunging waves:

$$D_n = \frac{H_D \xi^{2/3}}{\Delta_m \cdot 8 \cos \alpha} = \frac{0.7 \cdot 1.5^{2/3}}{0.95 \cdot 8 \cdot \cos 20} = 0.13m$$

Situation 2, surging waves:

$$D_n = \frac{H_D \xi^{2/3}}{\Delta_m \cdot 8 \cos \alpha} = \frac{0.7 \cdot 4^{2/3}}{0.95 \cdot 8 \cdot \cos 20} = 0.25m$$

What becomes clear in this example is that the shape of waves that enter the revetment makes quite a difference between gabion thickness. The wide scatter, that is present from the experiments, gives a certain degree of uncertainty. Therefore the curve fitted line of Pilarczyk's latest formula has taken some extra safety into account.

If the main hydraulic failure mechanisms are considered than failure is caused by uplift or sliding. Sliding is for a part indirectly also caused by uplift, because this initiates the process by decreasing the resistant force. The amount of uplift pressure is caused by the difference in waterlevel in the soil itself and the waterlevel outside due to wave action. This pressure is at its maximum if the wave is at its maximum run-down.

2.5.9 Motion of Fill Material

Wave attack can also start the movement of the fill material just as a water flow. For steel wire grids it is important to know if filling material will start to move, since it can lead to damage of the galvanized layer. The quality of the protection will also be influenced if too much fill material is moved inside the grid. During wave attack the motion of filling material occurs only if the Iribarren parameter is smaller than 3 (plunging waves).

Van der Meer 19 created a more detailed formula in which wave shape and damage are added parameters for the determination of particle stability in waves. Based on this formula a criteria is derived for fill material movement [PILARCZYK 1998].

$$\frac{H_D}{\Delta D_f} = \frac{F}{\sqrt{\xi}} \quad [38]$$

With:

F = Stability factor [-] 2 < F < 3

For surging waves ($\xi > 3$) the Iribarren parameter may be set constant at 3, the limiting factor for plunging waves. The stability factor F depends on the allowable movement of material. For initial movement a value of 2 is acceptable and for a maximum acceptable movement of stones a value of 3 is used. This is also an empirical relation, the accuracy it therefore questionable.

2.6 Comparison Between Gabions and Rip-Rap Protection

In the previous sections it became clear that gabions have several advantages over loose stone rip-rap protections. In this section the advantages, that are related to the stability of the structure itself, are summarized.

The Shields parameter indicates how much transport of material is accepted for loose stone rip-rap protections in a water flow. A higher parameter indicates less transport of material. The Shields parameter according to Pilarczyk and Maccaferri is respectively 0.070 and 0.10. This is roughly twice the value that is applied for rip-rap protections (0.047). This means that in the same hydraulic conditions, the average dimension of the rocks to be used is half the size that should be used for rip-rap.

The limitation condition for rip-rap protections is the "threshold of movement". Beyond this condition the lining slowly start to deform. When the fill material inside gabions start to move it will deform the gabion but it depends on the quality of the grid. A new equilibrium situation will develop if the wire mesh is strong enough. The deformation relation should still be fulfilled and the subsoil or filterlayer may not be exposed. Design formulas are based on no-, or little fill material movement, minimising the possibility.

With a smaller size of rock, used as a fill material, the velocity at the interface between gabion and subsoil is lower. The thickness of the protection will also be of influence the velocity at the interface. The application of smaller stones reduces the necessity for an extra gravel filter. A reduction of the size of the fill material will also reduce the hydraulic resistance of the channel. The contribution is that the capacity of the channel increases.

Advantage in saving material can also be gained if different structures are compared. Rip-rap revetments are made of a thicker layer of stones compared to a gabion mattress. Also at the toe construction material can be saved. Rip rap revetments often have a pile of stones to gain extra stability and to give the possibility to fill erosion pits along the lining, by the deformation that follows. The advantage of a gabion mattress is that some extra length can be placed at the bed. A smooth transition is made and some extra friction force can be absorbed caused by sliding gabions. Figure 2.32 gives a indication of the difference. Different variants can be made for toe-construction. In general, gabion mattresses solutions will use less material.



1: Loose stone rip-rap revetment

2: Reno mattress revetment

Figure 2.32: Advantages of gabions

The difference in stone size for revetments that are under influence of waves is comparable to that of gabions under current attack. The containing function results in a smaller size of fill material compared to rip-rap protections.

The influence of the gabion grid is not applied in any of these stability relations. A synthetic geogrid will not result in a more stable construction or a gabion or thinner mattress, though it should be noticed that some advantage can be gained when selecting the proper size of the fill material. All design rules are based on the concept of no-, or little fill material movement. For synthetic gabions it might be possible, to allow under certain circumstances, more movement of material. This could result in the application of smaller fill material.

2.7 Filter Layers

2.7.1 Function of a Filter Layer

Filter layers are present between the subsoil and the outer protective layer. The two main functions of filters are separation and filtration of these layers. The separation function prevents transport from base soil particles through the voids of the outer layer. Two types of filters can be distinguished. The geometrical closed filters and the geometrical open filters.

Closed filters are designed in such a way that the particles cannot move through the layers. Filters, constructed of this type are conservative, since they can stand any load as long as the upper layer is stable. Open filters consist of particles that are much larger than the base soil. During certain loads the base soil particles can protrude through the filter. Erosion will only take place if a certain threshold is exceeded. Below this level the filter construction will be stable. The design of such a filter is based on a critical gradient for which the filter is stable.

The presence of a filter can be in the form of a granular layer from which the gradation is of a smaller degree compared to the top layer. A filter can also be present in the form of a geotextile. A geotextile is a synthetic cloth which has a certain characteristic opening size O_x . This size should be small enough to prevent particles of the subsoil to erode and large enough to provide a certain permeability of the layer. The permeability is necessary to prevent the development of a too large uplift pressure.

2.7.2 Filter Layers for Current Exposed Gabions

If the current velocity between the interface of the gabion and subsoil is high enough than the wash out of particles can still occur. To prevent this a few measures can be taken. In the first place it is possible to use a thicker mattress, but this not the most cost effective solution. A better possibility is the application of a filter construction.

A solution is to apply a filter from smaller stones. These stones should be dumped on the subsoil before the gabion is placed. In this extra filter layer the turbulent flow velocity is further reduced and the wash out of material decreased. With this filter, water can flow through the layer and particles stay in place. What happens is that the flow is decelerated through the layer and changes from turbulent behaviour to laminar behaviour.

Simons approach for the design of filters

Simons determined the need of a filter construction based on the flow velocity between the interface of soil and gabion. *Simons 1984* [MAYNORD 1995] presented a formula to calculate this velocity, formula [39], which is an adapted form of Manning's formula. The roughness parameter is important for the velocity level at the interface. A rougher surface will result in more turbulence that dissipates energy and gives lower interface flow velocities. This formula is based on Simons experiments and is an empirical relation. The formula includes the effect of rock size, gradation and mattress thickness.

$$u_i = \frac{1.486}{n_f} \left(\frac{D_f}{2} \right)^{2/3} i^{1/2} \quad [39]$$

With:

u_i = velocity at the interface between the gabion and subsoil/mattress [m/s]
 n_f = roughness coefficient

For geotextiles the roughness coefficient is assumed $n_f = 0.02$ and if there is a gravel filter under the protection a roughness coefficient of $n_f = 0.025$ has to be applied. The hydraulic radius that is used in Manning's formula is replaced by the term of the average diameter of the fill material divided by 2. It is assumed that this represents the hydraulic radius. The velocity u_i must be compared with the velocity which the bottom can withstand without being eroded (u_c).

The critical velocity of the particles depends not only on the size of the particles but also on the cohesion of the soil. Simons splitted these two properties. For the non-cohesive soil formula [40] is suggested and for the cohesive soils a graph (Figure 2.33) expresses the critical velocity.

$$u_c = 16.1\sqrt{d} \quad [40]$$

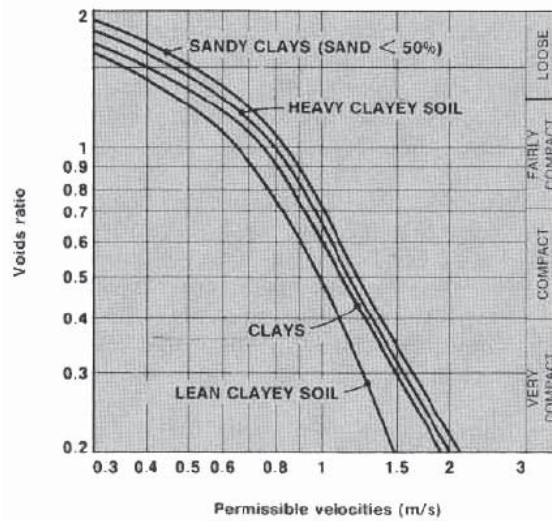


Figure 2.33: Critical velocity for the subsoil

If a geotextile is used it should be kept in mind that the velocity at the interface is reduced to 1/4 to 1/2 of the velocity u from formula [39]. If the interface velocity is still too high, a gravel filter layer should be applied. The thickness of these filters should be at least 15 to 20 cm for execution reasons and at least greater than formula [41]:

$$S = \frac{d_v}{f} \left[1 - \left(\frac{u_c}{u_i} \right)^2 \right] \quad [41]$$

Parameter f , the Darcy-Weisbach coefficient for flow friction through the particles, is assumed to be 0.05. The d_v value is a equivalent void diameter for the filter layer or subsoil layer below. This equivalent value is 1/5 of the d_{50} from the layer above. For optimization a combination of geotextile and a filterlayer can be used or a thicker filter layer can be applied.

The filters that are applied in these constructions are so called geometrically closed filters. In these filters it is impossible for grains to move through the pores of the upper layers. To establish this the gradation of the filter is based on several filter rules. This is to prevent migration of the filters through the gabion, migration of subsoil through the filter, and for internal stability and demixing. These filter rules were initially developed by *Terzaghi 1922* [SCHRIECK 2004].

$$\frac{d_{50}^{filter}}{d_{50}^{soil}} \leq 40 \quad 5 \leq \frac{d_{15}^{filter}}{d_{15}^{soil}} \leq 40 \quad \frac{d_{15}^{filter}}{d_{85}^{soil}} \leq 5 \quad [42]$$

Pilarczyk 1998 also presented some filter rules that are also based on Terzaghi's rules for a geometrical closed filter [43]. Pilarczyk did not develop a formula that gives the velocity at the interface gabion and filter/subsoil. The influence of the subsoil diameter is not taken into account. The general advise is, that for a flow velocity higher than 3 m/s or waves higher than 1 m, a geotextile should be applied in combination with a granular sublayer [PILARCZYK 2000]. The thickness of this filter should be about 20 cm and have a d_{50} that is one fifth of the top layer.

$$\frac{d_{15}^{gabion}}{d_{90}^{filter}} > 4 \quad \begin{matrix} d_{15}^{filter} > 10d_{50}^{subsoil} \\ d_{15}^{filter} > 5d_{50}^{subsoil} \end{matrix} \quad \text{if} \quad \begin{matrix} d_{50}^{subsoil} < 0.3mm \\ d_{50}^{subsoil} > 0.3mm \end{matrix} \quad \frac{d_{50}^{filter}}{d_{90}^{filter}} < 4 \quad [43]$$

2.7.3 Filter Layers for Gabions Exposed to Waves

In the previous chapters it came forward that all hydraulic failures can be related to sliding due to uplift and down-rush forces. In more permeable layers, the water pressure that originates is able to flow out in a better way. The permeability of the subsoil and filter layers is therefore of influence on the stability of the construction against sliding. In impermeable soils the water pressure can flow out less easy with the effect that the structure can start moving.

Another effect of water pressure fluctuations in less permeable soils, is that it can lead to geotechnical failure. Local slip-circle failure can occur. The water overpressure between the pores results in less compaction of the soil. The loss of compaction gives less internal friction and a higher possibility of slip-circle failure. The permeability of the subsoil is therefore very important for good functioning of the construction. An example in the difference of stability between permeable and impermeable soil is given in Figure 2.34. This model scale experiment is executed by Maccaferri with a gabion mattress of 0.15 m. The ability to sustain a certain amount of load differs considerably.

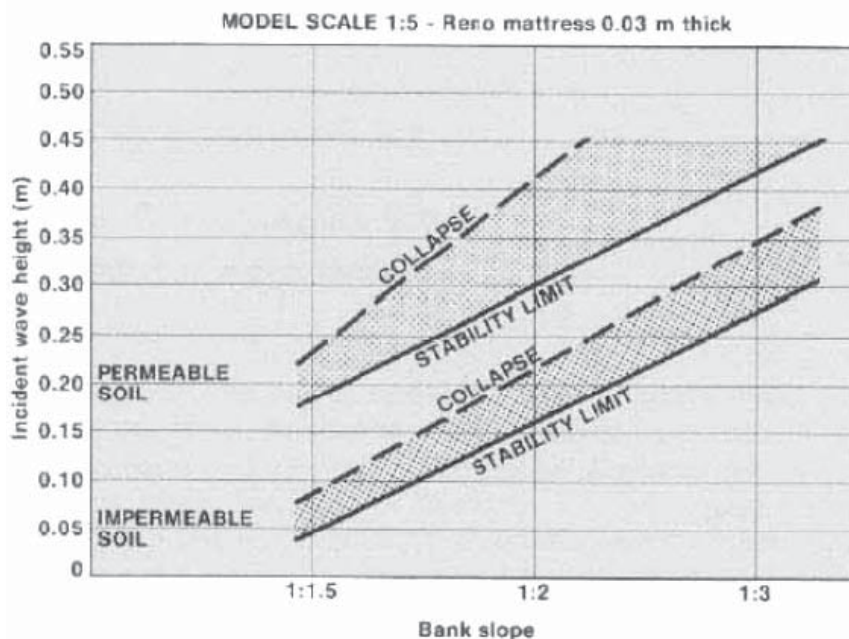


Figure 2.34: Influence of the soil permeability on the stability

To prevent this problem a filter construction can be applied. With this more permeable layer the uplift pressure will decrease and a better transition can be provided. Most of the scale experiments are based on sandy permeable soil. This should be kept in mind when a construction is designed on impermeable soil.

Between the gabion mattress and subsoil, a filter layer is present in the form of a geotextile or granular layer or a combination of both. In reality a gabion revetment consist out of a mattress with a geotextile for situations with waves lower than 1 m. For higher waves a granular filter layer, combined with a geotextile is advised [PILARCZYK 2000].

The two main functions of geotextiles, separation and filtration, are also a property of granular filters. It is however not the case that a geotextile can replace a granular filter. Granular filters also contribute with their thickness, weight and higher friction to the stability of the construction. The extra granular filter contributes to the damping of the pressure fluctuations on the covered layer.

The advantage of a granular filter compared to a geotextile, is that it has a better ability to transfer shear stresses, due to the increased friction factor. The disadvantage of granular filters is, that they are usually more expensive than geotextiles and especially difficult to construct under water within the required limits. A minimum thickness of 20 cm is necessary, which increases the costs.

The filter construction of a revetment is just as important as the gabion mattress cover layer. Proper tuning of the permeability is an essential condition for a good design. According to Maccaferri and Pilarczyk it is possible to place a gabion mattress on a geotextile, but there are certain limitations. Maccaferri makes this distinction by presenting a rather coarse formula that gives the flow velocity at the interface of filter and cover layer. When this is exceeded an extra granular filter layer is needed. Pilarczyk also presented a coarse boundary that gives a maximum wave height of 1 meter before a granular filter layer should be applied over the geotextile.

The contradiction in the functioning of filters is that a certain permeability is demanded to prevent uplift, so therefore a permeable granular layer or open geotextile would be appropriate. This in contrast to the fact that the interference with the subsoil particles should be prevented so a more closed filter or geotextile would be suitable, but at the expense of the permeability. Higher waves on the construction will result in more severe uplift forces created by out flowing water. Liquefaction of the subsoil might result in slip circle failure.

The permeability of the filter layer should therefore correspond to the amount of internal allowable pressure. This is the reason that for high waves gabion mattresses on geotextiles will not be able to fulfil their function since a certain degree of permeability and opening size is demanded which are properties contradict each other. In these cases an extra granular filter layer is needed.

2.7.4 Klein Breteler Filter Design Method.

The design of a filter is based on the permeability of the several layers in the revetment with the subsoil as a base. Forces are exerted on the soil particles. A geotextile can reduce these forces to a certain extent. A parameter defining these forces is the so called hydraulic gradient (i). The hydraulic gradient is a ratio that indicates the loss of head (pressure) over a certain distance. The critical gradient is best illustrated by Figure 2.35.

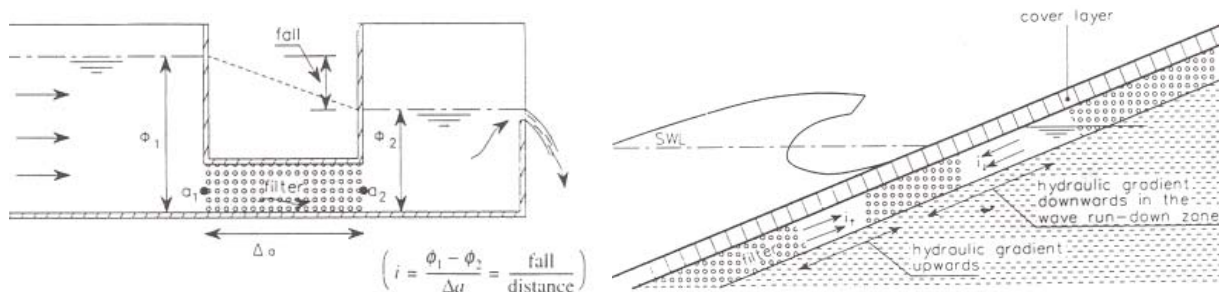


Figure 2.35: Hydraulic gradient

The magnitude of the hydraulic gradient is dependent on the permeability of the soil, the type of hydraulic loading (steady or dynamic) and the type of structure. The strength of the interface is characterized by the gradient when particles begin to move. This is called the critical gradient (i_{cr}). For revetment protections this value is governed by the maximum gradient of external loading along the protection. The stability criterion of a filter implies that the magnitude of the acting gradient (i) must be lower than the critical gradient. In a definition this reads:

$$i \leq i_{cr} \quad [44]$$

Hydronamical sand tight geotextiles prevent the erosion of the subsoil to a certain hydraulic load, described by the gradient i , on top of the geotextile. The main flow is assumed to be parallel to the geotextile. Flow deviates through the pores, a certain component of the velocity will flow through the geotextile. This will result in canals under the geotextile originated by movement of the smaller particles of the gradation. The design of a geotextile filter construction is based on the critical velocity that can flow along the filter before particles begin to move at the present velocity through the subsoil. The present hydraulic gradient is then used to calculate the velocity in the subsoil. This requires that the present filter velocity is smaller than the critical velocity for which initiation of sand transport takes place.

$$v_f \leq v_{f,cr} \quad [45]$$

Determination of the hydraulic gradient

The hydraulic parallel gradient (i_p) is influenced by the so-called leakage length (Λ). The amount of uplift is related to the ratio of the permeability of the cover layer and sub layers. This ratio is expressed by the leakage length. This length is a measure for the exchange between the external and internal loads. It is defined as:

$$\text{One layer:} \quad \Lambda = \left(\frac{d_f k_f d_t}{k_t} \right)^{0.5} \quad [46]$$

$$\text{Two layer:} \quad \Lambda = \left(\frac{(d_{f1} k_{f1} + d_{f2} k_{f2}) d_t}{k_t} \right)^{0.5} \quad [47]$$

With:

Λ	= Leakage length	[m]
d_f	= Thickness filter layer	[m]
d_t	= Thickness cover layer	[m]
k_f	= Permeability filter	[m/s]
k_t	= Permeability cover layer	[m/s]

The indices 1 and 2 represent the filter layer 1 and 2.

With the leakage length and the wave height, three situations can be distinguished:

- $\Lambda/H \ll 1$: The cover layer is relatively permeable. The exchange is relatively easy and there is hardly any head difference
- $\Lambda/H \gg 1$: The cover layer is relatively impermeable and the pressure fluctuation cannot be followed which results in large head difference.
- $\Lambda/H \approx 0.5$: In reality the leakage length will be between 0.5 and 0.3 m. This is the transition area

The problem with a revetment protection, that is placed directly on a geotextile is the leakage length which is influenced by the small thickness of the geotextile. The value for the leakage length does not give a proper result. For a representative value of the leakage length, the permeability of the subsoil should be filled in. For the thickness of the filter layer the depth to which the surface effects the subsoil should be filled in. A value of 0.5 m for sand and 0.10 m for clay may be used. [PILARCZYK 1998]

For situations in the transition area the following relation can be used to determine the hydraulic gradient in a construction [PILARCZYK 2000]:

Downward gradient:

$$i_{down} = \sin \alpha \quad [48]$$

Upward gradient:

$$i_{up} = \frac{\cos \alpha}{\tan \beta} \left\{ 1 - \exp \left(-\frac{\tan \beta}{2\Lambda \cos \alpha} \phi_b \right) \right\} - 0.5 \sin \alpha \cdot \exp \left(-\frac{\tan \beta}{2\Lambda \cos \alpha} \phi_b \right) \quad [49]$$

With:

$$\begin{aligned} \beta &= \text{The angle of the schematised wave front} & [^\circ] \\ \phi_b &= \text{The piezometric head on a slope due to the oncoming wave} & [m] \end{aligned}$$

In the formula the wave front is described and its pressure distribution is used to calculate the hydraulic gradient inside the revetment (Figure 2.36). In practise the upward directed gradient will always be normative. The parameters β and ϕ_b are defined by the following relationship CUR/RWS 1995 a,b [PILARCZYK 2000]:

$$\tan \beta = \frac{0.17}{\sqrt{\frac{H}{L_o}}} \quad [50]$$

$$\frac{\phi_b}{H} = 0.36 \xi_o \sqrt{\cot \alpha} \quad \text{with} \quad \frac{\phi_b}{H} \leq 2.2 \quad [51]$$

In which: $L_o = 1.56 T^2$.

The above described formulas [48] and [49] are valid between the following ranges:

$$\begin{aligned} 2 &\leq \cot \alpha \leq 4 \\ 0.01 &\leq H/L_o \leq 0.07 \\ 0.05 &\leq h/L_o \leq 0.2 \\ 2.5 &\leq h/L_o \leq 0.2 \end{aligned}$$

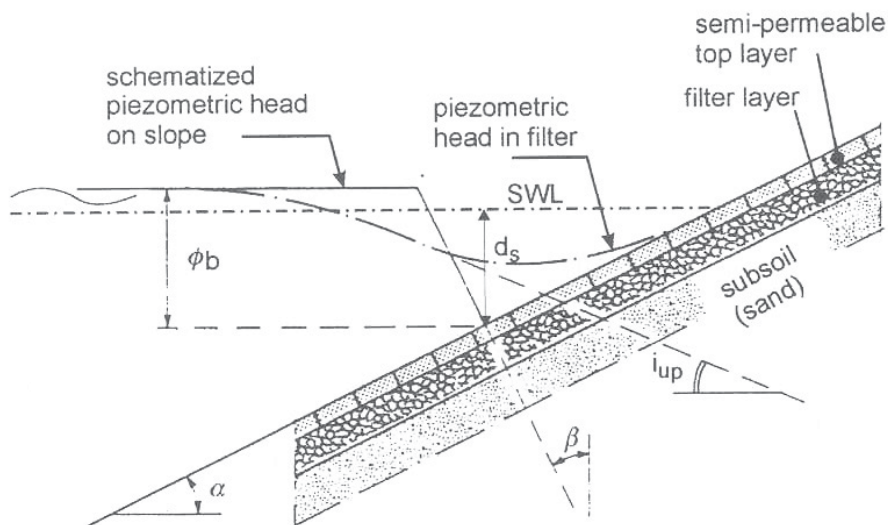


Figure 2.36: Internal pressure due to wave front

Filter velocity

The basic equation for determining the filter velocity (v_f) is the application of Darcy's equation:

$$v_f = k i^m \quad [52]$$

Darcy's equation is valid for laminar flow conditions. For laminar flow condition $m=1$. If a coarser granular subsoil is present with a turbulent flow condition the relation does not hold. In turbulent conditions the formula can also be applied, but the hydraulic gradient should be adapted by taking the root of the gradient, $m=0.5$. At a transition a approximation of $m=0.7$ is applied. In appendix A, information is presented about the relation between fill material size and flow condition.

Geotextile permeability requirement

The basic requirement is that the permeability of the geotextile is larger than the permeability of the subsoil k_b (m/s). The permeability of a geotextile indicated by a permeability coefficient k_g (m/s). The permeability of the geotextile should be a factor c larger than the subsoil.

$$k_g \geq c k_b \quad [53]$$

The value of the factor c depends on the type of subsoil and its permeability. *Giroud 1996* [PILARCZYK 2000] proposed that the variation of pore water pressure in the base soil must be small. Giroud developed a criteria based on the expected hydraulic gradient (i_s) in the base soil in the vicinity of a filter.

$$k_g \geq 10 k_b \cdot i_s \quad [54]$$

With:

Inland channel protection	$i_s = 1$
Shoreline protection	$i_s = 10$

Gabions used for inland protections have a factor c of 10. For more cohesive soils the c value can be taken between 50 and 100. The permeability of a geotextile can also be expressed by the more general definition: the permittivity ψ (1/s). It is defined as the permeability per unit thickness of geotextile T_g [m].

Soil thightness of a geotextile

To describe the soil thightness of a geotextile the opening size is of importance. This is expressed by the O_x parameter. A geotextile with a opening size of O_{90} corresponds with the average sand diameter of the fraction of which 90 % of the weight remains on the geotextile after sieving. What happens during the functioning of a geotextile is that a natural filter develops at the interface geotextile and subsoil. The smallest particles will wash out and a natural filter of the largest particles originates.

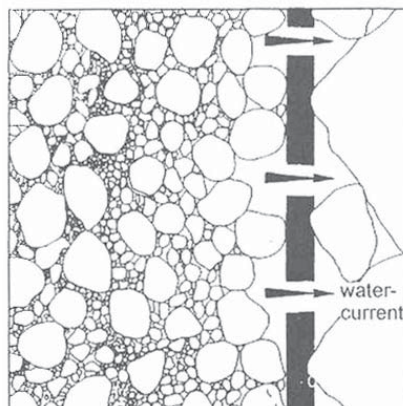


Figure 2.37: Functioning of a geotextile

The quantification of the soil thightness of a geotextile is expressed by the ratio between the opening size and the grain size of the subsoil particles (for example: O_{90}/D_{b90}). Both are based on a certain percentage that will pass the sieve. During time several design criteria have been developed for this criteria ratio. One of the first relations is developed by *Ogink 1975* [PILARCZYK 2000]. Based on a sandy subsoil the following relation was developed.

Ogink 1975: [55]

$$\begin{array}{ll} \text{Static flow} & O_{90}/D_{b90} \leq 1.8 \\ \text{Dynamic flow} & O_{98}/D_{b15} \leq 1.0 \end{array}$$

This relation is still used today, Although research that has been performed has yielded less strict criteria. Performance tests, executed by Delft Hydraulics, with geotextiles covered with gravel or rock have proven that geotextiles with increased openings can prevent erosion. The performance tests have proven that it is possible to apply a geotextile that does not meet the geometric sand thightness criteria. Klein Breteler therefore designed the criteria the following situation for dynamic flow conditions.

Klein Breteler 1990: [56]

$$O_{90}/D_{b90} \leq 2.5$$

From experience it came forward that for non-stationary cyclic conditions, like waves, the following criteria is used.

$$O_{98}/D_{b15} \leq 1.5$$

The performance tests of geotextiles based on a sandy subsoil have resulted in a design diagram developed by *Klein Breteler 1990* [PILARCZYK 2000]. With this diagram the critical gradient of a geotextile can be determined (Figure 2.38).

The Klein Breteler relation holds for non-cohesive soils with a base material condition of: $0.1 \text{ mm} < D_{b90} < 0.2 \text{ mm}$. Next to that, the uniformity coefficient should be smaller than 2. The uniformity coefficient (Cu) is a measure for the shape of the sieve curve of a gradation. If this is for example convex, concave or linear. The uniformity is expressed by:

$$Cu = \frac{D_{b60}}{D_{b10}} \quad [57]$$

Based on the permittivity of a geotextile the critical gradient for the involved situation can be determined. In Figure 2.38 an example situation is included. A geotextile with a permittivity of $0.7/s$ and a O_{90}/D_{90} - ratio of 2.0 a thickness of 1.2 mm under a filterlayer with a D_{15} of 30 mm and a porosity of 0.4 results in a critical gradient of 0.52. By comparing this value with the present gradient, the condition of formula [44] is checked. If the relation is not fulfilled than an extra granular filterlayer should be applied.

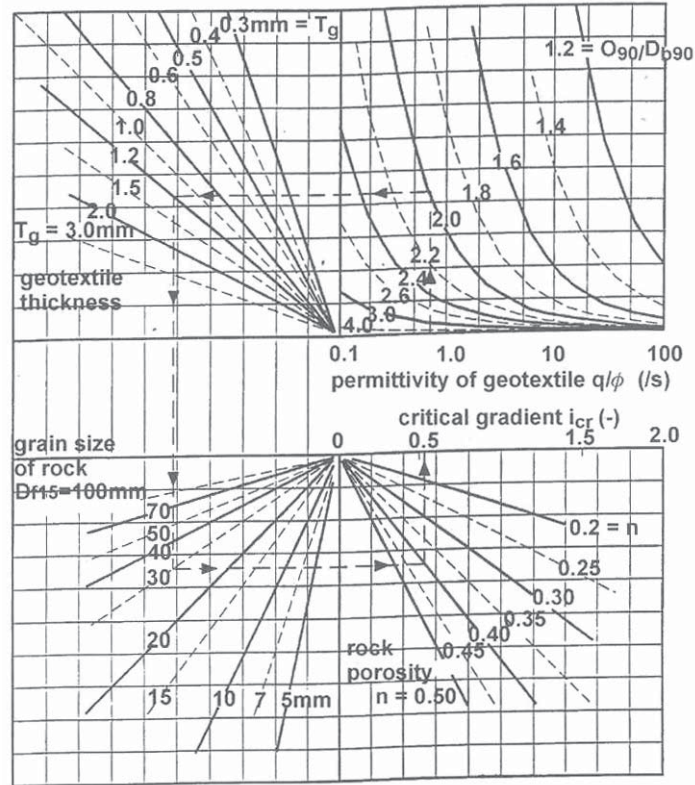


Figure 2.38: Klein Breteler design diagram for non-cohesive soil ,
 $0.1 \text{ mm} < D_{b90} < 0.2 \text{ mm}$, $Cu < 2$

The method as described by Klein Breteler is recommended for the design of revetment constructions based on a geotextile and a sandy subsoil. The velocity parallel to the filter interface, described by Klein Breteler, is given by formula [58].

$$v_{f,cr} = \left(10 \left(\frac{D_{b90}}{O_{90}} \right)^4 \cdot \frac{T_g}{D_{b90}} \cdot \left[\frac{w}{k_g} \right]^{1/2m} + \frac{n}{e} \right) \sqrt{\psi_s \Delta_s g D_{b50}} \quad [58]$$

With:

- ψ_s = Shields parameter of the sandy subsoil [-] See table 2.1
- m = Exponent in the equation related to the permeability [-]
- n = Porosity of the layer above [-]
- Δ_s = Relative density of the subsoil $(\rho_s - \rho_w / \rho_w) = 1.65$
- e = Coefficient related to the character of the flow. Formula [59]
- c_r = See table 2.1
- Re = Reynolds number [-] Formula [60]
- w = Fall velocity of the sand particles [m/s] Formula [61]
- ν = Kinematic viscosity of water [m²/s] = $1.3 \cdot 10^{-6} \text{ m}^2/\text{s}$ at 10 °C

$$e = c_r \text{ Re}^{-m^*} \quad [59]$$

$$\text{Re} = \frac{v_f D_{f15}}{\nu} \quad [60]$$

$$w = \frac{\Delta_s g D_{b15}^2}{18\nu} \quad [61]$$

The different numerical values for the parameters, c_r , m and the Shields parameter ψ_s , based on the D_{b50} of the subsoil are presented in table 2.1.

Db50 [mm]	c_r [-]	m^* [-]	ψ_s [-]
0.10	1.18	0.25	0.110
0.15	0.78	0.20	0.073
0.20	0.71	0.18	0.055
0.30	0.56	0.15	0.044
0.40	0.45	0.11	0.038
0.50	0.35	0.07	0.036
0.60	0.29	0.04	0.035
0.70	0.22	0.00	0.034
0.80	0.22	0.00	0.034
1.00	0.22	0.00	0.035

Table 2.2: Values of the coefficients c_r , m , ψ_s

With formula [58] the critical velocity can be calculated by checking the result with the present velocity. If relation [45] does not hold, a granular filter layer should be added. The above described determination of the critical value in a geotextile is based on non-granular uniform sand. The permeability of the subsoil plays an important role in the allowable critical gradient of a filter. A similar test program has been performed in which the behaviour of cohesive material was studied. The most important result from this test was, that the erosion could be prevented to a large hydraulic gradient compared to the unprotected situation. The test have resulted in the following criteria [PILARCZYK 2000]:

- 1) Good clay (40% lutum, 45% silt, 15% sand) $O_{90}/D_{b90} > 1$

$$i_{cr} = \frac{0.034}{n^2 D_{f15}} \quad [62]$$

- 2) Poor to medium clay (20% lutum, 45-60 % silt, 20-35% sand) $O_{90}/D_{b50} > 10$

$$i_{cr} = \frac{0.012}{n^2 D_{f15}} \quad [63]$$

- 3) $O_{90} > 1$, The method of Klein Breteler for sand as a base soil should be applied.

Based on the Klein Breteler design method it is better to judge if single geotextile filter satisfies the demands. Based on the permeability of the subsoil and the wave height an improved corresponding filter construction can be designed. When a geotextile is chosen it should be always be checked for blocking and clogging of the cloth.

2.7.5 Requirements due to Blocking and Clogging of a Geotextile

The permeability of geotextile can decrease if during time fine soil particles block the openings in the geotextile or if the particles migrate into the pores of the geotextile and get trapped. To prevent both of these mechanisms, requirements are formulated. These requirements should be checked before the design is constructed.

Blocking

The blocking of a geotextile happens if coarse particles migrate upstream and settle at the entrance of the geotextile apertures. This phenomenon is expected when a geotextile is used to retain particles of very low concentrated suspensions or when a lack of contact between soil and geotextile is present. Blocking though is rarely observed. The risk is present when:

- The aperture in the geotextile is very uniform
- The grain size of the subsoil is very uniform
- $0.5 < O_{90}/D_{b50} < 1$

Clogging

When fine particles are trapped in the openings, it will lead to a decrease of the permeability. This process can also be caused by organic matters, chemical deposit and bacterial growth. This process is time-dependent and takes place very slowly. No danger of clogging is present when the hydraulic gradient over geotextile and subsoil is smaller than 3 or when the subsoil is well graded.

2.8 Review on the Pilarczyk's Design Formula's for Gabions in Waves

In the previous sections the mechanisms that are present in a gabion revetment construction have been described. The driving force in the form of wave action causes an uplift pressure, which reduces the resistance to sliding. In combination with the down rush force a distortion of the equilibrium is possible with sliding as a result.

Pilarczyk developed a stability formula based on the breaker parameter. Section 2.5.1 showed that for higher Iribarren parameter values, the run-down increases. Therefore the forces on the revetment also increase. Due to this effect the mattress thickness increases for higher breaker parameters as can be seen in Pilarczyk's graph (Figure 2.31). The wave run-down effect is indirectly present in the formula of Pilarczyk. For this reason the Pilarczyk formula is more superior to the Maccaferri stability formula, in which only the wave height is taken into account.

The resistant force to sliding is based on the friction between the gabion and filter layer. The steepness of the slope influences the ability to absorb loads. This parameter comes forward in Pilarczyk's formula. The friction factor though is also of influence on the resistance against sliding. In the graph of Figure 2.27 the difference between a granular layer and geotextile is presented. In exact same conditions the granular filter layer will resist higher waves compared to a construction placed on the smoother geotextile. This aspect of friction is not taken into account in Pilarczyk's formula.

A second aspect that is not taken into account, is the ability to spread forces over the total length of the revetment, since they are mutually connected. When two slopes are compared with the same filter construction, but a different mattress length, than the longer version will be able to resist a higher wave load.

A third remark is the permeability of the construction. The amount of uplift pressure is not only dependent on the amount of run-down, but also on the permeability of the layers. The difference in water level will create a flow through the different layers. Constructions that are less permeable will experience higher uplift forces and therefore fail earlier. Adaptation of Pilarczyk's formula could be done by including the permeability of the construction.

Considering these effects with respect to Pilarczyk's design formula and graph, the expectation is that the shape of the line is correct. The position of the line in the graph can vary from situation to situation. Figure 2.39 represents the hypothesis based on a situation with increased mattress length and improved filter construction.

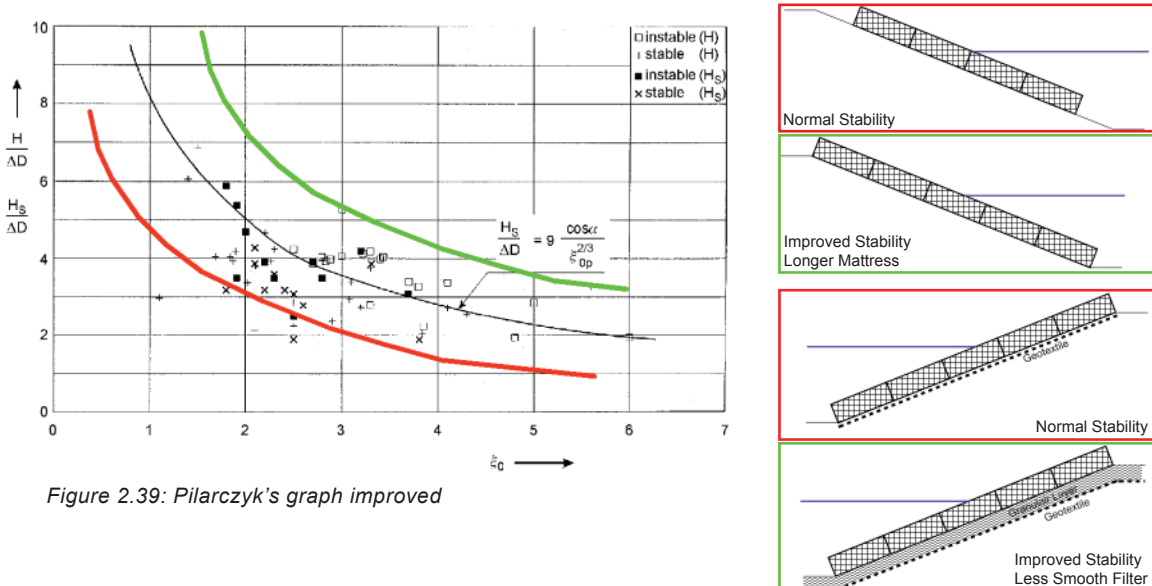


Figure 2.39: Pilarczyk's graph improved

For the description of gabion stability several parameters are of importance. Pilarczyk developed a formula, which resembles the failure of a revetment. Improvement of this relation is possible. Extra parameters that are of influence and should be included in the design rule for gabions are:

- The design in which mattress length and revetments shape are taken into account.
- The friction factor (f) between the mattress and filter layer.
- The permeability of the construction.

In the objectives states that improvement of the current design formula is one of the targets of this report. Based on the scale model tests an attempt is made to improve the current design rule in which the three extra parameters are included.

Chapter 3. Synthetic Materials for Gabions

3.1 Introduction

Chapter 1 gave a description about the advantages of synthetic materials above steel wire grids. Synthetic materials are available in all sorts of forms and with all sorts of properties. In this chapter the properties are described, that the material should have, in order to form a proper alternative for a synthetic gabion grid. The material fulfilling these requirements will be used for further development of synthetic gabions.

There are many suppliers of synthetic materials that have comparable properties. For this project a material will be chosen as an example. The choice will be made out of the assortment of company Texion Geosynthetics, since they participate in this project. Alternative materials from other suppliers could also be suitable for the construction of gabions, but are not mentioned in this report.

A first selection can be made from the synthetic materials in general, because many materials are not useful to investigate. In the field of civil engineering the application of synthetic materials has already been applied for more than 40 years. These so-called geosynthetic materials have emerged in a wide array of applications: transportation-, geotechnical-, environmental-, hydraulics engineering and various other applications. Gabion constructions fit in this profile and the application of a geosynthetic material is therefore appropriate. In the category of geosynthetics there is also a wide offer of different products with different qualities and for different purposes. The proper material is found in the category of geosynthetics.

The qualitative positive properties of steel wire gabions should also be found in a synthetic alternative. Replacing the grid by a synthetic alternative, brings some extra points of attention which are not found when a steel wire grid is applied. Section 3.2 describes the properties and attention points of a steel wire grid and respectively the synthetic grid. This is followed by section 3.3 that describes the present available geosynthetics. From this selection a choice is made for a geosynthetic material that is applicable for the gabion grid. Section 3.4 presents the characteristics of this material related to the requirements from section 3.2. From the suitable material finally a gabion needs to be constructed. Several connections are needed to create a volume, but also to construct a mutual connection between the gabions. Information about the construction of a volume is presented in section 3.5.

3.2 Material Properties

3.2.1 Material Requirements With Respect to Gabion Functioning

Steel wire gabions have certain qualities. These qualities should also be present in a synthetic gabion to provide a good alternative. The qualities of the synthetic material must be comparable or better than the ones of a steel wire grid. In the section below the key elements are summarized that should be present in the synthetic material.

- Open Structure

Gabions are very well able to absorb wave-energy. This is mainly dedicated to the open structure of the container that gives easy access to the porous fill material. The synthetic material should therefore have an open mesh structure. This gives the ability to create the same level of turbulence for the dissipation of energy and to decrease possible pressure build-up.

- Flexibility

The ability to follow soil deformations and scour holes to a certain degree is one of the main positive arguments for the application of gabions. The relative thin steel mesh structure of gabions results in a certain flexibility. Synthetic materials are in general more flexible than steel, so this quality can easily be met.

- Strength

The container material should have a strength that is well able to hold the fill material inside the gabion. The strength is needed for several reasons. In the first place it is possible that wave-, or current attack will result in forces acting on the grid. Secondly, the rearrangement of stones can lead to stress on the grid as a result of deformation.

Besides these forces in the utility phase, there can also be high loads present during the construction phase. This mainly depends on the way of execution. The assembly of gabions on location, placement and filling afterwards will not result in extreme high stresses inside the grid. In some situations it can be difficult to place mattresses and fill them afterwards, therefore the construction is assembled and filled on location and placed with help of mechanical equipment, like lifting cranes. When the gabion is lifted it should be capable to hold the weight of the fill material. The amount of stress in the grid depends on the way of lifting.

The strength of a steel wire grid depends mainly on the wire diameter. The wire diameter is mostly between 2.2 and 3 mm, together with a mesh type that lies between 60 x 80 mm and 80 x 120 mm. This results in a ultimate tensile strength of approximately 35 - 50 kN/m [CIRIA, CUR, CETMEF 2007], Depending on the dimensions of the grid.

- Stiffness

A container made from synthetic materials needs a certain flexibility to follow soil deformation, but an amount of stiffness is also required. The material needs rigidity to keep the shape in which it is built. Attack by waves or high current velocities could result in deformation of the element. The material needs a certain stiffness to prevent deformation. This aspect of the construction can be influenced by the design.

3.2.2 Material Requirements With Respect to Synthetic Properties

Besides the qualities that should be comparable to a steel grid, the use of synthetic materials brings some other points of attention that are not found in steel wire. These points are important to keep in mind for the development of a good quality construction. It mainly depends on material properties and chemical qualities.

- Leaching

As it was already mentioned in chapter 1, zinc protection will slowly dissolve and harm the environment. Especially for environmental friendly banks this can be a reason not to apply gabions. Synthetic materials do not have this problem, but can show a quality that also dissolves material in the water. This is called leaching. It is a process where particles are extracted from a solid by a liquid that solves these particles and wash them out. This principle can also harm the environment, though there are enough synthetic materials available that do not have this quality. The applied material should not harm the environment on this manner.

- Ultraviolet Resistance

Sunlight is an important cause of degradation of many materials, including polymers from which geosynthetics are made. Ultraviolet light, that is radiated by the sun, causes degradation of the material. The degradation is caused by the photons of light that break the polymers chemical bonds. Long-term exposure will result in decreasing material strength. By using additives the degradation can be limited considerably.

- Creep

Materials that are subjected to a certain stress for a longer time will slowly deform to release stresses. These stresses are below the yield of ultimate strength, but can result in material deformation. The material will deform and could become so large that a component can no longer perform its function. With respect to gabions, creep might result in elongation and deformation of the container, having the consequences that the fill material might simply move through the compartment. The rate of this damage is a function of material properties, exposure time, exposure temperature, and the load. From a first point of view this property is not concerning for gabions applied in bank protections, because the forces are considered to be relatively small. This in contrast to soil retaining walls where the load is of a higher order.

Next to elongation of the material, creep rupture can also occur. If a material is loaded for a considerable long time, rupture can occur at a stress that is considerable lower than the initial strength. The creep performance is an important element in the determination of the allowable amount of load on a grid.

- Frost

During winters it might occur that the material freezes. It is an important point of attention to investigate the behaviour of the material in low temperatures. Several winters can affect the material and frozen materials can behave differently. As a result of severe frost the material can become more rigid and show a sudden fracture. These days respectable manufacturers control their production processes in such a way that this mechanism does not form a threat.

- Vandalism

The possibility of vandalism is something to keep in mind. For steel wire gabions this is also one of the disadvantages. Fisherman can for example cut the wire open for the placement of their fishing tools, but also bonfires can cause damage of the construction. Synthetic gabions made are even more vulnerable to vandalism. Synthetic materials are generally softer and will melt as a result of high temperatures, like fire. This aspect cannot be solved by the choice of a certain material. The solution to prevent this is found in the accessibility of the bank and local rules.

- Biological Effects

The geosynthetic gabion material will be used in an environment where micro-organisms can degrade polymers. Organisms like bacteria and fungi can attach to the fibers to use the polymer as a feedstock. The possibilities that this can happen is relatively unlikely, because only few molecular chain endings are available to initiate the bio-degradation process.

- Chemical Effects

Synthetic materials can degrade fast if they interact with some sort of chemical content. For gabions this situation can occur. Chemical content that has ended up in the water could cause this. There are several synthetic materials available that have a good resistance to a wide range of chemicals. It should therefore be possible to build a mattress that is very well able to resist against most occurring chemical conditions. This also includes the sour degree in the environment.

- Durability

Finally the material has to be able to sustain the conditions to which it is exposed. Steel wire gabions are usually given a life-time-expectancy of 5 to 20 years [CUR/RWS 2000]. For the better PVC and Galfan protection systems there can be a durability of 40 years, according to the manufacturer Maccaferri. The expectations are of a rather coarse degree, since they will differ considerably depending on the type of hydraulic structure. Synthetic gabions must have a comparable or better life-expectancy to form a serious alternative. Several experiments of synthetic material are available that show the degradation during time. Elements as creep and UV-degradation play an important role in this process.

3.3 Geosynthetics

The majority of the geosynthetics are made from polymers (95%). Polymeric materials consist out of parts, the so-called monomers, that are repeated and connected in a molecular chain (poly). The number and sort of monomers together with the mutual bands in the chain influences the behaviour of the material. Longer molecular chains are heavier and show better qualities with respect to: tensile strength, elongation, impact strength, etc.

The links between the molecules themselves also form a important concept, because they separate polymeric materials in two major types. The so-called thermoplastic and thermoset polymers. A thermoplastic polymer can be repeatedly heated to its softening point, shaped and worked as desired and then cooled to preserve that remolded shape. Examples of thermoplastics are: polyethylene, polypropylene, polyvinyl chloride and polyester. In a thermoset polymer, the heating process cannot be repeated. Any additional heat after first forming will lead only to charring and degradation of the material. Examples of thermoset polymers are butyl, ethylene and propylene. Geosynthetic products almost entirely exist out of thermoplastic polymers. In general there are 8 sorts of geosynthetics, which all have different qualities.

1) Geotextiles

One of the largest groups, within the geosynthetics, are geotextiles. It is best described as a synthetic cloth that can be used for: separation, reinforcement, filtration and/or drainage. The textiles have a structure that prevents particles from moving but gives water the probability to flow through.

2) Geogrids

In contrast to the more closed geotextiles geogrids are plastics formed into a very open gridlike configuration with large apertures between the individual ribs. Geogrids have many applications, but the most applied function is reinforcement material.

3) Geonets

The primary function of a geonet is to convey liquid within the plane of its structure. It consists of parallel sets of ribs overlying similar sets at various angles for in-plane drainage.

4) Geomembranes

Geomembranes can be described as a very low permeable synthetic membrane lines or barriers that are used with any geotechnical engineering related material in order to control fluid migration in a human-made project. They find their application in pits for the deposition of contaminated soil.

5) Geosynthetic Clay Liners

This is a hydraulic barrier consisting of a layer of bentonite or other low permeable material supported by geotextiles and/or geomembranes, mechanically hold together by needling, stitching or chemical adhesives. These waterproof barriers are used for example as landfill covers or pollution control facilities.

6) Geopipe

Geopipe or just plastic pipe is buried underground for the discharge of fluids. It is well able to resist against the compressive loads.

7) Geofoam

A foam that is used to create extremely light blocks that are stacked side by side to form the base of a road or the core of a levee.

8) Geocomposites

This material consist out of a combination of geotextiles, geogrids, geonets and/or geomembranes. Also any of these four materials can be combined with another synthetic material or with soil.

Figure 3.1 gives an overview of all eight different geosynthetics.

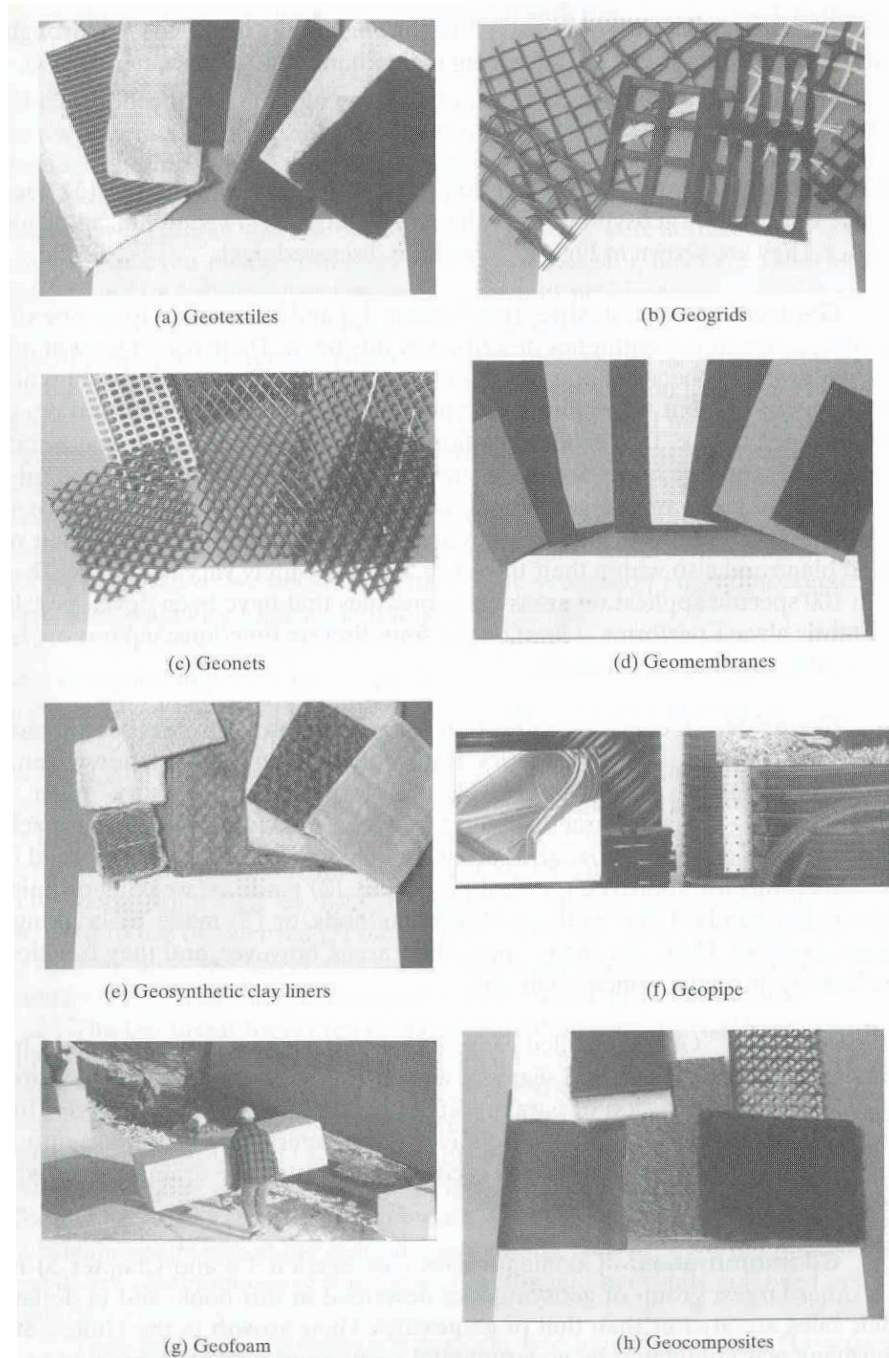


Figure 3.1: Geosynthetics

Using the material properties as feedback, most of the geosynthetics are not suitable for the construction of a gabion. A open structure of the grid is demanded in combination with a certain strength and flexibility. Only two types of materials seem appropriate from a first point of view. These are geogrids and geonets.

These two materials show comparable looks with the steel wire grid. The difference between these materials is the field of application. Geonets are used for their in-plane drainage capabilities, while geogrids are used for reinforcement purposes. Geonets have reasonable strength, but are exclusively used in drainage applications. Although geogrids and geonets look quite similar, geogrids form a much better alternative. Their use for reinforcement of constructions results in alternatives, which have better strength and stiffness properties. The use of geogrid has the most potential.

3.4 Geogrid Properties

3.4.1 Types of Geogrid

Geogrids are matrixlike materials with large open spaces. Typical sizes of these apertures are 10 to 100 mm between the ribs. The grid consists of longitudinal and transverse ribs, which can have different strength properties. The primary application of geogrids is soil reinforcement, retaining walls, revetments and roads.

With respect to stress absorption, there can be a distinction of two types. In certain fields of application the direction of major stresses is known as is the case for walls and slopes. For these constructions uniaxial geogrids are applied. Within these grids the ribs have different strength qualities in longitudinal and transverse direction. In situations where the stress comes from random directions, like in roads and foundations, biaxial geogrids are used. In biaxial geogrids the nodes in the grid are an important element in the transfer of the load from longitudinal to transverse ribs.

The stresses in the grid of a gabion are not from one single direction. The stresses during wave attack, deformation of fill material and even during placement of the gabion come from a random direction. The geogrid must therefore be able to transfer stresses in all directions and a biaxial grid is therefore used for the gabion application.

Biaxial geogrids are made from polypropylene or polyethylene sheet. Small holes are punched, in a regular pattern, in a sheet with a thickness of 2 to 8 mm. The sheet is then drawn biaxially with help of different roles and under controlled temperatures conditions (Figure 3.2). This process will cause the molecular chains to flow slowly into an elongated direction. With the molecular chains drawn in same direction the strength of the material is increased. The creep sensitivity of the elongated ribs is greatly reduced by the drawing process [KOERNER 2005]. Uniaxial grids are produced by drawing the material in just one direction. This results in more oval apertures. With respect to the containment of the filling material it is wisely to use uniform square openings.

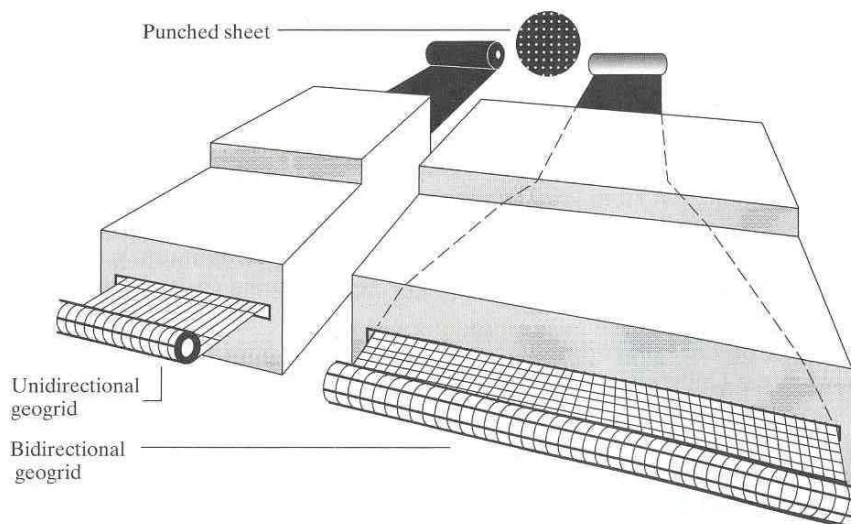


Figure 3.2: Manufacturing of uniaxial and biaxial geogrids

Another type of geogrid is a coated yarn-type geogrid. These geogrids are made of high-tension polyester yarns, woven into an open structure with the junctions being knitted together or physically intertwined. The entire grid is then coated with PVC, latex or bitumen for two-dimensional stability and to provide protection of the ribs during filling. These grids are relatively flexible with respect to homogenous geogrids. a certain stiffness is demanded from the material, Therefore this type of geogrid is not used. Besides this, it is also impossible to create boxes, since the junctions between the ribs have no significant strength. Finally, when the wire is cut raveling of the geogrid will occur.

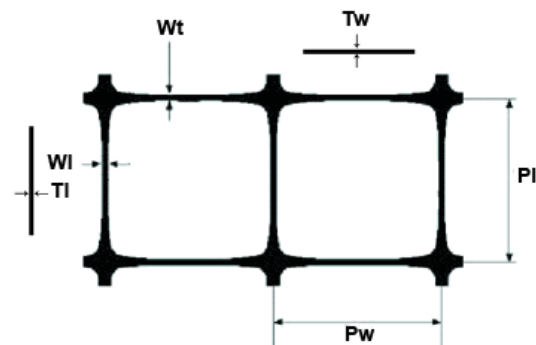
The last sort of geogrids are the so-called strap geogrids. These grids are produced from parallel straps of approximately 10 mm wide and 1 mm thick. The nodes are ultrasonically or laser bonded to provide junction strength. The stiffness of this grid is comparable to that of the homogeneous grid. This type of geogrid has the same disadvantage as the woven geogrids. The junctions are too weak compared to the rib strength. This type of grid is therefore not suitable for gabions.

The three alternatives all have a rib strength that is comparable. Woven geogrids and strap geogrids have the disadvantage that the junctions have no significant strength. The effect is that it is not possible to create boxes for the construction of a gabion. The junctions on the rib are too weak, which can lead to failure near connection points. Homogeneous geogrids have the same junction strength as the rib strength and are therefore the most appropriate solution.

In the assortment of Texion Geosynthetics there is one homogeneous geogrid that is able to fulfil to the stated demands. This is the so-called E'Grid geogrid. This is a biaxial grid made from polypropylene material. In table 3.1 an overview is given of the dimensions and strength properties.

Type	E'Grid 2020	E'Grid 2020L	E'Grid 3030	E'Grid 3030L	E'Grid 4040	E'Grid 4040L
Transverse width Pw [mm]	40	66	40	66	33	54
Longitudinal length Pl [mm]	40	66	40	66	33	54
Smallest transverse rib-width Wt [mm]	2.0	3.3	2.2	3.3	2.3	3.5
Smallest longitudinal rib-width Wl [mm]	2.4	4.0	2.7	4.0	2.6	4.5
Thickness transverse [mm]	1.0	1.0	2.0	1.5	2.3	1.8
Thickness longitudinal [mm]	0.8	0.9	1.4	1.4	2	1.6
Tensile strength longitudinal [kN/m]	20	20	30	30	40	40
Tensile strength transversal [kN/m]	20	20	30	30	40	40
Strain vs Force						
2% strain at a force F [kN/m]	7.4	7.4	10.8	12.5	14.0	14.0
5% strain at a force F [kN/m]	14.8	14.8	21.6	25.0	28.0	28.0

Table 3.1: E'grid geogrid dimensions



An interesting comparison is how the tensile strength differs from the strength of steel wire grids. Table 3.2 gives an overview of the most common mesh types and wire diameters used in river and coastal works with their ultimate tensile strength [CIRIA, CUR, CETMEF 2007b]. From this table it can be concluded that the E'grid geogrid 4040 version shows comparable strength properties.

Common Steel Wire Properties		
Mesh type	Wire diameter	Ultimate tensile strength
(mm)	(mm)	(kN/m)
60 x 80	2.2	35
80 x 100	2.7	43
80 x 100	3.0	51
100 x 120	3.0	43

Table 3.2: Common steel wire properties.

3.4.2 Reduction Factors

From the data in table 3.1 and 3.2 it can be concluded that the tensile strength of synthetic and steel gabion grid material is comparable. The synthetic material is a bit weaker than the steel wire mesh, but still of the same order. This does not mean that the gabion should be of a smaller size or different shape. During functioning on location the available strength, presented in table 3.2, will not be used till the ultimate level. The ultimate load on the grid will probably take place during installation on location, but also depends on the construction method. The strength properties therefore do not become a problem.

In the normal utility phase the geogrid can never be loaded to the ultimate tensile strength (T_{ult}). The allowable tensile strength (T_{allow}) must be lower than the ultimate tensile strength. The factor that is present between these two values is the so called safety factor. The value is based on reduction factors that represent ultra violet degradation (f_{UV}), chemical and biological degradation (f_{CBD}), creep over lifetime (f_{CR}), and installation damage (f_{ID}). Equation [64] shows the application to determine the relation between ultimate and allowable tensile strength. [KOERNER 2005].

$$T_{allow} = T_{ult} \left(\frac{1}{f_{UV} \cdot f_{CBD} \cdot f_{CR} \cdot f_{ID}} \right) \quad [64]$$

The factors that are applied are determined with help of several experiments.

Resistance to Ultraviolet Light

Exposure to ultraviolet light results in decreasing of the material strength. To provide protection and reduction of the amount of degradation, an extra additive is added to the polymer. The polymers are protected by adding a few percentages of carbon-black. Carbon-black is a so called competitive absorber. This means that it is able to capture and absorb the ultraviolet radiation and converting it into heat, which dissipates radiation harmless. This additive does not fully protect the polymer, but decreases the degradation process considerably.

The amount of degradation also depends on the amount of ultraviolet radiation. Locations with more sun hours and places with a closer distance to the sun, around the equator, will receive more UV radiation. This UV radiation is expressed in kilo Langleys (kLy). One kilo Langley stands for the amount of UV radiation energy in kJ that falls on one square centimetre. The Netherlands are for example subject to 70-80 kLy per year. The producer of the E'grid geogrid divided the world in three regions of radiation.

- Region A: Canada, Europe, central China
- Region B: USA, South America, Mediterranean coastal areas, Asia
- Region C: Central America, parts of South America, Middle East, India, Australia

U-V Exposure Level	Kilo Langleys per year	=120	120 - 160	=160
Region		A	B	C
Product				
E'GRID 2020		67	50	40
E'GRID 3030		>100	100	80
E'GRID 4040		>100	>100	92

Time to 75% of initial strength (years)

Table 3.3: E'grid geogrid strength UV degradation

Table 3.3 is based on several durability tests [BOSTD 2007]. By subjecting the material to a certain amount of radiation with special lamps the UV degradation can be simulated for several locations on the earth. The adding of carbon-black results in material that is very well able to resist UV radiation. Shading by for example vegetation give also positive contribution to the degradation process. For the estimation of the life-expectancy, the degradation of strength due to UV can be taken into account. Table 3.3 shows the time passing until 75% of the strength is left. The properties E'grid geogrid are rather good since for the heavier classes it takes more than 100 years to degrade until 75 % of the initial strength.

Biological, Chemical and Oxidation Degradation

Polypropylene is not affected by micro-organisms. It is not possible for organisms to settle on the material and effect the material properties. According to biological degradation tests (EN 12225) that have been executed, no results of degradation where found. [BOSTD 2007]

Chemical effects are hardly present. Polypropylene is also used for the storage of chemicals, manufacturing of fuel tanks and battery cases. The resistance to chemical attack is very good. Liquids with very high or very low pH-values can affect the material properties. For the situation in which gabion mattresses will be applied, chemical degradation does not play a role.

Polymers are sensitive to oxidation. This is a chemical process in which material degrades caused by oxygen. Especially polypropylene is susceptible to this process. High temperatures will start this process. Temperatures close to the melting point (165 °C for polypropylene) accelerate the process. These temperatures will normally not occur near gabions. A test where the sensitivity to oxidation at 100 °C and 110 °C was tested for 230 and respectively 112 days did not show any form of degradation [BOSTD 2007]. This is equivalent to more than 100 years of exposure at normal ambient temperatures. This is therefore not a concern for gabions. According to these test results the reduction factor for biological, chemical and oxidation degradation is good. The producer of E'grid geogrid gives a reduction factor of 1, for these types of possible degradation. The material is not affected by any of these processes.

Creep Performance

A good creep-performance is essential for the functioning of the construction. Creep can lead to more space in a compartment. This gives the possibility for the fill material to start moving in the basket. Under a certain amount of tension the grid will elongate. When developing a gabion, the pursuit is to keep deformation in control and reduce it to a minimum. This can be achieved by applying material that has relatively good creep-tension properties. The performance depends on the material properties, temperature, time and load.

The producer BOSTD did perform several creep performance tests. These test were performed on the uniaxial variant, with grids that are made from high density polyethylene. These grids have stronger tensile strength properties. The initial strength lies between 50 - 170 kN/m. Main target of these experiments has been the determination of the ultimate creep-limited strength (UCLS) properties. During strain-time experiments, failure is described as elongation of 20% or rupture of the grid.

The ultimate creep limited strength was determined in the experiments by applying accelerated creep testing methods. This type of experiment is based on the fact that the increased temperature will accelerate the amount of creep. By time-temperature-superposition the load-time curve can be determined. With this curve the ratio is determined between the initial strength and the ultimate-creep limited strength during time. The ratio is presented in table 3.4 [WRIGLEY 2007]

Creep failure ratio at 20 °C			
Design life	75 years	100 years	120 years
UCLS / IS	0.4079	0.4041	0.4018

Table 3.4: Creep failure ratio

The results in these tables are valid for geogrids that are continually loaded without unloading as for example in soil improvement constructions. It can be concluded that HDPE grids will have approximately 40% of the initial strength after considerable time. The reduction factor is the inverse of this ratio if the grid is continually loaded (2.5). According to *Koerner, 2005* the reduction factor for the ultimate creep limited strength is between 3 and 4.

Geogrids applied in gabions are not continually loaded. Gabions will only be loaded now and then, when severe wave-, or current attack occurs. Most part of the life-time there will be no-, or little stresses on the grid. After 100 years gabion geogrids will probably have more or less the same strength of the initial strength if UV degradation is not taken into account. The reduction factor can be less strict for geogrids applied in gabions.

The behaviour under lower load conditions is more important for geogrids applied in gabion mattresses. A certain amount of load leads to strain of the grid. This can result in a increasing volume of a compartment which can give movement of fill material. The strain of the material should therefore be limited. Figure 3.3 represents strain curves during time, for the uniaxial E'grid geogrid 50-170R.

A great amount of different samples were tested for varying time and load. Not every grid has the same initial strength. Due to normalising the load, based on the initial strength, a comparable behaviour in proportion to the initial strength is the result. In Figure 3.3 the isochronous creep curves for uniaxial E'grid at 20°C have been deviated [WRIGLEY 2007].

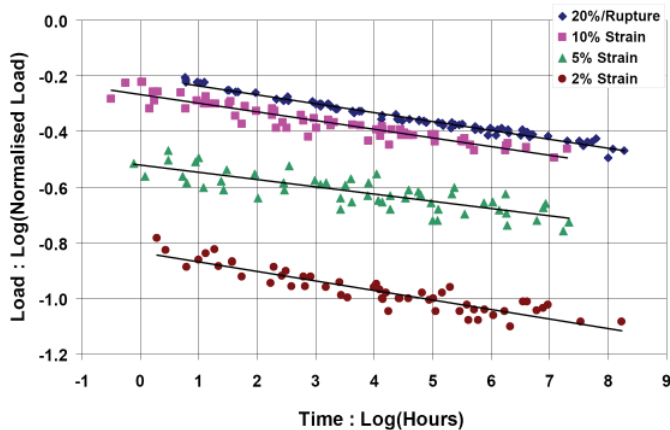


Figure 3.3: Strain curves uniaxial E'grid 50-170R

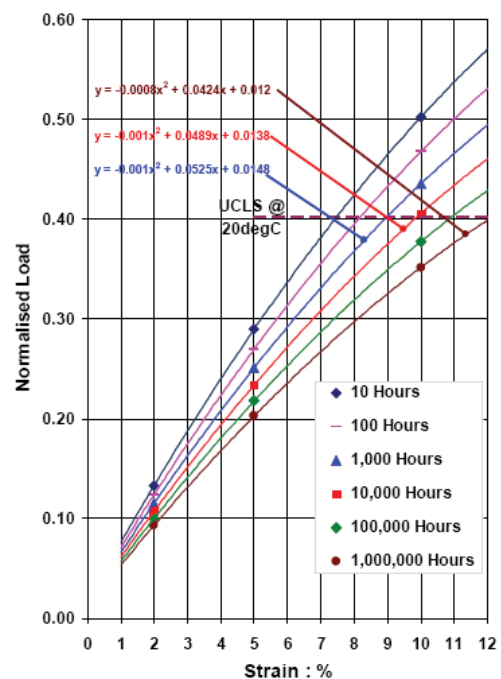


Figure 3.4: Isochronous creep curves

The BOSTD E'grid geogrid material from the type 50 - 170R is an uniaxial grid. In the gabion mattress, the biaxial variant is applied. There is no research available on the biaxial E'grid. This graph cannot be directly applied on the uniaxial E'grid, though the material shows similar behaviour and will show a comparable graph. The biaxial variant is made from a lighter polymer, which results in relative decreased strength qualities.

For both types of E'grid geogrid the amount of load for a 2% and 5% elongation is known. During these tests, time is not an issue and the load is assumed as a peak load compared to the other test situations. The $\log(\text{time})$ -value expressed in hours has a negative value, since the experiments takes only a few minutes. In table 3.5 these values are calculated for the uniaxial and biaxial E'grid geogrid. The relations in Figure 3.3 show more or less the same gradient for each level of strain. Based on the slope of the gradient the lines are interpolated and the position for the peak load stresses, with respect to the duration tests, are expressed in the graph of Figure 3.5. The accompanying $\log(\text{time})$ value is -7.7.

Considering the mutual relation between the different strain levels from Figure 3.4, it is possible to do a careful approximation of the isochronous creep curves for the biaxial E'grid geogrid. Comparing the polynomials of the different lines the factors increase by a certain value depending on the duration of the load. These are interpolated to determine the several isochronous creep curves, including the peak load curve, which should resemble the measured data. In Figure 3.6 the uniaxial stress curve is presented, based on the peak load in combination with the approached load. The relations between the uniaxial curves have been applied on the biaxial variant to create an approximation of the isochronous creep curves, presented in Figure 3.6.

Product	Initial Tensile Strength	Force 2% Strain	Force 5% Strain	Load Normalised 2% Strain	Load Normalised 5% Strain	Log(Norm) 2%	Log(Norm) 5%
Uniaxial	[kN/m]	[kN/m]	[kN/m]	[-]	[-]	[-]	[-]
50R	54	12.7	24.7	0.24	0.46	-0.63	-0.34
65R	68.7	16.1	30.9	0.23	0.45	-0.63	-0.35
90R	90	23.7	45.2	0.26	0.50	-0.58	-0.30
110R	112	29.9	56.5	0.27	0.50	-0.57	-0.30
130R	141.9	38	75.5	0.27	0.53	-0.57	-0.27
170R	176	52.5	103	0.30	0.59	-0.53	-0.23
Biaxial							
2020	20	7.4	14.8	0.37	0.74	-0.43	-0.13
2020L	20	7.4	14.8	0.37	0.74	-0.43	-0.13
3030	30	10.8	21.6	0.36	0.72	-0.44	-0.14
3030L	30	12.5	25	0.42	0.83	-0.38	-0.08
4040	40	14	28	0.35	0.70	-0.46	-0.15
4040L	40	14	28	0.35	0.70	-0.46	-0.15

Table 3.5: Creep failure ratio

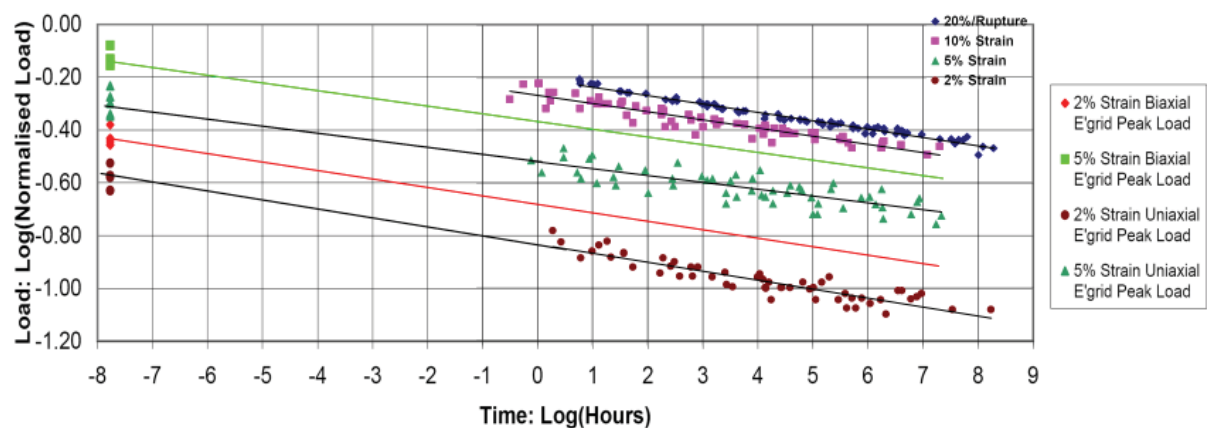


Figure 3.5: Strain curves uniaxial E'grid 50-170R

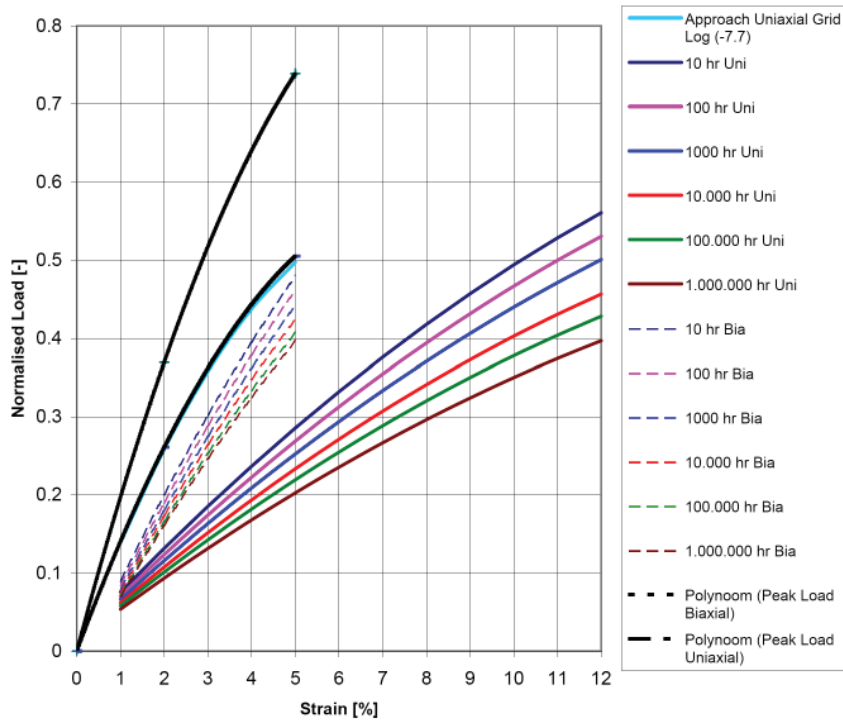


Figure 3.6: Approximated isochronous creep curves biaxial E'grid geogrid

The above stated graph describes the percentage of strain during a loading time that does not represent wave action. A downward directed tension force, on the grid, will be performed for a part of the wave period. The response of the material during a great amount of load repetitions is of interest. A material can behave elastic and plastic on constant loading and unloading. Elastic response of a material will result in the original length after relieving the tension. Steel responds elastic if the yield point is not reached. Plastic behaviour expresses strain in permanent deformation after relieving the tension. Figure 3.7 shows the difference.

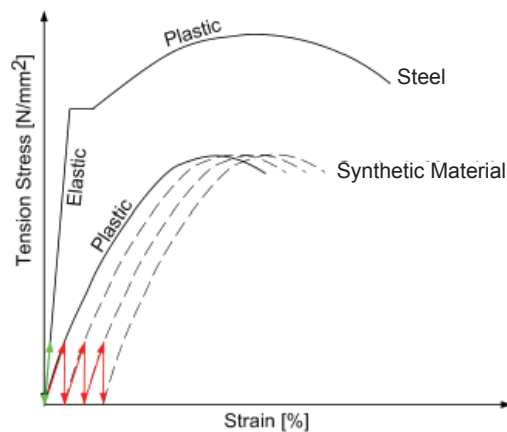


Figure 3.7: Stress-strain behaviour

If a gabion grid material would show plastic behaviour, then during a certain amount of waves, strain could develop to a considerable, inconvenient and permanent level. Elastic behaviour is a property that is desired. Thermoplastic materials, like the polypropylene geogrid, show several states of behaviour that depends on the structure of the molecules.

The molecules of steel are present in a crystal structure that are responsible for the elastic character. Steel is characterised by the sudden melting point. When this point is reached the crystal structure is broken and the material fluids. From this point the material behaves plastic. Thermoplastic materials more or less respond in the same way only with a less sudden point of loss of the crystal structure.

The characteristics can best be described in a elasticity - temperature relation. Elasticity is a degree for the stiffness of the material. This relation is presented in Figure 3.8. Three stages are present for thermoplastics: the glass-, rubber-, and plastic state. The transitions are characterised by the glass temperature (T_g) and fluid temperature (T_v). For normal polypropylene these temperatures are respectively $-15\text{ }^\circ\text{C}$ and $165\text{ }^\circ\text{C}$.

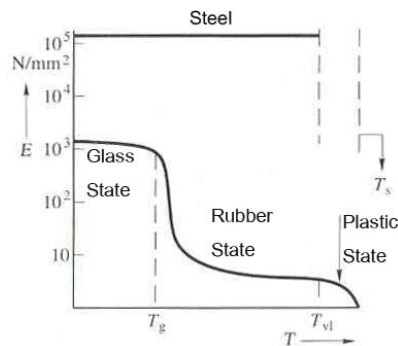


Figure 3.8: Thermoplastic behaviour

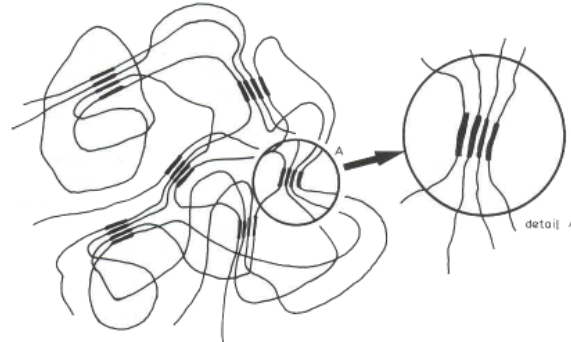


Figure 3.9: Crystallisation polymers

Below the glass temperature the chains experience mutual forces due to partly crystallisation (Figure 3.9). Due to these mutual forces the material generates a elastic resistance force. Above this temperature the material starts to behave more elastic. Due to the extrusion process the molecule chains are oriented and the crystallisation degree of the material improves. The effect of the molecule structure improvement is a better stiffness and ability to keep its original shape. A 100% crystallisation improvement would result in the same sudden failure as steel. For thermoplastic polymers this is not possible. Polypropylene has the ability for 70% crystallinity improvement [VERVER 2000]. Figure 3.10 shows the improvement of the behaviour.

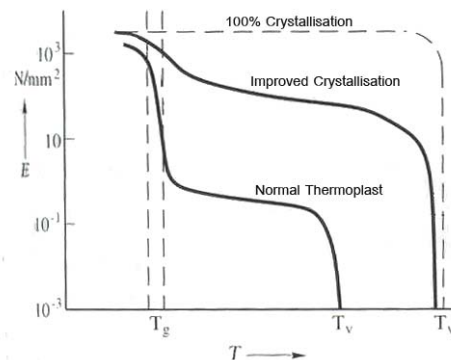


Figure 3.10: Crystallinity improvement

Based on the material properties it is expected that the amount of strain is fairly little with respect to the tensile strength of the material. The material will behave elastically in the utility phase. The total percentage of strain in gabions during life-time is expected to be very little, although it also depends on the amount of tension stress that a construction has to absorb. A full guarantee cannot be given based on the available results.

Construction of a Revetment.

There are three main options for the construction of gabion mattress revetment. The different methods are presented in Figure 3.11 to 3.13. The first solution is connecting and filling of the gabions on the bank in dry conditions. This method demands some extra labour force, but can also be applied in more remote areas that are not accessible with heavy machinery. In countries where labour is cheap this is a good method, because the operations are not difficult. Filling the gabions could also be done with the help of machinery.

The second solution is filling on the bank and later placement with a crane. This execution method can also be done to place mattresses below the water level, in contradiction to the first solution. Especially for the construction of embankments and riverbeds this method is applied. What should be kept in mind is that lifting the gabion can result in high stresses on the grid especially at the lifting points. To spread the load over the construction, a lifting frame can be used that is connected on several points of the grid. Synthetic material is even more vulnerable to high peak tensions and the elongation of the grid that it brings. The execution method, and especially careful lifting of synthetic gabions, should be taken into account during the development.

A third method that could be applied with large mattresses is the so called pontoon placement. This method is especially useful for deep water installation and large-scale placement. The mattress is prefabricated and placed on a barge or pontoon. By tilting the pontoon the mattress will slide down and cover the bed. Under water the mattresses are not connected, but they overlap each other in downward flow direction.



Figure 3.11: In-situ assembly



Figure 3.12: Crane placement



Figure 3.13: Pontoon placement

All these construction methods require a certain degree of planning and care. As happens during construction with of heavy machinery and perhaps careless crews, installation damage of the grid can occur. When constructions are examined afterwards loss of strength can be present. To take this aspect into account a factor for the installation damage is applied. Though this factor depends on the quality which a contractor can achieve. *Koerner 2005* gives reduction factors for the installation damage (f_{ID}) of 1.1 to 1.4.

Total Reduction Factor

If a revetment in the Netherlands is considered and a demanded lifetime would be 75 years the reduction factor of the three of types E'grid geogrid would be:

- UV Degradation (f_{UV})

The degradation due to UV radiation depends on the type of E'grid geogrid applied. In table 3.3 the number of years that is needed for 25 % reduction of the initial strength is presented. For now it is assumed that UV degradation is a linear process. If the values of table 3.3 are interpolated it would be a 28 % reduction for E'grid geogrid 2020 and 19 % reduction for the 3030 and 4040 version. This gives f_{UV} factors of respectively 1.39 and 1.23.

- Chemical and Biological Degradation (f_{CBD})

E'grid geogrids are not subjected to chemical or biological degradation. A f_{CBD} reduction factor of 1 is used.

- Creep (f_{CR})

E'grid geogrid applied in gabions will never be loaded until the ultimate level for a very long time. Most of the time there will be no tension on the grid. The problem is that accurate measurements of the loss of strength due to time and waves are not available. The most safe creep reduction factor would be based on the 60 % loss of strength from Wrigley research. This is a rather strict condition and does not reflect the gabion mattress situation. Gabions are subjected to lower stresses. A loss of 33 % of the initial strength is used as safe first approximation. A f_{CR} of 1.33 is applied.

- Installation Damage (f_{ID})

Assuming that the quality of the constructor is good a installation damage reduction factor of 1.1 is used.

If formula [64] is filled in than the general reduction factor of the material would be 0.50 for the 2020 version and 0.55 for the 3030 and 4040 version.

$$T_{allow} = T_{ult} \left(\frac{1}{f_{UV} \cdot f_{CBD} \cdot f_{CR} \cdot f_{ID}} \right)$$

$$T_{allow} = T_{ult} \left(\frac{1}{1.39 \cdot 1 \cdot 1.33 \cdot 1.1} \right)$$

$$T_{allow} = T_{ult} \left(\frac{1}{2} \right)$$

3.5 Construction of a Gabion

3.5.1 Creating a Volume

A construction has a certain strength that is equal to the weakest link in the chain. The E'grid geogrid seems a very good material for construction of the gabion, still a volume has to be constructed. This volume should be filled with material and closed to create a compartment. Gabions are connected to each other to create solid homogeneous protection. In this section the different connections, that could be used, are described.

Normally gabions are delivered as a package of panels and are assembled on location. The baskets are folded together and the ribs are joined together. This is done by using thicker wire, which laces the ribs are together. An alternative is the use of a pneumatic Spenax tool that connects the ribs by stainless rings (Figure 3.14). When the baskets are constructed they are filled with material and placed on their final location with a mechanical tool e.g. lifting crane or they can be placed and filled afterwards. Depending on the type of structure, its location and the availability of supporting equipment, a choice is made for a certain construction method.

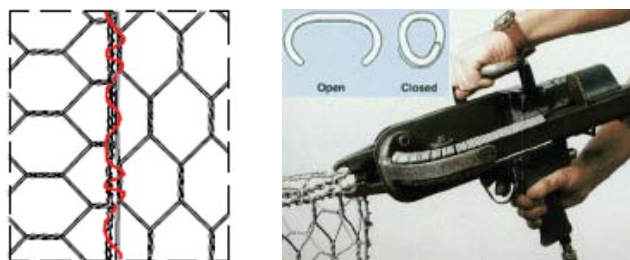


Figure 3.14: Lacing wire and spenax tool

Gabions that are made from E'grid geogrid, for example applied in a rubbish dump, are cold bent. It is also possible to bend the geogrid with heat. Polypropylene is a so-called thermoplastic polymer. A thermoplastic polymer can be repeatedly heated to its softening point, shaped or worked as desired and then cooled to preserve the remodelled shape. The melting temperature is around 165 °C, it is easily bend in the correct shape by heating it. Both bending methods have no effect on the strength of the material. The only difference is that the ribs from the cold bent grid can show a less smooth curvature of a few fibres. A few fibres let loose, but no fracture of the material occurs. Figure 3.15 shows a picture of a bent E'grid geogrid. It is clear that the heated grid on the left shows a smoother corner than the cold bent grid on the right. The little delamination does not have effect on the tensile strength of the material.



Figure 3.15: Bent E'grid geogrid

The bending quality can be used for the assembly of a gabion. A plate that is cut out in a certain shape is delivered on location, by bending certain ribs a volume can build. The side ribs and the lid have to be connected by a external connection. Figure 3.16 shows an example for setting up a mattress gabion. Some panels are added with external connections. In this figure a combination of bent ribs and external connections is presented. The external connections that are applied for mutual connection of the mattresses are not included in this figure.

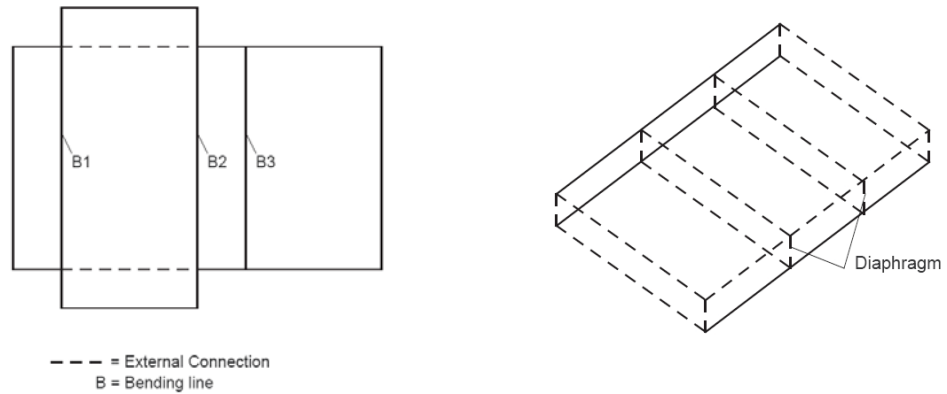


Figure 3.16: Bending plan and separate connections

3.5.2 External Connections

For closure of the volume it is possible to use a Spenax tool with stainless steel rings. These rings are an alloy and will not corrode and are able to resist high tension forces. A second possibility is the use of a synthetic system. Tie-wrap cable ties are for example a rigid solution. The connection is available till a tensile strength of 110 kg, made from UV-resistant material. Special tools are available, comparable to the Spenax tool, to connect the grids. Another potential advantage of these cable ties is that after some time when the stones are settled, the ties can be tightened again. The container needs a certain degree of overfill of material when this aspect is used.

A stainless steel version is also available. This cable has higher strength properties and is suitable for salt-water environments. When the durability and strength possibilities of synthetic cable wires is not good enough than the stainless steel version may provide a better result.

Another possibility is the use of helical connectors. These connectors are helix shaped and are braided through the grid. Figure 3.18 shows an example of such a connector. Disadvantage of this connector is that it is only available in protected steel wire. Protected in the same manner as the steel wire grids, that are applied in gabions these days. Applying these connectors is therefore not possible and a synthetic alternative is not available. Advantage of a connector like this is the tight closure of the grid. During lifting or loading of the grid the connector will spread the loads over the total length of the rib.

All these different techniques have been tried and used. From experience it came forward that the lacing of edges with HDPE wire of about 5 mm is the most successful technique. This method is comparable to the steel wire lacing and is now the most applied connection. It has similar material properties as the biaxial geogrid and provides proper transfer of stresses.



Figure 3.17: Cable ties



Figure 3.18: Helical connector



Chapter 4. Experiment Description

4.1 Introduction

From a first point of view the application of synthetic material, for the construction of gabions, seems appropriate. Several material tests could be executed to confirm the proper functioning of E'grid geogrids as a casing for synthetic gabions. Still there is a hesitation to apply this synthetic alternative in hydraulic structures. A general fear exists that synthetic materials are not strong enough, have less durability and show too much deformation during time.

From the material description it comes forward that the material E'grid geogrid is strong enough and that the durability of the material is comparable, or even better than that of steel wire grids. The main problem is the possible deformation of the geogrid. In the application of soil retaining walls, high loads are subjected to the construction, which results in bulging of the construction. Gabions that are used for bank erosion protections are subjected to waves, which results in loads on the grid of a general less severe degree. The doubt and lack of experience, with this type of construction, holds engineers back from applying synthetic gabions.

No fundamental research has been performed on the deformation of gabions under wave attack, but the same principle as with deformation in currents is present. Waves cause a redistribution of the material, if space inside the compartment is present. Development of extra space can already occur at the initial phase of the gabion functioning. The majority of the gabion mattresses are assembled on location and are then mechanically filled. Some assistance is present to ensure optimal filling and closure of the gabion.

The current idea is that after some time several waves have entered the bank and the material will be settled. The compaction of the fill material will improve. This results in more space inside the gabion and the process of deformation is initiated, since the fill material has space to move inside the compartment. Gabions placed on a slope, will be more sensitive to deformation. Gabions on land are therefore slightly overfilled before they are closed. Sometimes, after a couple of weeks the connection wires will be pulled tight to compensate the extra space that has developed by the improved degree of compaction. For gabions that are present on banks and even partly situated under water this method is not possible to apply. The loss of fill material coverage will take place on the upper side of the compartment. The process of erosion will take place at this part of the mattress and is therefore the most sensitive.

One of the intentions of this project is to study how synthetic gabions behave under wave attack. The concept of deformation is an important issue and will be one of the main points of interest. The influence of fill material, compaction and flexural rigidity of the grid are investigated.

Besides deformation, the failure mechanism due to sliding is of interest as explained in chapter 2. The current most useful formula from Pilarczyk does not take every aspect into account. The experiments in the wave flume will be used to develop a improved stability relation.

To gain better insight in the processes caused by wave-action, scale experiments are executed. With these experiments the effect of geogrid deformation and failure is investigated. Several scaled gabions will be tested in which different parameters are altered.

In this chapter a description of the laboratory experiments is presented, which are executed to investigate the effect of deformation and failure due to sliding. An important aspect of model tests is the proper scaling of the parameters. The first part of this chapter is devoted to this subject, followed by a description of the set-up and execution of the different model tests. The performed tests form a base for recommendations and potential improvement of the design rules.

4.2 Scale Experiments

4.2.1 Scaling of Parameters

The deformation of gabions is a complex system that depends on many parameters. The insight into this problem is not very clear and a numerical analysis is impossible to perform. A scale model experiment will give a better insight in the general behaviour of the construction, if properly executed.

The experiment is performed by building a slope inside a flume. On this slope a scaled gabion mattress is placed. The wave generator inside the flume subjects the revetment to wave attack. The experiment is performed on scale, therefore it is important that the different material parameters of the geogrid are properly scaled down, to develop a proper representation of reality. Especially for the aspect of deformation, proper scaling of the model material behaviour is necessary.

The degree of geogrid deformation depends on several aspects namely:

- The size, density and compaction of the fill material
- The stiffness of the wire mesh material
- The size of the compartments inside the mattress

The dimensions are scaled down with a factor, to fit the dimensions of the flume. Scaling will be done by dividing the physical parameters of the prototype by a scale factor. The scale factor is calculated by formula [65] from [DE VRIES 1976].

$$n_x = \frac{x_p}{x_m} \quad [65]$$

With:

- p = Subscript p is for the prototype situation.
- m = Subscript m is for the model situation.

There are three types of similarity that should be maintained between a model and the prototype:

- Geometric similarity: All geometrical dimensions are scaled down with the same factor.
- Kinematic similarity: The velocities are scaled down with the same factor.
- Dynamic similarity: The forces are scaled with the same scale factor.

The problem with scaling is that certain parameters cannot be scaled down or have certain restrictions. For example: the viscosity of water or gravity. Next to that, material properties cannot be scaled down infinitely. Large scale factors applied on sand will result in particle sizes of silt or clay that show cohesive behaviour and are therefore not representative.

Not every parameter can be scaled down. It is necessary to identify the processes of primary importance and determine the dominant forces. Then, it is necessary to scale the model and model-material properties so as to maintain, as closely as practicable, the same ratios between the primary forces in the model as in the prototype.

In hydraulic engineering the relevant forces are identified with dimensionless parameters. The two most important dimensionless parameters for an experiment of this type are: The Froude number and the Reynolds number. By scaling the included parameters in proportion to each other the dominant forces and processes will be maintained. The Froude or Reynolds number will be the same for the model and prototype. The problem is that both parameters cannot be satisfied. The explanation for this is explained in the next section

4.2.2 Scaling Method

The Froude number gives the ratio between the inertia and the square root of gravity. When a model is scaled based on a constant Froude number, than the relation between the scale factor of length and velocity differs. This means that if a model is geometrically scaled, than the velocity scale factor should be the root of the length scale factor. This is derived below. It should be kept in mind that the model is subjected to the same field of gravity acceleration, so: $n_g = 1$.

$$F_r = \frac{u}{\sqrt{gL}} \quad \frac{F_{r-p}}{F_{r-m}} = \frac{\frac{u_p}{\sqrt{L_p}}}{\frac{u_m}{\sqrt{L_m}}} = 1 \quad \text{so, } n_u = n_l^{1/2}$$

The Reynolds number gives a certain degree of turbulence that is present for a situation. This depends on flow velocity, object size and viscosity of the flow. If an experiment is Froudian scaled, than the Reynolds number will be influenced. The viscosity of the water cannot be adapted by the scaling factor and will be kept $n_\nu = 1$. The Froude relation between velocity and length will effect the Reynolds number. The relation is derived below.

$$\text{Re} = \frac{uL}{\nu} \quad \frac{\text{Re}_p}{\text{Re}_m} = \frac{u_p L_p}{u_m L_m} = n_l^{1/2} n_l = n_l^{3/2}$$

The effect of scaling based on the Froude number implies that the Reynolds number in the model is underestimated compared to the prototype situation. The effect is that the viscous forces become larger and the amount of turbulence is too low. Turbulence is a important aspect that can influence the deformation since pressure fluctuations cause the first movement of the fill material.

When the model is based on a constant Reynolds number, other effects will be scaled improperly. The velocity and length are inversely proportional. A higher velocity results in a smaller length parameter. The velocity is influenced by the wave height, which is scaled down in the model. This means that the length should be scaled up. This contradiction is improper for the use in the gabion scale model experiment.

The Reynolds number is important when viscous forces dominate. This is the case for low Reynolds numbers that are present in for example in slow flowing rivers. For constructions in waves this is not the case and higher degree of turbulence is present. According to *Ettema, 2000*: If a fully rough flow exists at full scale and model scale, than exact satisfaction of the Reynolds number is not needed. In most coastal scale models the Froude criteria is the most important to fulfil. The experiment is based on Froudian scaling.

4.3 Material Properties

4.3.1 Elasticity

Deformation depends on the quality and geometry of the material. For representative results all aspects of the gabion construction should be scaled down to the same degree. The geometrics of the different biaxial E'grid geogrid material is represented in table 3.1 chapter 3.

An important parameter that is expected to influence the sensitivity to deformation is the elasticity of the material. Elasticity is a degree for the stiffness or weakness of a material. This ratio is determined with Hooke's law [66].

$$E = \frac{\sigma}{\varepsilon} \quad [66]$$

In which σ is the tension and ε is the percentage of sample elongation. This law is only applicable in the part where the material responds elastic and therefore linear on the relation between tensile strength and strain percentage. Oriented materials have a plastic deformation behaviour as explained in Figure 3.7, so the relation does not hold exactly. For E'grid geogrid the tensile strength versus strain percentage is known. In Table 4.1 the different biaxial geogrid types are presented and the force related to a 2% strain percentage [BOSTD 2007].

For the approximation of the elasticity, the load for 2% strain values are used, since they more or less approach a linear relation (Figure 3.6). To determine the stress inside the grid the smallest cross-section surface of a rib is determined. By dividing this value through the 2 % elongation value the elasticity is determined. Table 4.1 shows the results. There is a variation between the values, because the material does not behave fully elastically.

Cross-section dimensions and Elasticity						
Type	E'Grid 2020	E'Grid 2020L	E'Grid 3030	E'Grid 3030L	E'Grid 4040	E'Grid 4040L
Smallest cross-section per rib [mm ²]	1.9	3.6	3.8	5.6	5.2	7.2
cross-section per meter grid [mm ²]	48	55	95	85	158	133
Tensile stress 2% strain, sigma [N/mm ²]	154	136	114	147	89	105
Elasticity 2% [N/mm ²]	7708	6783	5714	7366	4442	5250

Table 4.1: Elasticity

4.3.2 Flexural Rigidity

Not only the elasticity parameter of the material can influence the deformation, also the flexural rigidity of the geogrid might influence this. The shape of an element is of influence on the rigidity and normally included by calculating the moment of inertia. In combination with the elasticity these values are used to determine the sensitivity to bending. Geogrids do not have defined cross-section so this method can therefore not be applied.

The flexural rigidity of geogrids is a property that is of interest when the firmness of the compartment shape is concerned. This can be measured using the standard test *ASTM D1388a, 2007*. This is a test in which the flexural rigidity of fabric is determined. The length of overhang is measured when the tip of the specimen is depressed, under its own weight, to the point where the line joining the top of the edge of the platform makes a 41.5° angle with the horizontal. The length of overhang is measured and related to the mass per unit area. Figure 4.1 shows this so called cantilever test apparatus and the principle of the test. As an indication for the flexural rigidity: a grid with a rigidity value of 1000 g-cm is considered stiff [KOERNER 2005].

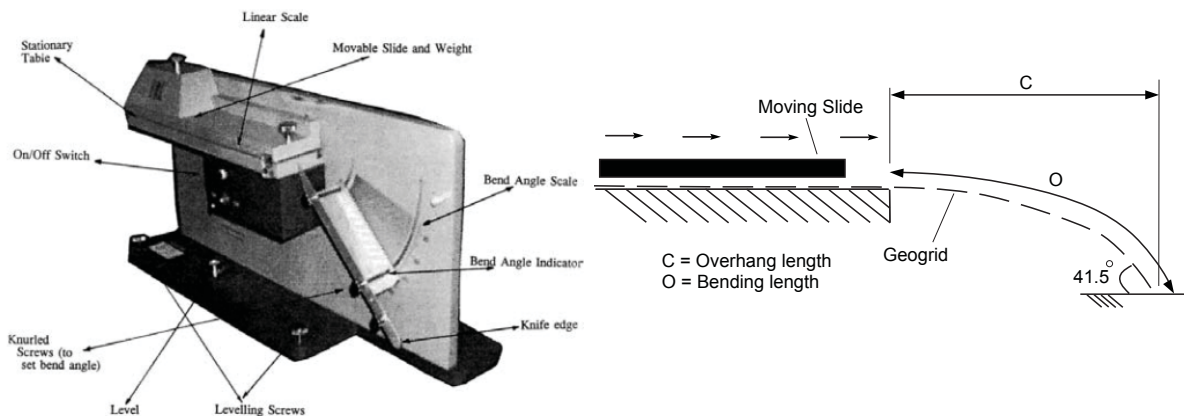


Figure 4.1: Cantilever test apparatus

The bending length (c) is calculated by dividing the overhang length (O) by 2. This value is used in the formula for the calculation of the flexural rigidity [ASTM D1388a, 2007].

$$G = 1.421 \cdot 10^{-6} * W * c^3 \quad [67]$$

With:

G	= Flexural rigidity	[μJ/m]
W	= Fabric mass per unit area	[mg/cm ²]
c	= Bending length = O/2	[mm]
O	= Overhang length	[mm]

The numerical factor present in the formula is not dimensionless. A dimension analysis is performed with the following result:

$$G = 1.421 \cdot W \cdot c^3$$

$$\frac{L^2 M}{T^2} / L = \frac{M}{L^2} \cdot L^3$$

$$\frac{LM}{T^2} = LM \left(\frac{1}{T^2} \right)$$

The numerical factor in formula [67] has a dimension T⁻².

In Table 4.2 the flexural rigidity values of E'grid geogrids are presented [BOSTD 2007] in the unit [g cm]. A different unit than applied in formula [67]. To get a better view on the sensitivity to bending, the related bending length is calculated with formula [67]. To transform the value expressed in the unit [gr cm] to [uJ/m] it divided by the value 1.421. With formula [67] the bending-, and overhang length are calculated.

Type	E'Grid 2020	E'Grid 2020 L	E'Grid 3030	E'Grid 3030 L	E'Grid 4040	E'Grid 4040 L
Flexural rigidity [g cm]	1400	1500	2800	2200	4300	3700
Flexural rigidity [μ J/m]	985	1056	1970	1548	3026	2604
Fabric mass [mg/cm ²]	20	20	30	30	50	50
Bending length c [m]	0.33	0.33	0.36	0.33	0.35	0.33
Overhang length c [m]	0.65	0.67	0.72	0.66	0.70	0.66

Table 4.2: Flexural rigidity

Besides a proper scaling of the elasticity that is necessary for a representative performance of the experiment, a good scaling of the resistance to bending is important. The flexural rigidity will be taken into account.

4.4 Scaling

4.4.1 Scaling of the Geometrics

The experiment is scaled based on the Froude relation. The geometrical parameters as length, width and thickness are scaled down in relation to each other. In order to scale down these properties, the following simple relation holds [68].

$$\frac{Pl_m}{Pl_p} = \frac{Wl_m}{Wl_p} = \frac{Tl_m}{Tl_p} = \frac{1}{N} \qquad \frac{Pt_m}{Pt_p} = \frac{Wt_m}{Wt_p} = \frac{Tt_m}{Tt_p} = \frac{1}{N} \qquad [68]$$

There is a linear relation between the scale factor and the one dimensional geometrical properties of the grid. When the difference between length and surface scales are considered, than a simple relation shows that the surface scale factor counts quadratic with respect to the length scale factor.

$$\frac{A_m}{A_p} = \left(\frac{1}{N}\right)^2 \qquad \text{so: } n_a = n_l^2$$

Based on the concept of geometrical scaling and fulfilling the Froude ratio, every scale factor for each parameter can be expressed in the length scale factor. In section 4.2 it is derived that the scale factor for velocity would be equal to the root of length scale factor. The different scale factors are derived below.

Length	L	n_l
Velocity	$u = \frac{\text{length}}{\text{time}}$	$n_u = n_l^{1/2}$
Time	$t = \frac{\text{length}}{\text{velocity}}$	$n_t = n_l^{1/2}$
Acceleration	$a = \frac{\text{velocity}}{\text{time}}$	$n_a = n_l^{1/2} / n_l^{1/2} = 1$
Force	$F = \text{mass} \cdot \text{acceleration}$	$n_F = \rho n_l^3$
Pressure	$\sigma = \frac{\text{force}}{\text{area}}$	$n_p = n_l$

4.4.2 Scaling of the Elasticity

Proper scaling of the material properties is important to be able to apply the experimental results on situations in the field. An important parameter is the elasticity, which should be scaled down by a factor n . The request is that the material applied in the model should show the same percentage of strain as a result of the scaled down force. The idealised tensile stress-strain behaviour is presented in Figure 4.2. With identical scaled material characteristics the percentage of strain should be equal for the model and the prototype: $\varepsilon_m = \varepsilon_p$

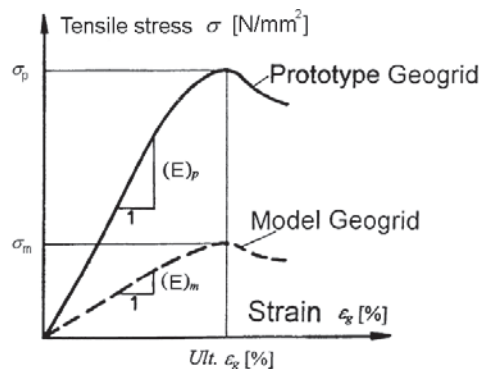


Figure 4.2: Idealized stress-strain behaviour

To fulfil this request equal strain percentages imply that the amount of tensile stress and the elasticity of the geogrid should be scaled down with a factor N. The definition of elongation is given by formula [69].

$$\varepsilon = \frac{F}{AE} \quad [69]$$

$$\frac{E_m}{E_p} = \frac{F_m}{F_p} \frac{A_p}{A_m} \frac{\varepsilon_p}{\varepsilon_m}$$

Based on the Froude relation, the following scale factor for the elasticity based on the geometrical scale is the result:

$$\frac{F_m}{F_p} = \left(\frac{L_m}{L_p} \right)^3 = \frac{1}{n_l^3} \quad \frac{A_p}{A_m} = \left(\frac{L_p}{L_m} \right)^2 = n_l^2 \quad \frac{\varepsilon_p}{\varepsilon_m} = 1$$

Filling in these different scale factors results in the factor for the elasticity, which is equal to the geometrical scaling factor as proven below. It should be noticed that changing the elasticity of a material can develop in different material behaviour.

$$\frac{E_m}{E_p} = \frac{L_m}{L_p} = \frac{1}{n_l}$$

4.4.3 Scaling of the Flexural Rigidity

The rigidity of the grid also influences the sensitivity to deformation. The expression of the flexural rigidity is indirectly influenced by the elasticity of the material. The elasticity should be scaled down by the same factor as the length. The effect of this relation is that a plastic model of a geogrid will tend to have unrealistic elasticity properties if the scale factor is too high. This can for example be seen if the cross section of a geogrid rib is taken into account. This surface will decrease quadratically and the model grid will loose too much of its flexural rigidity, though a compromise can be made.

Reasonable agreement can be achieved by ensuring that the overall moment of inertia is correct. For plastic models this can be done by exaggerating the thickness or width of the construction. The effect is that the structural density starts to deviate, but for the geogrid this is not a problem. The best approach to solve this problem is first by considering a simple deformation equation of a beam that is subjected to a moment [70]. In this formula shape and elasticity are included.

$$\frac{1}{r} = \frac{M}{EI} \quad [70]$$

With:

r	= Radius of curvature	[m]
E	= Elasticity modulus	[N/m ²]
M	= Moment	[Nm]
I	= Moment of inertia.	[m ⁴]

By applying the formula of *De Vries 1976* on this definition:

$$\frac{r_p}{r_m} = \frac{M_m}{M_p} \frac{E_p}{E_m} \frac{I_p}{I_m}$$

Based on the Froude scaling rule this results in:

$$\frac{I_m}{I_p} = \left(\frac{L_m}{L_p} \right)^5 \frac{E_p}{E_m} \quad [71]$$

The result is that the surface of inertia (I) should be scaled by a factor n_1^4 . This value falls in the line of expectations since the unit of area of inertia is m^4 . Depending on the scale factor n_1 , this area of inertia will decrease rapidly. Scaling of a geogrid is quite difficult since there is no defined area of inertia. A solution could be to approximate a single rib as a beam. Based on the dimension the scale factors can be applied.

With formula [71] the area of inertia is calculated by using the average values for the width and thickness of E'grid geogrid 4040L. Different scale factors are presented with different values of the width and thickness of a rib in combination with the accompanying elasticity. The results are presented in table 4.3. The conclusion from this table is that the scaling of geogrids can be done to a maximum scale factor of 4 to 5. Scaling based on this approach is rather inaccurate, since the ribs do not have a constant dimension. An improved solution of scaling is based on the product of EI.

$$I \propto W \cdot T^3$$

Scale [-]	I mm ⁴	W mm	T mm	E N/mm ²
1	19.7	4.0	1.7	5252
2	1.23	2.0	0.9	2626
2	1.23	1.0	1.1	2626
2	1.23	0.5	1.3	2626
3	0.24	1.0	0.6	1751
3	0.24	0.5	0.8	1751
4	0.08	1.0	0.4	1313
4	0.08	0.5	0.5	1313
5	0.03	1.0	0.3	1050
5	0.03	0.5	0.4	1050

Table 4.3: Scaled rib dimensions

4.4.4 Scaling the EI Parameter

In the table above the parameter for elasticity (E) and area moment of inertia (I) are scaled by the derived relations based on a constant Froude number. The effect is that scaling of a E'grid geogrid is restricted to certain values. Tolerance is present by considering the product EI. The combination of elasticity and area moment of inertia should be scaled with a factor n_1^5 . By scaling the elasticity more down than a factor n_1 , for example n_1^2 , the moment of inertia can be scaled down with factor n_1^3 . The scaled flexural rigidity will not be influenced in this way.

Besides this point of attention there is also a physical restriction. The elasticity of E'grid geogrid is already on the lower side in the spectrum of different material elasticity properties. A scale factor 3 would result in a model elasticity that is 9 times smaller. Grids with such a low elasticity are difficult to find, but will also show behaviour that will not correspond with the accompanying scale since the material has different properties.

A certain variation between the elasticity and area moment of elasticity is possible, but scaling factors cannot deviate too much from their origin. The best manner to check if the product EI fulfils the requirement is by performing a flexural rigidity test. The overhang length c is also a length which can be geometrically scaled by a factor n_1 .

The combination of the material elasticity and surface area of inertia come together and determine the flexural rigidity of a fabric. In the ASTM 1388 test, the flexural rigidity of a cloth is determined. An apparatus as described in the standard ASTM 1388 is not available, but an alternative method can be applied with a comparable result.

In mechanics all kinds of relations are available that give the relation between the load and deflection. In these formulas the elasticity and surface area of inertia are included. For a beam that is fixed at one side this relation is as follows:

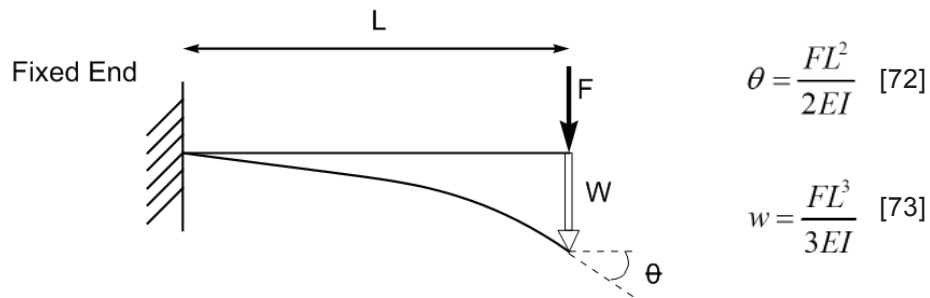


Figure 4.3: Deflection of a beam

Based on the figure above a relation between the force and the deflection can be set-up, to determine the scale factor between two materials. A piece of E'grid geogrid is taken and the deflection is measured for several lengths and several weights. The same is done for a piece of potential model material. The length and weight are scaled and the deflection should resemble the scaled deflection of the E'grid geogrid. A scale material based on a scale factor 5, should for example, have the following properties for length, deflection and force if the original E'grid geogrid material is 50 cm long and gives a deflection of 15 cm with a weight of 50 grams.

- Length:	$L_m = L_p / n$	$= 50 / 5$	$= 10$ cm
- Deflection:	$w_m = w_p / n$	$= 15 / 5$	$= 3$ cm
- Mass:	$F_m = F_p / n^3$	$= 50 / 5^3$	$= 4$ gr

4.4.5 Determination of the Scale Factor.

The scale factor will be determined based on the behaviour of the model material. Several samples of potential model grids were provided by suppliers. The firm Afcon has several small types of synthetic grids in their assortment mainly for the purpose of building outdoor bird cages. The type BKT 96 is a grid that looks comparable to that of E'grid geogrid. The grid is made from polypropylene and is produced on the same manner. Figure 4.4 shows a picture of the prototype material and the model material.

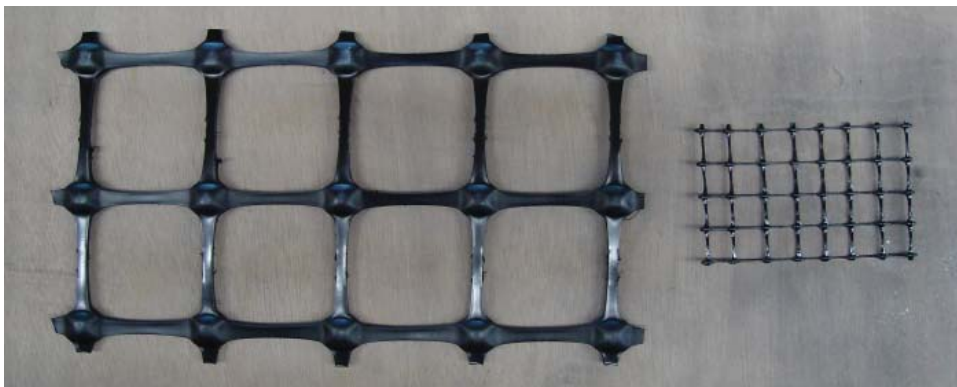


Figure 4.4: Prototype and model material

A piece of E'grid geogrid 4040L is taken and cut to a length of approximately 100 cm (18 apertures) and a width of 20 cm (4 apertures). This piece is clamped at one end. E'grid geogrid is not totally homogeneous the production process and rolling up of the grid results in some tension in the grid. Placed on a flat surface the grid follows a hollow shape. This is mainly due to the production process. Figure 4.5 shows the difference in deflection in two directions under its own weight. For this reason the experiment is performed in transversal and in longitudinal direction. For both directions the grid is also turned over. The grid is not fully flat and shows a convex (n-shape) or concave shape (u-shape).

To decrease the influence of the pre-stresses, that are present in the grid, a weight is used. The experiment is performed with two types of weights to create a solid base. A weight of 150 gram and of 250 gram have been used. Figure 4.6 shows the deflection due to a mass.



Figure 4.5: Difference in deflection due to the own-weight in longitudinal and transversal direction

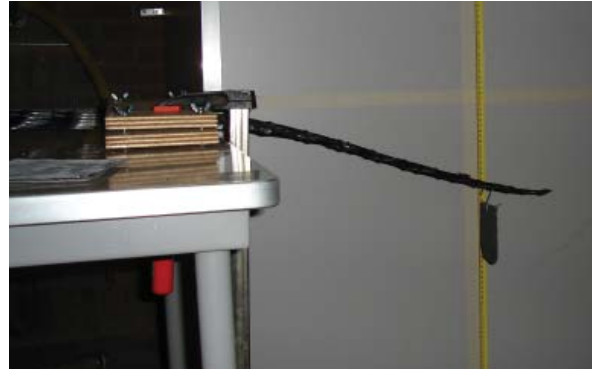


Figure 4.6: Measuring the deflection of E'grid geogrid with a mass

The results of the deflection of E'grid geogrid are presented in Figure 4.7. On beforehand it is not known what the scale factor is between the prototype material and model material. Three scale factors are tested: 4, 4.5 and 5. The scaled down deflection values of the prototype are used on the model material deflection.

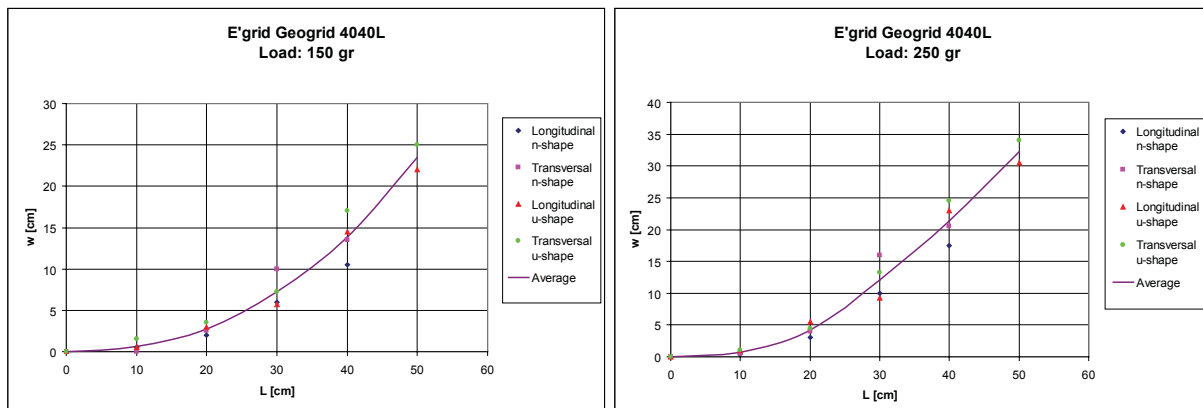


Figure 4.7: Deflection of the E'grid geogrid under a 150 and 250 gram mass

The deflection and the accompanying scale are presented in Figure 4.8. From this figure it can be concluded that for a scale of $n=4.5$, the model material fits the best. It should be noticed that for the longitudinal directions the model material does not fit the results. The reason for this is that the model material has a different structure. When a closer look is taken, it can be seen that the crossing ribs are not fully interconnected as in the E'grid geogrid. The ribs are laying over each other. The effect is that the material behaves different, depending on the side of the material. The transversal ribs are also thinner than the longitudinal ribs. For the construction of the model gabions this is taken into account. Each side of the material is in the proper direction.

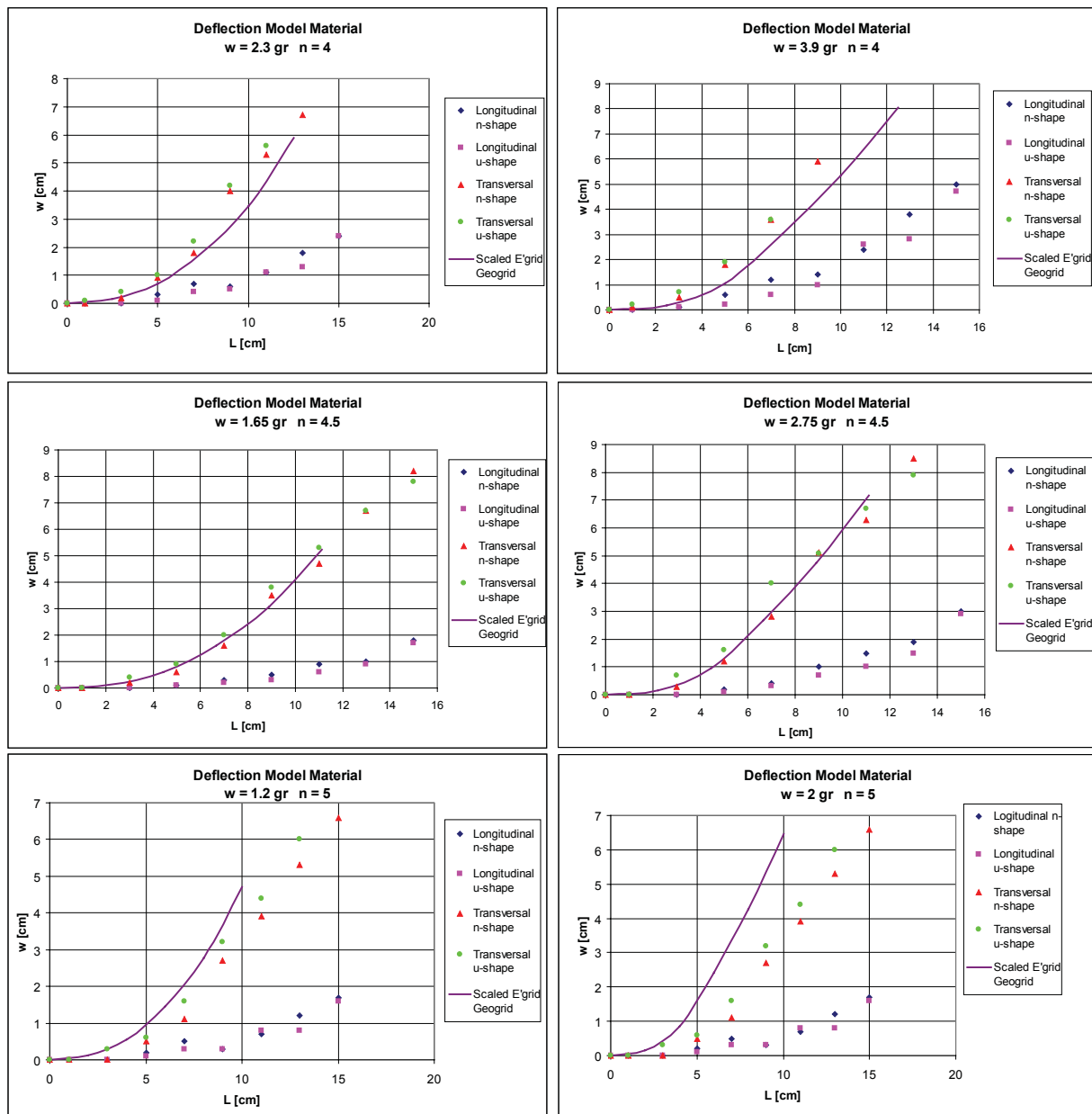


Figure 4.8: Determination of the model material scale based on the scaled E'grid geogrid deflection

4.5 Expected Failure Process

With the prototype scaled down experiments can be executed to investigate the deformation and sliding of gabions under wave attack. By altering different parameters during the experiment, it can be examined how these properties influence the functioning and behaviour of the gabion. Failure will be caused by insufficient coverage of the fill material on the filter, or by sliding of the mattress.

A good base for determining the proper method with respect to measuring and execution, is estimating the expected results and the order of these results. The processes that takes place in the protection can be divided in different classes, if the wave height is considered from low to high. The mechanism is described by the following steps:

1) Low Waves, No Movement

When very low waves are subjected on the bank and the stones are considered stable, no movement of fill material will take place. The fill material is also stable by itself if it is placed on a slope.

2) Low to Medium Waves, Little Movement

By increasing the waves, little movement of the fill material will take place. During this situation a first replacement of the particles, that are not hindered or blocked, is taking place. The smaller particles of the fill material will settle between the pores that are present between the larger stones, after little movement of the fill material. Resettlement and increased compaction is taking place until a equilibrium situation is the result. Deformation of the gabion grid has not started in this phase.

3) Medium Waves, Particle Vibration

With medium wave loading the forces on the particles increase. The larger particles inside the gradation will start moving if space is available. The friction force is a important aspect for preservation of the equilibrium situation of a particle. The coverage of the fill material gives a contribution to the stability of the stones. The friction is derived by partly protrusion of the fill material through the apertures. This is the so-called interlocking mechanism (Figure 4.9). The particles could move in downward direction, but are blocked by the grid. Vibration of the particles present in the upper layer could take place if they are not fixed by neighbouring particles.

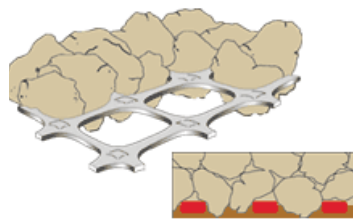


Figure 4.9: Interlocking of particles in a geogrid

4) Medium to High Waves, Geogrid Deformation

By increasing the wave height the flow velocity through the fill material will increase. During this moment the influence on the grid will start to become more important. Potential deformation of the geogrid is initiated when the uplift forces become too high and execute a pressure on the lid in upward direction. Extra space develops due to this process and resettlement of the fill material takes place.

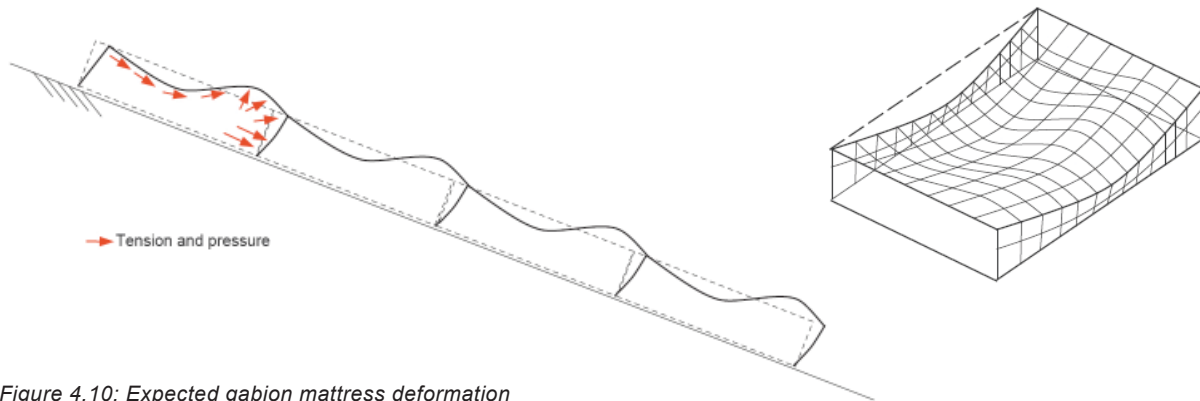


Figure 4.10: Expected gabion mattress deformation

It is not only expected that the lid of the mattress will deform into a curving shape, but that the diaphragms inside the mattress will show some degree of rotation. The whole construction will show some skewness. Deformation is a result of fill material accumulation, which gives certain pressures and tensions on the grid. Figure 4.10 gives an indication of the mechanism and stresses. In the lower part of the compartment pressure will develop, caused by the accumulated fill material.

The expectation is not that every gabion on the revetment will show the same degree of deformation. The highest degree of deformation will be found in the breaker zone area. The gabions in this zone will be subjected to the highest run-up and run-down velocities. Above and below this area only little degree of deformation will be present.

The amount of deformation will also differ from place to place inside the gabion. Main reason for this is that the vertical planes, which stand parallel to the angle of wave attack, generate some extra stiffness. E'grid geogrid is a quite stiff material that shows flexible behaviour on loads perpendicular to the plane. Loads that work parallel inside the plane are very well able to be absorbed without deformation. A certain resistance to deformation is expected around these planes.

5) High Waves, Failure of the Construction

The expectation is that in the above described situation, with a certain degree of deformation, an equilibrium situation will develop. By increasing the wave height two mechanisms of failure can be the result.

The first possible failure mechanism could be the deformation continues, which results in a shortage of coverage of the sublayer. The filter layer will be damaged and potential start of erosion will be initiated. This problem can be prevented by placing enough fill material in the compartments or by increasing the thickness of the mattress.

A second possibility of failure is sliding of the construction. The uplift forces generated by the waves, combined with the strong drag-, and shear forces can result in sliding or partly sliding of the whole mattress.

4.6 Experiment Program

4.6.1 Experiment Objectives

As mentioned in the introduction of this chapter, a general fear is present that synthetic gabions deform when these are subjected to waves. From the material description it comes forward that geogrid is suitable for the construction of synthetic gabions. The current design rules are based on the initiation and vibration of fill material movement. Synthetic material is not restricted to this requirement, so it creates possibilities for adapting the design formula.

The sensitivity to deformation of the gabion plays an important role in the functioning of the construction, but also in the acceptance of the construction. It is important that information about the potential deformation is available. It is therefore important to quantify, determine and investigate the sensitivity of the synthetic geogrid gabion to deformation. The role of the fill material plays an important role in quantifying this process. Aspects as: fill material size, compaction and shape will be implemented.

In the stability analysis for gabions it came forward that Pilarczyk's design formula does not take all aspects into account. There is space for improvement of the formula with respect to the friction, permeability and construction length. The expectation is that by altering these parameters, different stability curves develop which will have the same shape as Pilarczyk's stability relation.

Summarizing the following points are of interest for the objectives of this project:

Deformation of gabions:

- Description of the deformation process.
- Investigate the sensitivity to deformation by adapting the fill material properties.
- The influence of grid stiffness.
- Quantifying the deformation.

Stability of gabions:

- The influence of the filter permeability on the stability of the protection.
- The influence of the filter friction on the stability of the protection.
- The influence of the length of the revetment on the stability of the protection.
- Set up an advise for potential improvement of the design formula for a gabion revetment protection in waves.

4.6.2 Altering Parameters

The experiment program should result in information that covers a great amount of the possible unknown situations. Deformation and sliding are the causes for gabion revetment failure. By varying different parameters a better insight in the process of failure is achieved. With the experimental results recommendations and restrictions to the design will be made. In the coming section the experiment program is described. The following parameters will vary for the described reasons and objectives.

- Geogrid Stiffness

The contribution of the geogrid stiffness in the deformation process is not known. The mutual support of the fill material could result in an effect that the deformation will be of a rather limited degree if the filling degree of the compartment is good enough. Almost all experiments will be performed based on the scaled model of E'grid geogrid, which is considered as relatively stiff. As a comparison a experiment will be performed that consists out of a grid with considerable less flexural rigidity. Based on the difference in behaviour, recommendations can be made about the influence of grid stiffness.

- Fill Material

In steel wire gabions it is advised to use round fill material to minimise the effect of damaging the protective layer of the grid. Round fill material has less mutual friction and the expectation is that it will move easier through a compartment. Round fill material, like gravel, is also more expensive compared to angular rock. One of the advantages of synthetic geogrid is that it is possible to apply angular fill material. This material has better mutual friction properties that will potentially show less deformation compared to the same situation where round fill material is applied. To check the validity of this assumption a test will be performed in which the angularity of the fill material is altered. It is expected that deformation is also influenced by the size of the fill material. Three types of fill material are applied. Further information is presented in appendix B.

1) Gravel	16-32 mm	D_{50}	= 24 mm
2) Small Angular	10-20 mm	D_{50}	= 15 mm
3) Angular	16-32 mm	D_{50}	= 25 mm

- Compaction

One of the parameters that can influence the amount of deformation is the compaction degree of the fill material. The base of the deformation problem is an excess of space that develops during time on the short run by compaction improvement due to waves. On the long run potential elongation can cause deformation. Even more important is the bulging of the compartment lid caused by the uplift pressure of the waves. Increased compaction of the fill material could decrease these effects, because the interlocking effect improves. For the experiment two types of compaction will be used to research the influence of the compaction degree on the deformation process. Based on the experience, recommendations will be made to determine the amount of fill material in a compartment.

1) Normal Filling of the Mattress.

The mattress is filled based on the volume of the compartment. The porosity of the fill material is taken into account. In the calculations a porosity of 0.4 is used. Gabions will deform and protrude partly so the applied porosity is between 0.35 and 0.40

2) Improved Compaction.

By improving the compaction less space for fill material transport is available. The desired effect is that less deformation will be the result. By subjecting the compartment to vibrations the compaction will increase. But also the bottom side should be slightly lifted to let particles protrude. Closure of the compartment is done under tension of the connection. The lid of the compartment will have a more curved shape.

- Fill Material Size

Altering this parameter is interesting with respect to the functioning of the gabion. On one side the larger and heavier fill material will be relatively less sensitive to the wave action, but it might be possible that on the top side of the compartment not enough coverage of stones is present when the deformation process starts. A smaller type of fill material might be transported more easily through the grid, but if a equilibrium situation is reached, a better coverage of the total compartment could be achieved.

- Slope Angle

A steeper slope results in easier movement of the fill material, though if a equilibrium situation is reached then the amount of deformation might be comparable. Besides the deformation, failure of the revetment caused by sliding is an important mechanism. Using different slopes creates a wider base for an improved stability relation. Slopes of 1:1.5, 1:2 and 1:3 are used. A slope of 1:1.5 is more or less the maximum allowable steepness for gabion revetment protections. A slope angle of 1:3 is a situation which is more common.

- Wave Height and Iribarren Number

The wave height and shape are the main parameters on which the design rule of Pilarczyk is based. In the stability analysis it came forward that this is quite an important parameter with respect to the run-down. The expectation is that different filters and designs will result in different stability relations. To create a base for a certain stability relation it is important that a number of test is performed for a particular situation, with different Iribarren numbers. The bandwidth of the breaker parameter lies between 1.5 and 5. The wave height will depend on the Iribarren number. To approximate the moment of failure, the waves will be increased step by step. By recording the initiation of motion and following the process of deformation, information is gathered about the role of the fill material.

- Filter Influence

The layer that is present under the protective layer is of equal importance for stability of the construction. A proper designed filter is important to transfer the uplift pressures. In gabion revetments the filter consists of a geotextile, or a combination of granular layer and a geotextile. By performing experiments with different filter layers the added value of a granular layer, on the stability and deformation, can be judged.

- Mattress Design

Thicker mattresses have more potential to resist against wave attack, since the weight of the compartment increases, the resistant force of the mattress increases. Three different mattress thicknesses are used. A 30, 40 and 55 mm variant. This done to cover the stability relation for the smaller breaker parameters, which will fail with higher waves. There are some restriction to the maximum wave height. Therefore thinner mattresses are used, because the thicker variant might not fail due to sliding.

The second argument for thickness variation is the influence on the deformation and especially the sensitivity to this process. Thicker mattresses have a better ability to cover the sublayer than a thinner mattress with the same filling degree.

4.6.3 Experiment Program

The experiment description is divided in two categories. The scale tests consists of two main points of interest: deformation and failure due to sliding. Table 4.5 gives an overview of the deformation test program. In appendix D the experiment results are presented, and a more complete description of each experiment is given.

Test [-]	Dn [mm]	ξ [-]	α [-]	Compaction [-]	Fill [-]	Filter [-]
D1*	40	3	1:1.5	Normal	Small Angular	Granular
D2	40	3	1:1.5	Normal	Gravel	Granular
D3	55	4.5	1:1.5	Normal	Gravel	Granular
D4	40	3	1:1.5	Increased	Angular	Granular
D5	30	3	1:1.5	Normal	Small Angular	Granular
D6	40	3	1:1.5	Increased	Small Angular	Granular
D7	55	3.5	1:1.5	Normal	Gravel	Granular
D8	55	3.5	1:1.5	Normal	Small Angular	Granular

* Experiment D1 is performed with a weak grid

Table 4.5: Deformation test program

Table 4.6 gives an overview of the sliding experiments. In total 8 different revetment situations are tested. Each colour, in the table, represents a revetment construction. The varying factor is the mattress length or filter construction type. To develop a stability relation for each revetment construction the situations are tested for several Iribarren parameters. Figure 4.11 gives a schematic overview of all situations.

Test S12 and S13 are not used in a stability relation. The results are used to validate the mutual relations between the different runs. More details about each test are implemented in appendix D: Experiment Results.

Originally the test program consisted out of 6 runs. During the execution of the tests S22 and S25, it came forward that the experiments could not be performed, since it was not possible to create failure of the revetment. The capacity of the wave generator was insufficient to create a wave of such a degree that the mattress would slide down. For this reason the runs 7 and 8, based on a 1:2 slope, were added.

Run [-]	Test [-]	Dn [mm]	ξ [-]	α [-]	Mattress [-]	Fill [-]	Filter [-]
1	S1	40	3	1:1.5	Long Rev	Gravel	Granular
	S2	55	5	1:1.5	Long Rev	Gravel	Granular
	S3	55	4	1:1.5	Long Rev	Gravel	Granular
	S4	55	3.5	1:1.5	Long Rev	Gravel	Granular
	S5	55	3	1:1.5	Long Rev	Small Angular	Granular
	S6	30	2	1:1.5	Long Rev	Small Angular	Granular
	S7	30	3	1:1.5	Long Rev	Small Angular	Granular
2	S8	30	2	1:1.5	Short Rev	Small Angular	Granular
	S9	55	5.5	1:1.5	Short Rev	Small Angular	Granular
	S10	55	3	1:1.5	Short Rev	Gravel	Granular
	S11	55	4	1:1.5	Short Rev	Gravel	Granular
	S12	40	2	1:1.5	Long Rev	Small Angular	Gran + Geo
	S13	40	3	1:1.5	Long Rev	Small Angular	Gran + Geo
3	S14	30	1	1:3	Short Rev	Small Angular	Geotextile
	S15	40	2	1:3	Short Rev	Angular	Geotextile
	S16	55	4	1:3	Short Rev	Angular	Geotextile
4	S17	30	1	1:3	Long Rev	Small Angular	Geotextile
	S18	40	2	1:3	Long Rev	Angular	Geotextile
	S19	30	3	1:3	Long Rev	Small Angular	Geotextile
	S20	55	4	1:3	Long Rev	Angular	Geotextile
5	S21	30	1.5	1:3	Long Rev	Small Angular	Gran + Geo
	S22	30	3	1:3	Long Rev	Small Angular	Gran + Geo
	S23	40	4.5	1:3	Long Rev	Small Angular	Gran + Geo
6	S24	40	1.5	1:3	Short Rev	Small Angular	Gran + Geo
	S25	30	3	1:3	Short Rev	Small Angular	Gran + Geo
	S26	40	4.5	1:3	Short Rev	Small Angular	Gran + Geo
7	S27	30	1.5	1:2	Short Rev	Small Angular	Geotextile
	S28	55	3	1:2	Short Rev	Small Angular	Geotextile
	S29	30	1	1:2	Short Rev	Small Angular	Geotextile
8	S30	30	2	1:2	Short Rev	Small Angular	Gran + Geo
	S31	30	2.5	1:2	Short Rev	Small Angular	Gran + Geo
	S32	30	3	1:2	Short Rev	Small Angular	Gran + Geo
	S33	30	4.5	1:2	Short Rev	Small Angular	Gran + Geo

Table 4.6: Sliding test program

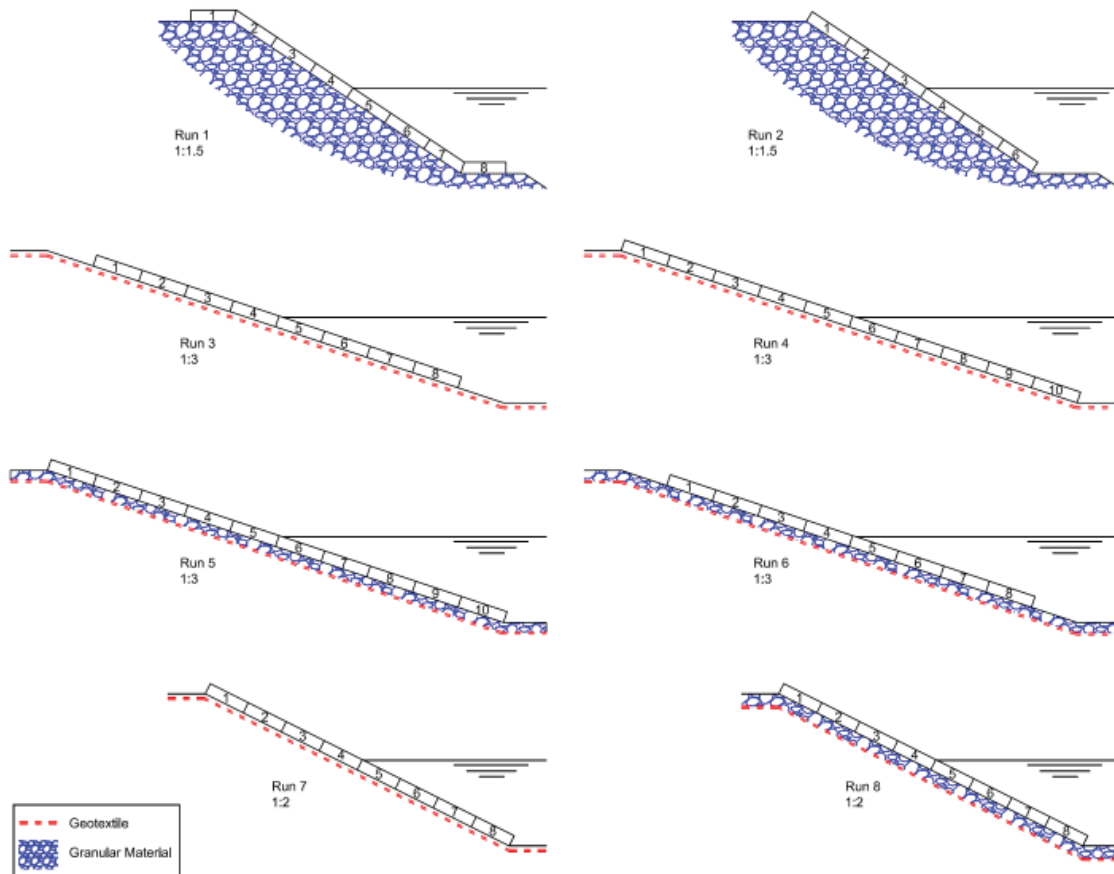


Figure 4.11: Revetment design representative for each run

Run 1 and 2

A homogeneous sublayer, consisting of granular material. The slope angle is of such a steep degree that the crown and toe compartment have considerable influence on the stability. A design like this is quite common. Run 2 is also performed on a homogeneous sublayer, only without the toe-, and crown compartment.

Run 3 and 4

This design is based on the smoother geotextile filter layer. The influence of the decreased friction factor and permeability of the filter are the main parameters of interest. Due to the decreased friction factor is the slope angle adapted to 1:3. The difference between the runs is that run 4 is executed with a relative shorter mattress.

Run 5 and 6

Run 5 and 6 are performed on a 1:3 slope and based on a different filter alternative. A geotextile and granular filter combination is applied. The increased friction between the mattress and filter should improve the stability. During the execution it came forward that the wave generator could not create waves to let the mattress slide down.

Run 7 and 8

The set-up of the runs 5 and 6 consisted a relative too gentle slope. The original test program was adapted by adding run 7 and 8, consisting of a 1:2 slope. Run 7 is executed on a geotextile filter. Run 8 is performed on a geotextile and granular filter combination.

4.7 Experiment Set-up

4.7.1 Wave Flume

The experiments are performed in a wave flume with an overall length of 13 m. The flume consists out of four main parts.

- 1) The slope on which the mattress is placed. During the experiments the slope angle is adapted.
- 2) A set of wave gauges to measure the different wave parameters.
- 3) A wave generator. This machine is only capable of generating regular waves. A wave spectrum is not possible with this device.
- 4) Reflection compensation is placed behind the wave generator to absorb the developed waves behind the machine.

Figure 4.12 and 4.13 give a general overview of the set-up together with some dimensions.



Figure 4.12: Overview experiment set-up

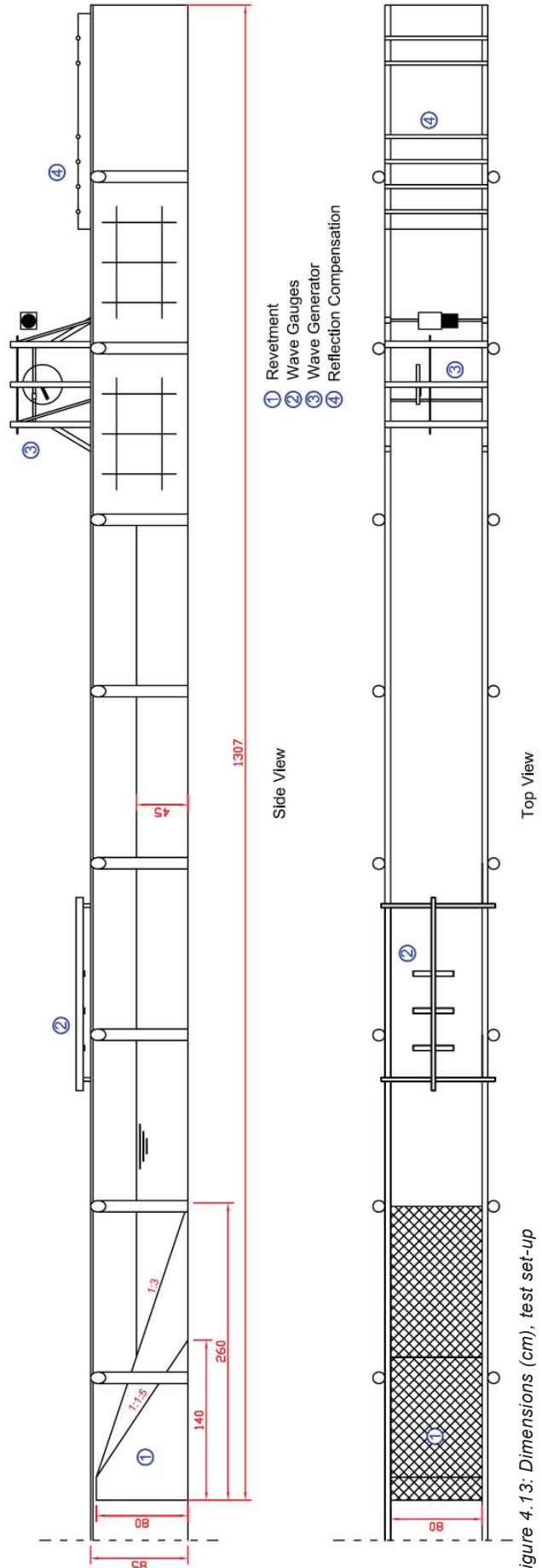


Figure 4.13: Dimensions (cm), test set-up

4.7.2 Construction of the Gabion Model Mattress

The experiment is performed based on a gabion mattress with a compartment prototype dimension of 1 meter wide and 2 meter long. Scaling with a factor 4.5 results in compartments of 22 x 45 cm.

The flume has a width of 80 cm. Placing two compartments next to each other would not be possible and unwise, since side effects are present along the glass side wall. A stroke of one complete compartment is placed in the middle of the flume. To simulate the mutual support, compartments half of the original length are placed on both sides. Figure 4.14 represents the mattress construction.

In a normal situation the lid is placed over several compartments. To decrease the building time, of the experiment, is the mattress divided in strokes of two. During filling of the elements only one side of each compartment has to be opened.

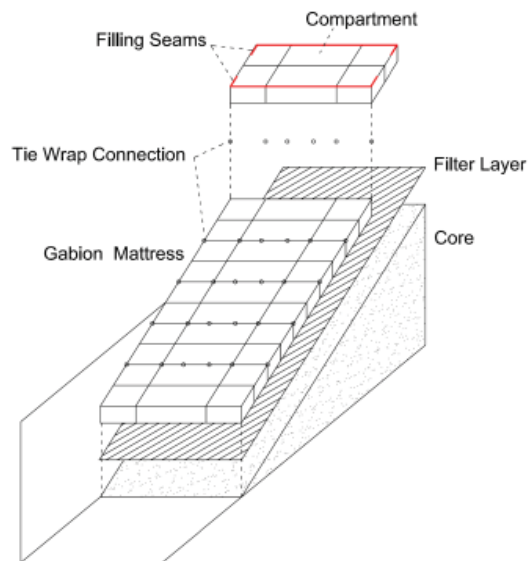


Figure 4.14: Mattress construction



If the slope of core material is placed, a filter layer is constructed. In the situation of a geotextile filter, the cloth is cut into its shape and placed over the core. When a granular filter is applied the thickness of the layer should be one fifth of the original situation. The minimum thickness of a filter layer in a prototype situation is 20 cm. In the scale model this is 4 - 5 cm. The size of the granular filter layer for this experiment will be 4 - 8 mm with an angular shape. The core material consists out of the same granular material.

The compartment strokes are filled outside the flume, closed and placed inside the flume. The strokes are placed and connected with tie-wraps. By connecting the compartments with enough tie-wraps a homogeneous mattress connection is gained.

4.7.3 Measurements

Revetment Measurements

The deformation of the geogrid is measured by using a level instrument that is placed on a cart that rides over the flume. Along the rail a ruler will be placed in combination with an indicator on the cart. Based on this indicator the coordinates in the X-direction along the flume can be found.

The difference in height will be measured with a level instrument. By lowering the level of the depth gauge, the z-coordinate can be determined. To prevent measurement errors caused by a steep point, that could protrude in a pore of the mattress, a half sphere is placed at the end. The measuring of rip-rap constructions is based on the same method. The diameter of the sphere should be two times the D_{50} of the cover layer. The average size of the fill material is 15 mm. A sphere with a diameter of 30 mm is placed under depth gauge. Figure 4.15 represents a cross section of the measuring method.

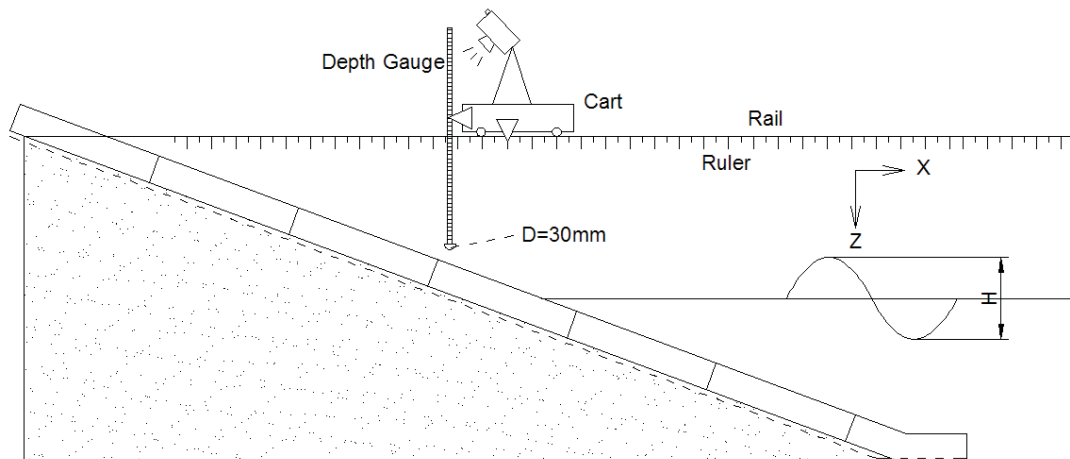


Figure 4.15: Cross section measurement method

The Y-coordinate is measured by placing a ruler on the cart. Along this ruler the depth gauge can be moved. Based on fixed X-, and Y-coordinates the altering Z-coordinate can be measured from one specific point. Measuring the deformation will be performed along the in advance determined points. Higher amounts of deformation will take place along the water line. The intensity of the measuring points will therefore be the higher in this area.

Along the revetment the wave run-up and wave run-down will be measured. This is done by writing down the increase and decrease of the water level on the side of the flume for every wave step. Afterwards, when the wave height is determined, the accompanying run-up and run-down levels are added.

Wave Measurements

The waves are measured with an acoustic system. Three wave gauges are placed over the flume. The equipment gives of an acoustic signal. These signals reflect on the water surface. The time it takes for a signal to travel the distance is measured by the wave gauges. Based on the velocity of sound through air, the wave height is measured. Figure 4.16 gives a schematic representation of the method.

Three wave gauges are used. The reason for this is that the wave period and wave height of the reflected wave can be measured. These values are calculated based on a Matlab script. Disadvantage of the acoustic system is that noise in the measuring data can originate. During high waves or rapid water level fluctuations some signals reflect on the bottom of the flume. This creates peaks in the data. Before the data is used, for wave parameter calculations, it is filtered by a different script. In appendix C the filter method is described.

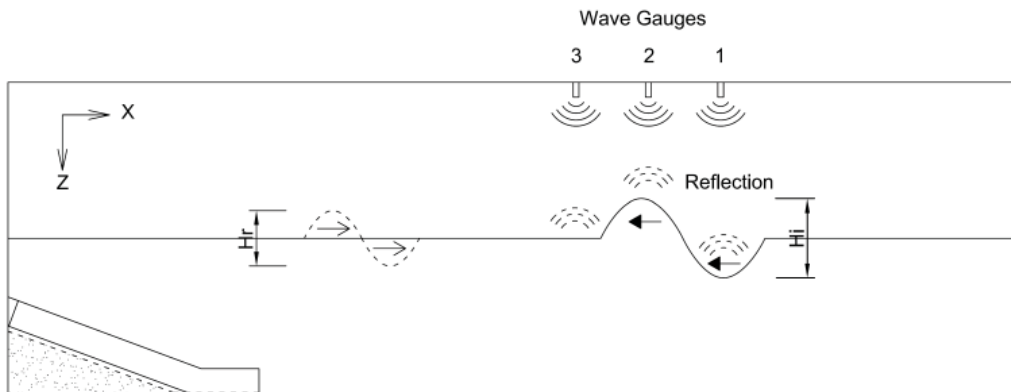


Figure 4.16: Acoustic wave measurement

4.7.4 Work Method

The experiment is performed by increasing the waves during different stages. In the description below, these phases are presented in combination with the measurements that are performed. A certain amount of waves must have reached the protection before it can be concluded that the situation is stable. The wave generator is only capable of producing regular waves. For the experiments it is assumed that after 500 waves, without any increasing deformation or sliding, the situation is stable.

Stage 1) Still Water Level

In this situation the mattress is measured in its original position. The values serve a reference for further deformed conditions.

Stage 2) Small Waves H = 5 cm

In stage two the revetment is loaded with small waves. The applied height is 5 centimetre. The idea behind this stage is to create the possibility for settlement of the fill material and potential replacement for small particles. No further elevation measurements are performed.

Stage 3) Medium Waves H = 10 cm

Compartments subjected to medium waves will show some deformation, mostly present at the water line. Compartments that show visual deformation are measured. Compartments that show no deformation are not measured, the same level as the reference values are used.

Stage 4) High Waves Increasing to H = 15 cm

Further deformation develops, but a equilibrium situation originates during several waves. Only the he visual deformed gabions are measured. Compartments that are not deformed are checked with their original position and shape.

Stage 5) Extra High Waves H = 20 cm

The waves are increased from 15 to 20 centimetre. The moment of failure is approached, since a clear boundary with respect to stability is not present. Failure due to sliding or insufficient coverage are the two main possibilities. If after 20 centimetre waves no failure has yet occurred, then the deformed revetment is measured again. It interesting to check if the equilibrium situation of the previous step still holds or if further deformation has developed.

Stage 6) Loading Until Failure

In the final stage the revetment is loaded with waves until failure occurs, if this has not already happened during the previous stages.

Revetment failure for mattress protections can occur in two ways: Inadmissible deformation or sliding of the cover layer. Failure due to deformation is defined by the fact that internal coverage of the compartment is no longer satisfying. A coverage of half the original gabion thickness is demanded. If this value decreases further, then the filter layer is exposed to flow velocities that could finally cause erosion.

The problems due to deformation can be prevented by placing enough fill material in the compartments. The second potential failure mechanism becomes sliding of the revetment. If a mattress starts sliding down the process will only accelerate itself since the anchoring length becomes shorter. Some support of the compartments below will add to the stability, but finally bulging and severe deformation of the toe structure will be the result. The boundary due to sliding is therefore set at a distance of 5 cm. When this value is passed during the experiment the construction is considered as failed.

The gabion revetment fails if:

Coverage	< 0.5 D_n
Sliding	> 5 cm

Chapter 5. Observations, Test Results and Data Analysis

In this chapter the observations of the different tests are presented. The processes and mechanisms are described followed by the test results that should confirm the observations. Finally a data analysis is performed on the test results. In this analysis several relations and recommendations are deviated.

5.1 Deformation Observations

5.1.1 Fill Material Behaviour and Grid Interaction

The function of the grid is to retain the fill material that would normally erode under certain wave conditions. It is known that a grid gives a certain contribution to the stability of the fill material. During the experiments it became more clear how this contribution is expressed.

Distinction is made between two types of fill material compaction. In the first situation the volume of the compartment was considered fixed. Based on this volume a amount of stones is placed in the compartment. The amount material is related to a void ratio of about 0.38. If a rip-rap construction would be constructed with the same material, than the void ratio of the protection would be the same.

During the experiments, with a normal compaction degree, it was noticed that displacement of fill material did not occur in the form of particle transport. Small waves, until 10 cm, resulted in a stable particle situation where no movement could be observed. Increasing the waves gave a resettlement of the fill material in total. The order of particles did not change. What happens is that fill material deforms as a whole. The more or less plane shape of the lid is transformed into a more bulging shape. Visual movement of particles cannot be seen, since the displacement is of a very little degree. Only in the upper part of the compartment, space developed. Due to the resettlement, the particles create a tension on the grid that works in retroaction back on the particles. The fill material compresses itself inside the compartment. Due to this process the particles experience a pressure which results in a more homogeneous group behaviour of the fill material.

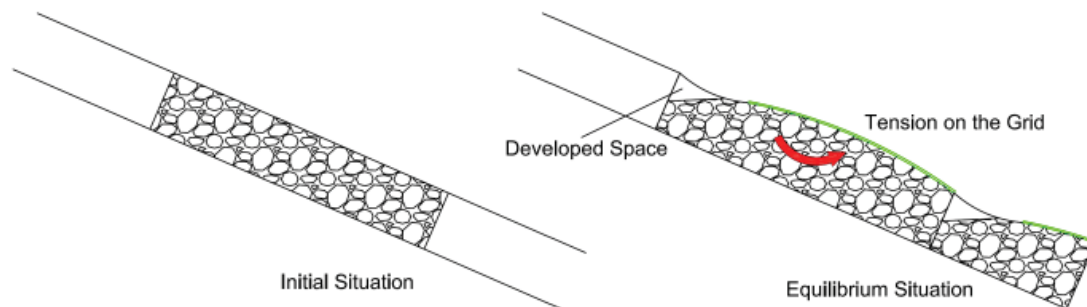


Figure 5.1: Deformation process

The part of the fill material that is present in the lower section of the compartment has no possibility for movement. Due to the developed tension and the mutual blocking of the particles, no transport or vibration occurs. The particles that directly interact with the grid are also unable to move, because of the interlocking effect (Figure 4.9). Vibration occurred only for a few particles that had some space available, caused by the surrounding of that specific location. The order of vibration was only a few millimeters. The effect of the grid is that due to the tension that originates together on the fill material, a group functioning of the particles develops. Raising the wave height does not result in further deformation of a compartment. If the fill material is in an equilibrium situation, no further movement is possible.

The bulging effect of the compartment lid results in the development of space in the upper part of the compartment. This is where a shortage of fill material originates. It forms the most sensitive area in a compartment. In this upper part, the fill material did show movement, since there is no mutual blocking of the particles.

Three mattress thicknesses are tested for deformation. It came forward that the compartment lid will always develop the same bulging shape, independent of the mattress thickness. The mattresses contained material, which all had the same filling degree, though the thinnest mattress showed the least favorable situation. The developed space is for each compartment the same, but for the thinnest mattress this is relatively the largest. The upper part of a compartment can become uncovered and erosion through the mattress can originate. Figure 5.2 represents the effect and shows that thinner mattresses are relatively more sensitive to this process.

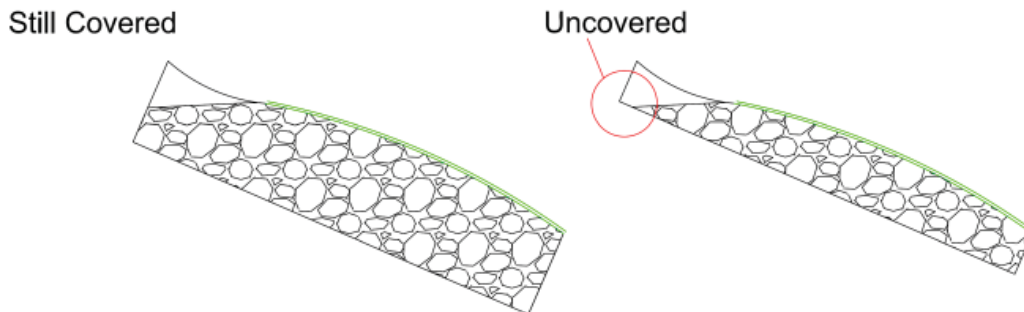


Figure 5.2: Influence Thickness

The effect is visible when two experiments are compared. Experiment D5 is executed with a 30 mm mattress and experiment D8 with an 55 mm mattress. Both had the same filling degree and fill material. In Figure 5.3 it is visible that for the thinner 30 mm mattress the grid failed due to a loss of coverage in the upper part of the compartment. The thicker mattress also shows a development of space, but the sublayer is still covered. Particles from the sublayer did not erode through the mattress.



Figure 5.3: 30 mm mattress normal filling, exp D5



Figure 5.4: 55 mm mattress normal filling, exp D8

5.1.2 Increased Compaction

The compartment of a gabion mattress should not be considered as a fixed volume. Some flexibility will always be present, especially in the lid of a compartment. The influence of flexibility can be eliminated if the final deformed shape is applied during the revetment construction. If during closure of the compartment, the lid is stretched over the fill material than the degree of deformation will be limited for a great part. The fill material is placed under the pre-tension that would normally develop due to resettlement of the fill material. In fact this is an anticipation on the development of space that would normally occur.

Experiment D4 and D6 are performed with an increased amount of fill material inside the compartment. The degree of filling is described as increased compaction. This is not a fully correct naming. The percentage of voids in the material does not decrease, but the amount of material relative to a considered fixed volume is increased. The compartments are simply filled with some extra material and closed under tension.

The extra fill material in the compartment results in bulging of the entire compartment lid. The surface of the mattress is no longer flat. The figures 5.5 and 5.6 show the shape of an increased filled mattress.



Figure 5.5: Experiment D4 improved mattress

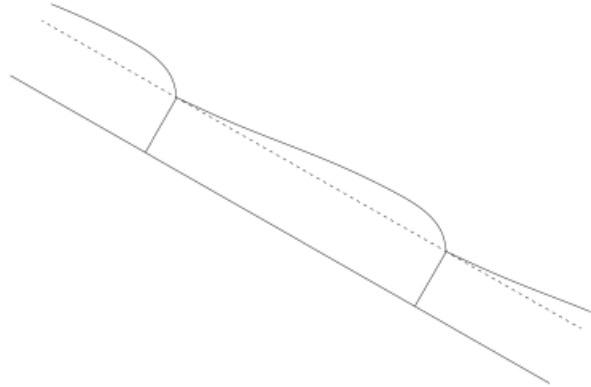


Figure 5.6: Cross-section mattress shape

During wave action the mattresses of experiment D4 functioned extremely well. It should be remarked that some degree of space developed. The cause of this, is that the compartments are filled outside the flume. During placement on the slope a little distortion of the compartment shape results in a certain loss of grid tension. Due to little compression the width decreases and tension is released from the compartment lid. After some waves the material resettled and some space developed in the upper part. This amount of space is very little and did not effect the functioning of the mattress. The picture of Figure 5.5 has been taken after 23 cm wave attack.

Experiments D4 and D6 are performed with a 40 mm mattress and increased filling of the compartments. The difference is that for experiment D4 small angular fill material is used and for D6 the large angular fill material. Small fill material has a better ability to follow the bulging shape compared to a larger variant. Increased filling of experiment D6 was gained with using relative less material, due to the larger size of the particles.

More or less the same behaviour was shown during the test. The difference was that the size of the fill material is relatively too large. A recommendation of manufacturers and Pilarczyk is to apply fill material with a d_{50} that is 1.8 - 2 times smaller than the mattress thickness D_n . The angular fill has a d_{50} of 24.5 mm. In combination with a 40 mm mattress from experiment D6 this recommendation is exceeded. The effect during the experiment was that the fill material did not show any deformation, though the turbulence through the mattress was too high. Over the total width of the compartment, particles from the sublayer eroded through the mattress. The upper part of the a compartment, which is the weakest, showed the greatest amount of protruded particles. Figure 5.7. represents the situation. The space that developed in this area resulted in more intense turbulent conditions. The sublayer was covered, but due to the large stones and relative small mattress thickness the sublayer material protruded through the voids.



Figure 5.7: Experiment D6 too large fill material

5.1.3 Influence of the Mutual Connections

If no mutual connections are present, the deformation of a compartment will increase considerably. A mutual connection results in a more fixed shape of the revetment. Bulging of a compartment results in a tension stress that is transferred to the surrounding compartments. The effect is that these compartments will experience tightening of the volume. Based on the mutual influence, these compartments will keep their shape better. Figure 5.8 explains the principle.

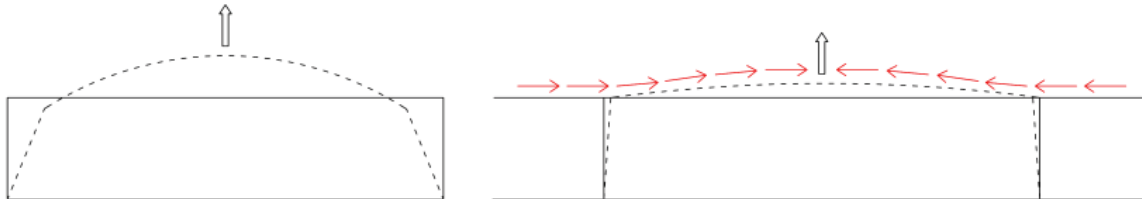


Figure 5.8: Influence of mutual connections, left: no connection, right connection

The most intensely loaded compartment, is the compartment just below the water level. In this area the first initial deformation is observed. This compartment will affect the quality of the neighboring compartments. It implicates that the compartment deserves extra attention during the construction of a revetment.

A second aspect that is influenced by the connection is the possibility of a separated mattress. When the deformation tests were performed, certain mattresses were fixed to the board to prevent failure, caused by sliding. Reason for this was to simulate an infinite long mattress that was unable to fail due to sliding.

The experiment is executed with sections that consist out of two compartments. The compartment sections are linked with tie-wraps that connect only the upper ribs. On the under side of the compartments are the ribs not connected. During a high degree of wave attack little sliding developed. The compartments stayed in position, only the low side moved. Figure 5.9 shows the effect.

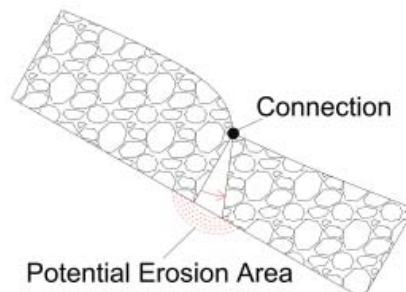


Figure 5.9: Sliding due to insufficient connections

In reality a mattress consists of six compartments. Revetment protections longer than one mattress are no exception. A connection between two mattresses should be made for the upper and lower ribs. If this is not done, there might be a risk that space originates between mattresses with erosion as a result.

The size of the fill material can influence the sensitivity to deformation. The effect of a larger fill material is that it cannot follow the shape of the bulging compartment lid as accurately as the relatively smaller fill material. During increased filling of the compartments relatively more small material can be placed in a compartment.

5.2 Sliding Observations

Run 1 and 2 - Slope 1:1.5 - Filter: Granular Sublayer

These two test series are performed on the most steep slope. Gabion mattresses will never be applied on steeper slopes, caused by the friction factor restriction. During the experiments it became clear that the longer revetment, with crown and toe compartments, have a increased stability. During a stable situation no movement or forms of uplift pressure on the mattress are noticed.

The mattress on the slopes showed a sudden failure. By increasing the waves a little the mattress failed by sliding down a considerable length. Just before the moment of failure a characteristic sound of resettling stones, present in the core, could be heard. In reality this way of failure means that no warning signal of potential developing damage will be given. Quick improvement of the revetment during severe conditions is not possible. Sliding of the mattress did not result in compression of lower compartments. The mattress slides down evenly over the total length of the revetment. Figure 5.11 shows two pictures of the before and after situation.

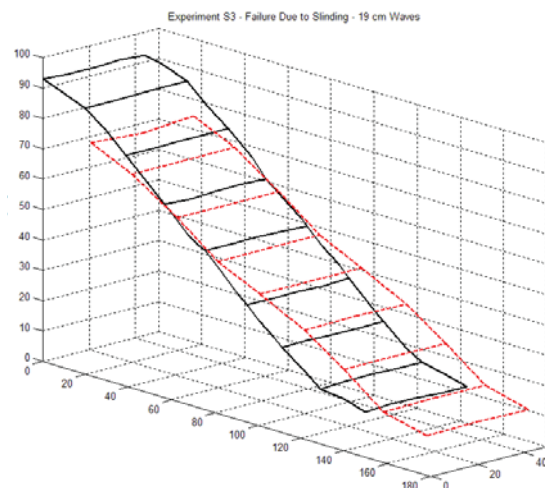


Figure 5.11: Start and finish of experiment S3

During sliding of the mattress, the material from the sublayer is taken down. In the right picture some of this material came through the edge. After sliding of the revetment a clear S-profile developed in the situation with the crown and toe compartment (Figure 5.12). In run 2 no crown-, and toe compartments are used. The sublayer kept its original shape and a S-profile did not develop.



Figure 5.12: S-profile, experiment S3



The effect of a crown construction does not only contribute with its weight, the shape also creates some extra resistance with help of the subsoil, present in the corner under mattress. The internal friction of the subsoil in this part contributes to the overall stability. In figure 5.13 a cross section is drawn in which the mechanism is explained. During the failure of the tests from run 1 this area was always taken down during failure.

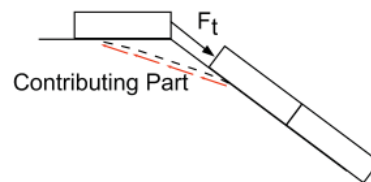


Figure 5.13: Contribution of a crown element

Due to this effect, the horizontal compartments of the crown construction contribute even more to the stability compared to a situation in which they are placed on the slope.

Run 3 and 4 - Slope 1:3 - Filter: Geotextile

Slopes with a 1:3 gradient are relatively gentle. In the literature the use of a geotextile combined with a gabion mattress in a wave climate can be applied until a certain level. Pilarczyk proposed a maximum wave height of 1 meter before a granular layer should be applied. According to the more detailed method of Klein Breteler (chapter 2) a better estimation of the need for a granular layer can be made.

The failure on the more gentle slope developed differently than the steep slope with a granular sublayer. During the experiment it could be noticed that at a certain wave height, the mattress started to show uplift around the water level. The mattress did not slide down, but showed only movement of the mattress due to the uplift pressure on the underside on the geotextile. Increasing the waves resulted in a longer and more intense movement of the mattress.

During even higher waves, the uplift expressed itself as passing wave through the mattress, following in the same frequency as the outer waves only with a phase difference. It was visible that the water level inside the core tried to follow the water level in the flume. Figure 5.14 shows the process.

During uplift a compartment is not able to absorb the driving forces. The compartment compresses the lower compartment very little and creates a tension force on the upper compartment. This process is of such a small level that movement is not visible during a single wave period. When a great number of waves traveled over the revetment it can be seen that the mattress is slowly moving down. The best way to compare the failure of the mattress is by the movement of a crawling caterpillar.

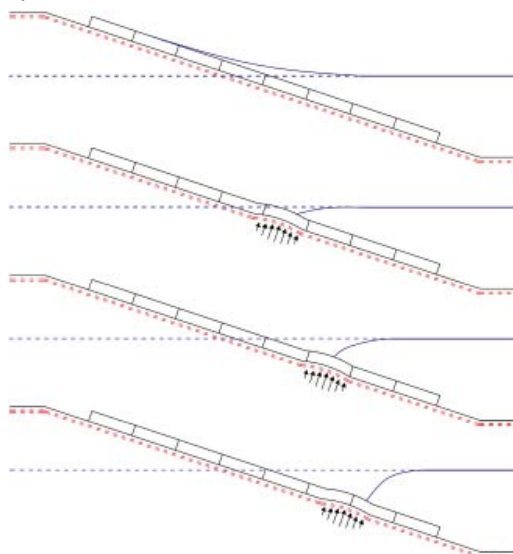


Figure 5.14: Movement in the mattress due to uplift pressure

The effect of the slowly moving mattress is resulting in bulging of the lower compartments, which are compressed by the higher placed elements. Figure 5.15 shows a picture of a lower compartment in the mattress, which is compressed. Elements on a higher position in the mattress show tension between the compartments. The development of space, between the transitions, originated due to the presence of only a upper rib connection. In the beginning of the experiments the elements are placed against each other. In reality the connection is more homogeneous due to the application of thicker wire, instead of the tie-wrap connection applied in the model.



Figure 5.15: Bulging of a compartment



Figure 5.16: Tension between two compartments

The mechanism of uplift, shown by Figure 5.14, is the result of a too low permeability of the geotextile. The mattress did not fail, but in reality a situation like this could cause problems on the long term. The turbulence that develops under the geotextile can cause transport of subsoil and a the slope angle could redefine itself. A proper designed filter will contribute to the stability of a construction.

Run 5 and 6 - Slope 1:3 - Filter: Granular and Geotextile

To prevent problems with uplift, seen in run 3 and 4, an extra granular filter layer can prevent this problem. A better transition is created and the uplift pressure is reduced. The tests of run 5 and 6 could not be further executed. The maximum wave height that could be generated inside the flume is 30 cm. During varying Iribarren parameters the construction did not fail.

The granular filter has a increased friction factor and a better ability to absorb the wave forces. For this reason the tests in run 3 and 4 could be executed and the tests in run 5 and 6 did not, due to the increased friction of the granular layer. During the tests nothing happened and the situation was fully stable. Some fill material moved, but the compartments with improved filling, around the water line, showed no form of deformation or movement.

Run 7 - Slope 1:2 - Filter: Geotextile

To replace run 5 and 6 two extra test runs are performed. Run 7 is performed on a 1:2 slope with only a geotextile filter. For a geotextile filter this is a relative steep slope and at the boundary of stability in a still water situation. Failure of the revetment occurred at relatively low wave heights. The failure mechanism is more or less of the same principle as with test runs 3 and 4. The difference is that the steps of the caterpillar effect are longer and failure occurs within a number of waves when the process is initiated.

Run 8 - Slope 1:2 - Filter: Granular and Geotextile

The addition of a granular layer resulted in a much more stable revetment. The revetment resisted a much higher wave level before failure occurred, compared to the situation with only a geotextile. At the moment of failure the geotextile did hardly move. The mattress moved down together with a part of the granular layer, though enough material was left to cover the geotextile. This means that the sliding plane lies between the mattress and granular layer.



Figure 5.17: Sliding of the mattress

Sliding of the mattress occurred in more or less the same way as during the tests in run 1 and 2. At the moment of failure, the mattress slides down a certain distance. In a few waves the mattress slides down several small distances until a new equilibrium is developed, which is based on increasing length of the supporting toe. On the upper part of the slope an area became uncovered.

5.3 Deformation Test Results

In the figures below the influence of increased compaction is presented. Figure 5.18 shows the development of the mattress profile during wave action. The mattress was filled with gravel in a 55 mm thick mattress. It is visible that in the fifth compartment, just below the water line, most deformation originates. The bulging is clearly visible, the centre of the compartment rises (yellow area) at cost of the coverage in the upper part.

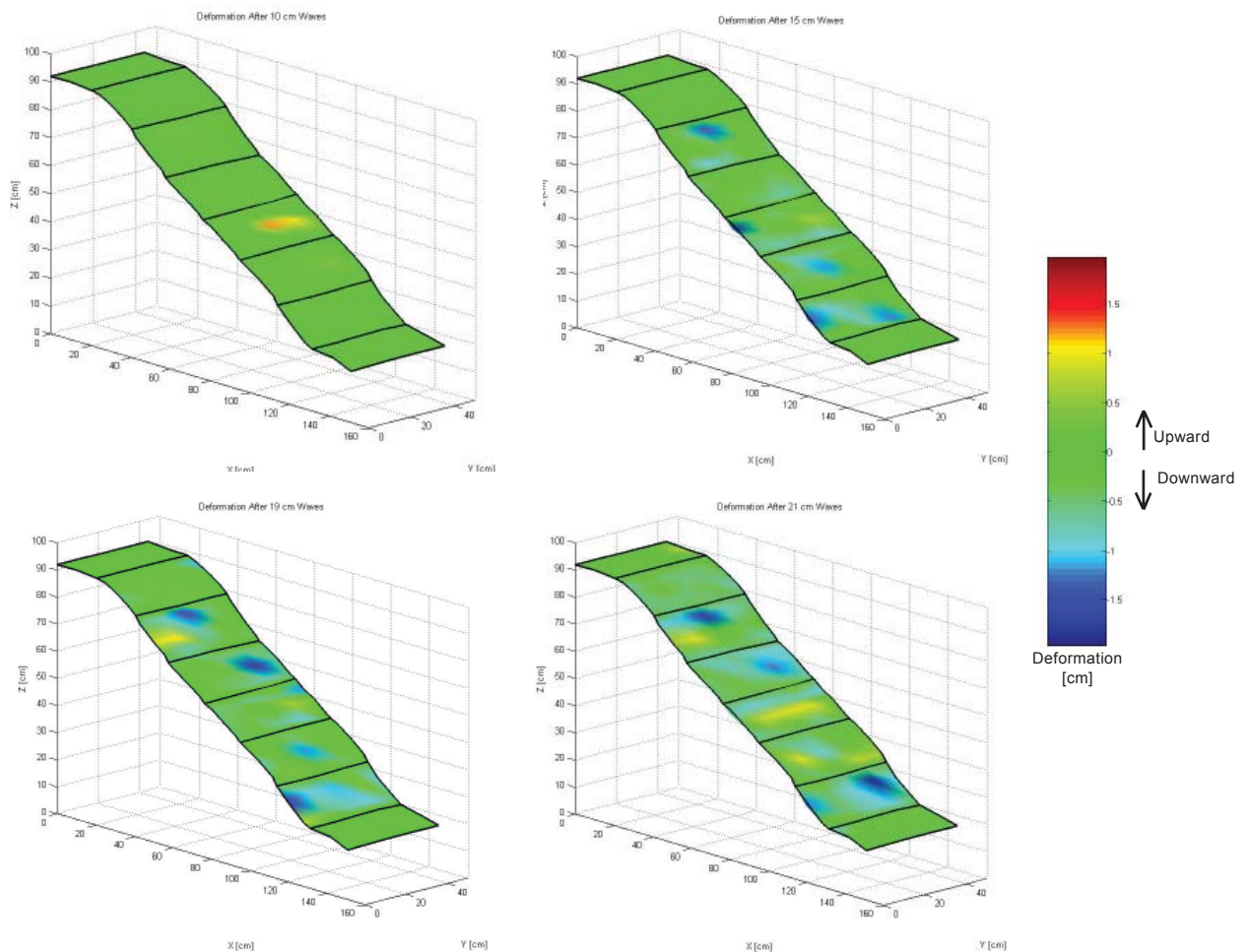


Figure 5.18: Development of deformation experiment D7; 55 mm thickness, normal compaction, gravel fill material

Experiment D6 is executed with small angular fill material. In this case the 55 mm thick mattress is used. The compartments 3 to 6 were filled with extra material, which resulted in a mattress with more curved compartments.

The different steps of figure 5.19 show that there is a rearrangement of material present. The firmness of the compartments is better compared to the previous revetment. The development of bulging parts (yellow spots) in the mattress is not visible. The tension on the fill material creates a homogeneous group behaviour of the fill material

The influence of the mutual connections between the compartments is also visible. The compartment just below the waterline is experience the first deformation. This deformation results in increased tension on the neighbouring compartments, which further decreases the possibilities to deformation due to the increased tension.

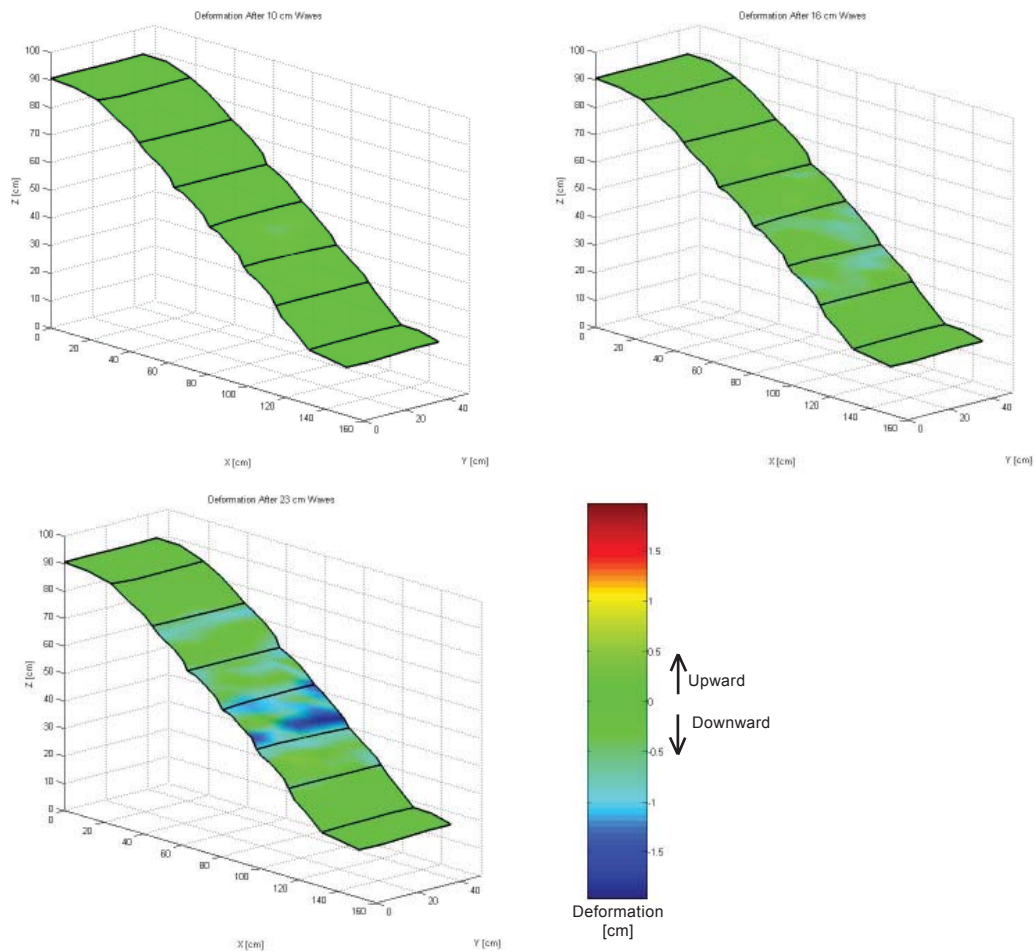


Figure 5.19: Development of deformation experiment D6; 55 mm thickness, increased amount of fill material, small angular fill material

5.4 Sliding Test Results

Section 2.7 presented a review on Pilarczyk's design formula. The summarized comments on the stability relation are:

- The effect that the mattress length is not taken into account
- The friction between the mattress and filter is not implemented
- The permeability of the structure is not used.

If these parameters would be implemented than the stability relation would not follow a single line, as in Pilarczyk's formula, but would consist out of a infinite number of relations depending on the design and local situation. Figure 2.39, from chapter 2, represents a situation with a improved and decreased stability relation, due to a different mattress length, or filter construction.

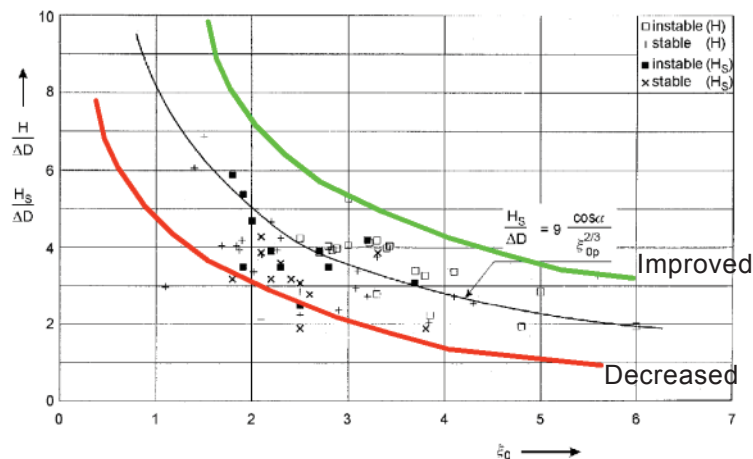


Figure 2.39: Pilarczyk's graph with different stability relations

Each line, that will represent a stability relation, will show the descending shape that depends on the Iribarren parameter. The descending behaviour can be described with an exponential function $e^{-\xi}$. A second term should be added that describes the position of each stability relation in the graph. Due to a difference in mattress length the relation will shift in up-, or downward direction. The descending shape will always be present and expressed by the exponent term. The constant c determines the position of the line in the graph. A coarse form of the preliminary stability relation is [74]:

$$\frac{H}{\Delta_m D_n} = c + e^{-\xi} \quad [74]$$

The mutual relation between the shifting term (c) and descending term ($e^{-\xi}$) should be related, in the proper way, to each other. The influence of the descending term should be adapted by a second parameter c_2 . The effect of this parameter is that the sensivity of the term is adapted to the shifting term.

The Iribarren number influences the descending degree of the exponential term. The influence of the Iribarren number should possibly also be corrected, just as in the original Pilarczyk design formula. The third parameter that is added is c_3 , to correct the Iribarren number. The general developed stability relation, including added parameters that needs to be determined, is:

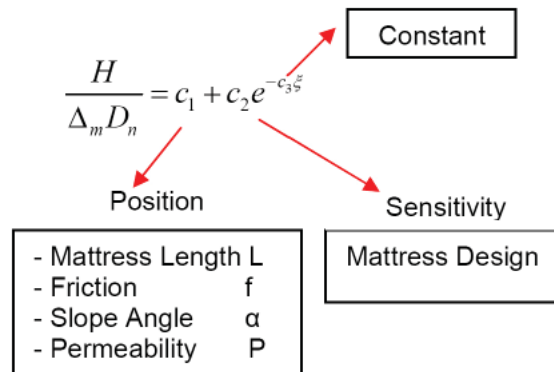
$$\frac{H}{\Delta_m D_n} = c_1 + c_2 e^{-c_3 \xi} \quad [75]$$

The position of the stability relation, determined by c_1 , can best be explained by the ability to absorb a certain amount of tension force. A longer mattress will be able to absorb a higher tension force directed in downward degree. The same applies for a mattress placed on a less steep slope or for a sublayer with a increased friction factor. These processes will result in a higher position in the graph of the stability relation. The permeability of a filterlayer is also of influence on the stability. A less permeable construction due to a less favourable filter set-up will experience higher uplift forces. Due to this uplift effect less tension force can be absorbed and the revetment will fail earlier. A less permeable construction will result in a lower c_1 value.

The parameter c_2 determines the influence of the descending degree of the curve. This variable depends on the design. Horizontal compartments in the shape of crown-, berm-, or toe constructions will effect the stability curve in two ways. The mattress length which is increased so the c_1 will become higher, but horizontal compartments contribute relatively more to the stability, which will give a more steep curve of the stability relation.

The value c_3 is a coefficient that effects the influence of the Iribarren value. It can stretch or compress the stability relation. This value is a constant in the formula.

Summarizing, the following parameters are of influence on the variables c_1 and c_2 and the constant c_3 :



During the execution of the test program it was not always possible to adjust the wave generator in such way that the exact wave height and Iribarren parameter could be created. Most of the times, the result was close to the preliminary objective. Table 5.1 presents the wave height for each moment of failure. The stability parameter for the moment of failure is also presented in the table.

Run [-]	Test [-]	H _i m	H _r m	K _r -	T s	ξ -	Run-up cm	Run-down cm	D _n mm	Δ_m -	H _i / $\Delta_m D_n$
1	S1	0.19	0.09	0.31	1.7	3.3	20.2	9.2	40	0.99	4.72
	S2	0.15	0.08	0.51	2.2	4.9	14.3	12.7	55	0.99	2.68
	S3	0.19	0.09	0.49	2.1	4.1			55	0.99	3.51
	S4	0.20	0.06	0.32	2.0	3.7	19.4	11.3	55	0.99	3.60
	S5	0.28	0.14	0.50	1.8	2.9			55	1.00	5.04
	S6	0.22	0.06	0.29	1.5	2.7	21.2	6.0	30	1.00	7.32
	S7	0.24	0.05	0.21	1.3	2.2	19.8	6.1	30	1.00	8.01
2	S8	0.13	0.03	0.24	0.9	1.9	10.0	3.7	30	1.00	4.43
	S9	0.09	0.05	0.57	2.5	6.9	10.6	5.9	55	1.00	1.68
	S10	0.17	0.05	0.28	1.4	2.7	14.1	6.8	55	0.99	3.14
	S11	0.12	0.05	0.41	1.7	4.0	12.7	7.2	55	0.99	2.28
S12	0.14	0.03	0.19	0.9	1.9	8.1	3.0	40	1.00	3.56	
S13	0.14	0.04	0.30	1.4	3.2	7.9	5.6	40	1.00	3.52	
3	S14	0.23	0.02	0.10	1.2	1.0	12.2	7.2	30	1.00	7.53
	S15	0.15	0.04	0.24	1.9	2.1	11.4	6.9	40	0.96	3.99
	S16	0.11	0.05	0.48	3.2	3.9	16.0	8.8	55	0.96	2.14
4	S17	0.27	0.03	0.10	1.6	1.3	21.9	10.8	30	1.00	9.09
	S18	0.20	0.04	0.19	2.2	2.1	19.5	8.3	40	0.96	5.07
	S19	0.17	0.07	0.42	3.0	3.0	26.9	11.7	30	1.00	5.63
	S20	0.18	0.12	0.68	4.0	3.9	30.8	12.6	55	0.96	3.33
7	S27	0.10	0.03	0.27	0.8	1.5	4.1	1.6	30	1.00	3.50
	S28	0.13	0.03	0.22	1.4	2.4	8.0	3.4	55	1.00	2.36
	S29	0.11	0.06	0.52	0.7	1.2	2.0	1.5	30	1.00	3.71
8	S30	0.25	0.04	0.15	1.6	1.9	20.9	6.7	30	1.00	8.33
	S31	0.22	0.03	0.12	1.9	2.6	18.8	10.2	30	1.00	7.35
	S32	0.18	0.02	0.13	2.2	3.2	18.2	12.8	30	1.00	6.01
	S33	0.15	0.10	0.65	2.9	4.5	27.1	14.3	30	1.00	5.15

Table 5.1: Test Results

The moment of failure is plotted in figure 5.20. For each experiment the stability parameter ($H/\Delta_m D_n$) is determined which is plotted against the Iribarren number of that situation.

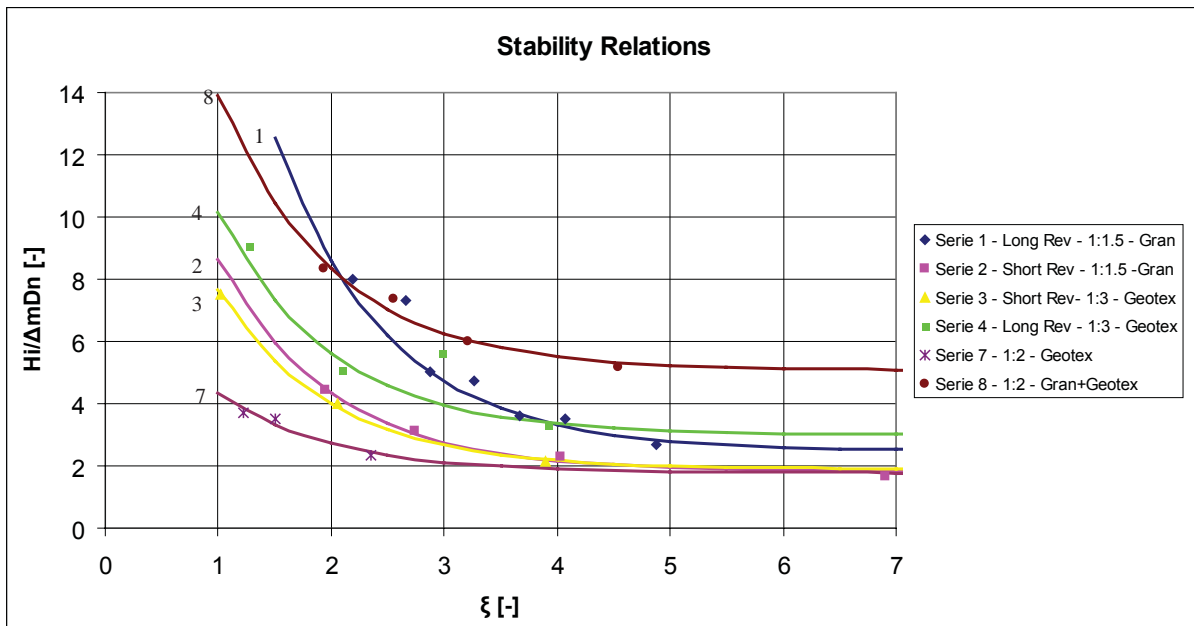


Figure 5.20: Sliding test results

Through every run, a decaying exponential function is drawn, which is based on the least squares curve fitting method. This is based on formula [75] which consists of two variables c_1 and c_2 . The constants in the formula are determined by creating a matrix E , which consists out of two vectors with the length equal to the amount of test results. The first vector consists of one's the second vector consist out of the exponent of the value x . The least square solution is determined by: $c=E^{-1}y$. Matrix c contains the values of the two parameters. The values of c_1 and c_2 are presented in table 5.2.

Parameter	Run 1	Run 2	Run 3	Run 4	Run 7	Run 8
C1	2.5	1.8	1.9	3.5	1.8	5.1
C2	54	19	16	19	7	24

Table 5.2: c-values

The fitting of the data is based c_3 value of 1. The curve fits well and it is not necessary to adapt the constant for a proper fitting of the data. The formula can be based on the Iribarren parameter.

Considering the stability relations of runs 2, 3, 4 and 8, it can be concluded that they follow more or less the same curvature (Figure 5.21). In table 5.2 it can be seen that the value for c_2 is of the order 20 for these runs. The geometrical design of these mattresses consists only of elements placed on a slope, for this reason they all have more or less the same shape. The difference in the c_1 value is devoted to the mattress length, filter construction, or slope angle.

The influence of increased mattress length becomes clear in the difference between runs 3 and 4, in which run 4 was executed with a longer mattress and therefore has a higher position in the graph. Run 8 is performed on a more steep slope, but due to the increased friction factor it is possible that this revetment can absorb a higher downward directed tension force, caused by the waves. For this reason the stability relation is on a relative higher position in the graph.

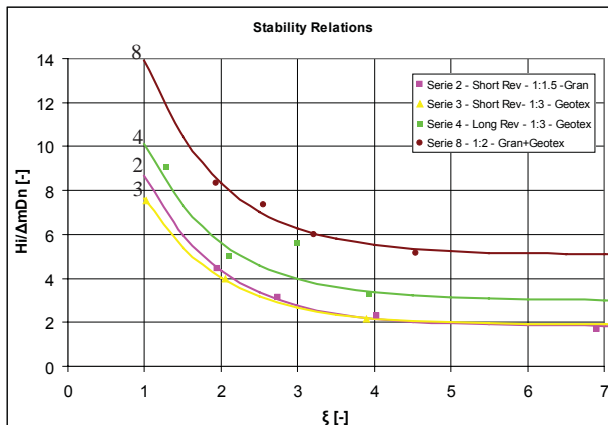


Figure 5.21: Comparable curve shape

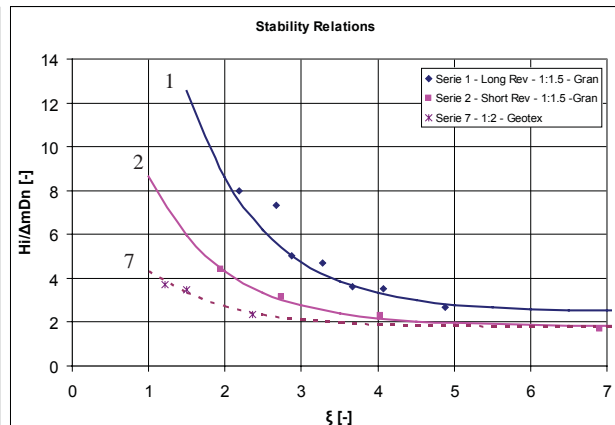


Figure 5.22: Difference curve shape

Figure 5.22 presents the three stability curves that show a difference in curvature. Run 1, 3 and 7 show different behaviour. First attention is given to the results from run 7. These results are performed on a 1:2 slope with a geotextile filter. In a still water situation the mattress is almost out of the equilibrium and will slide down due to a little disturbance. The quality of the results from run 7 are inferior and will not be taken into account in the further analysis. Therefore the line from run 7 is presented dotted in Figure 5.22.

As described in the runs from Figure 5.21, all the stability relations have more or less the same curvature. Considering run 1 with the rest of the stability relations it shows different curvature of the stability relation, especially for the smaller Iribarren numbers. Run 1 is the only series of experiments that is performed with a crown and toe compartment. The increased length of the mattress results in an upward shift of the stability relation, compared to run 2 which is based on the same slope. The horizontal compartments give an extra contribution relative to an inclined compartment. For the smaller Iribarren parameters the waves have a shorter period which results in a shorter moment of tension force that needs to be absorbed. The subsoil, present under the crown, interacts and gives extra stability. Longer waves not only give a deeper run-down, but also result in uplift-, and tension forces that are present for a longer moment of time. Due to the increased forces the subsoil is no longer able to give that extra contribution. The mattress will slide down including the contributing subsoil, resulting in the s-profile. In the analysis section of this chapter a beginning will be made for the determination of the c_1 and c_2 value.

5.5 Run-up, Run-down and Reflection

In this section the run-up, run-down and reflection results of the deformation and sliding experiments are presented. Some available relations are drawn through the graphs to see how the results fits the available data from the literature.

5.5.1 Run-up Test Results

In Figure 5.23 two graphs are plotted over each other in which run-up test results are plotted. The coloured data points are the points that came forward from the gabion experiments. The black and white data points are the results from the experimental work of *Van Der Meer & Stam 1992* [CUR, CIRIA, CETMEF 2007]. Both data series cannot be directly compared. The results of *Van Der Meer & Stam 1992* are based on irregular waves in which the data points are based on 2% of the highest waves. The y-axis of the graph represent the $R_{2\%}/H_i$ value. The difference is that the gabion experiments are based on regular waves. The run-up level is therefore based on a constant average wave height and cannot be directly compared with the results from *Van Der Meer & Stam 1992*. For the gabion test results the y-axis of the graph represents the $R_{50\%}/H_i$ value.

The degree of run-up does not only depend on the height of the incoming wave, but is also influenced by the roughness of the outer layer and the permeability of the structure. A smooth outer layer like asphalt will show a higher run-up level compared to a more rough protection like rip-rap, in which more turbulence develops and more energy is dissipated. The same effect accounts also for a more permeable structure. Through the voids of a granular filter, kinetic wave energy is able to dissipate. The less impermeable the sublayer is, the less energy can be dissipated which results in higher run-up. A geotextile filter is therefore considered as a impermeable sublayer.

In the gabion test results the influence of filter permeability is visible. The scatter cloud of the mattresses that is placed on the granular layer is at a lower position in the graph, compared to the other two filter layer alternatives in which a geotextile is applied. The runs in which a geotextile is applied, show a general higher run-up. With this theory a distinction should also be visible between the geotextile filter and granular + geotextile filter. The difference in core permeability is of such a small level that this cannot be concluded.

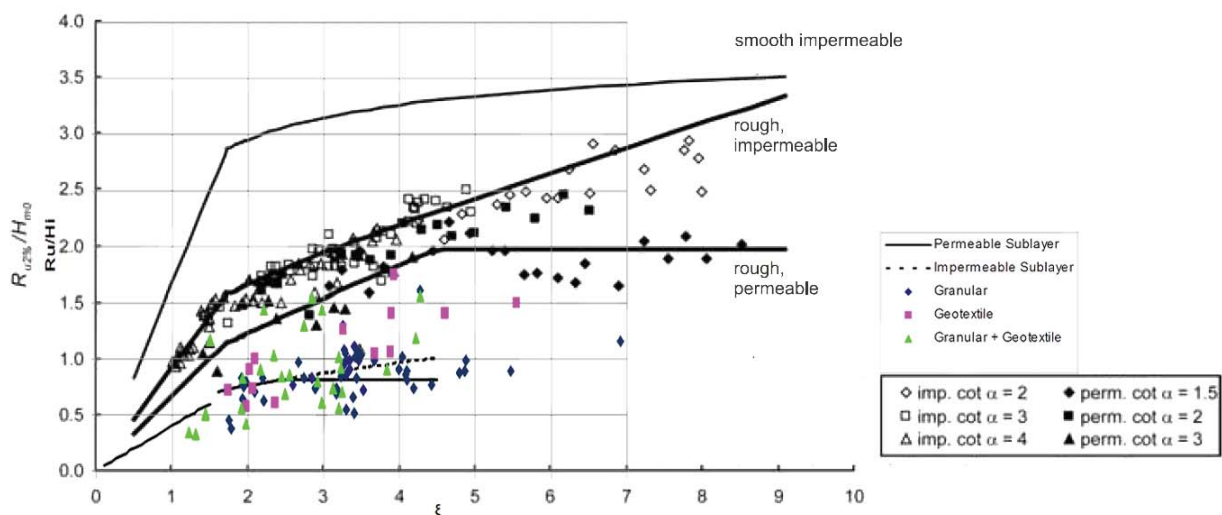


Figure 5.23: Run-up test results

Van Der Meer & Stam 1992 [CUR, CIRIA, CETMEF 2007] developed a prediction formula for rough slopes based on the exceedance level of different wave heights [76]. For each exceedance percentage the factors in the formula were determined. Table 5.3 represents the different factors of formula [76]. Through the gabion run-up data, which is based on regular waves the $R_{u,50\%}/H_i$ is drawn.

$$\begin{array}{ll}
 \text{Impermeable and Permeable core} & \frac{R_{u,n\%}}{H_s} = a\xi \quad \xi < 1.5 \\
 \text{Impermeable and Permeable core} & \frac{R_{u,n\%}}{H_s} = b\xi^c \quad \xi > 1.5 \\
 \text{Permeable core} & \frac{R_{u,n\%}}{H_s} = d
 \end{array} \quad [76]$$

Run-up level n%	a	b	c	d
0.1	1.12	1.34	0.55	2.58
1	1.01	1.24	0.48	2.15
2	0.96	1.17	0.46	1.97
5	0.86	1.05	0.44	1.68
10	0.77	0.94	0.42	1.45
50	0.47	0.60	0.34	0.82

Table 5.3: Coefficients equations formula [76]

If a comparison is made between the two scatter clouds of Van Der Meer & Stam and the gabion experiments than there is a difference in the way the data fits the curve. The Van Der Meer & Stam data give a more consistent scatter cloud. The gabion run-up scatter cloud is much wider distributed.

The explanation for this difference in the relative smaller thickness of the outer layer compared to a rip-rap construction that is applied in the research of Van Der Meer & Stam. Due to the grid it is possible to construct a relative thinner construction. The amount of turbulence that is created in the outer layer is relatively less compared to a thicker layer. The effect is a increased influence of the filter layer. The thinner a mattress is, the more influence a filter layer will have on the amount of run-up. When a thin mattress is placed on a geotextile it will show a higher level of run-up compared thicker mattress in the same situation. This effect will increase for the conditions with higher wave numbers, since less wave energy will dissipate, as can be seen in the data from Van Der Meer & Stam, Figure 5.23.

The test data from Van Der Meer & Stam have a certain standard deviation which is used to determine the confidence limits. For impermeable structures the variation coefficient (σ/μ) is 6% and for permeable structures 9% Van Der Meer & Stam 1992 [CUR, CIRIA, CETMEF 2007]. With these values the 95% confidence limits are determined for the $R_{u,50\%}/H_i$ value from formula [76].

In figure 5.24 the confidence limits are presented including the subdivided data, based on the mattress thickness. The mattresses that are placed on the granular sublayer, show a more or less a consistent result. A coarser distribution of the data is especially present in the situation of thin mattresses applied on a filter including a geotextile. The disadvantage of subdividing the data is that the amount of information per situation becomes less. The situation of a 40 mm mattress applied on a granular + geotextile filter seems to show a little better resemblance of formula [76] compared to the thinner 30 mm variant, though the situation contains only 4 data points and this statement cannot be made. Unfortunately there is no more data available, in the 40 mm and 55 mm variant, to create a better foundation for this theory. The same counts for the comparison between the 30 and 55 mm mattress placed on only a geotextile. There are simply not enough data points available for a proper conclusion.

To develop a improved relation for the amount of run-up, based on a thin cover layer, more research is necessary. The only conclusion that can be made at this point is that the confidence interval for gabion mattress shows a wider variation.

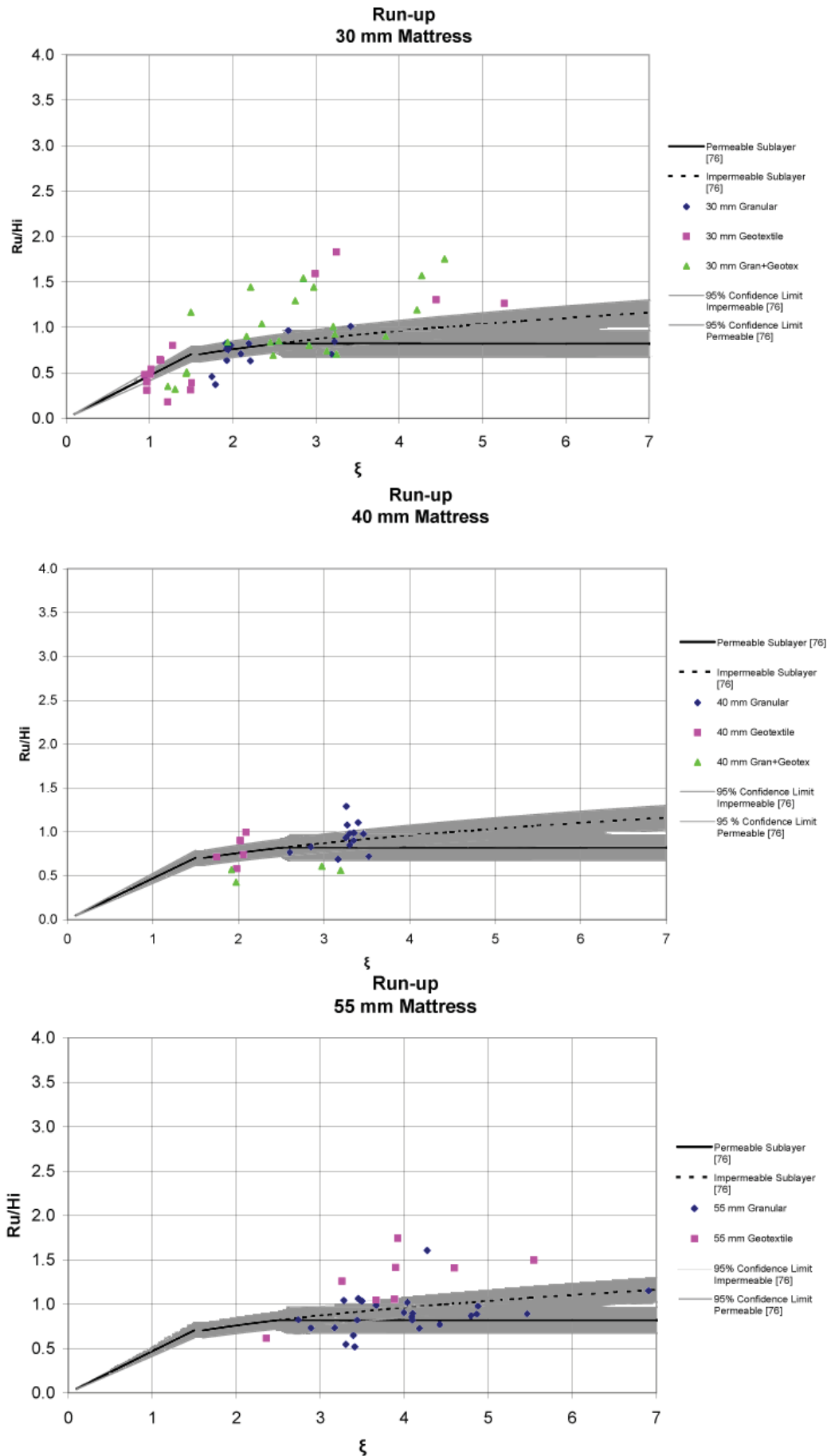


Figure 5.24: Subdivided run-up data

5.5.2 Run-down Test Results

The influence of the filter permeability is of influence on the amount of run-down. Increased turbulence results in lower draw down effects. Confirmation of this is visible in Figure 5.25. The mattress placed on the most permeable granular sublayer, shows the least relative amount of run-down.

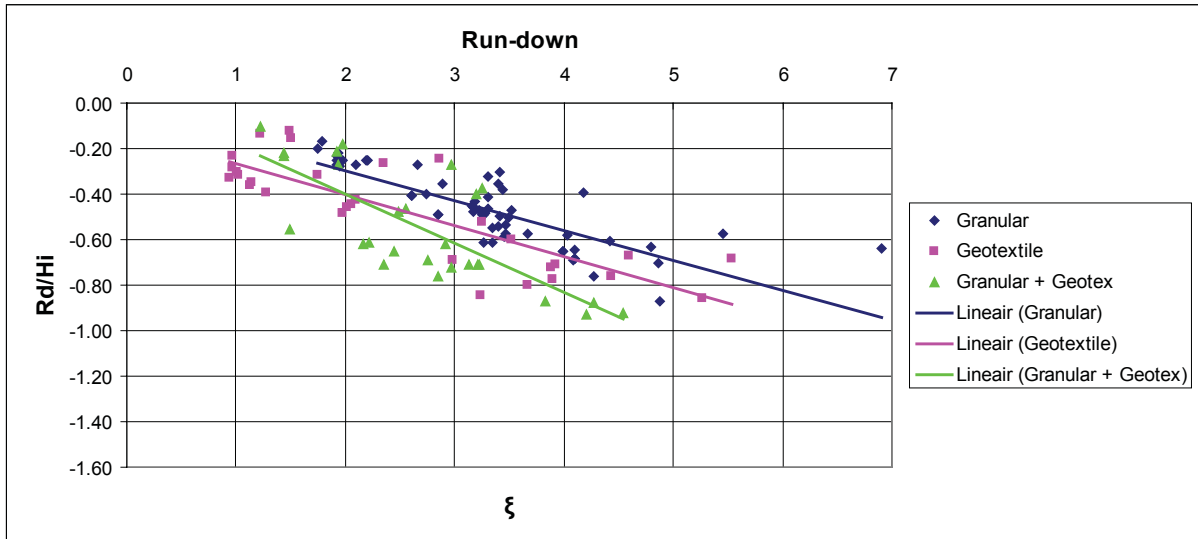


Figure 5.25: Run-down test results

Curve fitting with a current prediction formula from the literature does not give a satisfying result. The proposed formula of *Battjes 1974* [SCHIERECK 2001] [77] for regular waves does not resemble the data set. The reason for this is that the formula is based on a smooth impermeable slope. Therefore the relation is not presented in the graph.

$$R_d/H = (1-0.4 \xi) \xi \quad [77]$$

The quantification of run-down is in general ill defined. The formulas that are available are mainly based on the $R_{2\%}/H_i$ value. A comparable formula in which different exceeding levels can be determined, as in *Van Der Meer & Stam* [76] does not exist. Most of the basic formulas are based on a linear relationship of the form $R_d/H = a\xi + b$. In Figure 5.25 the linear trend is added for each filter layer based on the linear regression through the data.

This results in the following relations:

Granular	$R_d/H = -0.132 \xi - 0.032$
Geotextile	$R_d/H = -0.136 \xi - 0.132$
Granular + Geotextile	$R_d/H = -0.215 \xi + 0.028$

A comparable conclusion can be drawn with respect to the wave run-up results. A wide degree of scatter is present, probably caused by the increased influence of the filter layers.

5.5.3 Reflection Test Results

Reflection is expressed with the Iribarren parameter. Steeper slopes will reflect more wave energy and longer waves will result in less dissipation. An increasing wave parameter gives a higher reflected wave. The degree of reflection can further be influenced by the roughness of the outer layer and the permeability of the construction. In Figure 5.26 the gabion reflection data is presented (coloured points) together with test results from earlier experiments (black and white points).

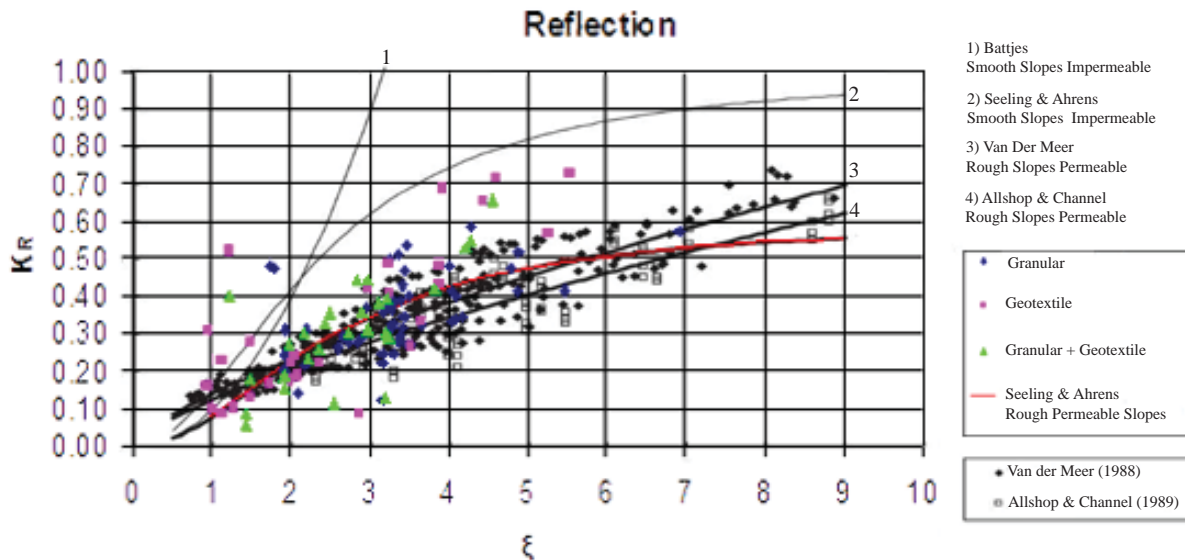


Figure 5.26: Reflection test results

Battjes 1974 [CUR, CIRIA, CETMEF 2007] was the first who developed a reflection formula based on the Iribarren parameter. The research has been performed on a smooth outer layer placed on a impermeable core. From the data, based on regular waves, a steep curve is the result. With the same revetment conditions *Seeling & Ahrens 1981* [CUR, CIRIA, CETMEF 2007] developed a different relation for smooth impermeable slopes. These relations are both not applicable for a gabion revetment, since the experiments consisted out of rough slopes.

Van Der Meer 1988 and *Allshop & Channel 1989* [CUR, CIRIA, CETMEF 2007] performed reflection tests based on rough slopes and a permeable revetment construction. For both situations the data scatter is presented in Figure 5.26, including the curve fitted line. It should be noticed that the tests are based on irregular waves.

The work of *Seeling & Ahrens 1981* is based on regular waves and also describes a relation for rough slopes with permeable conditions [78]. This relation fits the data from the literature and gabion experiments reasonable (red line). Unfortunately there is no formula available, in the current literature, that describes the reflection based on a rough slope with a impermeable sublayer. If this relation would exist it would be present between the Van Der Meer and Seeling & Ahrens relation for impermeable smooth slopes.

Seeling & Ahrens:
$$K_R = \frac{0.6\xi^2}{(6.6 + \xi^2)} \quad [78]$$

Again the remark is made that the scatter cloud of the gabion experiments show a increased variation. The probable explanation for this is that the sublayer has influence on the reflection, since gabion mattresses are relatively thin compared to rip-rap constructions. Mattresses placed on a geotextile show a slight divergence in upward direction. The amount of data is too limited to give further recommendations or conclusions.

5.6 Analysis Deformation

During the deformation tests it came forward that the compartments with an increased amount of fill material, creating a tension on the grid, resulted in a proper function of the mattress. When gabion mattress revetments are constructed, the intension should always be to close the compartments with a certain tension on the grid.

The ideal construction method of a mattress it performed in such a way that the compartments are first normally filled. Followed by a partly closure of the lowest compartment. Extra fill material should then be placed in the lowest compartment, in combination with elements that could vibrate the filling. The compartment can than be filled to the maximum and closed under tension, along the upper rib. Based on this filling process, mattresses should be filled in upward direction (Figure 5.27).

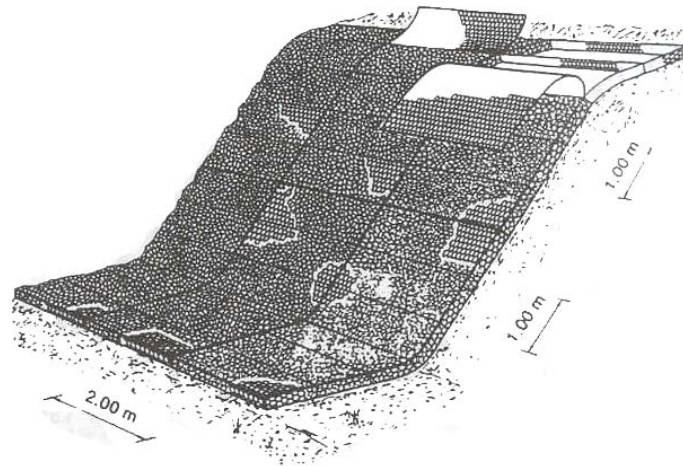


Figure 5.27: Filling the mattress

When pre-fabricated and filled mattresses are used it is important to preserve the shape of the compartments. In this way the tension will be kept on the grid. Revetments constructed in this way will benefit from the application of a more rigid grid material, although the handling of the mattress during construction is also of considerable influence. Prefab placement will need a proper quality control.

The amount of fill material that can be added extra, based on the fixed volume of a compartment depends on the size of the fill material. Smaller particles are better able to follow the curved shape of the compartment lid, which results in the adding of some relative extra material. With formula [79] the volume of the bulging part of a compartments is calculated.

$$V_{b,c} = V_{c,f} - \frac{M_{c,if}}{\rho_s \cdot (1-n)} \quad [79]$$

With:

- $V_{b,c}$ = Volume due to bulging compartment.
- $V_{c,f}$ = Volume fixed compartment
- $M_{c,if}$ = Mass increased filled compartment

In table 5.4 the results of formula [79] are presented for the the 4 compartments of experiment D4 and D6, which are executed with angular and small angular fill material.

Mattress Information					
Experiment	Compartment	Width	V _{c,f}	Mass	V _{b,c}
-	-	cm	cm ³	kg	cm ³
D4	3	21.5	3913	7.90	975
	4	20.5	3690	7.40	888
	5	21.5	3849	7.70	915
	6	22.0	3916	7.80	910
				Average	922
D6	3	22.5	4028	9.05	1446
	4	21.5	3849	8.55	1322
	5	21.0	3822	8.55	1349
	6	20.0	3640	7.85	1107
				Average	1306

Table 5.4: Deformation volume

For small fill material the extra volume was 1300 cm³ on average. For the larger angular fill material this was 920 cm³. Based on the fixed volume of the mattress this means a 34 % extra volume based on a 40 mm mattress and 24% extra volume for the larger angular fill material. The corresponding D_n/D_{50} are 2.6 and 1.6. A very coarse relation could be developed based on these results, though the resemblance with the reality would be minimal.

The amount of fill material that can be added depends also on many different other factors. If the length of the compartment lid is slightly wider than the base it results in a increase of fill material volume that could be added. The most important aspect is that the compartments should be filled in such a way that the compartments are filled and closed, with a little tension on the grid without leaving space on beforehand.

5.7 Analysis Sliding Test Results

In the section that presents the test results, a first step is taken in the analysis of gabion mattress failure due to sliding. Increased revetment length or friction, results in a relative higher position of the stability relation in the graph (Figure 5.20). The construction permeability will also influence the shape of the curve. In this section a start is made for a method to determine the factors c_1 and c_2 .

5.7.1 Parameter Analysis of Factor c_1

In a stability formula, like Pilarczyk's, a relation is presented between the stability parameter and the Iribarren number. The stability parameter includes the ratio between wave height, mattress thickness and relative mass. Identical revetment constructions with different thicknesses can be compared with the stability parameter. A thicker mattress will be able to absorb a higher wave height. With the stability parameter constructions are expressed in proportion to each other.

The factor c_1 will shift the stability relation in up-, or downward direction. The factor c_1 value resembles the degree in which a certain revetment design is able to absorb wave forces based on friction, slope angle, mattress length and construction permeability. For the first part of the analysis the permeability is left out of consideration.

Slope Angle and Friction Influence

A volume placed on a flat surface will move sideways if it is exposed to a tension force equal to the gravity force multiplied by the friction factor. If the friction factor is 0.7, than the capacity to sideward movement is 70 % of the gravity force. Increasing the slope angle will decrease the amount of force that is necessary to move the object in downward direction. The capacity of the object, to absorb a tension force, decreases. The degree of possible tension force absorption can be expressed by a factor R. This relation represents the ratio between the resistant force and driving force as formulated in chapter 2. From formula [30] it came forward that this ratio is equal to the ratio between the friction coefficient and slope angle. The ratio R is formulated as:

$$R = \frac{F_r}{F_d} = \frac{f}{\tan(\alpha)} \quad [-] \quad [80]$$

An R-value of 1 implicates that the mattress will slide down due to an infinitely small downward directed tension force. An R-value of 2 means that the object is able to resist an tension force that is equal to driving force. An important note is that the R-value gives no indication about the quantity of tension force that can be absorbed. Increasing the mass, thickness or length will result in the same constant R-value. The amount of tension force that can be absorbed will be higher for the thicker or longer mattress, though this cannot be concluded from the R-value.

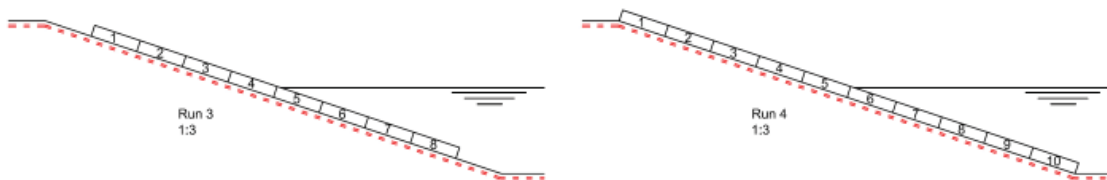


Figure 5.28: Constant R-value for run 3 and 4

If two identical mattresses are compared with different R-values, than the mattress with the highest R-value will have the best stability properties. In the stability relation this is expressed as a higher value for c_1 .

Mattress Length and c_1 Relation

In Figure 5.20 that represents the different stability relations, it becomes clear that for identical slope conditions (run 3 and 4), with the different mattress length, extra stability can be gained. Both revetments have the same R-value. Due to the increased mattress length is the c_1 -value higher for run 4. A relation between the relative length and c_1 value should be developed.

A compartment with a certain length and weight will be able to absorb a certain amount of tension force. Connecting two compartments will result in a double amount of tension force that can be absorbed. In view of the design formula [81] this means that the stability number and c_1 -value doubles, under the condition that the Iribarren number is large and the permeability is left out of consideration for now.

$$\frac{H}{\Delta_m D_n} \approx c_1 \quad \text{for } \xi \gg \text{large} \quad [81]$$

The combination of a certain mattress length and R-value will determine the value for c_1 . A relation between the R-value and mattress length is developed to determine the value for c_1 . A long and short mattress on a slope will have a constant R-value. The mattress length is used to express the c_1 value. The mattress length should be expressed as a dimensionless parameter to use the scaled test results in reality.

The graph of Figure 5.29 represents the theory. A longer mattress will show a further point on the line of a certain R-value and will therefore give a higher c_1 value. In theory a infinite number of R-lines can be drawn in the graph of Figure 5.29. With a graph like Figure 5.29 it would be possible to determine c_1 value for every situation.

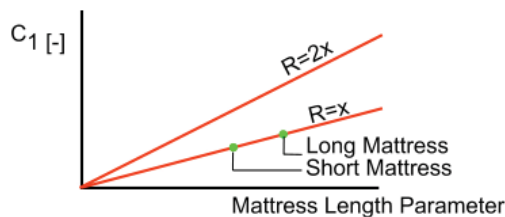


Figure 5.29: Parameter relation

Contribution of Submerged Compartments

The first coarse relation that is set up, does not take the influence of submerged compartments into account. Compartments submerged in a fluid experience an uplift force, which is equal to the displaced volume multiplied by the density of the fluid. The effect of this, is that the amount of tension force that can be absorbed by a compartment, is higher above water than if it is submerged. The following example explains the difference:

Element	= 1 m
α	= 20°
f	= 0.7
F_g	= 1000 N
Δ	= 1.65

The driving force and resistant force for the situation above water is:

$$\begin{aligned} F_d &= \sin(\alpha) * F_g & F_r &= \cos(\alpha) * F_g * f \\ F_d &= \sin(20) * 1000 & F_r &= \cos(20) * 1000 * 0.7 \\ F_d &= 342 \text{ N} & F_r &= 658 \text{ N} \end{aligned}$$

This part is able to absorb: $F_t = F_d - F_r = 316 \text{ N}$

The submerged element should be corrected for the uplift pressure of the water. This is implemented with the relative density parameter Δ (formula [2]). Assuming that the fill material has a density of 2650 kg/m³, a relative density parameter of 1.65 is given. The effective mass under water is:

$$F_{g,relative} = \frac{F_g}{\Delta} = \frac{1000}{1.65} = 606 N$$

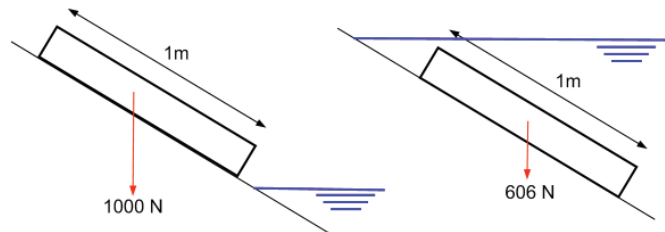


Figure 5.30: Contribution submerged compartments

The driving force and resistant force for the situation under water is:

$$\begin{aligned} F_d &= \sin(\alpha) * F_{g,relative} & F_r &= \cos(\alpha) * F_{g,relative} * f \\ F_d &= \sin(20) * 606 & F_r &= \cos(20) * 606 * 0.7 \\ F_d &= 207 N & F_r &= 399 N \end{aligned}$$

This part is able to absorb:

$$F_{t,relative} = F_d - F_r = 192 N$$

The capacity of the submerged compartment is decreased with a factor ($F_t / F_{t,relative} = 316/192$) 1.65, which is equal to the relative density parameter. Formulated differently, this means that a compartment under water should be 1.65 times longer than a compartment above water to be able to absorb the same amount of tension strength. The relative length, taking into account the submerged compartments, is expressed by formula [82].

$$L_{rel} = X + \frac{(L_m - X)}{\Delta} \quad [82]$$

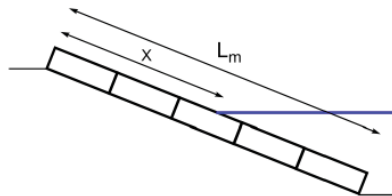


Figure 5.31: Parameters for relative length determination

Mattress Length Parameter

The capacity of a mattress depends on the R-value, thickness and the length of the structure. To make a distinction, based on the length a dimensionless mattress length parameter is introduced. The dimensionless length parameter is expressed by the ratio between relative mattress length and wave length (L).

$$\frac{L_{rel}}{L} = \frac{X + \frac{(L_m - X)}{\Delta}}{L} \quad [83]$$

By including the wave length an extra variable is introduced. The effect of this variable is described with an example. If a constant mattress length is considered than a longer wave will result in a relative shorter mattress. In Figure 5.29 this results in a lower c_1 value while the actual mattress length has not changed. From the experiments it came forward that a construction with a constant length will always have the same c_1 value independent of the Iribarren parameter.

To be able to use the dimensionless mattress length parameter a general stability relation is developed. This can be done by moving the c_1 parameter to the other side of the equation. With equation [84] all experimental results fall on the same line for the runs 2,3,4 and 8. The effect of horizontal compartments is left out of consideration for now. The result is plotted in Figure 5.32

$$\frac{H}{\Delta_m D_n} - c_1 = c_2 e^{-\xi} \quad [84]$$

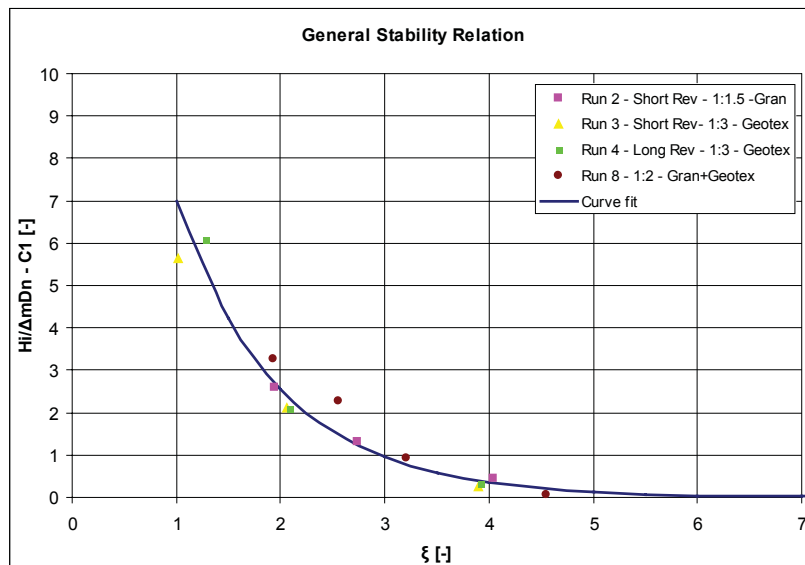


Figure 5.32: General stability relation

The formula of the curve fitted line is:

$$\frac{H}{\Delta_m D_n} - c_1 = 19e^{-\xi} \quad [85]$$

In the theory that describes the relation between the R-value and c_1 -value it is explained that constructions with different mattress length can have the same R-value. The difference in mattress length results in a different position on the line that presents the relation between the relative length and corrected stability relation. Figure 5.29 shows this. In Figure 5.33 the stability parameter, corrected with the c_1 value is plotted against the dimensionless mattress length parameter.

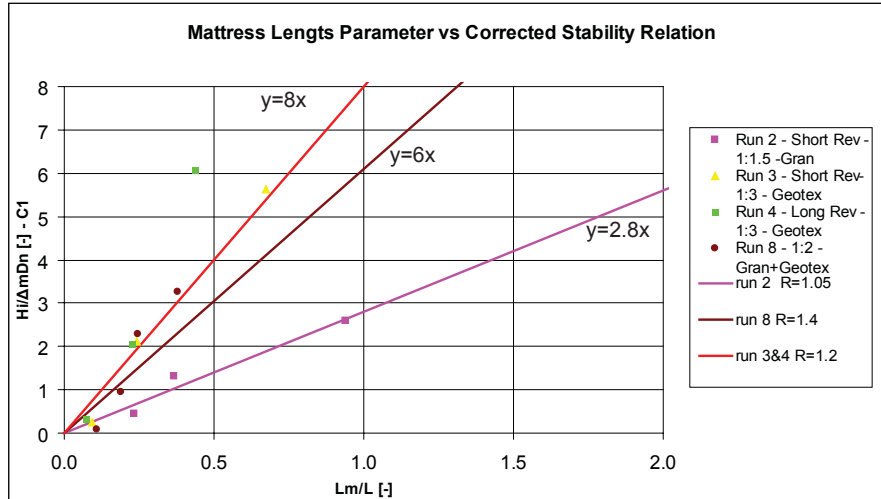


Figure 5.33: Mattress length parameter vs corrected stability relation

A linear relation is drawn through the results from the different runs. In theory the results from experiments 3 and 4 should follow the same line. For the relative smaller mattress length parameter this expectation is satisfied, though at a higher level there is some deviation between the two points. It should be noticed that the amount of results is rather limited for a solid confirmation.

Based on the gradient of the different lines the relation can be further developed for situations with other slope angles. A distinction is made between the difference in permeability of the structures, since the amount of uplift is of influence on the stability of a structure. This is based on the relative increase or decrease of the tension force that can be absorbed by an element with respect to the original situation. This is expressed in a ratio r which is deviated as follows:

$$r = \frac{F_{r,dep} - F_{d,dep}}{F_{r,or} - F_{d,or}} = \frac{\cos(\alpha_{dep}) \cdot F_g \cdot f - \sin(\alpha_{dep}) \cdot F_g}{\cos(\alpha_{or}) \cdot F_g \cdot f - \sin(\alpha_{or}) \cdot F_g} = \frac{\cos(\alpha_{dep}) \cdot f - \sin(\alpha_{dep})}{\cos(\alpha_{or}) \cdot f - \sin(\alpha_{or})} \quad [86]$$

The subscript *dep* and *or* stand for the dependent and original situation. The result of this ratio can be used to adapt the gradient of the three formulas, placed in Figure 5.33. These relations represent the original on which the rest is based. A relative twice as strong situation will result in a curve that is twice as steep as the original. Formula [87] represents the derivation of the original relation. If the slope angle approaches the value for which $R = 1$ than the c_1 value will be 0 just as the stability parameter.

$$\frac{H}{\Delta_m D_n} - c_1 = (B \cdot r) \frac{L_m}{L} \quad [87]$$

With:

B = Gradient of the original experimental determined relation (Figure 5.33).

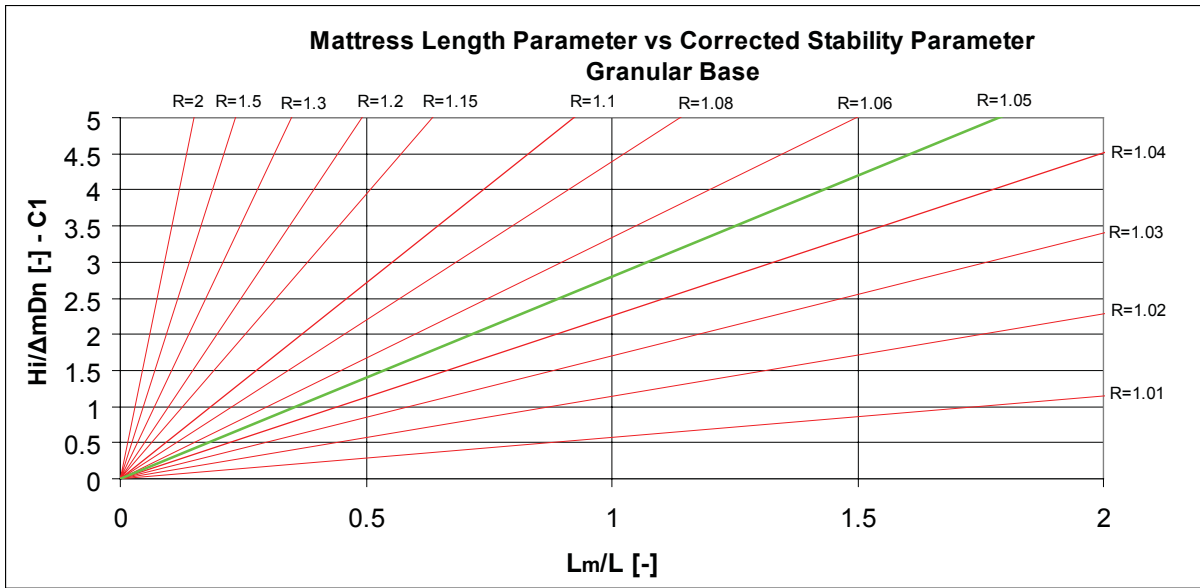


Figure 5.34: Relation between corrected stability parameter and mattress length for permeable granular slopes

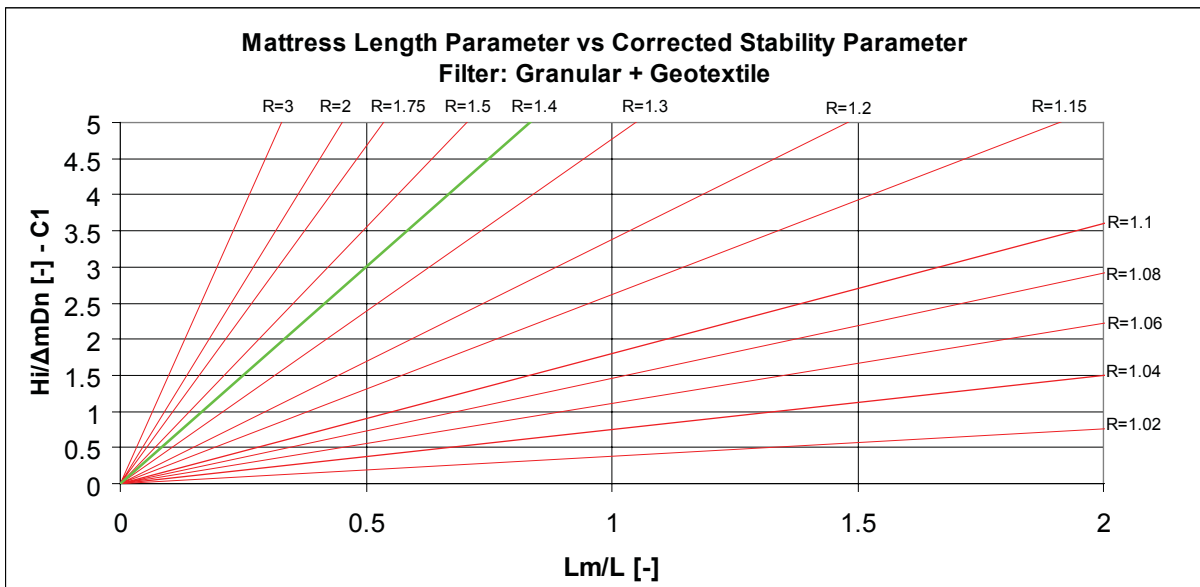


Figure 5.35: Relation between corrected stability parameter and mattress length for slopes on a granular + geotextile filter

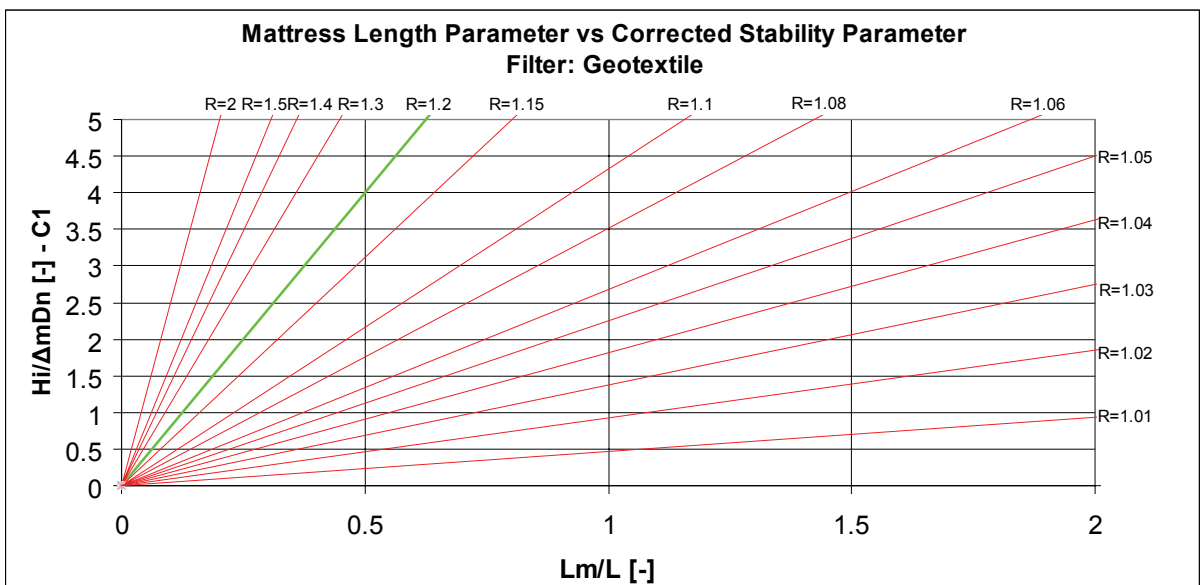


Figure 5.36: Relation between corrected stability parameter and matteress length for slopes on a geotextile

Design method

In the following example it presented how to use the graphs for the design of a revetment. A situation is given in which the following parameters are known.

Slope angle	α	= 30°
Granular + Geotextile filter	f	= 0.7
Capacity ratio	R	= 1.2
Wave height	H	= 1 m
Wave length	L	= 10 m
Iribarren parameter	ξ	= 1.8
Relative density material in a gabion	Δ_m	= 1

A choice is made for a certain mattress thickness $D_n = 0.20$. This gives a stability parameter of:

$$\frac{H}{\Delta_m D_n} = \frac{1}{1 \cdot 0.20} = 5$$

The graph from Figure 5.32 or formula [85] can be used to determine the c_2 value. From this result the parameter c_1 can be deviated.

$$\frac{H}{\Delta_m D_n} - c_1 = c_2 e^{-\xi}$$

$$\frac{1}{1 \cdot 0.20} - c_1 = 19 e^{-1.8}$$

$$c_1 = 5 - 3 = 2$$

The corresponding relative length parameter can be determined by using the graph from Figure 5.35. Filling in the determined parameters gives a relative length parameter of $L_m/L = 0.85$. The relative length of the mattress in this condition should be: $0.85 \cdot 10 = 8.5$ m.

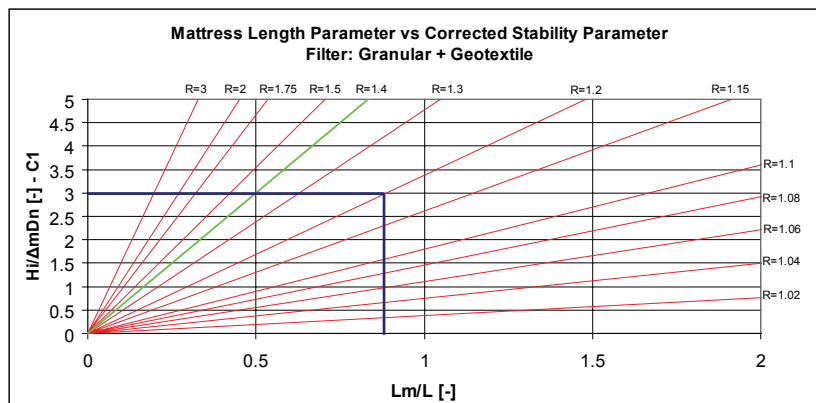


Figure 5.37: Determination mattress length parameter

If a thicker mattress is applied, than the mattress length becomes shorter. If a mattress thickness $D_n = 0.25$ m is used it gives a stability parameter of 4. This results in a relative mattress length of 6.5 m. With this method it is possible to optimise the use of fill material that should be applied. It remarked that it is always important to keep the degree of run-up and run-down into account when a mattress is calculated. A short mattress could be economical, but erosion around the mattress can still develop if this aspect is not taken into account. This aspect is especially important, since the run-up and run-down values show a wider variation around the average that is given by relations from literature.

Evaluation

In the Figures 5.34 and 5.35 it can be seen that for a line with a certain R-value the gradient is steeper for more permeable constructions. This is the effect of the uplift force, which influences the stability in a negative way for less permeable constructions.

The deviation of other R-values is based on the results from the experiments and are expressed in the ability of tension force absorption. The assumption is made that a linear relation is present between the increase of c_1 and the tension force that can be absorbed by a construction. This assumption is not fully correct. For increased R-values the slope angle decreases, but it results in a increase of the c_1 value that becomes unrealistically high. This implies that the linear relation between the relative length and corrected stability parameter is not fully correct. The mutual relation between the R-values based on the increased ability of tension force absorption should be corrected for the amount of uplift that develops. The uplift parameter will bend the graph to a more flat shape for a larger relative mattress length.

The analysis is performed on a limited amount of data. Extra series of tests have to be executed to gain a better relation between the relative length parameter and the R-value. This should be done for several slope angles to create a solid base for a better and more reliable design graph.

Contribution of Crown and Toe Compartments

In a gabion revetment, horizontal compartments can be placed at the toe, berm or crown. These elements contribute in two ways to the stability. In the first place the compartments do not experience a downward directed force component. In the second place the tension force on the mattress will always be in the downward direction. The amount of force needed to move the compartment improves due to the $\cos(\alpha)$ term.

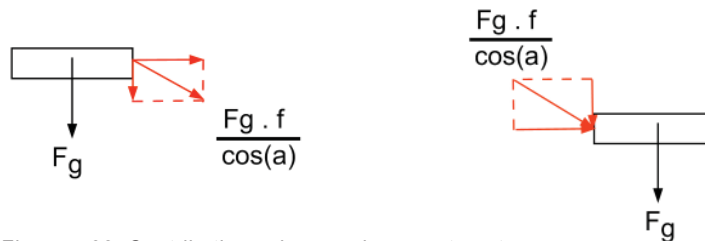


Figure 5.38: Contribution submerged compartments

To implement the influence of crown and toe compartments the length is expressed in the relative length of a compartment on the slope. Written in a relation this results in:

$$S_c = \frac{F_{horizontal}}{F_{slope}} = \frac{\frac{f \cdot F_g}{\cos(\alpha)}}{f \cdot F_g \cdot \cos(\alpha) - \sin(\alpha) \cdot F_g} = \frac{f}{\cos(\alpha) \cdot (f \cdot \cos(\alpha) - \sin(\alpha))} \quad [88]$$

$$S_t = \frac{F_{horizontal}}{F_{slope}} = \frac{\frac{f \cdot F_g}{\cos(\alpha)}}{f \cdot F_g \cdot \cos(\alpha) - \sin(\alpha) \cdot F_g} = \frac{f}{\cos(\alpha) \cdot (f \cdot \cos(\alpha) - \sin(\alpha)) \Delta} \quad [89]$$

For toe constructions the same relations holds, but it is corrected for the relative density in water. The result from formula [88] is divided by the parameter Δ [89]. Figure 5.39 shows the relation for crown and toe constructions based on the friction factors for geotextile and granular material.

From Figure 5.39 it can be deviated that the contribution of a horizontal compartment is depending on the slope angle and friction factor. A crown compartment with a friction force of 0.7 based on a 20° slope will contribute 2.4 times more than a inclined compartment.

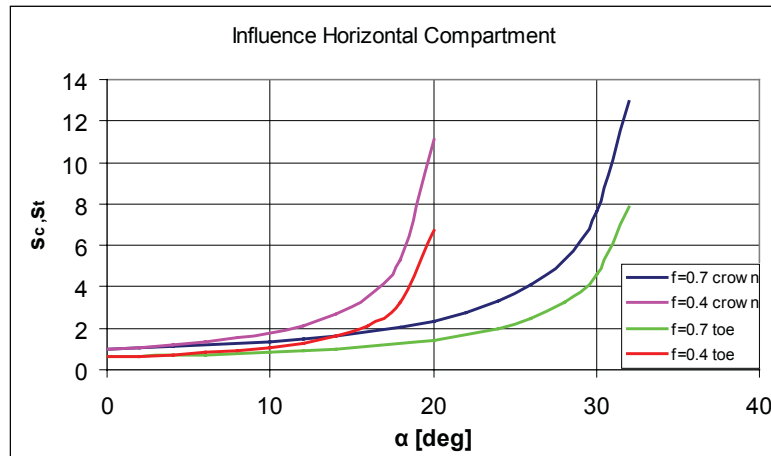


Figure 5.39: Contribution horizontal compartments

The influence of horizontal compartments can be implemented in the dimensionless mattress length ratio with formula [90]

$$\frac{L_{rel}}{L} = \frac{X + \frac{(L_m - X)}{\Delta} + s_c \frac{L_c}{X} + s_t \frac{L_t}{X}}{L} \quad [90]$$

For increased slope angles the factor s_c and s_t increases rapidly towards the condition in which $R=1$. The system will not respond static as expressed by Figure 5.39. The subsoil under the crown interacts with the horizontal compartment. For the relative smaller slope angles the graph might be useful, but for increasing slope angles the interaction with the subsoil starts to become important.

The graph of Figure 5.39 should therefore be corrected for the expression of the relative length. To adapt the graph a comparison can be made between a situation without crown and toe compartment (run 2) and a situation with horizontal compartments (run 1). Run 2 had a c_1 value of 1.83. Run 1 is based on the same slope only with a crown and toe compartment added giving a c_1 value of 2.5. Using these values in Figure 5.34 it comes forward that the dimensionless length is increased from 0.64 to 0.89 due to the horizontal compartments.

The contribution of horizontal compartments on the relative length depends on the angle of the slope. But the bearing capacity of the soil is also of importance, since the subsoil in the corner of the revetment is compressed. Increasing the length of a crown compartment will not result in a linear increasing of the relative length. The influence of the subsoil bearing capacity becomes important and the effect of increased length becomes less important.

If a serie of experiments would devoted to the contribution of horizontal elements than a better relation could be developed for the contribution. Based on the static relation a factor could be developed that corrects the influence of the subsoil failure at a certain point. The influence of the crown length should also be taken into account.

5.7.2 Parameter Analysis of Factor c_2

Horizontal compartments do not only influence the c_1 value but also have influence the sensitivity of the descending part of the stability relation. In Figure 5.22 the influence of the parameter c_2 is examined. All the runs show more or less the same curvature, giving a c_2 value of the order 20. Run 7 was rejected due to insufficient reliability of the experimental results. The R-value was around the value 1, giving unreliable results.

In Table 5.5 the c_2 -values are presented. The influence of the horizontal compartments is expressed in a c_2 -value that is more than doubled with respect to revetments with only inclined compartments. A direct relation cannot be developed with only one result for this mattress design. The conclusion that can be drawn is that horizontal compartments have influence on the shape of the stability relation. This comes especially forward in situations with lower Iribarren values. A possible explanation is that the subsoil bearing capacity is of influence. Lower Iribarren parameters show shorter waves, resulting in a faster and shorter presence of the load on the mattress. The subsoil might be better able to absorb this. The loads of longer waves is present for a longer period of time. This effect will result in deformation of the subsoil if the load is present long enough.

If more experimental results will become available, in which the influence of horizontal compartments is examined, then it will become possible to develop a relation for the parameter c_2 . In this relation the slope angle and horizontal compartment will determine the behaviour of this function. When a solid relation is developed it becomes possible to further implement the influence of revetment design on the stability. Based on this relation it would be able to describe a more general stability relation in which formula [84] is also divided by the value of c_2 . A single relation will represent all possibilities a stability relation.

Parameter	Run 1	Run 2	Run 3	Run 4	Run 7	Run 8
C2	54	19	16	19	7	24

Table 5.5: C_2 values

Chapter 6. Conclusions and Recommendations

In this chapter the conclusions of the thesis work is presented. It is followed by recommendations for the design and building of gabion mattresses. An important aspect is also the advise for further research.

6.1 Conclusions

6.1.1 Objectives

In chapter 1 several objectives have been created containing the aspects material, deformation and stability of synthetic gabions. Summarizing the following aspects are the objectives of this thesis:

1) Material

- Formulation of the demands for a synthetic grid material.
- Confirmation of the application of a synthetic material.

2) Deformation

- Determination of the grid material influence on the deformation.
- Determination of the influence of fill material shape, size and filling degree on the deformation.
- Recommendations for the construction of gabions.

3) Design Formula

- Improvement of the current design formula.

In order to reach the objectives, with respect to deformation and improvement of the design formula, scale experiments have been executed in a wave flume. During these test the following parameters have been varied:

-Wave parameters

Wave height (H), Wave period (T), Wave length (L)

- Revetment dimensions

Slope angle (α), Filter permeability, Friction (f),

- Gabion dimensions

Mattress length (L_m), Mattress thickness (D_n), Grid rigidity

- Fill material dimensions

Filling degree, Material size (D_r), Angularity

6.1.2 Material

Demands have been formulated for the properties of a grid material. Aspects as strength, ultraviolet degradation, sensitivity to installation damage, creep and chemical and biological degradation are taken into account. The application of E'grid geogrid in mattress gabions is a potential good alternative. In almost every aspect the E'grid geogrid contains properties that are comparable or better than a steel wire grid. The main disadvantages, corrosion and environmental pollution, of a steel wire grid gabion are not present in a synthetic geogrid alternative.

The strength capacity of the material depends on the dimensions of the mattress. Longer and heavier mattresses need to be able to absorb the tension force generated by the waves. The highest amount of tension force will develop is the ultimate limit state. A design should always be checked on the potential tension forces that can develop just before a mattress fails.

In view of creep that might develop, due to the tension forces, some extra research might be necessary to confirm the behaviour of the material during long time presence of short loading and unloading periods. These loads should represent the severe wave action that could be exposed on a structure. The tension should approach the moment of failure just before sliding. With these results a limit could be set for the maximum construction dimensions of a certain grid type. The expectation is that the development of creep is rather limited. E'grid geogrid is applied in road constructions in which many load variations develop during the passing of traffic. The expectation is that the E'grid geogrid will function properly during time with respect to creep.

The thought of the potential danger of wearing due to vibration of particles is irrelevant. The impulse of particles on the grid is of such small level that wearing will not cause any problems during the life-time of the construction. Due to the mutual blocking of the particles hardly any vibration is present.

6.1.3 Deformation

The scale experiments gained insight in the processes that occur during the functioning of gabions in waves. The main conclusion with respect to fill material is that the angularity is not of importance on the deformation process. The filling degree of the compartment determines the amount of deformation that can develop. If a compartment is not properly filled, than the fill material will bulge, resulting in the development of space on the upper side of the compartment. This could finally result in erosion through the mattress. The fill material that is transformed into the bulging compartment shape, results in a small tension on the grid. The developed tension results in more homogeneous behaviour of the fill material, since the grid exerts a pressure on the fill material. Due to this effect the amount of deformation does not depend on the angularity of the fill material. As long as there is mutual blocking of the particles no deformation will develop.

If a compartment is filled, it should always be filled until the grid is closed under tension. By applying this construction method the potential bulging shape that might develop is anticipated. The lid of the compartment will show a bulging shape, but material transport in the compartment becomes impossible. The interlocking effect of the grid and the mutual blocking of the particles, results in a homogeneous behaviour of the element. Influence of the grid rigidity is negligible on the amount of deformation that can develop. The anticipated and tightened compartment shape results in a limited amount of deformation in which grid rigidity has no influence. The importance of the flexural rigidity is of minor influence on the functioning of the construction.

A higher grid rigidity, though facilitates the construction phase of a revetment. The shape of a compartment should be preserved if it filled on site and placed afterwards. During movement, fill material can resettle itself and force the compartment in a less favourable shape. Careful lifting is important to gain a proper quality of the revetment. Filling on the slope itself will improve the initial quality of the construction, since the filling process and demanded result can be better controlled.

Some degree of deformation will always develop during time. Designing thin mattresses with a considerable compartment width compared to the thickness will result more easily in failure due to uncovered spots in the upper side of the compartment. The amount of space that can develop in wider compartments is relatively larger and will result more easily in uncovered areas. This aspect should always be taken into account when compartment sizes are applied that differ from standard dimensions.

The size of the fill material that is applied in a mattress has certain restrictions. The $D_{r,50}$ size of a mattress should always fulfil the relation of minimal $0.5 \cdot D_n$. Mattresses with relative too large fill material will subject the sublayer to a more intense turbulent environment, resulting in potential erosion of the sublayer. This can especially be present at the transitions between compartments. Larger fill material will also result in larger filter material that will be necessary.

The influence of fill material on the degree of deformation is rather limited. A compartment will always transform in more or less the same deformed shape, independent of the fill material size. There is a difference in the amount of fill material that is placed in a compartment. Relatively smaller fill material is able to follow the shape of the deformed mattress better compared to larger fill material. The amount of extra fill material that is necessary to close the compartment under tension is smaller for larger fill material.

6.1.4 Run-up, Run-down and Reflection

The run-up, run-down and reflection test results showed a difference with already available data from the literature. In the literature data is available from earlier performed tests. These tests are mostly based on scale model experiments from rip-rap revetment constructions. Data for this type of parameters never show a consistent relation, but form a scatter cloud around a certain average. Along the average of these data points a relation is developed with a certain deviation.

The difference with the gabion scale model tests is a wider scatter cloud of the data points. The data shows a larger variation. An acceptable and possible explanation is the influence of the relative thin outer layer of a gabion revetment protection. Rip-rap consists of a relative thicker layer which provides a better ability for wave energy absorption. Due to the thin outer layer of a gabion mattress the sublayer has more influence on the amount of wave energy absorption. Mattresses placed on a smooth and relative impermeable geotextile show a relative higher degree of run-up compared to the more permeable granular sublayer.

A relation cannot be developed, due to the relative small amount of data. The conclusion that can be made is that gabion mattresses show a wider variation in the expected amount of run-up, run-down and reflection. This aspect should be taken into account when a construction is designed.

6.1.5 Design Formula

Pilarczyk presented the current most useful formula for a stability relation of mattresses in waves. The Iribarren parameter is implemented which indirectly takes the run-down effect into account. The course of Pilarczyk's stability relation is correct, but there are some limitations. Aspects as friction, mattress length and permeability are not taken into account, which influence the stability of a construction. In the scale experiments the missing parameters are varied, which resulted in different stability relations (Figure 5.20). It is established that stability relations depend on slope angle, mattress geometry, friction and permeability characteristics of a specific design. Based on these results a start is made for a improved gabion mattress design formula in waves.

From the experimental results it comes forward that all the stability relation graphs have more or less the same shape for mattresses fully placed on a slope. The influence of increased length or improved friction is expressed by shifting of the entire stability relation in upward direction. The location of a stability relation is expressed by a parameter c_1 . This so called shifting factor c_1 influences the stability relation and depends on mattress length, friction, slope angle and permeability of the revetment construction.

From the experimental results it came forward that the runs performed with mattresses placed on a slope with their total length show a comparable course of the stability relation. The experiments that contained horizontal compartments on the crown or toe show a different more steep course of the stability relation. To describe the decaying course of the stability relation an exponential function has been applied which depends on the Iribarren parameter. The stability relation is described in the form:

$$\frac{H}{\Delta_m D_n} = c_1 + c_2 e^{-\xi}$$

The parameter c_2 describes influence of the stability course with respect to the shifting factor. These two parameters need to be determined to set up a stability relation for a certain situation. The determination of c_1 is based on the amount of tension force that can be absorbed by a construction before it slides down. It consists out of two parameters. The ratio R that describes the capacity of a element on a slope to absorb a certain amount of tension force. This is independent of the size or thickness of an element. The length of the mattress in that specific situation determines the c_1 value. A dimensionless length parameter has been developed to include the influence of the mattress length. The influence of the submerged part is taken into account by including the relative density parameter.

$$R = \frac{F_r}{F_d} = \frac{f}{\tan(\alpha)} \qquad \frac{L_{rel}}{L} = \frac{X + \frac{(L_m - X)}{\Delta}}{L}$$

The influence of permeability cannot be based on the tension force absorption. The different experimental relations between length and the R -value are therefore divided in three different groups that represent a certain type of filter construction. The relation for different R -values is based on an increase or decrease of the amount of tension force that can be absorbed. This results in the graphs of Figure 5.34 - 5.36, page 117.

The comments on these graphs are the unrealistically high values that can develop if the slope angle decreases to a certain degree. For high R -values the results are considered to be unreliable. The linear transformation of the test results is not fully correct. The development of uplift has influence on this process and will probably effect the shape of the graphs. More specified test results are necessary to improve the graphs.

From the experimental results it becomes clear that the course (c_2) of the stability relation is constant for revetment designs with compartments that are all placed on a slope. The value for c_2 is in the order of 20 for these situations.

The adding of horizontal compartments effects the stability relation in two ways. The relative length increases, but also a barrier is formed underneath the horizontal crown compartment. The bearing capacity of the subsoil will interfere in the stability when a horizontal crown compartment is placed. Especially for the lower Iribarren numbers an improved stability condition develops due to horizontal compartments. Smaller Iribarren numbers result in shorter waves that exert their tension force for a shorter amount of time. The bearing capacity is able to absorb the pressure that comes forward. Longer waves result in a longer period of pressure that is present on the subsoil underneath the crown compartment. It creates the ability for the subsoil to deform underneath until a slide plane originates.

Toe structures also effect the stability, but do not have the advantage of the extra subsoil barrier resistance. Their function is expressed by supporting the mattress. Heavy toe constructions with respect to the mattress will not prevent the mattress from sliding. The toe structure can be stable, but the mattress can slide down, resulting in bulging of the mattress.

Only one run with horizontal compartments is performed. Further analysis and recommendations are possible if the influence of the horizontal compartments are researched more intensively. Aspects as soil bearing capacity, slope angle and compartment length will play a considerable role of influence on this aspect. A result that could come forward from this research is a factor that corrects the static relation for the increased relative length.

6.2 Recommendations

6.2.1 Confirmation of Material Application

The development of creep is expected to be limited to a minimum. This is not completely excluded. Therefore it is recommended to perform a material test that represents the cyclic tension force on the anchoring zone of the mattress. This represents the tension force, caused by wave action just before the moment failure. With these results it is possible to set maximum mattress dimensions for each type of grid.

The vibration of fill material is also limited to a few particles if the compartments are properly filled. Wearing of the grid due to vibrating particles will not occur, though it might be useful to perform a wearing test in which particles move for a considerable amount of time over a sample. These results can take away the uncertainty that failure due to wearing might develop.

6.2.2 Run-up, Run-down, Reflection

In the test results the run-up, run-down and reflection data showed a wider scatter cloud compared to the test results based on rip-rap. The filter layer has more influence, since less turbulence can be created by the thinner mattress. A clear relation could not be developed. More specified research is necessary to investigate this effect.

The set up of the experiment must be adapted for a improvement of the results. It is recommended to apply a better wave reflection compensation to eliminate resonance in the flume, which can lead to a difference between the measured and actual present wave dimensions. Next to that the scale of the experiment should be decreased to prevent potential errors due to scaling. Based on these adaptations it is possible to gather a improved quality of data. Based on this data it might be possible to describe the influence of the mattress thickness and filter permeability in a formula.

6.2.3 Stability Relation

For further improvement of the stability relation it is important that research is performed with the objective to develop a relation between shift parameter c_1 , the tension force absorption ratio R and the dimensionless length parameter.

The linear approach that was applied between the ability to absorb tension force and c_1 is not fully correct and results in unrealistic high values for the stability parameter. The expectation is that due to uplift different mutual relation between the lines become visible. Due to a lack of data, caused by a too wide variety of experimental runs it was only possible to develop a first approach for a improved stability relation. More specified research should be performed for the three structure permeability groups, based on mattress that are all placed on the slope.

If more research becomes available for the determination of the c_1 value and a improved relation is created than the next step is to improve the relation influence of horizontal compartments. Crown and toe compartments do not only influence the c_1 value by increasing the relative length. They also effect the steepness of the stability relation c_2 . Both of these aspects form a subject for further improvement of the stability relation, taking into account the influence of design.

This research has to take into account the length of horizontal compartments, the bearing capacity of the soil and the slope angle. With these relations the contribution of horizontal compartments can be determined more accurately. Based on the mutual relations between the stability graphs, it might be possible to create a more general formula in which all stability relations are scaled to a main relation. Based on the determination of the shift factor c_1 and curvature parameter c_2 an individual relation can be developed from this general main stability relation.

List of Symbols

Symbol	Definition	Value	Unit
B	Width of a river		m
C	Chezy coefficient		(m/s) ^{1/2}
c	Bending length		mm
C _f	Friction coefficient		-
C _r	Coefficient for the character of the flow		-
C ₁	Stability relation shift factor		-
C ₂	Stability course factor		-
C ₃	Stability shape factor	1	-
Cu	Uniformity coefficient		-
d	Particle diameter		m
d*	Dimensionless particle diameter		-
dA	Compartment width		m
d _f	Thickness filter layer		m
d _t	Thickness cover layer		m
d _n	Nominal particle diameter		m
d _v	Equivalent void diameter		m
d _x	Grain diameter where x% of the grain mass has a smaller diameter		m
D _f	Size of gabion fill material		m
D _n	thickness of the gabion		m
e	Coefficient related to the character of the flow		-
E	Elasticity		N/mm ²
f	Friction factor		-
f	Darcy-Weisbach coefficient		-
f _{CBD}	Reduction factor chemical and biological degradation		-
f _{CR}	Reduction factor creep		-
f _{ID}	Reduction factor installation damage		-
f _{UV}	Reduction factor ultra violet radiation		-
F	Revetment stability factor		-
F _d	Downward directed force		N
F _g	Gravity force		N
F _r	Froude number		-
F _{r1,2}	Resistant force		N
F _t	Tension force		N
g	Acceleration of gravity	9.81	m/s ²
G	Flexural rigidity		μJ/m
h	Water depth		m
H	Wave height		m
H _D	Design wave height		m
H _i	Height incoming waves		m
H _r	Reflected wave height		m
H _s	Significant wave height, average of ¹ / ₃ of highest waves		m
i	Gradient		-
i _{cr}	Critical gradient		-
i _{down}	Downward gradient		-
i _s	Expected hydraulic gradient		-
i _{up}	Upward gradient		-
I	Moment of inertia		m ⁴
k _b	Permeability coefficient subsoil		m/s
k _f	Permeability coefficient filter layer		m/s
k _g	Permeability coefficient geotextile		m/s
k _n	Roughness		m

k_t	Permeability coefficient cover layer	m/s
K_d	Hudson element shape coefficient	-
K_h	Depth factor	-
K_r	Wave reflection coefficient	-
K_s	Slope factor	-
K_T	Turbulence factor	-
L	Wave length	m
L_m	Mattress length	m
m	Gradient flow condition parameter	-
m^*	Exponent related to the permeability	-
m^+	Coefficient particle fall velocity and geotextile thickness	-
M	Mass of an element	kg
	Moment	Nm
$M_{c,if}$	Mass increased filled compartment	kg
m_s	Mass of a stone	kg
n	Fill material porosity	-
n_r	Roughness coefficient	-
n_x	Scaling factor of a parameter x	-
O	Overhang length	mm
O_x	Geotextile opening size in which x% of the weight remains on the cloth	m
P_w	Geogrid transverse rib width	m
P_l	Geogrid longitudinal rib width	m
r	Centre line radius river	m
	Radius of curvature	m
	Tension force ratio	-
R	Hydraulic radius	m
	Tension force absorption ratio	-
Re	Reynold number	-
Re^*	Particle Reynolds number	-
R_d	Run-down	m
$R_{d2\%}$	Run-down for 2% of the highest waves	m
R_u	Run-up	m
s_c	Relative length factor crown	-
s_t	Relative length factor toe	-
T_{allow}	Allowable tensile strength	kN/m
T_{ult}	Ultimate tensile strength	kN/m
T_g	Thickness geotextile	m
T_p	Wave period at peak of spectrum	s
u	Mean flow velocity	m/s
u_b	Velocity at gabion surface	m/s
u_c	Critical flow velocity	m/s
u_i	velocity at the interface gabion and base soil/mattress	m/s
u^*	Shear stress velocity	m/s
$V_{b,c}$	Volume due to bulging compartment	m ³
$V_{c,f}$	Volume fixed compartment	m ³
V_s	Volume of a stone	m ³
v_f	Filter velocity	m/s
$v_{f,cr}$	Critical filter velocity	m/s
w	Fall velocity of a particle	m/s
w	Deflection	m
W	Fabric mass	mg/cm ²
W_t	Geogrid transverse rib width	m
W_l	Geogrid longitudinal rib width	m
X	Mattress length above water	m

α	Slope angle (perpendicular to flow direction)		°
α_b	Slope angle of river bottom (parallel to flow direction)		°
β	Angle of the schematised wave front		°
Δ	Relative density of a stone in water		-
Δ_m	Relative density of granular material in water		-
Δ_s	Relative density of the subsoil		-
Δ_z	Gabion deformation parameter		-
ε	Percentage of sample elongation		-
θ	Angle of internal friction		°
	Rotation		rad
Φ	Stability parameter		-
Φ_b	Piezometric head on a slope due to oncoming wave		m
Λ	leakage length		m
ρ_s	Density of stone		kg/m ³
ρ_w	Density of water	1000	kg/m ³
σ	Tension		N/mm ²
τ	Shear stress		N/mm ²
τ_b	Bottom shear stress		N/mm ²
τ_c	Critical bottom shear stress		N/mm ²
τ_m	Bank shear stress		N/mm ²
τ_s	Critical bank shear stress		N/mm ²
ν	Kinematic viscosity	$1.3 \cdot 10^{-6}$	m ² /s
Ψ	Shields parameter		-
	Permittivity		1/s
Ψ_{cr}	Critical shear stress parameter		-

Definitions

English	Dutch	Definition
Cohesion	Cohesie	The resistance due to the mutual forces between particles.
Creep	Kruip	Deformation and loss of initial strength of material which is loaded for a longer period.
Crown	Kruin	The horizontal part on the top of a revetment protection.
Current	Stroom, stroming	A flow of water.
Erosion	Erosie	The wearing away of land by the action of natural forces.
Filter	Filter	Intermediate layer consisting of granular material and/or a geotextile to prevent fine particles of the under layer from being washed out through the voids of the upper layer.
Gabion	Schanskorf	Container made of an open wired mesh filled with rock, stones or crushed concrete that is used for structural purposes.
Galvan Protection	Galvan bescherming	Protection of steel with a zinc-aluminium alloy based on the galvanizing process.
Galvanizing	Galvaniseren	Protecting of steel with a zinc layer, which is electronically applied.
Geogrid	Geogrid	A geosynthetic material consisting of connected parallel sets of intersecting ribs with apertures of sufficient size for interference with surrounding soil or stones.
Geotextile	Geotextiel	Synthetic permeable cloth that is used for separation or as a filter.
Pore Pressure	Poriën druk	The pressure of air or water in the voids between the particles.
Revetment	Bekleding	A protection of a slope formed by a cover layer and filter layer(s), used to protect the bank against erosion.
Rip-rap	Stortsteen	Randomly placed loose stone used for protection against erosion.
Run-down	Golf afloop	The downward movement of waves on a bank or wall below the average water level.
Run-up	Golf oploop	The upward movement of wave on a bank or wall above the average water level.
Scour	Ontgronding	Erosion of under water material by waves and/or currents around structures.
Shear stress	Schuifspanning	The drag force exerted by flowing water on the wetted perimeter of a river or channel, defined as a force per unit area.
Soil Bioengineering	Geo-Bio engineering	Erosion protection based on vegetation or a combination with structural elements.
Spanax tool	Spanax werktuig	A tool to connect ribs with steel rings.
Stake	Stek	Part of a plant that is placed as a base for further development of that specific type of vegetation.
Toe	Teen	The horizontal part on the bottom of a revetment protection.
Turbulence	Turbulentie	Irregular velocity fluctuations around an average value
Up-lift pressure	Opwaartse druk	Upward pressure subjected on the particles of an upper layer due to the resistance of out flowing water.
Wave Height	Golf hoogte	The vertical distance between the trough and crest.
Wave Period	Golf periode	The time for a wave to traverse a distance equal to the wave length.

References

- ASTM D1388a (2007), Standard Test Method for Stiffness of Fabrics, *ASTM, United States*
- BOSTD a (2007), Designing with E'GRID products, Technical factors
- CIRIA, CUR, CETMEF (2007) The rock manual, The use of rock in hydraulic engineering, *C683 CIRIA, London, 275-277*
- CUR/RWS (1995) Design manual for pitched slope protections, CUR report 155, *A.A. Balkema, Rotterdam*
- CUR/RWS (2000) Manual on the use of rock in hydraulic engineering, CUR report 169, *Taylor & Francis, 6-56*
- CUR 200 (1999) Natuurvriendelijke oevers, Aanpak en toepassingen, *CUR, Gouda*
- CUR 201 (1999) Natuurvriendelijke oevers, Belasting en sterkte, *CUR, Gouda*
- CUR 202 (1999) Natuurvriendelijke oevers, Oeverbeschermingsmaterialen, *CUR, Gouda*
- ETTEMA R. (2000), Hydraulic Modeling, *ASCE, Reston, USA*
- GRAY D.H., SOTIR R.B. (1996) Biotechnical and soil bioengineering slope stabilization, A practical guide for erosion control, *John Wiley & Sons, New York*
- KOERNER, R.M. (2005) Designing with geosynthetics, *Pearson Prentice Hall, USA, 42-43*
- MACCAFERRI (1985) Flexible lining in Reno mattress and gabions for canals and canalized water courses, *Maccaferri, Bologna*
- MAYNORD S.T. (1995) Gabion-mattress channel-protection design, *J. of Hydraulic Engineering ASCE, 121(7) 519-522*
- MORGAN R.P.C., RICKSON R.J. (1995) Slope stabilization and erosion control, A bioengineering approach. *E & FN Spon, London*
- PILARCZYK, K.W. (1998) Dikes and revetments, *A.A. Balkema, Rotterdam*
- PILARCZYK, K.W. (2000) Geosynthetics and geosystems in hydraulic and coastal engineering , *A.A. Balkema, Rotterdam*
- SCHIERECK, G.J. (2001) Introduction to bed bank and shore protection, *Delft University Press, Delft*
- VAN DER MEER, J.W., STAM, C.J.M. (1992) Wave run-up on smooth and rock slopes, *J. of WPC and OC, 118(5) 534-550, New York*
- VERVER, M.W. (2000) Materiaalkunde, *Educatieve Partners Nederland, Houten*
- VISWANADHAMA, B.V.S., KÖNIG, D. (2004), Studies on scaling and instrumentation of a geogrid, *J. of Geotextiles and Geomembranes, Elsevier*
- VRIES, M. de (1976) Waterloopkundig Onderzoek, Collegehandleiding b 80, Technische Universiteit Delft, Afdeling Waterbouw, *Delft*
- WRIGLEY, N.E. (2007) The creep-limited strength of E'grid 50-170R, BOSTD Geosynthetics, *New-grids Limited, Qingdao*

Internet

<http://www.etsong.com>

<http://www.geogrid.be>

<http://www.hy-tengabions.com>

<http://www.newgrids.com>

<http://www.texion.be>

<http://www.wikipedia.com>

List of Figures

- Figure 1.1: From: www.maccafferri.com
Figure 1.2: From: www.hy-tengabions.com
Figure 1.3: Left figure: CIRIA, CUR, CETMEF (2007) The rock manual, The use of rock in hydraulic engineering, page 274
Right figure: www.hy-tengabions.com
Figure 1.4: MACCAFERRI, Gabions and Reno mattresses, page 11
- Figure 2.1: Gabion link middle east, Design Guidelines, chapter 4
Figure 2.2: Gabion link middle east, Design Guidelines, chapter 6
Figure 2.3: CUR 201 (1999) Natuurvriendelijke oevers belasting en sterkte. Rijkswaterstaat DWW
Figure 2.4: AGOSTINI, R (1976) Flexible linings for canals and canalised water courses, page 33
Figure 2.5: MACCAFERRI, (1985) Flexible lining in Reno mattress and gabions for canals and canalized water courses, page 74
Figure 2.6: STEPHONSON, D (1979) Rockfill in hydraulic engineering, page 107
Figure 2.7: MACCAFERRI, River training works problems and solutions, page 19
Figure 2.8: MACCAFERRI, River training works problems and solutions, page 17
Figure 2.9: Wikipedia internet site, search term: gabions
Figure 2.10: GRAY D.H., SOTIR R.B. (1996) Biotechnical and soil bioengineering slope stabilization, a practical guide for erosion control, page 217
Figure 2.11: MACCAFERRI, Gabions and Reno mattresses, General Brochure, page 19
Figure 2.12: SCHIERECK, G.J. (2001) Introduction to bed bank and shore protection, page 50
Figure 2.13: SCHIERECK, G.J. (2001) Introduction to bed bank and shore protection, page 53
Figure 2.14: SCHIERECK, G.J. (2001) Introduction to bed bank and shore protection, page 55
Figure 2.15: SCHIERECK, G.J. (2001) Introduction to bed bank and shore protection, page 26
Figure 2.16: MACCAFERRI, (1985) Flexible lining in Reno mattress and gabions for canals and canalized water courses, page 40
Figure 2.17: MACCAFERRI, (1985) Flexible lining in Reno mattress and gabions for canals and canalized water courses, page 42
Figure 2.18: MACCAFERRI, (1985) Flexible lining in Reno mattress and gabions for canals and canalized water courses, page 43
Figure 2.19: MACCAFERRI, (1985) Flexible lining in Reno mattress and gabions for canals and canalized water courses, page 42
Figure 2.20: SCHIERECK, G.J. (2001) Introduction to bed bank and shore protection, page 153
Figure 2.21: CIRIA, CUR, CETMEF (2007) The rock manual, The use of rock in hydraulic engineering, page 488
Figure 2.22: SCHIERECK, G.J. (2001) Introduction to bed bank and shore protection, page 159 and 162
Figure 2.23: SCHIERECK, G.J. (2001) Introduction to bed bank and shore protection, page 157
Figure 2.24: PILARCZYK, K.W. (1998) Dikes and revetments, page 326
Figure 2.28: PILARCZYK, K.W. (1998) Dikes and revetments, page 337
Figure 2.29: PILARCZYK, K.W. (1998) Dikes and revetments, page 371
Figure 2.31: PILARCZYK, K.W. (1998) Dikes and revetments, page 374
Figure 2.32: MACCAFERRI, (1985) Flexible lining in Reno mattress and gabions for canals and canalized water courses, page 44
Figure 2.33: MACCAFERRI, (1985) Flexible lining in Reno mattress and gabions for canals and canalized water courses, page 43
Figure 2.34: MACCAFERRI, (1985) Flexible lining in Reno mattress and gabions for canals and canalized water courses, page 48
Figure 2.35: PILARCZYK, K.W. (2000) Geosynthetics and geosystems in hydraulic and coastal engineering, page 121
Figure 2.36: PILARCZYK, K.W. (2000) Geosynthetics and geosystems in hydraulic and coastal engineering, page 126
Figure 2.37: PILARCZYK, K.W. (2000) Geosynthetics and geosystems in hydraulic and coastal engineering, page 133
Figure 2.38: PILARCZYK, K.W. (2000) Geosynthetics and geosystems in hydraulic and coastal engineering, page 144

- Figure 3.1: KOERNER, R.M. (2005) Designing with geosynthetics, page 6
Figure 3.2: KOERNER, R.M. (2005) Designing with geosynthetics, page 42
Figure 3.3: WRIGLEY, N.E. (2007) The creep-limited strength of E'grids 50-170R, BOSTD, page 18
Figure 3.4: WRIGLEY, N.E. (2007) The creep-limited strength of E'grids 50-170R, BOSTD, page 19
Figure 3.8: VERVER, M.W. (2000) Materiaalkunde, page 294
Figure 3.9: VERVER, M.W. (2000) Materiaalkunde, page 296
Figure 3.10: VERVER, M.W. (2000) Materiaalkunde, page 297
Figure 3.11: CIRIA, CUR, CETMEF (2007) The rock manual, The use of rock in hydraulic engineering, page 1062
Figure 3.12: MACCAFERRI, Gabions and Reno mattresses, page 17
Figure 3.13: AGOSTINI, R (1976) Flexible linings for canals and canalised water courses, page 56
Figure 3.14: MACCAFERRI, River training works, problems and solutions, page 11
Figure 3.18: Hy-ten gabion solutions, www.hy-tengabions.uk

Figure 4.1: ASTM D1388 (2007), Standard Test Method for Stiffness of Fabrics, page 2
Figure 4.2: VISWANADHAMA, B.V.S., KÖNIG, D. (2004), Studies on scaling and instrumentation of a geogrid, J. of Geotextiles and Geomembranes, page 313
Figure 4.9: Tensar International, www.tensarinternational.com

Figure 5.23: CIRIA, CUR, CETMEF (2007) The rock manual, The use of rock in hydraulic engineering, page 495
Figure 5.26: CIRIA, CUR, CETMEF (2007) The rock manual, The use of rock in hydraulic engineering, page 522
Figure 5.27: PILARCZYK, K.W. (1998) Dikes and revetments, page 370

List of Tables

- Table 2.1: CUR 202 (1999) Natuurvriendelijke oevers, Oeverbeschermingsmaterialen, CUR, Gouda, Appendix A
- Table 2.2: PILARCZYK, K.W. (2000) Geosynthetics and geosystems in hydraulic and coastal engineering, page 145
- Table 3.1: www.newgrids.com
- Table 3.2: CIRIA, CUR, CETMEF (2007) The rock manual, The use of rock in hydraulic engineering, page 275
- Table 3.3: www.newgrids.com
- Table 3.4: WRIGLEY, N.E. (2007) The creep-limited strength of E'grids 50-170R, BOSTD, page 6
- Table 3.5: www.newgrids.com
- Table 4.1: WRIGLEY, N.E. BOSTD
- Table 4.2: WRIGLEY, N.E. BOSTD
- Table 5.3: [CUR, CIRIA, CETMEF 2007] Rock Manual, The use of rock in hydraulic engineering, page 495

Appendix A: Soil Parameter Information

A.1 Permeability Characteristics

Table A1: Permeability Values and Flow Characteristics for Various Materials

Material	d_{50} ($< 63 \cdot 10^{-3}$ m) or d_{n50} (m)	Permeability, k (m/s)	Character of flow
Clay	$< 2 \cdot 10^{-6}$	10^{-10} - 10^{-8}	laminar
Silt	$2 \cdot 10^{-6}$ - $63 \cdot 10^{-6}$	10^{-8} - 10^{-6}	laminar
Sand	$63 \cdot 10^{-6}$ - $2 \cdot 10^{-3}$	10^{-6} - 10^{-3}	laminar
Gravel	$2 \cdot 10^{-3}$ - $63 \cdot 10^{-3}$	10^{-3} - 10^{-1}	transition
Small rock	$63 \cdot 10^{-3}$ - 0.4	10^{-1} - $5 \cdot 10^{-1}$	turbulent
Large rock	0.4 - 1	$5 \cdot 10^{-1}$ - 1	turbulent

From: SCHIERECK (2000), Bed Bank and Shoreline Protection, page 101

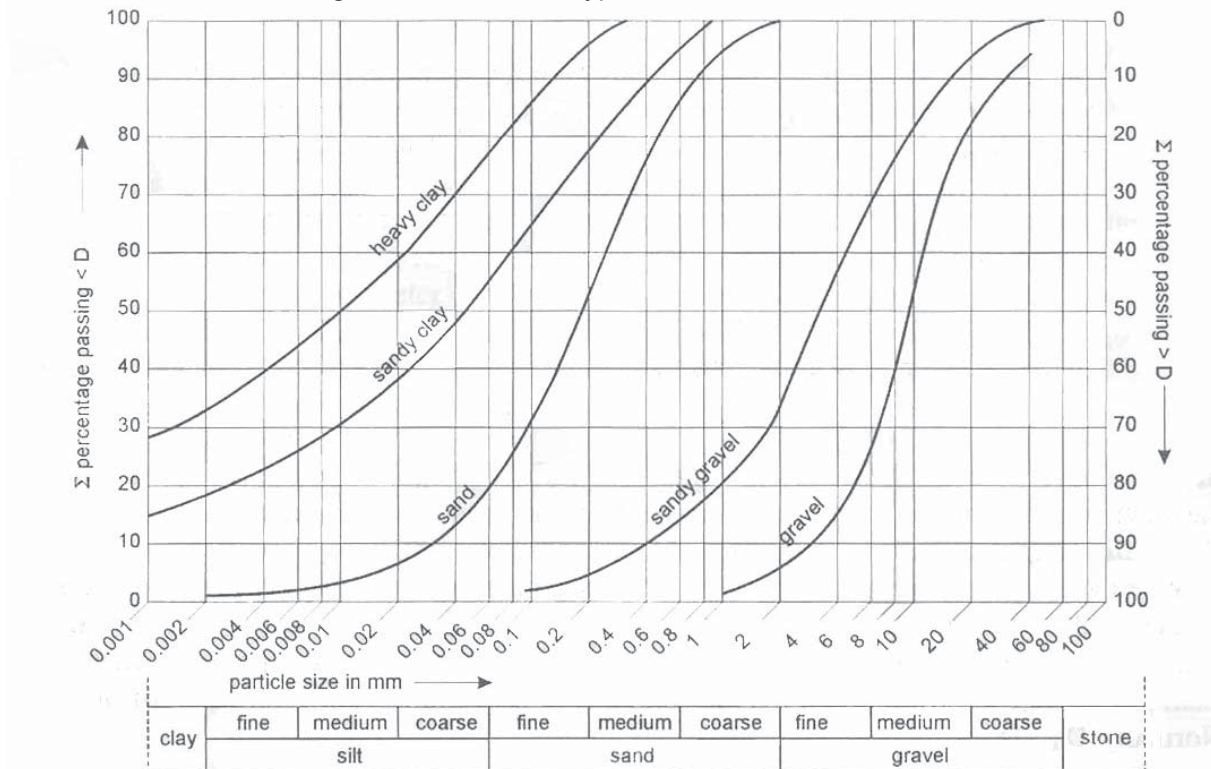
Table A2: Permeability Values of Sand Containing Hardly Any Silt

Grain size, D_{b50} [mm]	Permeability, k [mm/s]
0.10	0.06
0.15	0.14
0.20	0.24
0.30	0.54
0.40	1.00

From: PILARCZYK (2000), Geosynthetics and Geosystems in Hydraulic and Coastal Engineering, page 131

A.2 Sieving Curves Typical Dutch Soil

Figure A1: Overview Typical Dutch Sieve Curves



From: PILARCZYK (2000), Geosynthetics and Geosystems in Hydraulic and Coastal Engineering, page 131

Appendix B: Fill Material Information

B.1 Types of Fill Material

During the experiment several types of fill material are used. The application of different sorts of fill material are used to research the effect of shape and size on the deformation of gabions. The potential influence of the fill material on the stability of the construction is also taken into account. The following three types of stones are used during the experiment:

- Round fill material, gradation 16-32 mm.
- Small angular fill material, gradation 10-20 mm.
- Angular fill material, gradation 16-32 mm.

Figure B.1 shows samples of the types of fill material. In this appendix the properties of the fill material are represented in aid of the several parameters to be filled in.



Figure B.1: Round-, small angular-, and angular fill material

B.2 Fill Material Density

The density of the stones (ρ_m) is determined based on the increased volume and weight when a sample of stones are dropped into a measuring cylinder filled with water. The cylinder is partly filled with water to eliminate the effect of the pores. The result of this test is the density of the rock without pores. The working method is as follows:

- A measuring cylinder is partly filled with water. The volume of water is read from the scale on the measuring cylinder.
- A sample of stones is placed on a scale and the weight is measured (m_s).
- The sample of stones are then added to the measuring cylinder. The water level is higher than the stone level so the influences of pores is eliminated. The cylinder is shaken to release included air bubbles that can influence the test result.
- The rise of the water level is then measured from the scale. Based on the difference in water volume the volume of stones is determined (V_s).
- With formula B1 the density of the stones (ρ_m) can be calculated.

$$\rho_m = \frac{m_s}{V_s} \quad [B1]$$

- To create a proper base for the density of the stones the test is repeated three times with different samples of stones for every test. Based on the average of these three results the density is determined.

Figure B.2 shows the materials used for the determination of the stone density.



Figure B.2: Scale and measuring cylinder

Table B.1 shows the results of the determined densities.

Test	1	Mass	Volume
Gravel 16-32 mm		gr	ml
Cylinder with water		702.05	275
Stone mass		400.94	
Total		1102.99	425
Stone volume			150
ρ_m		2673	kg/m ³

Test	1	Mass	Volume
Small ang 10-20 mm		gr	ml
Cylinder with water		742.25	315
Stone mass		456.2	
Total		1198.45	485
Stone volume			170
ρ_m		2684	kg/m ³

Test	1	Mass	Volume
Angular 16-32 mm		gr	ml
Cylinder with water		757.84	327
Stone mass		343.06	
Total		1100.9	457
Stone volume			130
ρ_m		2639	kg/m ³

Test	2	Mass	Volume
Gravel 16-32 mm		gr	ml
Cylinder with water		720.65	290
Stone mass		486.15	
Total		1206.8	475
Stone volume			185
ρ_m		2628	kg/m ³

Test	2	Mass	Volume
Small ang 10-20 mm		gr	ml
Cylinder with water		724.81	295
Stone mass		457.87	
Total		1182.68	467
Stone volume			172
ρ_m		2662	kg/m ³

Test	2	Mass	Volume
Angular 16-32 mm		gr	ml
Cylinder with water		699.68	270
Stone mass		298.11	
Total		997.79	387
Stone volume			117
ρ_m		2548	kg/m ³

Test	3	Mass	Volume
Gravel 16-32 mm		gr	ml
Cylinder with water		697.47	267
Stone mass		420.41	
Total		1117.88	425
Stone volume			158
ρ_m		2661	kg/m ³

Test	3	Mass	Volume
Small ang 10-20 mm		gr	ml
Cylinder with water		754.93	325
Stone mass		448.88	
Total		1203.81	494
Stone volume			169
ρ_m		2656	kg/m ³

Test	3	Mass	Volume
Angular 16-32 mm		gr	ml
Cylinder with water		760.75	330
Stone mass		381.93	
Total		1142.68	475
Stone volume			145
ρ_m		2634	kg/m ³

Average	ρ_m		
		2654	kg/m ³

Average	ρ_m		
		2667	kg/m ³

Average	ρ_m		
		2607	kg/m ³

Table B.1: Density of gravel-, small angular-, angular fill material

B.3 Fill Material Sieving Curves

The fill material has a certain gradation. The supplier of the material gives a gradation of the fill material that is rather coarse. Sieving curves are made to get a better indication of the fill material size and distribution. With these graphs the d_{50} of the different fill materials is determined.

The sieve curves are determined according to two methods. For the larger stones, the round gravel and angular rock, the curve based on the individual weight of the stones. The sieve curve of the smaller angular rock is determined by using sieves of different sizes. Based on the weight that is present on a sieve, the curve is determined.

For the larger stone types (16-32 mm) a random sample of 100 stones was taken. Every stone is placed on a scale and the weight is noted. The density of the material is determined in section B.2. Based on this result the nominal size of the stones can be determined with use of formula B2:

$$d_n = \left(\frac{m_s}{\rho_s} \right)^{1/3} \quad [B2]$$

The result of this formula is the size in the form of a cube. This size can be converted into d_{50} by applying formula B3 [SCHRIERECK 2001].

$$\frac{d_{n50}}{d_{50}} = 0.84 \quad [B3]$$

Based on the mass of the stones the the data can be sorted from small to large stones. A cumulative distribution is made based on the weight of the stones compared to the the total weight of the sample. Figure B.3 en B.4 gives the results of the applied approach. The d_{50} of the round gravel is 23.7 mm. For the angular material the d_{50} is 24.5 mm.

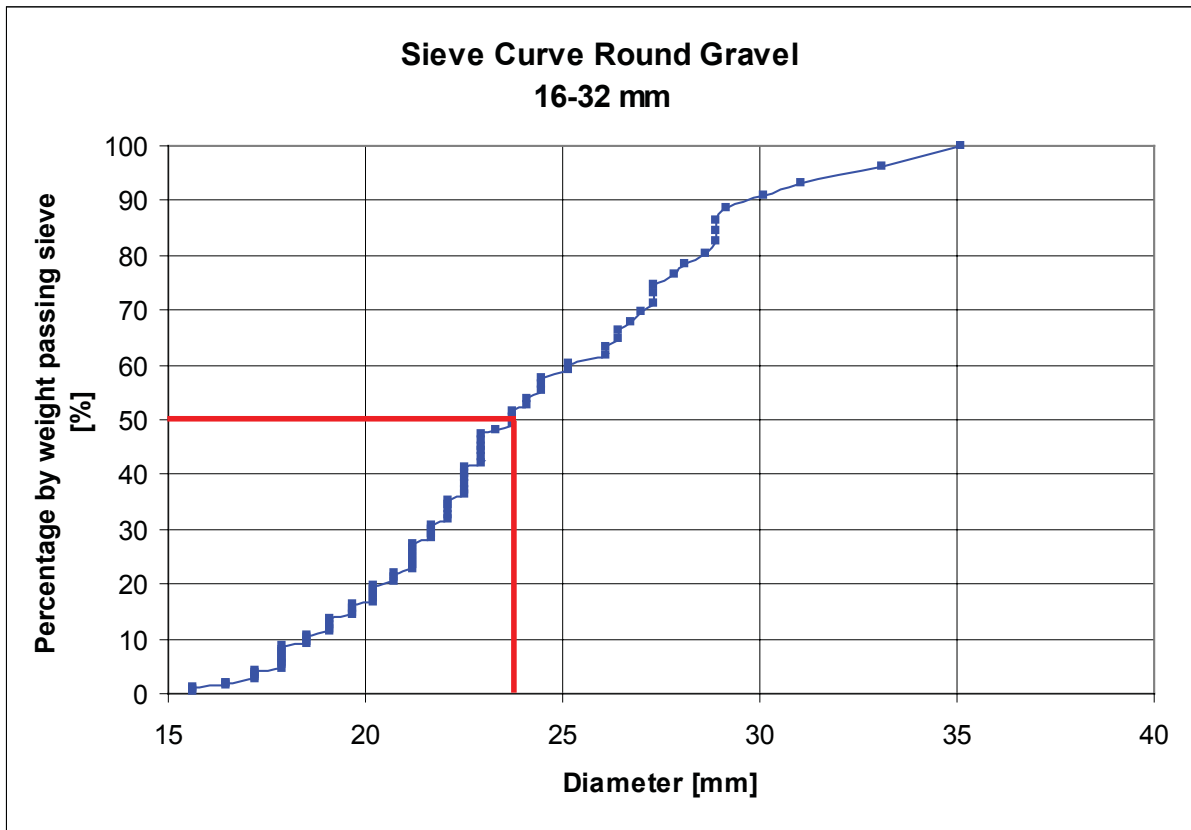


Figure B.3: Sieve curve round gravel 16-32 mm

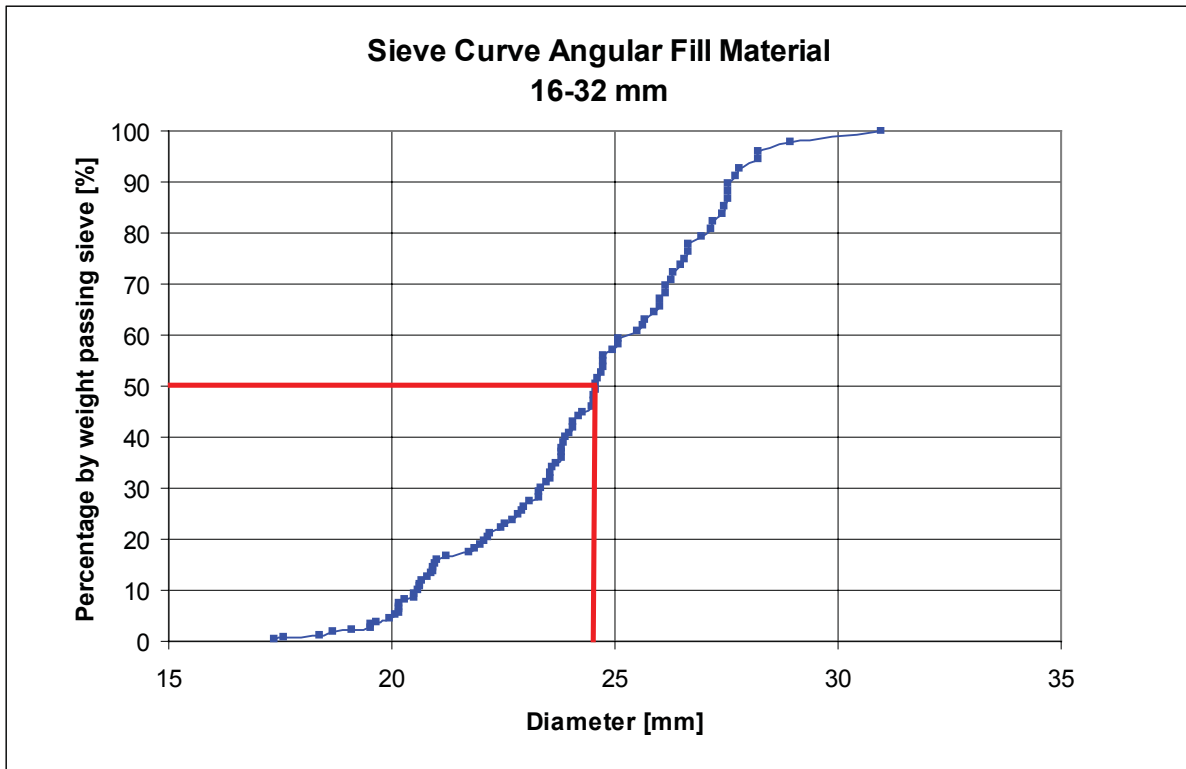


Figure B.4: Sieve curve angular fill material 16-32 mm

For the smaller angular gravel (10-20 mm) sieves are applied for the determination of the sieving curve. Sieves with sizes of respectively 6, 12, 16, 20 and 28 mm where used. By taking a sample of stones and sieving this quantity a certain distribution originates over the sieves. The mass present on every sieve is measured on a scale. Based on the percentage of the total weight a cumulative distribution can be drawn.

This method was repeated three times with different samples to generate a solid result. Table B.2 represents the results from the three test. In figure B.5 the test results are graphically represented. The d_{50} of the small angular material is approximately 15.4 mm.

Test 1				Test 2				Test 3			
Sieve [mm]	Mass [gr]	Percentage [%]	Cumulative [%]	Sieve [mm]	Mass [gr]	Percentage [%]	Cumulative [%]	Sieve [mm]	Mass [gr]	Percentage [%]	Cumulative [%]
0	0.00	0.0	0.0	0	0.00	0.0	0.0	0	0.00	0.0	0.0
6	50.47	4.1	4.1	6	44.16	4.0	4.0	6	62.45	5.7	5.7
12	141.25	11.6	15.7	12	153	13.7	17.7	12	122.38	11.2	16.9
16	497.45	40.8	56.6	16	483.21	43.4	61.1	16	472.59	43.2	60.2
20	528.9	43.4	100.0	20	433.42	38.9	100.0	20	435.49	39.8	100.0
28	0.00	0.0	100.0	28	0.00	0.0	100.0	28	0.00	0.0	100.0
Total	1218.07	100.0	100.0	Total	1113.79	100.0	100.0	Total	1092.91	100.0	100.0

Table B.2: Sieving results of the small angular fill material.

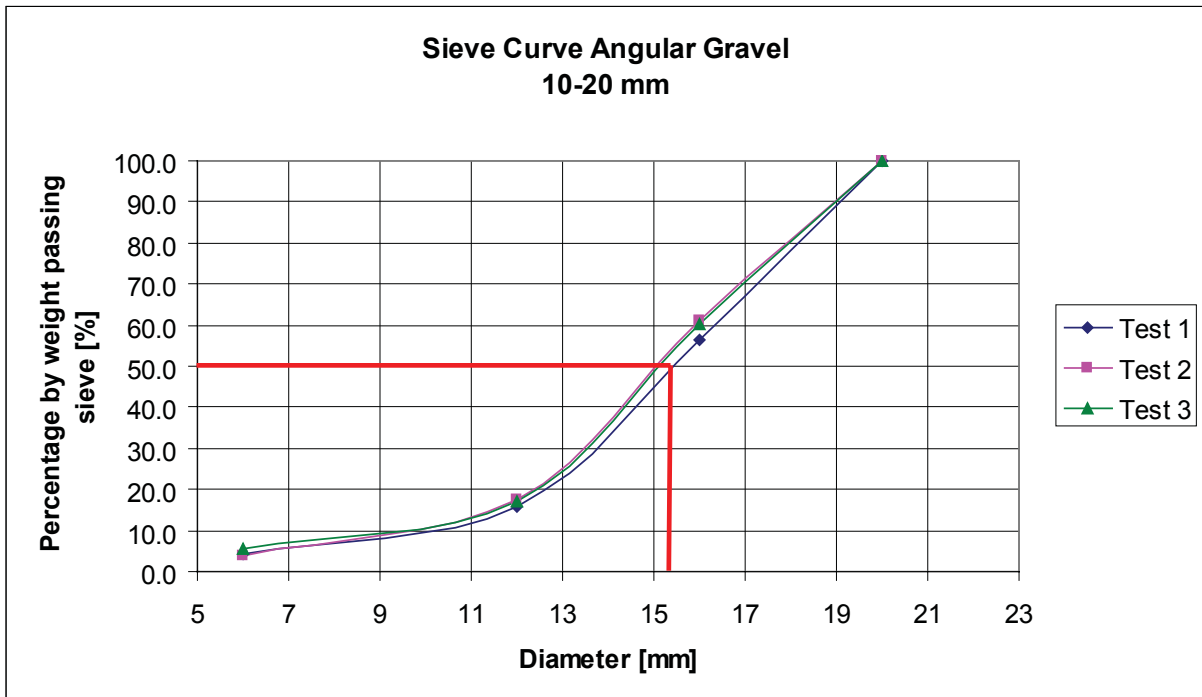


Figure B.5: Sieve curve angular fill material 10-20 mm

Appendix C: Wave Data Filter

C.1 Filtering Wave Data

The waves are measured with an acoustic system which consists out of three gauges. By measuring the wave height in three locations with known distances the period, incoming wave height and reflected wave height can be calculated. This is based on a Matlab program.

Disadvantage of the acoustic measuring system is that at a certain point peaks in the data originate due to increased wave steepness or propagation velocity. The sensor misses the signal that reflected on the water surface and measures the bottom of the flume. The next measuring point measures the water level again. This results in the data. Figure C.1 shows an example of these peaks.

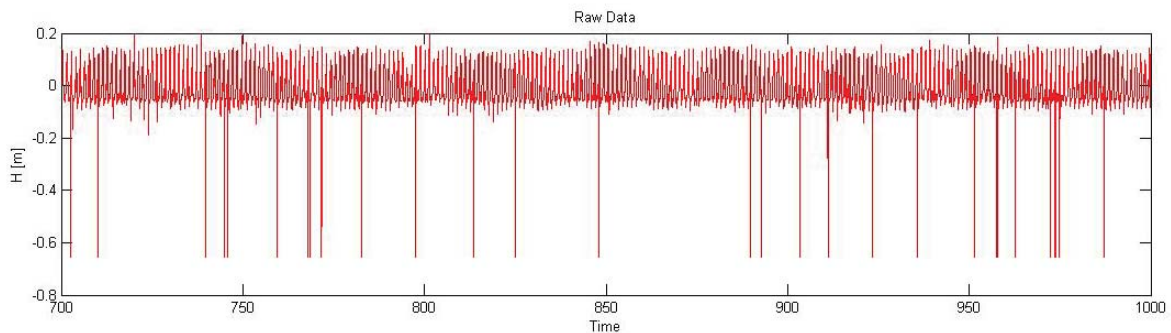


Figure C.1: Unfiltered data

The noise in the data disturbs the results from the Matlab script. Values for the wave height and period are influenced. For this reason the wave data is filtered. The waterlevel is measured with a frequency of 50 Hz. When a peak develops this is for one or two measuring points. Difference in waterlevel is unrealistic for these points. The data is filtered in such a way that if the distance between two following points is too large the value of the first measuring point is used. Between the two points a constant straight line is drawn. Figure C.2 shows the graph for filtered wave data.

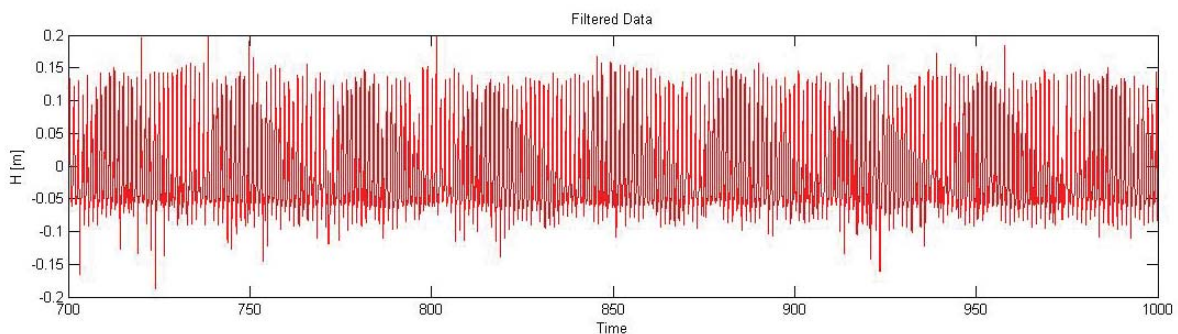


Figure C.2: Filtered data

C.2 Matlab Script

The data is filtered based on the following Matlab script:

```
% Unfiltered Data
g=[time sensor 3 sensor2 sensor1];

% Graphs Unfiltered Data
subplot(231), axis([0 600 -0.15 0.15])
plot(g(:,1), g(:,2), 'k')
subplot(232), axis([0 600 -0.15 0.15])
plot(g(:,1), g(:,3), 'r')
subplot(233), axis([0 600 -0.15 0.15])
plot(g(:,1), g(:,4), 'b')

% Filter Sensor 3
for i=2:1:(length(g)-1);
    disp(length(g))
    if g(i,2)-g(i-1,2)<-0.10 || g(i,2)-g(i-1,2)>0.10;
        g(i,2)=g(i-1,2);
    end;
    disp(i)
end;

% Filter Sensor 2
for i=2:1:(length(g)-1);
    disp(length(g))
    if g(i,3)-g(i-1,3)<-0.10 || g(i,3)-g(i-1,3)>0.10;
        g(i,3)=g(i-1,3);
    end;
    disp(i)
end;

% Filter Sensor 1
for i=2:1:(length(g)-1);
    disp(length(g))
    if g(i,4)-g(i-1,4)<-0.10 || g(i,4)-g(i-1,4)>0.10;
        g(i,4)=g(i-1,4);
    end;
    disp(i)
end;

% Graphs Filtered Data
subplot(234), axis([0 600 -0.15 0.15])
plot(g(:,1), g(:,2), 'k')
subplot(235), axis([0 600 -0.15 0.15])
plot(g(:,1), g(:,3), 'r')
subplot(236), axis([0 600 -0.15 0.15])
plot(g(:,1), g(:,4), 'b')

%Storage Filtered data
save exp.. -ascii -tabs
```

Appendix D: Experiment Results

D.1 Deformation Tests XI

D.1.1	Experiment D1	XII
D.1.2	Experiment D2	XIII
D.1.3	Experiment D3	XV
D.1.4	Experiment D4	XVII
D.1.5	Experiment D5	XIX
D.1.6	Experiment D6	XXI
D.1.7	Experiment D7	XXIII
D.1.8	Experiment D8	XXVI

D.2 Sliding Tests XXVII

D.2.1	Experiment S1 - Run 1	XXVIII
D.2.2	Experiment S2 - Run 1	XXIV
D.2.3	Experiment S3 - Run 1	XXX
D.2.4	Experiment S4 - Run 1	XXXI
D.2.5	Experiment S5 - Run 1	XXXII
D.2.6	Experiment S6 - Run 1	XXXIII
D.2.7	Experiment S7 - Run 1	XXIX
D.2.8	Experiment S8 - Run 2	XXXV
D.2.9	Experiment S9 - Run 2	XXXVI
D.2.10	Experiment S10 - Run 2	XXXVII
D.2.11	Experiment S11 - Run 2	XXXVIII
D.2.12	Experiment S12	XXXIV
D.2.13	Experiment S13	XXXX
D.2.14	Experiment S14 - Run 3	XLI
D.2.15	Experiment S15 - Run 3	XLII
D.2.16	Experiment S16 - Run 3	XLIII
D.2.17	Experiment S17 - Run 4	XLIV
D.2.18	Experiment S18 - Run 4	XLV
D.2.19	Experiment S19 - Run 4	XLVI
D.2.20	Experiment S20 - Run 4	XLVII
D.2.21	Experiment S22 - Run 5	XLVIII
D.2.22	Experiment S25 - Run 6	XLIX
D.2.23	Experiment S27 - Run 7	XLX
D.2.24	Experiment S28 - Run 7	LI
D.2.25	Experiment S29 - Run 7	LII
D.2.26	Experiment S30 - Run 8	LIII
D.2.27	Experiment S31 - Run 8	LIV
D.2.28	Experiment S32 - Run 8	LV
D.2.29	Experiment S33 - Run 8	LVI

D.1 Deformation Tests

D.1.1 Experiment D1

Test Parameters D1						
α	1:1.5	-	Crown	24	cm	
ξ	3	-	L1	68	cm	
D_n	40	mm	L2	60	cm	
Δ_m	1.00	-	Toe	22	cm	
ρ_s	2667	kg/m ³				
Fill Material	Small Angular					
Compaction	Normal					
Filter	Granular					
Remark	Extra Weak Grid					

Mattress Information						
Compartment	Width	Volume	Mass	ρ_b	n^*	Grid
-	cm	cm ³	kg	kg/m ³	-	-
1	24.0	4224	6.9	1634	0.39	Normal
2	23.5	4183	6.9	1650	0.38	Normal
3	22.5	4185	6.9	1649	0.38	Weak
4	22.5	4230	7.0	1655	0.38	Weak
5	23.0	4324	7.1	1642	0.38	Weak
6	23.5	4230	7.0	1655	0.38	Weak
7	22.0	3960	6.5	1641	0.38	Normal
8	22.0	3916	6.4	1634	0.39	Normal

Wave Results						
H_i	H_r	K_r	T	ξ	Run-up	Run-down
m	m	-	s	-	cm	cm
0.046	0.0160	0.35	0.99	3.9	3.6	1.9
0.109	0.0352	0.32	1.32	3.3	9.3	4.5
0.150	0.0579	0.39	1.55	3.3	14.7	7
0.177	0.0691	0.39	1.72	3.4	19.6	9.6

Reference		11 cm Waves					15 cm Waves					18 cm Waves				
x	A(0)	B(11)	C(22)	D(33)	E(44)	A(0)	B(11)	C(22)	D(33)	E(44)	A(0)	B(11)	C(22)	D(33)	E(44)	
cm	cm	cm	cm	cm	cm	cm	cm	cm	cm	cm	cm	cm	cm	cm	cm	
0.0	90.4	90.5	90.8	90.5	90.8	90.4	90.5	90.8	90.5	90.8	90.4	90.5	90.8	90.5	90.8	
11.5	90.2	89.7	89.2	89.6	90.5	90.2	89.7	89.2	89.6	90.5	90.2	89.7	89.2	89.6	90.5	
23.5	88.2	87.6	88.0	88.2	88.5	88.2	87.6	88.0	88.2	88.5	88.2	87.6	88.0	88.2	88.5	
32.5	85.6	85.8	85.9	85.8	85.5	85.6	85.8	85.9	85.8	85.5	85.6	85.8	85.9	85.8	85.5	
39.5	81.6	83.3	82.8	82.5	80.7	81.6	83.3	82.8	82.5	80.7	81.6	83.3	82.8	82.5	80.7	
45.0	77.8	77.5	77.3	76.9	77.3	77.9	77.7	77.5	77.0	77.3	77.9	77.6	77.5	77.0	77.2	
48.0	73.2	73.4	74.4	74.5	75.1	73.5	73.1	74.4	74.5	75.2	73.7	73.6	74.4	74.0	74.0	
54.5	70.4	70.1	70.4	71.0	71.9	70.4	70.1	69.9	71.0	71.7	70.5	70.2	69.2	71.5	71.0	
61.5	67.0	66.4	66.5	67.2	66.4	67.0	66.3	66.6	67.5	66.8	66.6	66.0	66.7	67.2	66.8	
63.5	64.8	64.3	64.1	64.1	64.0	64.8	64.3	64.0	64.0	64.0	64.7	64.0	64.0	63.8	63.9	
67.0	62.0	61.8	62.2	61.8	62.7	61.8	61.8	61.8	61.8	62.5	61.7	61.9	62.3	61.9	62.3	
73.5	58.2	58.3	58.9	58.0	58.9	58.4	58.4	58.9	57.7	58.8	58.0	58.5	58.5	57.5	58.5	
78.0	55.8	56.2	56.5	56.0	56.0	55.7	56.1	56.5	56.3	56.0	55.7	56.0	56.5	56.3	56.5	
82.0	52.3	52.1	52.2	52.2	52.4	52.2	52.2	52.2	52.0	52.3	52.2	52.1	52.1	52.0	52.1	
85.5	48.9	49.7	49.2	49.5	50.0	48.9	49.7	49.1	49.3	49.8	48.6	47.7	48.5	49.0	48.8	
92.5	44.7	44.6	45.3	45.8	45.6	44.5	44.6	45.0	45.7	45.5	45.6	45.3	46.3	45.3	46.0	
98.0	42.0	41.7	41.6	42.1	42.1	42.0	41.7	41.6	42.0	41.8	41.9	41.5	41.4	41.8	41.6	
100.0	39.1	38.9	38.5	39.1	39.4	39.1	38.8	38.6	39.0	39.4	38.9	38.6	38.5	38.9	39.2	
103.0	37.8	37.7	37.5	37.6	37.7	37.8	37.7	37.5	37.6	37.7	37.8	37.4	37.3	37.4	37.2	
109.5	34.3	34.0	34.5	34.3	34.5	34.3	34.0	34.5	34.3	34.5	34.1	34.0	34.5	34.0	34.2	
116.5	29.6	29.3	29.2	29.2	29.8	29.6	29.3	29.2	29.2	29.8	29.5	28.8	29.0	28.9	29.6	
119.0	26.5	26.3	26.2	26.2	26.5	26.5	26.3	26.2	26.2	26.5	26.3	25.9	25.8	26.0	26.4	
122.5	23.2	24.7	25.2	24.8	24.4	23.2	24.7	25.2	24.8	24.4	23.2	24.7	25.2	24.8	24.4	
128.5	21.1	21.8	22.2	22.0	22.1	21.1	21.8	22.2	22.0	22.1	21.1	21.8	22.2	22.0	22.1	
133.5	19.4	19.7	20.0	19.9	19.8	19.4	19.7	20.0	19.9	19.8	19.4	19.7	20.0	19.9	19.8	
137.5	17.5	17.8	17.5	17.5	17.5	17.5	17.8	17.5	17.5	17.5	17.5	17.8	17.5	17.5	17.5	
146.5	17.4	18.9	18.4	18.8	17.7	17.4	18.9	18.4	18.8	17.7	17.4	18.9	18.4	18.8	17.7	
157.5	16.5	16.8	16.8	17.2	17.4	16.5	16.8	16.8	17.2	17.4	16.5	16.8	16.8	17.2	17.4	

D.1.2 Experiment D2

Test Parameters D2						
α	1:1.5	-	Crown	24	cm	
ξ	3	-	L1	68	cm	
D_n	40	mm	L2	60	cm	
Δ_m	0.99	-	Toe	22	cm	
ρ_s	2654	kg/m ³				
Fill Material	Gravel					
Compaction	Normal					
Filter	Granular					
Remark	Failed at 19 cm					

Mattress Information						
Compartment	Width	Volume	Mass	ρ_b	n^*	Grid
-	cm	cm ³	kg	kg/m ³	-	-
1	24.0	4224	6.90	1634	0.38	Normal
2	23.5	4136	6.80	1644	0.38	Normal
3	21.5	3784	6.20	1638	0.38	Normal
4	21.5	3784	6.20	1638	0.38	Normal
5	22.0	3872	6.40	1653	0.38	Normal
6	21.0	3696	6.10	1650	0.38	Normal
7	22.0	3872	6.40	1653	0.38	Normal
8	22.5	3960	6.47	1634	0.38	Normal

Wave Results						
H_i	H_r	K_r	T	ξ	Run-up	Run-down
m	m	-	s	-	cm	cm
0.051	0.019	0.37	0.80	2.9	1.5	1.0
0.138	0.036	0.26	1.16	2.6	10.6	5.6
0.163	0.045	0.27	1.38	2.8	13.5	8.0
0.187	0.086	0.31	1.70	3.3	20.2	9.2

Reference		14 cm Waves					16 cm Waves					19 cm Waves Deformation Due to Sliding				
x	A(0)	B(11)	C(22)	D(33)	E(44)	A(0)	B(11)	C(22)	D(33)	E(44)	x	A	B	C	D	E
cm	cm	cm	cm	cm	cm	cm	cm	cm	cm	cm	[-]	0	11	22	33	44
0.0	94.0	93.9	93.5	93.5	94.0	94.0	93.9	93.5	93.5	94.0	13.0	85.3	84.7	84.1	83.6	84.5
12.0	92.6	93.2	93.4	93.2	92.7	92.6	93.2	93.4	93.2	92.7	25.0	81.2	81.4	81.1	81.8	81.6
22.0	88.7	88.3	88.4	88.3	88.5	88.7	88.3	88.4	88.3	88.5	35.0	76.5	76.0	76.2	76.5	77.0
33.0	81.5	82.3	82.4	81.1	81.8	81.5	82.3	82.4	81.1	81.8	47.0	69.6	70.0	70.1	69.9	69.3
41.0	77.0	77.7	76.8	76.7	75.8	77.0	77.7	76.8	76.7	75.8	55.0	64.3	64.5	64.0	64.3	64.1
43.5	74.2	74.9	73.9	73.3	73.3	74.2	74.9	73.3	73.4	73.8	62.5	60.0	61.0	61.2	60.2	59.6
51.0	69.3	70.0	70.1	69.0	68.5	68.9	70.1	69.8	70.5	69.7	70.0	56.9	57.1	56.9	57.4	55.3
58.0	64.8	66.4	66.3	65.4	65.0	64.5	66.0	66.1	65.6	65.0	72.0	54.2	54.4	54.0	54.1	53.9
61.5	61.9	61.9	62.2	62.5	62.5	61.2	61.5	61.2	61.8	62.4	77.0	50.8	51.6	51.0	51.5	51.1
70.0	57.4	57.6	57.5	57.5	57.0	57.2	57.7	57.5	57.5	56.9	85.0	48.9	48.9	49.3	49.0	48.2
75.0	54.8	55.0	55.1	55.3	53.8	54.7	55.4	55.5	55.6	53.9	93.5	45.4	45.2	45.3	45.5	45.3
81.0	51.8	51.1	51.1	50.5	50.7	50.8	50.7	49.9	50.1	49.8	98.0	43.2	43.3	42.4	43.2	43.2
87.0	47.9	48.2	48.0	47.6	46.3	46.9	48.0	48.5	48.2	46.3	105.0	39.9	42.0	41.5	41.0	40.1
94.0	42.1	43.3	43.4	42.5	41.0	42.6	43.5	43.9	43.0	41.3	113.0	35.2	36.2	36.7	36.3	35.6
98.0	38.6	39.0	39.1	38.6	38.6	37.9	38.2	38.2	37.7	38.5	120.0	31.0	33.2	32.5	32.8	30.6
105.0	34.0	35.2	35.0	34.6	34.0	33.8	34.5	34.7	34.7	33.8	125.0	28.4	29.7	30.7	30.5	28.1
110.0	30.0	31.8	31.6	30.7	30.4	31.0	31.7	32.6	31.8	30.7	130.0	26.0	26.5	26.9	26.3	25.4
114.5	28.0	28.6	28.0	27.5	27.8	27.5	28.2	27.5	27.0	27.4	134.5	22.8	23.9	24.4	22.8	22.6
120.5	23.5	24.4	25.2	24.0	23.6	24.1	24.5	25.0	24.0	23.5	141.5	18.6	20.5	21.0	19.9	18.8
129.0	18.7	18.6	18.7	18.9	18.9	18.8	18.7	20.2	20.0	19.0	147.5	16.0	16.2	16.3	16.1	15.8
140.0	15.7	16.8	16.6	15.8	15.6	15.7	16.8	16.6	15.8	15.6	158.5	12.9	14.4	14.1	12.9	12.9
150.0	13.3	13.4	13.8	13.0	13.0	13.3	13.4	13.8	13.0	13.0	168.0	11.7	11.6	11.5	11.5	11.7

D.1.3 Experiment D3

Test Parameters D3						
α	1:1.5	-	Crown	24	cm	
ξ	4.5	-	L1	68	cm	
D_n	55	mm	L2	60	cm	
Δ_m	0.99	-	Toe	22	cm	
ρ_s	2654	kg/m ³				
Fill Material	Gravel					
Compaction	Normal					
Filter	Granular					
Remark	Failed at 19 cm					

Mattress Information						
Compartment	Width	Volume	Mass	ρ_b	n^*	Grid
-	cm	cm ³	kg	kg/m ³	-	-
1	20.0	4840	8.00	1653	0.38	Normal
2	23.0	5566	9.10	1635	0.38	Normal
3	22.5	5445	8.90	1635	0.38	Normal
4	22.0	5324	8.70	1634	0.38	Normal
5	22.0	5324	8.70	1634	0.38	Normal
6	22.5	5445	8.90	1635	0.38	Normal
7	21.0	5082	8.40	1653	0.38	Normal
8	22.0	5324	8.70	1634	0.38	Normal

Wave Results						
H_i	H_r	K_r	T	ξ	Run-up	Run-down
m	m	-	s	-	cm	cm
0.114	0.045	0.40	1.66	4.1	10.2	7.8
0.164	0.079	0.48	1.94	4.0	14.8	10.7
0.192	0.094	0.49	2.14	4.1		

19 cm Waves Deformation Due to Sliding

x	A(0)	C(22)	E(44)
cm	cm	cm	cm
22.5	76.9	75.6	76.9
34	72.6	74	72.6
41.5	70.5	70.5	70.5
52	65.8	66.8	65.8
62	60.5	60.2	60.5
73	54.9	55.2	54.9
81	50	49.9	50
85	48.9	47.9	48.9
93	45.7	46.4	45.7
100.4	43.3	43.1	43.3
110.2	41.1	42	41.1
121.5	35.8	36.3	35.8
131	31.8	32.4	31.8
134	30.4	31.3	30.4
139.5	26.6	26.8	26.6
149	21.5	22	21.5
156	18.6	18.8	18.6
158	16.6	16.8	16.6
167	14.5	16	14.5
178	13	13.3	13

16 cm Waves

A(0)	B(11)	C(22)	D(33)	E(44)
cm	cm	cm	cm	cm
93.1	92.4	92.4	92.7	92.2
91.0	91.5	91.6	91.9	91.1
87.6	87.5	87.6	87.9	87.9
82.5	82.7	83.5	81.7	81.7
76.0	76.0	76.0	76.1	76.1
67.9	68.2	68.4	69.0	67.9
62.5	62.5	62.9	63.0	62.5
60.3	60.0	60.1	61.4	60.5
56.0	56.9	57.0	57.1	55.7
53.8	53.7	53.8	53.4	53.4
51.6	51.6	51.6	51.5	51.7
46.3	47.0	46.3	46.6	45.5
40.0	41.6	41.1	41.2	29.5
38.0	38.1	38.1	38.1	38.2
34.0	34.6	34.6	34.5	33.5
29.9	30.8	31.2	30.6	29.1
27.5	27.6	27.7	27.4	27.7
22.1	22.0	22.7	21.9	21.0
18.0	18.4	18.4	18.3	18.2
16.9	17.6	17.2	17.6	16.5
14.8	15.2	15.0	14.6	14.4

11 cm Waves

A(0)	B(11)	C(22)	D(33)	E(44)
cm	cm	cm	cm	cm
93.1	92.4	92.4	92.7	92.2
91.0	91.5	91.6	91.9	91.1
87.6	87.5	87.6	87.9	87.9
82.5	82.7	83.5	81.7	81.7
76.0	76.0	76.0	76.1	76.1
68.1	68.6	70.0	70.5	69.0
63.6	63.5	63.2	63.6	63.5
60.6	60.3	60.1	61.9	61.2
56.2	57.5	57.5	57.6	56.6
53.9	54.4	54.5	55.0	53.5
52.1	52.4	52.0	51.9	51.8
46.2	48.2	46.4	46.6	46.7
41.1	41.6	41.2	42.0	41.8
38.5	38.3	38.4	38.5	38.5
34.0	34.6	35.1	34.9	34.7
31.2	30.6	30.9	31.6	31.0
27.7	27.8	27.7	27.7	27.6
22.0	21.9	22.5	21.6	20.8
18.0	18.4	18.4	18.3	18.2
16.7	17.4	17.3	17.4	16.5
14.8	15.2	15.0	14.6	14.4

Reference

x	A(0)	B(11)	C(22)	D(33)	E(44)
cm	cm	cm	cm	cm	cm
0.0	93.1	92.4	92.4	92.7	92.2
8.2	91.0	91.5	91.6	91.9	91.1
19.6	87.6	87.5	87.6	87.9	87.9
29.0	82.5	82.7	83.5	81.7	81.7
38.6	76.0	76.0	76.0	76.1	76.1
49.7	68.3	69.2	69.6	69.8	69.1
56.2	63.6	63.1	63.5	63.6	63.4
59.5	61.5	60.7	60.3	62.3	61.4
67.2	55.7	57.7	57.5	58.2	56.7
72.2	53.6	54.3	54.8	55.0	53.9
75.2	52.2	52.3	52.3	52.0	51.7
82.2	47.4	47.7	47.4	47.7	46.6
90.2	41.2	41.8	42.3	42.7	42.2
94.7	38.5	38.4	38.5	38.4	38.6
100.2	34.6	34.7	35.3	35.1	35.0
107.2	30.5	31.6	31.0	30.6	30.1
110.6	27.8	27.9	27.7	27.7	27.8
121.2	22.2	22.0	23.0	22.0	21.1
128.7	18.0	18.4	18.4	18.3	18.2
139.2	16.9	17.6	17.2	17.6	16.5
149.5	14.8	15.2	15.0	14.6	14.4

D.1.4 Experiment D4

Test Parameters D4						
α	1:1.5	-	Crown	24	cm	
ξ	3	-	L1	68	cm	
D_n	40	mm	L2	60	cm	
Δ_m	0.96	-	Toe	22	cm	
ρ_s	2607	kg/m ³				
Fill Material	Angular					
Compaction	Increased					
Filter	Granular					
Remark	Fixed Mattress					

Mattress Information						
Compartment	Width	Volume	Mass	ρ_b	n^*	Grid
-	cm	cm ³	kg	kg/m ³	-	-
1	24.0	4224	6.90	1634	0.38	Normal
2	23.5	4183	6.90	1650	0.38	Normal
3	21.5	3913	7.90	2019	0.24	Increased
4	20.5	3690	7.40	2005	0.24	Increased
5	21.5	3849	7.70	2001	0.25	Increased
6	22.0	3916	7.80	1992	0.25	Increased
7	22.0	3960	6.50	1641	0.38	Normal
8	22.0	3916	6.40	1634	0.38	Normal

Wave Results						
H_i	H_r	K_r	T	ξ	Run-up	Run-down
m	m	-	s	-	cm	cm
0.067	0.008	0.12	0.98	3.2	4.5	3.0
0.113	0.025	0.22	1.28	3.2	7.8	5.2
0.158	0.045	0.28	1.60	3.3	14.3	8.7
0.218	0.117	0.54	1.94	3.5	21.3	12.5

Reference		11 cm Waves				16 cm Waves				22 cm Waves					
x	A(0)	B(11)	C(22)	D(33)	E(44)	A(0)	B(11)	C(22)	D(33)	E(44)	A(0)	B(11)	C(22)	D(33)	E(44)
cm	cm	cm	cm	cm	cm	cm	cm	cm	cm	cm	cm	cm	cm	cm	cm
0.0	92.1	92.1	91.8	91.9	91.6	92.1	92.1	91.8	91.9	91.6	92.1	92.1	91.8	91.9	91.6
11.0	92.0	93.1	92.5	92.0	91.4	92.0	93.1	92.5	92.0	91.4	92.0	93.1	92.5	92.0	91.4
23.0	91.0	91.4	91.1	90.8	90.3	91.0	91.4	91.1	90.8	90.3	91.0	91.4	91.1	90.8	90.3
33.0	87.3	88.1	87.5	87.3	86.5	87.3	88.1	87.5	87.3	86.5	87.3	88.1	87.5	87.3	86.5
40.5	82.6	83.2	83.4	83.0	81.6	82.6	83.2	83.4	83.0	81.6	82.6	83.2	83.4	83.0	81.6
44.0	79.9	80.1	79.8	79.3	79.2	79.9	80.1	79.8	79.3	79.2	79.9	80.1	79.8	79.3	79.2
48.0	77.8	77.8	77.9	77.8	78.1	77.8	77.8	77.9	77.8	78.1	77.8	77.8	77.9	77.8	78.1
54.0	72.6	74.2	75.2	73.3	73.8	72.6	74.2	75.2	73.3	73.8	72.6	74.2	75.2	73.3	73.8
58.5	70.1	70.3	71.5	70.1	70.1	70.1	70.3	71.5	70.1	70.1	70.1	70.3	71.5	70.0	69.7
62.3	67.0	67.4	66.8	66.7	66.3	67.0	67.4	66.8	66.7	66.3	67.0	67.3	67.2	66.6	66.1
64.0	65.6	66.6	65.0	66.0	65.2	64.2	66.6	64.9	65.6	65.0	64.2	66.6	65.4	65.6	65.1
67.5	64.5	65.9	65.2	65.0	64.3	64.6	65.4	64.1	64.1	63.9	64.2	65.1	64.2	63.6	63.5
74.0	59.8	62.0	62.2	60.6	59.7	59.5	61.4	61.9	60.5	59.6	59.0	60.9	61.2	60.5	59.4
76.5	57.3	57.7	57.7	57.7	57.6	57.0	57.3	57.1	57.1	57.0	56.5	57.0	56.8	56.9	56.6
80.0	55.4	56.0	55.7	55.4	56.1	55.5	56.0	55.3	54.6	54.5	55.7	55.5	54.8	55.0	54.7
86.0	52.5	53.1	53.5	53.1	53.8	52.0	52.0	52.7	52.7	52.8	51.5	51.7	52.3	52.5	52.5
92.0	49.6	49.7	49.8	49.2	49.3	49.1	49.6	49.2	49.4	49.1	48.5	49.2	48.8	49.2	48.7
94.5	46.6	46.6	46.5	45.9	46.4	46.1	46.0	46.1	45.5	45.7	45.5	45.2	45.6	45.8	45.6
98.0	44.5	45.8	44.8	45.1	44.3	44.5	45.0	45.0	44.7	44.1	43.7	44.1	43.6	44.2	43.0
104.0	41.0	42.2	42.0	42.3	42.1	40.3	42.0	41.7	42.2	41.1	40.8	42.0	41.1	41.9	41.3
109.5	38.8	38.3	38.7	38.5	37.7	38.3	37.6	38.4	38.2	37.2	37.7	37.2	37.8	37.4	37.7
112.5	35.2	35.2	35.3	35.1	34.2	35.2	35.2	35.3	35.1	34.2	35.2	35.2	35.3	35.1	34.2
116.0	30.5	32.3	32.5	32.1	31.2	30.5	32.3	32.5	32.1	31.2	30.5	32.3	32.5	32.1	31.2
121.5	27.6	29.7	29.6	28.4	26.5	27.6	29.7	29.6	28.4	26.5	27.6	29.7	29.6	28.4	26.5
127.5	23.5	23.8	23.6	23.4	22.7	23.5	23.8	23.6	23.4	22.7	23.5	23.8	23.6	23.4	22.7
137.5	19.6	20.9	20.0	20.4	19.5	19.6	20.9	20.0	20.4	19.5	19.6	20.9	20.0	20.4	19.5
146.5	15.7	16.2	16.5	16.5	16.5	15.7	16.2	16.5	16.5	16.5	15.7	16.2	16.5	16.5	16.5

D.1.5 Experiment D5

Test Parameters D5						
α	1:1.5	-	Crown	24	cm	
ξ	3	-	L1	68	cm	
D_n	30	mm	L2	60	cm	
Δ_m	1.00	-	Toe	22	cm	
ρ_s	2667	kg/m ³				
Fill Material	Small Angular					
Compaction	Normal					
Filter	Granular					
Remark	Fixed Mattress					

Mattress Information						
Compartment	Width	Volume	Mass	ρ_b	n^*	Compaction
-	cm	cm ³	kg	kg/m ³	-	-
1	23.0	3174	5.20	1638	0.39	Normal
2	21.5	2967	4.90	1651	0.38	Normal
3	21.0	2898	4.80	1656	0.38	Normal
4	22.5	3105	5.10	1643	0.38	Normal
5	22.5	3173	5.20	1639	0.39	Normal
6	21.5	3032	5.00	1649	0.38	Normal
7	22.5	3071	5.05	1644	0.38	Normal
8	23.0	3140	5.20	1656	0.38	Normal

Wave Results						
H_i	H_r	K_r	T	ξ	Run-up	Run-down
m	m	-	s	-	cm	cm
0.077	0.020	0.26	1.07	3.2	4.5	3.0
0.090	0.032	0.36	1.15	3.2	6.4	3.9
0.133	0.050	0.37	1.41	3.2	11.2	6.3
0.176	0.075	0.43	1.72	3.4	17.8	8.8

Reference		9 cm Waves					13 cm Waves					18 cm Waves				
x	A(0)	B(11)	C(22)	D(33)	E(44)	A(0)	B(11)	C(22)	D(33)	E(44)	A(0)	B(11)	C(22)	D(33)	E(44)	
cm	cm	cm	cm	cm	cm	cm	cm	cm	cm	cm	cm	cm	cm	cm	cm	
0.0	91.4	91.1	91.5	91.5	92.3	91.4	91.1	91.5	91.5	92.3	91.4	91.1	91.5	91.5	92.3	
11.1	90.4	91.0	90.8	90.6	90.8	90.4	91.0	90.8	90.6	90.8	90.4	91.0	90.8	90.6	90.8	
20.5	90.2	90.3	90.2	90.3	90.5	90.2	90.3	90.2	90.3	90.5	90.2	90.3	90.2	90.3	90.5	
23.5	89.2	89.7	89.5	89.9	89.2	89.2	89.7	89.5	89.9	89.2	89.2	89.7	89.5	89.9	89.2	
31.5	86.9	88.6	88.5	88.0	87.8	86.9	88.6	88.5	88.0	87.8	86.9	88.6	88.5	88.0	87.8	
38.6	82.7	85.2	84.3	84.5	82.3	82.7	85.2	84.3	84.5	82.3	82.7	85.2	84.3	84.5	82.3	
41.0	81.6	82.2	82.4	82.0	81.9	81.6	82.2	82.4	82.0	81.9	81.6	82.2	82.4	82.0	81.9	
44.0	78.6	79.2	79.3	79.7	79.0	78.6	79.2	79.3	79.7	79.0	78.6	79.2	79.3	79.7	79.0	
50.5	74.3	74.4	74.6	74.1	74.8	74.3	74.4	74.6	74.1	74.8	74.3	74.4	74.6	74.1	74.8	
56.4	69.7	71.0	70.4	71.0	70.4	69.7	71.0	70.4	71.0	70.4	69.7	71.0	70.4	71.0	70.4	
58.6	68.1	67.9	67.9	67.9	67.8	68.1	67.9	67.9	67.9	67.8	68.1	67.9	67.9	67.9	67.8	
61.5	65.4	65.6	66.3	66.0	66.2	65.4	65.5	66.3	66.1	66.2	65.4	65.5	66.3	66.0	66.2	
68.5	62.0	62.2	62.3	63.0	61.6	61.9	62.0	62.2	62.8	61.6	61.6	61.8	62.1	62.9	61.5	
73.9	58.3	59.0	59.0	58.9	57.3	58.1	59.0	58.6	59.1	57.1	58.2	59.1	58.5	59.0	57.0	
77.3	56.0	56.1	56.1	55.9	55.8	56.1	56.0	56.0	55.8	55.9	55.9	55.8	55.7	55.5	55.7	
80.5	52.6	52.1	52.4	53.2	53.0	52.3	51.5	51.9	52.8	53.0	51.7	51.3	51.7	52.0	51.5	
86.6	48.3	49.0	48.2	49.0	48.8	48.1	49.0	47.8	49.0	49.7	48.6	49.6	48.1	49.5	50.0	
91.5	44.5	45.0	44.8	45.7	45.9	44.4	44.8	44.6	45.5	45.7	44.5	45.5	44.7	46.1	46.4	
93.3	43.2	43.1	43.1	43.2	43.2	43.1	43.0	43.0	43.2	43.2	43.1	43.0	43.0	43.4	43.2	
96.5	41.2	41.4	41.2	41.6	41.0	41.0	41.3	41.4	41.5	41.0	40.7	41.3	41.1	41.2	40.5	
103.5	37.6	37.6	38.1	37.2	37.4	37.5	37.4	38.0	37.2	37.3	37.5	37.2	38.2	37.7	37.2	
110.9	33.0	33.1	33.7	33.3	33.0	33.0	33.0	33.4	33.4	33.2	33.5	33.0	33.2	33.3	33.1	
112.5	31.6	31.5	31.6	31.4	31.7	31.6	31.4	31.6	31.4	31.6	31.5	31.3	31.5	31.4	31.5	
116.5	29.5	29.0	29.5	29.7	29.1	29.5	29.0	29.5	29.7	29.1	29.5	29.0	29.5	29.7	29.1	
122.5	26.0	26.9	26.7	26.7	26.5	26.0	26.9	26.7	26.7	26.5	26.0	26.9	26.7	26.7	26.5	
128.5	22.5	23.2	24.1	23.2	22.8	22.5	23.2	24.1	23.2	22.8	22.5	23.2	24.1	23.2	22.8	
131.5	20.7	21.2	21.0	20.7	20.4	20.7	21.2	21.0	20.7	20.4	20.7	21.2	21.0	20.7	20.4	
141.5	17.9	18.8	18.7	18.2	17.8	17.9	18.8	18.7	18.2	17.8	17.9	18.8	18.7	18.2	17.8	
151.5	16.4	16.4	16.5	16.0	15.9	16.4	16.4	16.5	16.0	15.9	16.4	16.4	16.5	16.0	15.9	

D.1.6 Experiment D6

Test Parameters D6						
α	1:1.5	-	Crown	24	cm	
ξ	3	-	L1	68	cm	
D_n	40	mm	L2	60	cm	
Δ_m	1.00	-	Toe	22	cm	
ρ_s	2667	kg/m ³				
Fill Material	Small Angular					
Compaction	Increased					
Filter	Granular					
Remark	Fixed Mattress					

Mattress Information						
Compartment	Width	Volume	Mass	ρ_b	n^*	Compaction
-	cm	cm ³	kg	kg/m ³	-	-
1	24.0	4224	6.90	1634	0.39	Normal
2	23.5	4183	6.90	1650	0.38	Normal
3	22.5	4028	9.05	2247	0.16	Increased
4	21.5	3849	8.55	2222	0.17	Increased
5	21.0	3822	8.55	2237	0.16	Increased
6	20.0	3640	7.85	2157	0.19	Increased
7	22.0	3960	6.50	1641	0.38	Normal
8	22.0	3916	6.40	1634	0.39	Normal

Wave Results						
H_i	H_r	K_r	T	ξ	Run-up	Run-down
m	m	-	s	-	cm	cm
0.086	0.016	0.18	0.98	2.8	4.4	1.9
0.093	0.025	0.27	1.29	3.5	6.7	4.4
0.167	0.053	0.32	1.60	3.3	15.6	8.2
0.233	0.119	0.51	1.94	3.3	23.0	14.3
0.245	0.123	0.50	1.94	3.3	31.7	15.1

Reference		9 cm Waves					17 cm Waves					23 cm Waves				
x	A(0)	B(11)	C(22)	D(33)	E(44)	A(0)	B(11)	C(22)	D(33)	E(44)	A(0)	B(11)	C(22)	D(33)	E(44)	
cm	cm	cm	cm	cm	cm	cm	cm	cm	cm	cm	cm	cm	cm	cm	cm	
0.0	90.4	90.5	90.4	90.4	90.6	90.4	90.5	90.4	90.4	90.6	90.4	90.5	90.4	90.4	90.6	
12.0	89.7	89.6	89.1	89.6	90.4	89.7	89.6	89.1	89.6	90.4	89.7	89.6	89.1	89.6	90.4	
24.0	87.6	86.9	87.0	87.1	87.2	87.6	86.9	87.0	87.1	87.2	87.6	86.9	87.0	87.1	87.2	
33.0	83.0	83.5	84.4	83.5	83.5	83.0	83.5	84.4	83.5	83.5	83.0	83.5	84.4	83.5	83.5	
41.0	79.7	79.2	80.2	79.1	79.0	79.7	79.2	80.2	79.1	79.0	79.7	79.2	80.2	79.1	79.0	
45.0	76.6	76.5	76.4	76.3	76.4	76.6	76.5	76.4	76.3	76.4	76.6	76.5	76.4	76.3	76.4	
49.0	73.7	74.4	74.7	75.1	74.7	73.5	74.3	74.5	74.9	74.5	72.8	73.6	73.9	74.1	73.6	
56.0	70.6	72.0	72.0	71.6	70.9	70.5	72.0	72.0	71.7	70.9	70.5	71.5	71.8	71.7	71.0	
61.0	67.1	68.4	68.8	68.7	67.4	67.1	68.4	69.0	68.7	67.4	67.2	68.5	68.8	68.5	66.8	
63.0	64.1	64.1	64.1	64.0	63.9	64.0	64.1	64.0	63.9	63.9	63.4	63.6	63.6	63.5	63.0	
67.0	63.2	63.2	63.3	63.3	62.5	63.0	63.1	63.3	62.7	62.1	62.3	62.8	63.1	62.7	61.4	
73.0	60.2	61.0	62.2	62.4	59.7	60.0	61.0	62.1	62.2	59.9	59.6	60.9	61.4	61.5	59.9	
78.0	57.3	58.6	58.8	58.8	56.5	57.0	58.6	59.0	58.8	56.3	57.2	58.2	58.6	58.7	55.6	
81.0	53.6	54.2	54.3	54.4	54.3	53.6	54.1	54.3	54.4	54.3	52.5	53.0	53.3	53.4	52.9	
85.5	52.6	53.0	52.6	51.8	51.9	52.4	52.9	52.4	51.7	51.6	51.9	51.8	51.5	51.5	50.6	
90.5	49.5	50.1	50.6	50.8	48.7	49.4	50.0	50.2	50.5	48.5	49.2	50.2	50.1	49.8	47.9	
96.0	46.5	47.3	47.3	46.6	45.2	46.5	47.1	47.1	46.5	45.2	46.4	47.1	47.1	46.0	44.8	
98.5	42.9	43.1	42.7	42.5	42.1	42.8	43.0	42.9	42.5	42.0	42.5	42.8	42.6	42.2	41.7	
101.0	41.0	41.0	41.3	41.0	40.9	41.0	41.1	41.1	41.1	40.6	40.7	41.0	40.8	40.3	40.1	
106.0	39.1	39.0	38.8	39.1	38.0	39.0	39.0	38.8	39.1	37.9	38.4	38.8	38.3	38.3	37.7	
112.5	35.2	36.2	36.8	36.2	34.5	35.1	36.1	36.6	36.2	34.4	35.0	35.8	36.3	36.2	34.8	
115.0	32.2	32.3	32.2	32.2	32.2	32.2	32.3	32.1	32.1	32.2	31.8	31.9	31.9	32.2	31.8	
118.0	28.5	28.6	28.8	29.1	29.6	28.5	28.6	28.8	29.1	29.6	28.5	28.6	28.8	29.1	29.6	
125.0	24.5	26.9	26.9	26.7	24.8	24.5	26.9	26.9	26.7	24.8	24.5	26.9	26.9	26.7	24.8	
131.8	19.7	20.0	20.1	20.3	20.1	19.7	20.0	20.1	20.3	20.1	19.7	20.0	20.1	20.3	20.1	
141.0	18.7	19.5	20.5	20.4	19.9	18.7	19.5	20.5	20.4	19.9	18.7	19.5	20.5	20.4	19.9	
151.0	17.4	17.2	17.6	18.0	18.0	17.4	17.2	17.6	18.0	18.0	17.4	17.2	17.6	18.0	18.0	

D.1.7 Experiment D7

Test Parameters D7						
α	1:1.5	-	Crown	24	cm	
ξ	3.5	-	L1	68	cm	
D_n	55	mm	L2	60	cm	
Δ_m	0.99	-	Toe	22	cm	
ρ_s	2654	kg/m ³				
Fill Material	Gravel					
Compaction	Normal					
Filter	Granular					
Remark	Fixed Mattress					

Mattress Information						
Compartment	Width	Volume	Mass	ρ_b	n^*	Compaction
-	cm	cm ³	kg	kg/m ³	-	-
1	20.0	4840	8.00	1653	0.38	Normal
2	23.0	5566	9.20	1653	0.38	Normal
3	22.5	5445	8.90	1635	0.38	Normal
4	22.0	5324	8.70	1634	0.38	Normal
5	22.0	5324	8.70	1634	0.38	Normal
6	22.5	5445	8.90	1635	0.38	Normal
7	21.0	5082	8.40	1653	0.38	Normal
8	22.0	5324	8.70	1634	0.38	Normal

Wave Results						
H_i	H_r	K_r	T	ξ	Run-up	Run-down
m	m	-	s	-	cm	cm
0.084	0.021	0.25	1.15	3.30	4.6	2.7
0.115	0.028	0.25	1.29	3.17	8.4	5.5
0.147	0.040	0.27	1.60	3.47	15.4	7.9
0.196	0.079	0.40	1.86	3.50	20.3	9.9
0.208	0.122	0.58	2.34	4.27	33.4	15.8

Reference x cm	12 cm Waves					15 cm Waves					20 cm Waves				
	A(0) cm	B(11) cm	C(22) cm	D(33) cm	E(44) cm	A(0) cm	B(11) cm	C(22) cm	D(33) cm	E(44) cm	A(0) cm	B(11) cm	C(22) cm	D(33) cm	E(44) cm
0.0	91.8	91.8	91.7	91.7	91.7	91.8	91.8	91.7	91.7	91.7	91.8	91.8	91.7	91.7	91.7
10.5	91.9	91.8	91.5	91.6	91.1	91.9	91.8	91.5	91.6	91.1	91.9	91.8	91.5	91.6	91.1
20.5	91.1	91.1	91.1	91.1	90.9	91.1	91.1	91.1	91.1	91.1	91.1	91.1	91.1	91.1	90.9
25.2	90.3	88.9	88.9	90.3	89.4	90.3	88.9	88.9	90.3	89.4	90.3	88.7	88.7	90.0	88.3
32.5	86.8	86.6	86.7	87.0	86.2	86.8	86.6	86.7	87.0	86.2	86.3	86.4	86.5	86.9	86.1
37.5	83.9	84.2	84.5	84.5	83.5	83.9	84.2	84.5	84.5	83.5	83.6	83.9	84.3	84.3	83.6
40.9	81.5	81.4	81.1	81.2	81.1	81.5	81.4	81.1	81.2	81.1	81.4	81.4	80.9	81.0	80.9
43.0	78.9	79.0	79.1	78.1	78.8	78.9	78.7	78.8	77.8	78.8	78.4	78.2	77.6	77.6	78.8
50.5	73.5	73.0	73.6	74.3	72.7	73.5	73.0	73.5	74.3	72.7	74.4	74.1	72.9	74.2	72.6
56.0	70.1	70.7	70.3	70.1	68.9	69.9	70.6	70.0	70.1	68.9	69.8	70.0	69.9	69.9	68.5
57.7	67.8	67.7	67.8	67.5	67.2	67.7	67.7	67.7	67.5	67.2	67.4	67.2	67.6	67.6	67.2
60.5	66.0	66.0	65.4	66.2	66.0	66.0	66.0	65.4	66.2	66.0	65.8	65.9	64.9	65.7	65.6
67.5	62.3	61.8	62.2	62.2	62.4	62.3	61.6	62.1	62.2	62.4	62.2	61.5	61.9	60.5	61.8
74.0	58.8	58.4	58.0	58.7	58.3	58.8	58.4	57.8	58.6	58.1	58.6	58.1	57.5	58.0	57.8
76.5	56.6	56.7	56.8	56.7	57.2	56.6	56.6	56.9	56.9	57.2	56.5	56.6	56.8	56.9	57.1
80.5	55.2	55.2	54.9	53.7	54.5	55.1	55.0	55.0	53.7	54.5	54.7	54.8	54.3	53.2	53.3
86.5	51.6	51.5	51.5	51.4	51.7	51.6	51.5	52.7	52.5	51.8	51.2	51.2	51.5	52.0	51.9
92.9	48.0	47.7	48.6	48.1	47.6	48.0	47.6	48.5	48.0	47.7	47.5	47.0	48.0	47.1	47.6
95.1	46.1	46.3	46.5	46.5	46.5	46.2	46.3	46.5	46.4	46.5	45.8	46.2	46.4	46.4	46.4
99.5	44.1	44.7	44.3	44.1	44.5	44.1	44.7	44.2	44.2	44.5	44.3	43.9	43.7	43.9	44.3
105.4	41.0	40.4	41.4	40.7	41.2	40.7	40.5	41.1	41.0	41.2	40.6	40.3	40.2	40.6	41.0
112.0	36.9	36.3	36.5	37.1	37.0	37.0	36.2	36.3	37.1	37.0	36.8	36.6	36.4	36.7	37.1
114.1	34.1	33.9	34.0	34.3	34.4	34.0	34.0	33.9	34.4	34.3	33.9	33.8	33.9	34.1	34.2
119.5	29.6	30.9	30.5	30.8	29.5	29.6	30.9	30.5	30.8	29.5	28.2	29.9	29.4	31.0	28.6
128.3	23.3	25.6	24.9	25.2	24.1	23.3	25.6	24.9	25.2	24.1	23.2	25.1	24.2	24.2	23.6
131.5	22.1	22.1	22.4	22.6	22.2	22.1	22.1	22.4	22.6	22.2	22.1	22.1	22.4	22.6	22.2
142.0	21.2	21.0	21.3	21.0	20.4	21.2	21.0	21.3	21.0	20.4	21.2	21.0	21.3	21.0	20.4
151.0	18.2	18.5	18.7	18.7	18.7	18.2	18.5	18.7	18.7	18.7	18.2	18.5	18.7	18.7	18.7

21 cm Waves

A(0) cm	B(11) cm	C(22) cm	D(33) cm	E(44) cm
91.8	91.8	91.7	91.7	91.7
91.9	91.8	91.5	91.6	91.9
91.1	91.1	91.1	91.1	90.9
89.7	88.6	88.4	89.9	89.3
86.3	86.4	86.3	86.5	85.8
83.4	83.7	84.0	84.2	82.8
81.4	80.9	80.8	80.8	80.7
78.0	77.9	77.4	77.3	78.4
74.1	73.9	73.6	74.0	72.6
69.7	70.2	70.0	69.6	68.2
67.3	67.1	67.2	67.2	66.8
65.8	65.2	64.8	65.2	65.1
61.9	61.5	61.5	60.9	61.6
58.4	58.1	57.7	58.3	57.7
56.4	56.4	56.5	56.9	57.0
54.5	54.2	54.1	53.0	53.5
51.4	52.3	52.4	52.3	51.8
47.4	47.2	48.4	47.5	47.5
45.8	46.1	46.2	46.2	46.2
43.9	44.1	43.7	44.1	44.6
40.7	41.3	40.5	40.6	41.5
36.8	35.8	36.6	37.8	37.6
33.8	33.8	33.6	34.0	34.2
28.3	30.5	29.5	28.8	28.5
23.4	25.2	24.2	24.2	23.7
21.2	22.1	22.2	22.5	22.1
21.2	21.0	21.3	21.0	20.4
18.2	18.5	18.7	18.7	18.7

D.1.8 Experiment D8

Test Parameters D8						
α	1:1.5	-	Crown	24	cm	
ξ	3.5	-	L1	68	cm	
D_n	55	mm	L2	60	cm	
Δ_m	1.00	-	Toe	22	cm	
ρ_s	2667	kg/m ³				
Fill Material	Small Angular					
Compaction	Normal					
Filter	Granular					
Remark	Fixed Mattress					

Mattress Information						
Compartment	Width	Volume	Mass	ρ_b	n^*	Compaction
-	cm	cm ³	kg	kg/m ³	-	-
1	20.0	4840	8.00	1653	0.38	Normal
2	22.0	5324	8.60	1615	0.39	Normal
3	21.5	5203	8.50	1634	0.39	Normal
4	21.0	5082	8.40	1653	0.38	Normal
5	22.0	5324	8.70	1634	0.39	Normal
6	22.5	5445	8.90	1635	0.39	Normal
7	21.0	5082	8.40	1653	0.38	Normal
8	22.0	5324	8.70	1634	0.39	Normal

Wave Results						
H_i	H_r	K_r	T	ξ	Run-up	Run-down
m	m	-	s	-	cm	cm
0.079	0.025	0.31	1.15	3.41	4.1	2.4
0.108	0.037	0.35	1.36	3.44	8.9	4.1
0.178	0.065	0.37	1.66	3.28	18.5	8.6
0.201	0.094	0.47	1.86	3.45	21.4	11.8

Reference		20 cm Waves					18 cm Waves					11 cm Waves				
x	A(0)	B(11)	C(22)	D(33)	E(44)	A(0)	B(11)	C(22)	D(33)	E(44)	A(0)	B(11)	C(22)	D(33)	E(44)	
cm	cm	cm	cm	cm	cm	cm	cm	cm	cm	cm	cm	cm	cm	cm	cm	
0.0	91.5	90.8	91.6	91.6	91.6	91.5	90.8	91.6	91.6	91.6	91.5	90.8	91.6	91.6	91.6	
9.3	91.5	91.8	91.4	91.6	91.6	91.5	91.8	91.4	91.6	91.6	91.5	91.8	91.4	91.6	91.6	
20.1	90.5	90.8	90.7	90.9	91.0	90.5	90.8	90.7	90.9	91.0	90.5	90.8	90.7	90.9	91.0	
26.5	89.6	89.6	89.3	88.9	88.8	89.5	89.5	89.3	88.8	88.8	89.5	89.5	89.3	88.8	88.8	
34.5	86.7	86.4	86.6	86.1	85.6	86.5	85.9	86.3	85.4	85.4	86.5	85.9	86.3	85.4	85.6	
41.5	82.3	82.1	81.8	81.6	81.1	82.1	82.2	82.0	81.6	81.1	82.1	82.2	82.0	81.6	81.1	
44.5	78.4	78.7	78.1	79.7	78.6	77.7	78.4	78.0	79.0	78.6	77.7	78.4	78.0	79.0	78.6	
51.5	75.0	74.7	75.1	74.7	74.1	73.6	74.4	74.0	74.5	73.0	73.6	74.4	74.0	74.5	73.0	
57.5	71.1	70.1	71.0	70.9	70.1	70.1	70.2	70.4	70.8	69.6	70.1	70.2	70.4	70.8	69.6	
59.0	69.4	69.2	69.3	69.2	68.9	69.3	69.1	69.2	69.0	68.8	69.3	69.1	69.2	69.0	68.8	
62.5	66.2	66.0	67.0	66.8	66.5	65.7	65.0	66.4	66.2	65.7	65.7	65.0	66.4	66.2	65.7	
69.5	63.5	63.1	62.7	63.0	63.5	62.0	61.9	61.9	62.3	62.4	62.0	61.9	61.9	62.3	62.4	
75.5	59.3	59.7	59.1	59.3	59.0	59.2	59.3	59.2	58.2	59.0	59.2	59.3	59.2	58.2	59.0	
77.3	57.9	57.7	57.6	57.8	57.6	57.8	57.7	57.5	57.7	57.5	57.7	57.5	57.5	57.7	57.5	
81.4	54.1	55.0	55.1	55.0	53.9	53.6	54.7	54.4	54.7	53.8	53.6	54.7	54.4	54.7	53.8	
87.5	50.6	51.2	51.4	51.4	50.6	50.7	51.4	51.4	51.2	50.5	50.7	51.4	51.4	51.2	50.5	
91.5	48.2	48.5	48.2	48.1	47.7	48.2	48.3	48.0	48.0	47.5	47.9	48.3	48.0	48.0	47.5	
94.9	45.6	46.2	45.9	45.6	45.4	45.5	46.1	45.9	45.7	45.3	45.7	46.1	45.9	45.7	45.3	
98.5	43.0	42.2	43.8	43.8	42.9	42.7	42.1	43.5	43.7	42.8	42.0	41.3	43.1	42.3	41.8	
104.7	38.5	38.7	39.7	40.5	39.1	38.4	38.6	39.5	40.0	39.1	38.3	38.5	38.7	39.0	38.5	
112.0	34.3	35.3	35.4	36.0	35.1	34.4	34.9	34.4	35.5	35.1	35.1	35.0	34.5	35.5	35.1	
113.7	33.3	33.2	33.2	33.0	33.3	33.2	33.2	33.2	33.0	33.2	33.1	33.0	33.0	32.8	33.2	
117.9	29.0	29.3	29.5	30.1	29.8	29.0	29.3	29.5	30.1	29.8	28.4	29.1	28.8	30.1	30.0	
127.5	23.6	24.2	24.8	23.6	23.4	23.6	24.2	24.8	23.6	23.4	23.2	23.1	23.6	23.4	23.4	
130.9	21.0	21.0	21.0	20.7	20.5	21.0	21.0	21.0	20.7	20.5	21.0	21.0	21.0	20.7	20.5	
140.5	19.9	19.9	19.9	20.1	19.2	19.9	19.9	19.9	20.1	19.2	19.9	19.9	19.9	20.1	19.2	
150.9	18.2	18.2	18.4	18.4	18.2	18.2	18.2	18.4	18.4	18.2	18.2	18.2	18.4	18.4	18.2	

D.2 Sliding Tests

D.2.1 Experiment S1 - Run 1

Test Parameters S1 - Run 1						
α	1:1.5	-	Crown	24	cm	
ξ	3	-	L1	68	cm	
D_n	40	mm	L2	60	cm	
Δ_m	0.99	-	Toe	22	cm	
ρ_s	2654	kg/m ³				
Fill Material	Gravel					
Compaction	Normal					
Filter	Granular					
Remark						

Mattress Information						
Compartment	Width	Volume	Mass	ρ_b	n^*	Grid
-	cm	cm ³	kg	kg/m ³	-	-
1	24.0	4224	6.90	1634	0.38	Normal
2	23.5	4136	6.80	1644	0.38	Normal
3	21.5	3784	6.20	1638	0.38	Normal
4	21.5	3784	6.20	1638	0.38	Normal
5	22.0	3872	6.40	1653	0.38	Normal
6	21.0	3696	6.10	1650	0.38	Normal
7	22.0	3872	6.40	1653	0.38	Normal
8	22.5	3960	6.47	1634	0.38	Normal

Wave Results						
H_i	H_r	K_r	T	ξ	Run-up	Run-down
m	m	-	s	-	cm	cm
0.051	0.019	0.37	0.80	2.9	1.5	1.0
0.138	0.036	0.26	1.16	2.6	10.6	5.6
0.163	0.045	0.27	1.38	2.8	13.5	8.0
0.187	0.086	0.31	1.70	3.3	20.2	9.2

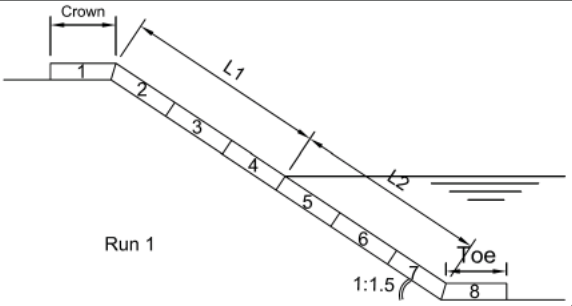
D.2.2 Experiment S2 - Run 1

Test Parameters S2 - Run 1						
α	1:1.5	-	Crown	24	cm	
ξ	4.5	-	L1	68	cm	
D_n	55	mm	L2	60	cm	
Δ_m	0.99	-	Toe	22	cm	
ρ_s	2654	kg/m ³				
Fill Material	Gravel					
Compaction	Normal					
Filter	Granular					
Remark						

Mattress Information						
Compartment	Width	Volume	Mass	ρ_b	n^*	Grid
-	cm	cm ³	kg	kg/m ³	-	-
1	20.0	4840	8.00	1653	0.38	Normal
2	23.0	5566	9.10	1635	0.38	Normal
3	22.5	5445	8.90	1635	0.38	Normal
4	22.0	5324	8.70	1634	0.38	Normal
5	22.0	5324	8.70	1634	0.38	Normal
6	22.5	5445	8.90	1635	0.38	Normal
7	21.0	5082	8.40	1653	0.38	Normal
8	22.0	5324	8.70	1634	0.38	Normal

Wave Results						
H_i	H_r	K_r	T	ξ	Run-up	Run-down
m	m	-	s	-	cm	cm
0.059	0.019	0.33	1.18	4.1	3.5	2.4
0.087	0.036	0.41	1.72	4.9	7.7	6.1
0.146	0.075	0.51	2.24	4.9	14.3	12.7

D.2.3 Experiment S3 - Run 1

Test Parameters S3 - Run 1						
α	1:1.5	-	Crown	24	cm	
ξ	4.5	-	L1	68	cm	
D_n	55	mm	L2	60	cm	
Δ_m	0.99	-	Toe	22	cm	
ρ_s	2654	kg/m ³				
Fill Material	Gravel					
Compaction	Normal					
Filter	Granular					
Remark						

Mattress Information						
Compartment	Width	Volume	Mass	ρ_b	n^*	Grid
-	cm	cm ³	kg	kg/m ³	-	-
1	20.0	4840	8.00	1653	0.38	Normal
2	23.0	5566	9.10	1635	0.38	Normal
3	22.5	5445	8.90	1635	0.38	Normal
4	22.0	5324	8.70	1634	0.38	Normal
5	22.0	5324	8.70	1634	0.38	Normal
6	22.5	5445	8.90	1635	0.38	Normal
7	21.0	5082	8.40	1653	0.38	Normal
8	22.0	5324	8.70	1634	0.38	Normal

Wave Results						
H_i	H_r	K_r	T	ξ	Run-up	Run-down
m	m	-	s	-	cm	cm
0.114	0.045	0.40	1.66	4.1	10.2	7.8
0.164	0.079	0.48	1.94	4.0	14.8	10.7
0.192	0.094	0.49	2.14	4.1		

D.2.4 Experiment S4 - Run 1

Test Parameters S4 - Run 1						
α	1:1.5	-	Crown	24	cm	
ξ	4.5	-	L1	68	cm	
D_n	55	mm	L2	60	cm	
Δ_m	0.99	-	Toe	22	cm	
ρ_s	2654	kg/m ³				
Fill Material	Gravel					
Compaction	Normal					
Filter	Granular					
Remark						

Mattress Information						
Compartment	Width	Volume	Mass	ρ_b	n^*	Grid
-	cm	cm ³	kg	kg/m ³	-	-
1	20.0	4840	8.00	1653	0.38	Normal
2	23.0	5566	9.10	1635	0.38	Normal
3	22.5	5445	8.90	1635	0.38	Normal
4	22.0	5324	8.70	1634	0.38	Normal
5	22.0	5324	8.70	1634	0.38	Normal
6	22.5	5445	8.90	1635	0.38	Normal
7	21.0	5082	8.40	1653	0.38	Normal
8	22.0	5324	8.70	1634	0.38	Normal

Wave Results						
H_i	H_r	K_r	T	ξ	Run-up	Run-down
m	m	-	s	-	cm	cm
0.102			1.7	4.4	7.9	6.2
0.137			1.82	4.1	11.8	9.5
0.196	0.064	0.32	1.95	3.7	19.4	11.3

D.2.5 Experiment S5 - Run 1

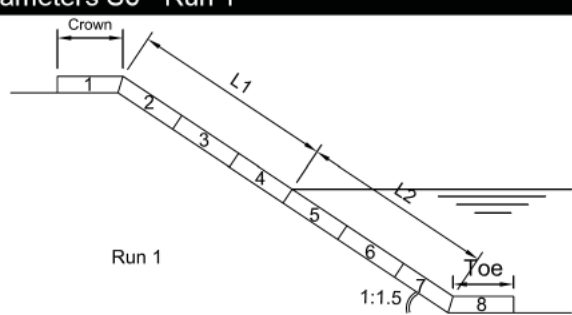
Test Parameters S5 - Run 1						
α	1:1.5	-	Crown	24	cm	
ξ	3	-	L1	68	cm	
D_n	55	mm	L2	60	cm	
Δ_m	1.00	-	Toe	22	cm	
ρ_s	2667	kg/m ³				
Fill Material	Small Angular					
Compaction	Normal					
Filter	Granular					
Remark						

Mattress Information						
Compartment	Width	Volume	Mass	ρ_b	n^*	Grid
-	cm	cm ³	kg	kg/m ³	-	-
1	20.0	4840	8.00	1653	0.38	Normal
2	22.0	5324	8.60	1615	0.39	Normal
3	21.5	5203	8.50	1634	0.39	Normal
4	21.0	5082	8.40	1653	0.38	Normal
5	22.0	5324	8.70	1634	0.39	Normal
6	22.5	5445	8.90	1635	0.39	Normal
7	21.0	5082	8.40	1653	0.38	Normal
8	22.0	5324	8.70	1634	0.39	Normal

Wave Results						
H_i	H_r	K_r	T	ξ	Run-up	Run-down
m	m	-	s	-	cm	cm
0.277	0.138	0.50	1.82	2.9		

D.2.6 Experiment S6 - Run 1

Test Parameters S6 - Run 1					
α	1:1.5	-	Crown	24	cm
ξ	2	-	L1	68	cm
D_n	30	mm	L2	60	cm
Δ_m	1.00	-	Toe	22	cm
ρ_s	2667	kg/m ³			
Fill Material	Small Angular				
Compaction	Normal				
Filter	Granular				
Remark					



Mattress Information						
Compartment	Width	Volume	Mass	ρ_b	n^*	Grid
-	cm	cm ³	kg	kg/m ³	-	-
1	23.0	3174	5.20	1638	0.39	Normal
2	21.5	2967	4.90	1651	0.38	Normal
3	21.0	2898	4.80	1656	0.38	Normal
4	22.5	3105	5.10	1643	0.38	Normal
5	22.5	3172.5	5.20	1639	0.39	Normal
6	21.5	3031.5	5.00	1649	0.38	Normal
7	22.5	3071.25	5.05	1644	0.38	Normal
8	23.0	3139.5	5.20	1656	0.38	Normal

Wave Results						
H_i	H_r	K_r	T	ξ	Run-up	Run-down
m	m	-	s	-	cm	cm
0.052	0.025	0.47	0.66	2.4	1.6	0.9
0.094	0.113	1.20	0.66	1.8	3.5	1.6
0.122	0.017	0.14	0.88	2.1	8.7	3.3
0.153	0.031	0.20	0.90	1.9	12.6	3.6
0.220	0.064	0.29	1.50	2.7	21.2	6.0

D.2.7 Experiment S7 - Run 1

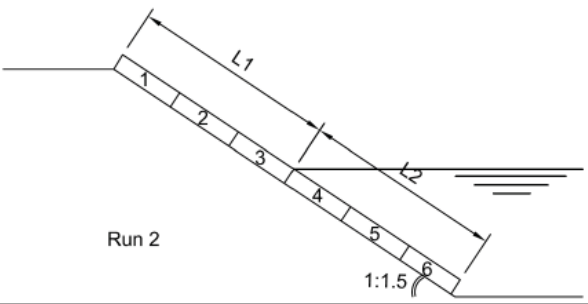
Test Parameters S7 - Run 1						
α	1:1.5	-	Crown	24	cm	
ξ	30	-	L1	68	cm	
D_n	40	mm	L2	60	cm	
Δ_m	1.00	-	Toe	22	cm	
ρ_s	2667	kg/m ³				
Fill Material	Small Angular					
Compaction	Normal					
Filter	Granular					
Remark						

Mattress Information						
Compartment	Width	Volume	Mass	ρ_b	n^*	Grid
-	cm	cm ³	kg	kg/m ³	-	-
1	23.0	3174	5.20	1638	0.39	Normal
2	21.5	2967	4.90	1651	0.38	Normal
3	21.0	2898	4.80	1656	0.38	Normal
4	22.5	3105	5.10	1643	0.38	Normal
5	22.5	3172.5	5.20	1639	0.39	Normal
6	21.5	3031.5	5.00	1649	0.38	Normal
7	22.5	3071.25	5.05	1644	0.38	Normal
8	23.0	3139.5	5.20	1656	0.38	Normal

Wave Results						
H_i	H_r	K_r	T	ξ	Run-up	Run-down
m	m	-	s	-	cm	cm
0.120	0.037	0.31	0.92	2.2	7.6	3
0.158	0.038	0.24	0.92	1.9	12.0	3.5
0.172	0.043	0.25	0.96	1.9	13.3	4.3
0.203	0.037	0.18	1.07	2.0	16.3	5.1
0.240	0.049	0.21	1.29	2.2	19.8	6.1

D.2.8 Experiment S8 - Run 2

Test Parameters S8 - Run 2					
α	1:1.5	-			
ξ	1.5	-	L1	68	cm
D_n	30	mm	L2	64	cm
Δ_m	1.00	-			
ρ_s	2667	kg/m ³			
Fill Material	Small Angular				
Compaction	Normal				
Filter	Granular				
Remark					

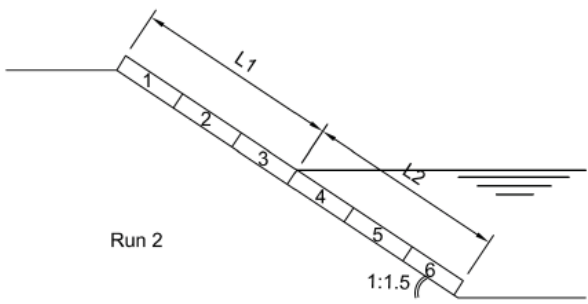


Mattress Information						
Compartment	Width	Volume	Mass	ρ_b	n^*	Grid
-	cm	cm ³	kg	kg/m ³	-	-
1	23.0	3174	5.20	1638	0.39	Normal
2	21.5	2967	4.90	1651	0.38	Normal
3	21.0	2898	4.80	1656	0.38	Normal
4	22.5	3105	5.10	1643	0.38	Normal
5	22.5	3172.5	5.20	1639	0.39	Normal
6	21.5	3031.5	5.00	1649	0.38	Normal

Wave Results						
H_i	H_r	K_r	T	ξ	Run-up	Run-down
m	m	-	s	-	cm	cm
0.124	0.059	0.48	0.74	1.7	5.7	2.5
0.123	0.038	0.31	0.81	1.9	7.8	3.3
0.133	0.032	0.24	0.85	1.9	10.0	3.7

D.2.9 Experiment S9 - Run 2

Test Parameters S9 - Run 2					
α	1:1.5	-			
ξ	5.5	-	L1	68	cm
D_n	55	mm	L2	64	cm
Δm	1.00	-			
ρ_s	2667	kg/m ³			
Fill Material	Small Angular				
Compaction	Normal				
Filter	Granular				
Remark					

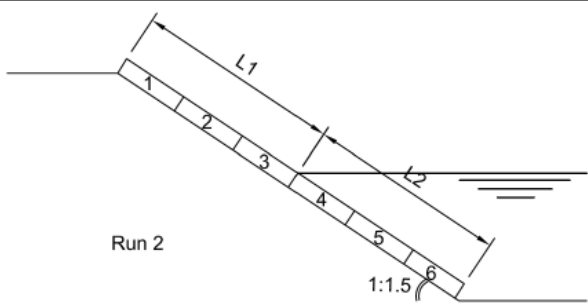


Mattress Information						
Compartment	Width	Volume	Mass	ρ_b	n^*	Grid
-	cm	cm ³	kg	kg/m ³	-	-
1	20.0	4840	8.00	1653	0.38	Normal
2	23.0	5566	9.10	1635	0.39	Normal
3	22.5	5445	8.90	1635	0.39	Normal
4	22.0	5324	8.70	1634	0.39	Normal
5	22.0	5324	8.70	1634	0.39	Normal
6	22.5	5445	8.90	1635	0.39	Normal

Wave Results						
H_i	H_r	K_r	T	ξ	Run-up	Run-down
m	m	-	s	-	cm	cm
0.060	0.021	0.36	1.45	4.9	4.1	3.4
0.070	0.029	0.41	1.73	5.5	6.2	4.0
0.097	0.046	0.47	1.79	4.8	8.4	6.1
0.092	0.053	0.57	2.52	6.9	10.6	5.9

D.2.10 Experiment S10 - Run 2

Test Parameters S10 - Run 2					
α	1:1.5	-			
ξ	3	-	L1	62	cm
D_n	55	mm	L2	62	cm
Δm	0.99	-			
ρ_s	2654	kg/m ³			
Fill Material	Gravel				
Compaction	Normal				
Filter	Granular				
Remark					

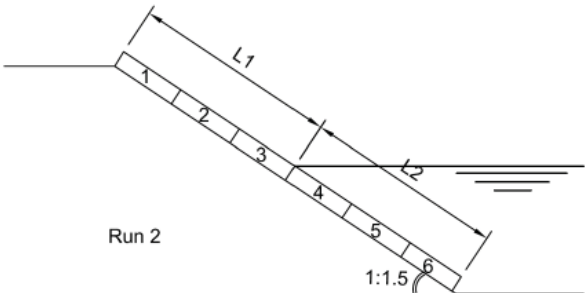


Mattress Information						
Compartment	Width	Volume	Mass	ρ_b	n^*	Grid
-	cm	cm ³	kg	kg/m ³	-	-
1	22.5	5445	8.90	1635	0.38	Normal
2	22.0	5324	8.70	1634	0.38	Normal
3	22.0	5324	8.70	1634	0.38	Normal
4	22.5	5445	8.90	1635	0.38	Normal
5	21.0	5082	8.40	1653	0.38	Normal
6	22.0	5324	8.70	1634	0.38	Normal

Wave Results						
H_i	H_r	K_r	T	ξ	Run-up	Run-down
m	m	-	s	-	cm	cm
0.076	0.026	0.35	1.38	4.2	5.5	3.0
0.099	0.029	0.29	1.28	3.4	6.4	3.5
0.145	0.042	0.29	1.32	2.9	10.6	5.1
0.171	0.048	0.28	1.36	2.7	14.1	6.8

D.2.11 Experiment S11 - Run 2

Test Parameters S11 - Run 2						
α	1:1.5	-				
ξ	4	-	L1	62	cm	
D_n	55	mm	L2	63	cm	
Δ_m	0.99	-				
ρ_s	2654	kg/m ³				
Fill Material	Gravel					
Compaction	Normal					
Filter	Granular					
Remark						



Mattress Information						
Compartment	Width	Volume	Mass	ρ_b	n^*	Grid
-	cm	cm ³	kg	kg/m ³	-	-
1	22.5	5445	8.90	1635	0.38	Normal
2	22.0	5324	8.70	1634	0.38	Normal
3	22.0	5324	8.70	1634	0.38	Normal
4	22.5	5445	8.90	1635	0.38	Normal
5	21.0	5082	8.40	1653	0.38	Normal
6	22.0	5324	8.70	1634	0.38	Normal

Wave Results						
H_i	H_r	K_r	T	ξ	Run-up	Run-down
m	m	-	s	-	cm	cm
0.093	0.031	0.34	1.50	4.1	7.6	6.0
0.124	0.051	0.41	1.71	4.0	12.7	7.2

D.2.12 Experiment S12

Test Parameters S12						
α	1:1.5	-	Crown	23	cm	
ξ	2	-	L1	68	cm	
D_n	40	mm	L2	80	cm	
Δ_m	1.00	-				
ρ_s	2667	kg/m ³				
Fill Material	Small Angular					
Compaction	Increased					
Filter	Granular + Geotex					
Remark	Adapted Revetment					

Mattress Information						
Compartment	Width	Volume	Mass	ρ_b	n^*	Grid
-	cm	cm ³	kg	kg/m ³	-	-
1	24.0	4224	6.90	1634	0.39	Normal
2	23.5	4183	6.90	1650	0.38	Normal
3	22.5	4027.5	9.05	2247	0.16	Increased
4	21.5	3848.5	8.55	2222	0.17	Increased
5	21.0	3822	8.55	2237	0.16	Increased
6	20.0	3640	7.85	2157	0.19	Increased
7	22.0	3960	6.50	1641	0.38	Normal
8	22.0	3916	6.40	1634	0.39	Normal

Wave Results						
H_i	H_r	K_r	T	ξ	Run-up	Run-down
m	m	-	s	-	cm	cm
0.106	0.029	0.27	0.77	2.0	4.5	1.9
0.142	0.027	0.19	0.87	1.9	8.1	3.0

D.2.13 Experiment S13

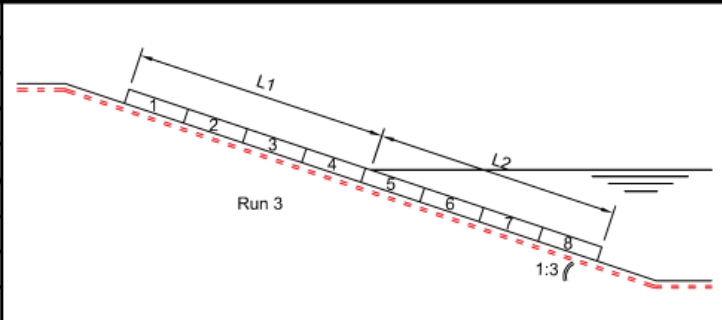
Test Parameters S13						
α	1:1.5	-	Crown	23	cm	
ξ	4	-	L1	62	cm	
D_n	40	mm	L2	63	cm	
Δ_m	1.00	-	Toe	22	cm	
ρ_s	2667	kg/m ³				
Fill Material	Small Granular					
Compaction	Increased					
Filter	Granular + Geotex					
Remark	Long Revetment					

Mattress Information						
Compartment	Width	Volume	Mass	ρ_b	n^*	Grid
-	cm	cm ³	kg	kg/m ³	-	-
1	24.0	4224	6.90	1634	0.39	Normal
2	23.5	4183	6.90	1650	0.38	Normal
3	22.5	4027.5	9.05	2247	0.16	Increased
4	21.5	3848.5	8.55	2222	0.17	Increased
5	21.0	3822	8.55	2237	0.16	Increased
6	20.0	3640	7.85	2157	0.19	Increased
7	22.0	3960	6.50	1641	0.38	Normal
8	22.0	3916	6.40	1634	0.39	Normal

Wave Results						
H_i	H_r	K_r	T	ξ	Run-up	Run-down
m	m	-	s	-	cm	cm
0.104	0.032	0.31	1.15	3.0	6.3	2.8
0.141	0.042	0.30	1.44	3.2	7.9	5.6

D.2.14 Experiment S14 - Run 3

Test Parameters S14 - Run 3						
α	1:3	-				
ξ	1	-	L1	85	cm	
D_n	30	mm	L2	84	cm	
Δm	1.00	-				
ρ_s	2667	kg/m ³				
Fill Material	Small Angular					
Compaction	Increased					
Filter	Geotextile					
Remark						

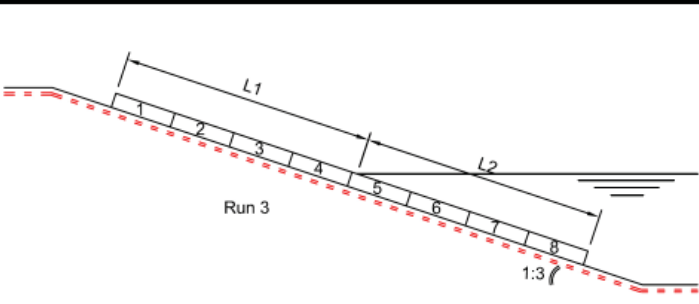


Mattress Information						
Compartment	Width	Volume	Mass	ρ_b	n^*	Grid
-	cm	cm ³	kg	kg/m ³	-	-
1	22.0	3135	7.10	2265	0.15	Normal
2	23.0	3174	7.20	2268	0.15	Normal
3	22.0	3102	7.10	2289	0.14	Normal
4	22.5	3172.5	7.20	2270	0.15	Normal
5	23.0	3105	7.10	2287	0.14	Normal
6	22.0	2970	6.80	2290	0.14	Normal
7	23.0	3105	7.10	2287	0.14	Normal
8	21.0	2835	6.50	2293	0.14	Normal

Wave Results						
H_i	H_r	K_r	T	ξ	Run-up	Run-down
m	m	-	s	-	cm	cm
0.071	0.011	0.15	0.94	1.5	2.7	1.2
0.188	0.018	0.10	1.05	1.0	9.1	5.7
0.226	0.022	0.10	1.16	1.0	12.2	7.2

D.2.15 Experiment S15 - Run 3

Test Parameters S15 - Run 3						
α	1:3	-				
ξ	2	-	L1	85	cm	
D_n	40	mm	L2	86	cm	
Δ_m	1.00	-				
ρ_s	2667	kg/m ³				
Fill Material	Angular					
Compaction	Increased					
Filter	Geotextile					
Remark						

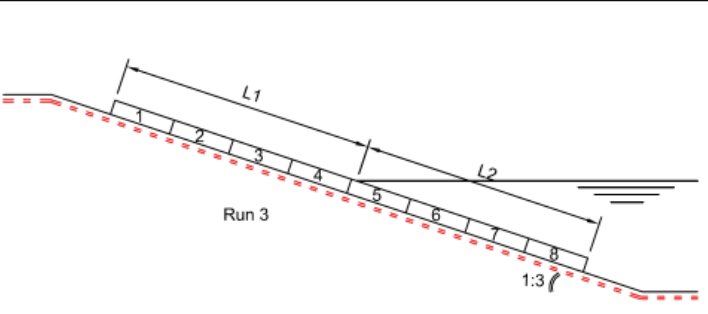


Mattress Information						
Compartment	Width	Volume	Mass	ρ_b	n^*	Grid
-	cm	cm ³	kg	kg/m ³	-	-
1	24.0	4224	6.90	1634	0.37	Normal
2	23.5	4183	6.90	1650	0.37	Normal
3	21.5	3913	7.90	2019	0.23	Increased
4	20.5	3690	7.40	2005	0.23	Increased
5	21.5	3848.5	7.70	2001	0.23	Increased
6	22.0	3916	7.80	1992	0.24	Increased
7	22.0	3960	6.50	1641	0.37	Normal
8	22.0	3916	6.40	1634	0.37	Normal

Wave Results						
H_i	H_r	K_r	T	ξ	Run-up	Run-down
m	m	-	s	-	cm	cm
0.085	0.005	0.06	1.16	1.7	3.2	2.1
0.146	0.024	0.17	1.60	1.7	10.4	4.6
0.154	0.037	0.24	1.94	2.1	11.4	6.9

D.2.16 Experiment S16 - Run 3

Test Parameters S16 - Run 3					
α	1:3	-			
ξ	4	-	L1	85	cm
D_n	55	mm	L2	87	cm
Δ_m	1.00	-			
ρ_s	2667	kg/m ³			
Fill Material	Angular				
Compaction	Normal				
Filter	Geotextile				
Remark					

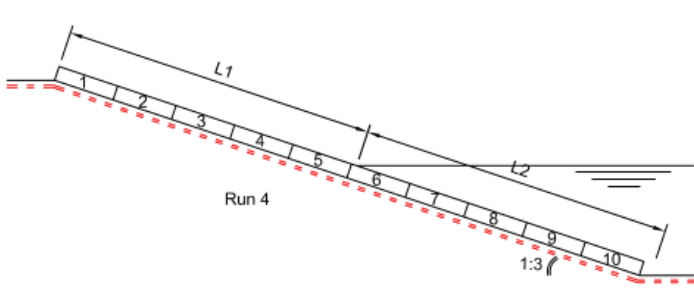


Mattress Information						
Compartment	Width	Volume	Mass	ρ_b	n^*	Grid
-	cm	cm ³	kg	kg/m ³	-	-
1	22.0	5505.5	8.50	1544	0.41	Normal
2	20.0	4950	8.50	1717	0.34	Normal
3	21.0	5139.75	8.30	1615	0.38	Normal
4	21.5	5321.25	8.60	1616	0.38	Normal
5	21.0	5197.5	8.50	1635	0.37	Normal
6	21.0	5197.5	9.10	1751	0.33	Normal
7	22.0	5445	8.70	1598	0.39	Normal
8	21.0	5197.5	8.30	1597	0.39	Normal

Wave Results						
H_i	H_r	K_r	T	ξ	Run-up	Run-down
m	m	-	s	-	cm	cm
0.069	0.018	0.27	2.22	3.5	5.1	4.1
0.099	0.043	0.43	2.94	3.9	10.5	7.2
0.113	0.054	0.48	3.15	3.9	16.0	8.8

D.2.17 Experiment S17 - Run 4

Test Parameters S17 - Run 4					
α	1:3	-			
ξ	1	-	L1	109 cm	
D_n	30	mm	L2	109 cm	
Δ_m	1.00	-			
ρ_s	2667	kg/m ³			
Fill Material	Small Angular				
Compaction	Increased				
Filter	Geotextile				
Remark					

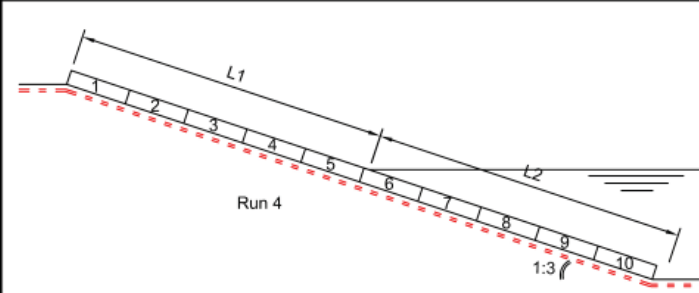


Mattress Information						
Compartment	Width	Volume	Mass	ρ_b	n^*	Grid
-	cm	cm ³	kg	kg/m ³	-	-
1	22.0	3036	6.90	2273	0.15	Normal
2	23.0	3174	7.20	2268	0.15	Normal
3	22.0	3135	7.10	2265	0.15	Normal
4	23.0	3174	7.20	2268	0.15	Normal
5	22.0	3102	7.10	2289	0.14	Normal
6	22.5	3172.5	7.20	2270	0.15	Normal
7	23.0	3105	7.10	2287	0.14	Normal
8	22.0	2970	6.80	2290	0.14	Normal
9	23.0	3105	7.10	2287	0.14	Normal
10	21.0	2835	6.50	2293	0.14	Normal

Wave Results						
H_i	H_r	K_r	T	ξ	Run-up	Run-down
m	m	-	s	-	cm	cm
0.110	0.034	0.31	0.77	1.0	3.4	2.6
0.147	0.024	0.16	0.89	1.0	5.9	4.2
0.196	0.031	0.16	1.00	0.9	9.4	6.4
0.200	0.045	0.23	1.22	1.1	12.7	7.0
0.254	0.022	0.09	1.36	1.1	16.4	9.2
0.273	0.029	0.10	1.60	1.3	21.9	10.8

D.2.18 Experiment S18 - Run 4

Test Parameters S18 - Run 4					
α	1:3	-			
ξ	2	-	L1	106 cm	
D_n	40	mm	L2	112 cm	
Δ_m	0.96	-			
ρ_s	2607	kg/m ³			
Fill Material	Angular				
Compaction	Increased				
Filter	Geotextile				
Remark					

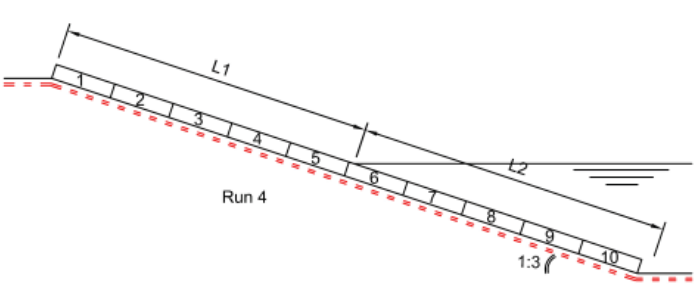


Mattress Information						
Compartment	Width	Volume	Mass	ρ_b	n^*	Grid
-	cm	cm ³	kg	kg/m ³	-	-
1	24.0	4224	6.90	1634	0.37	Normal
2	23.5	4183	6.90	1650	0.37	Normal
3	23.0	4324	8.40	1943	0.25	Normal
4	22.0	4136	7.80	1886	0.28	Normal
5	21.5	3913	7.90	2019	0.23	Normal
6	20.5	3690	7.40	2005	0.23	Normal
7	21.5	3848.5	7.70	2001	0.23	Normal
8	22.0	3916	7.80	1992	0.24	Normal
9	22.0	3960	6.50	1641	0.37	Normal
10	22.0	3916	6.40	1634	0.37	Normal

Wave Results						
H_i	H_r	K_r	T	ξ	Run-up	Run-down
m	m	-	s	-	cm	cm
0.067	0.003	0.20	1.15	1.8	3.3	2.1
0.105	0.018	0.17	1.54	2.0	6.1	5.1
0.160	0.036	0.22	1.94	2.0	14.4	7.3
0.196	0.036	0.19	2.22	2.1	19.5	8.3

D.2.19 Experiment S19 - Run 4

Test Parameters S19 - Run 4					
α	1:3	-			
ξ	1	-	L1	109 cm	
D_n	30	mm	L2	109 cm	
Δ_m	1.00	-			
ρ_s	2667	kg/m ³			
Fill Material	Small Angular				
Compaction	Increased				
Filter	Geotextile				
Remark					

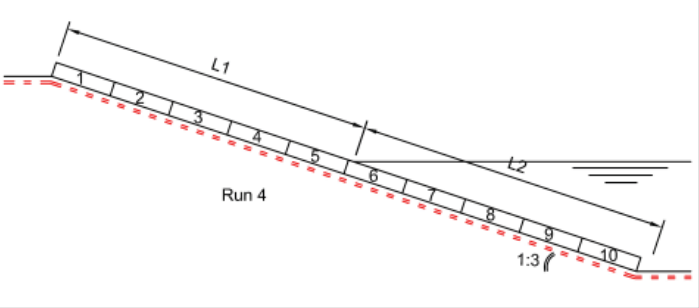


Mattress Information						
Compartment	Width	Volume	Mass	ρ_b	n^*	Grid
-	cm	cm ³	kg	kg/m ³	-	-
1	22.0	3036	6.90	2273	0.15	Normal
2	23.0	3174	7.20	2268	0.15	Normal
3	22.0	3135	7.10	2265	0.15	Normal
4	23.0	3174	7.20	2268	0.15	Normal
5	22.0	3102	7.10	2289	0.14	Normal
6	22.5	3172.5	7.20	2270	0.15	Normal
7	23.0	3105	7.10	2287	0.14	Normal
8	22.0	2970	6.80	2290	0.14	Normal
9	23.0	3105	7.10	2287	0.14	Normal
10	21.0	2835	6.50	2293	0.14	Normal

Wave Results						
H_i	H_r	K_r	T	ξ	Run-up	Run-down
m	m	-	s	-	cm	cm
0.072	0.041	0.57	3.39	5.3	9.1	6.2
0.117	0.076	0.65	3.65	4.4	15.3	8.9
0.162	0.078	0.48	3.13	3.2	29.6	13.7
0.169	0.071	0.42	2.95	3.0	26.9	11.7

D.2.20 Experiment S20 - Run 4

Test Parameters S20 - Run 4				
α	1:3	-		
ξ	4	-	L1	116 cm
D_n	55	mm	L2	100 cm
Δm	0.96	-		
ρ_s	2607	kg/m ³		
Fill Material	Angular			
Compaction	Normal			
Filter	Geotextile			
Remark				

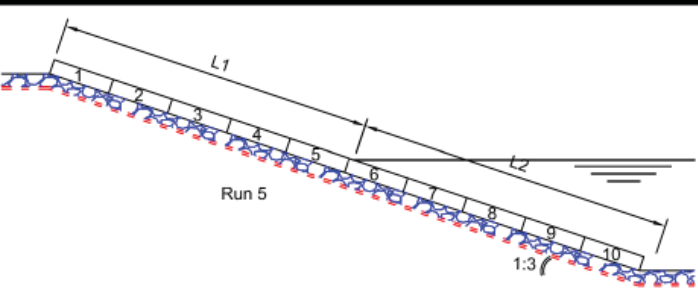


Mattress Information						
Compartment	Width	Volume	Mass	ρ_b	n^*	Grid
-	cm	cm ³	kg	kg/m ³	-	-
1	22.5	5630.625	8.90	1581	0.39	Normal
2	24.0	6006	9.10	1515	0.42	Normal
3	22.0	5505.5	8.50	1544	0.41	Normal
4	20.0	4950	8.50	1717	0.34	Normal
5	21.0	5139.75	8.30	1615	0.38	Normal
6	21.5	5321.25	8.60	1616	0.38	Normal
7	21.0	5197.5	8.50	1635	0.37	Normal
8	21.0	5197.5	9.10	1751	0.33	Normal
9	22.0	5445	8.70	1598	0.39	Normal
10	21.0	5197.5	8.30	1597	0.39	Normal

Wave Results						
H_i	H_r	K_r	T	ξ	Run-up	Run-down
m	m	-	s	-	cm	cm
0.098	0.032	0.33	2.76	3.7	10.3	7.9
0.141	0.058	0.41	2.94	3.3	17.8	7.4
0.129	0.094	0.73	4.78	5.5	19.3	8.8
0.155	0.111	0.72	4.35	4.6	21.9	10.4
0.177	0.121	0.68	3.96	3.9	30.8	12.6

D.2.21 Experiment S22 - Run 5

Test Parameters S22 - Run 5				
α	1:3	-		
ξ	3	-	L1	124 cm
D_n	30	mm	L2	96 cm
Δ_m	1.00	-		
ρ_s	2667	kg/m ³		
Fill Material	Small Angular			
Compaction	Increased			
Filter	Granular + Geotex			
Remark	NO FAILURE			

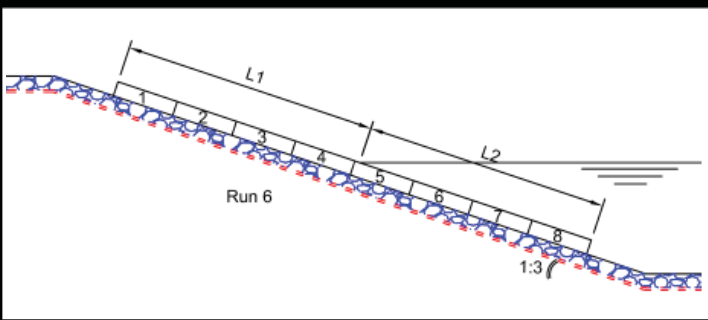


Mattress Information						
Compartment	Width	Volume	Mass	ρ_b	n^*	Grid
-	cm	cm ³	kg	kg/m ³	-	-
1	22.0	3036	6.90	2273	0.15	Normal
2	23.0	3174	7.20	2268	0.15	Normal
3	22.0	3135	7.10	2265	0.15	Normal
4	23.0	3174	7.20	2268	0.15	Normal
5	22.0	3102	7.10	2289	0.14	Normal
6	22.5	3172.5	7.20	2270	0.15	Normal
7	23.0	3105	7.10	2287	0.14	Normal
8	22.0	2970	6.80	2290	0.14	Normal
9	23.0	3105	7.10	2287	0.14	Normal
10	21.0	2835	6.50	2293	0.14	Normal

Wave Results						
H_i	H_r	K_r	T	ξ	Run-up	Run-down
m	m	-	s	-	cm	cm
0.109	0.036	0.33	1.94	2.4	9.1	7.1
0.155	0.040	0.26	2.22	2.3	16.1	11.0
0.140	0.042	0.30	2.47	2.7	18.1	9.7
0.291	0.052	0.18	1.94	1.5	34.0	16.2

D.2.22 Experiment S25 - Run 6

Test Parameters S25 - Run 6				
α	1:3	-		
ξ	3	-	L1	86 cm
D_n	30	mm	L2	87 cm
Δm	1.00	-		
ρ_s	2667	kg/m ³		
Fill Material	Small Angular			
Compaction	Increased			
Filter	Granular + Geotext			
Remark	NO FAILURE			

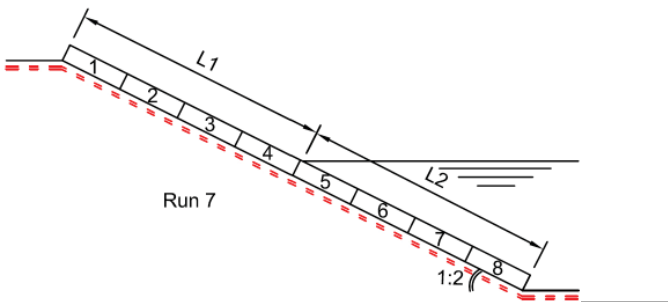


Mattress Information						
Compartment	Width	Volume	Mass	ρ_b	n^*	Grid
-	cm	cm ³	kg	kg/m ³	-	-
1	22.0	3135	7.10	2265	0.15	Normal
2	23.0	3174	7.20	2268	0.15	Normal
3	22.0	3102	7.10	2289	0.14	Normal
4	22.5	3172.5	7.20	2270	0.15	Normal
5	23.0	3105	7.10	2287	0.14	Normal
6	22.0	2970	6.80	2290	0.14	Normal
7	23.0	3105	7.10	2287	0.14	Normal
8	21.0	2835	6.50	2293	0.14	Normal

Wave Results						
H_i	H_r	K_r	T	ξ	Run-up	Run-down
m	m	-	s	-	cm	cm
0.098	0.035	0.36	1.87	2.5	6.8	4.7
0.166	0.050	0.30	2.12	2.2	15.0	10.3
0.134	0.059	0.44	2.61	3.0	19.3	9.7
0.146	0.065	0.44	2.61	2.8	22.5	11.1
0.192	0.045	0.24	2.33	2.2	27.7	11.8

D.2.23 Experiment S27 - Run 7

Test Parameters S27 - Run 7					
α	1:2	-			
ξ	1.5	-	L1	80	cm
D_n	30	mm	L2	90	cm
Δm	1.00	-			
ρ_s	2667	kg/m ³			
Fill Material	Small Angular				
Compaction	Increased				
Filter	Geotextile				
Remark					

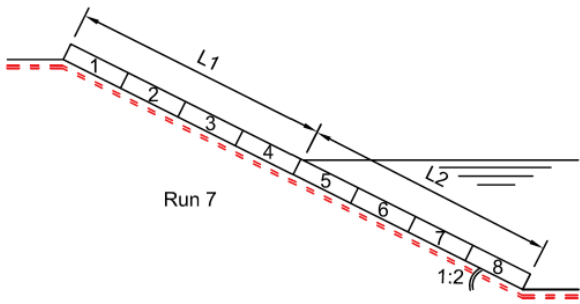


Mattress Information						
Compartment	Width	Volume	Mass	ρ_b	n^*	Grid
-	cm	cm ³	kg	kg/m ³	-	-
1	22.0	3135	7.10	2265	0.15	Normal
2	23.0	3174	7.20	2268	0.15	Normal
3	22.0	3102	7.10	2289	0.14	Normal
4	22.5	3172.5	7.20	2270	0.15	Normal
5	23.0	3105	7.10	2287	0.14	Normal
6	22.0	2970	6.80	2290	0.14	Normal
7	23.0	3105	7.10	2287	0.14	Normal
8	21.0	2835	6.50	2293	0.14	Normal

Wave Results						
H_i	H_r	K_r	T	ξ	Run-up	Run-down
m	m	-	s	-	cm	cm
0.096	0.013	0.13	0.74	1.5	3.0	1.2
0.105	0.029	0.27	0.78	1.5	4.1	1.6

D.2.24 Experiment S28 - Run 7

Test Parameters S28 - Run 7					
α	1:2	-			
ξ	3	-	L1	85	cm
D_n	55	mm	L2	83	cm
Δ_m	0.96	-			
ρ_s	2607	kg/m ³			
Fill Material	Angular				
Compaction	Normal				
Filter	Geotextile				
Remark					

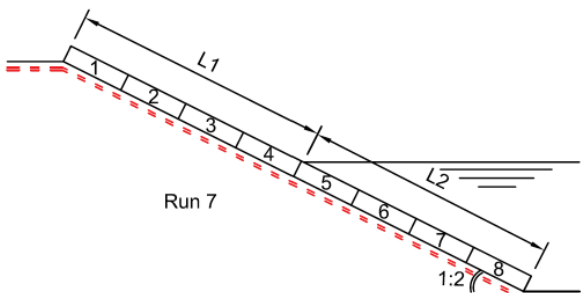


Mattress Information						
Compartment	Width	Volume	Mass	ρ_b	n^*	Grid
-	cm	cm ³	kg	kg/m ³	-	-
1	22.0	5505.5	8.50	1544	0.41	Normal
2	20.0	4950	8.50	1717	0.34	Normal
3	21.0	5139.75	8.30	1615	0.38	Normal
4	21.5	5321.25	8.60	1616	0.38	Normal
5	21.0	5197.5	8.50	1635	0.37	Normal
6	21.0	5197.5	9.10	1751	0.33	Normal
7	22.0	5445	8.70	1598	0.39	Normal
8	21.0	5197.5	8.30	1597	0.39	Normal

Wave Results						
H_i	H_r	K_r	T	ξ	Run-up	Run-down
m	m	-	s	-	cm	cm
0.061	0.005	0.09	1.13	2.9	2.5	1.5
0.130	0.029	0.22	1.36	2.4	8.0	3.4

D.2.25 Experiment S29 - Run 7

Test Parameters S29 - Run 7					
α	1:2	-			
ξ	1	-	L1	86	cm
D_n	30	mm	L2	83	cm
Δ_m	1.00	-			
ρ_s	2667	kg/m ³			
Fill Material	Small Angular				
Compaction	Increased				
Filter	Geotextile				
Remark					

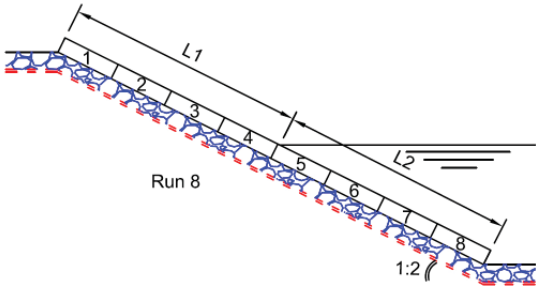


Mattress Information						
Compartment	Width	Volume	Mass	ρ_b	n^*	Grid
-	cm	cm ³	kg	kg/m ³	-	-
1	22.0	3135	7.10	2265	0.15	Normal
2	23.0	3174	7.20	2268	0.15	Normal
3	22.0	3102	7.10	2289	0.14	Normal
4	22.5	3172.5	7.20	2270	0.15	Normal
5	23.0	3105	7.10	2287	0.14	Normal
6	22.0	2970	6.80	2290	0.14	Normal
7	23.0	3105	7.10	2287	0.14	Normal
8	21.0	2835	6.50	2293	0.14	Normal

Wave Results						
H_i	H_r	K_r	T	ξ	Run-up	Run-down
m	m	-	s	-	cm	cm
0.055	0.022	0.40	0.65	1.7	0.9	0.4
0.111	0.058	0.52	0.65	1.2	2.0	1.5

D.2.26 Experiment S30 - Run 8

Test Parameters S30 - Run 8						
α	1:2	-				
ξ	2	-	L1	87	cm	
D_n	30	mm	L2	84	cm	
Δ_m	1.00	-				
ρ_s	2667	kg/m ³				
Fill Material	Small Angular					
Compaction	Increased					
Filter	Granular + Geotex					
Remark						

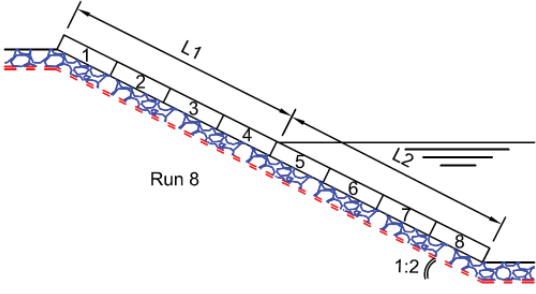


Mattress Information						
Compartment	Width	Volume	Mass	ρ_b	n^*	Grid
-	cm	cm ³	kg	kg/m ³	-	-
1	22.0	3135	7.10	2265	0.15	Normal
2	23.0	3174	7.20	2268	0.15	Normal
3	22.0	3102	7.10	2289	0.14	Normal
4	22.5	3172.5	7.20	2270	0.15	Normal
5	23.0	3105	7.10	2287	0.14	Normal
6	22.0	2970	6.80	2290	0.14	Normal
7	23.0	3105	7.10	2287	0.14	Normal
8	21.0	2835	6.50	2293	0.14	Normal

Wave Results						
H_i	H_r	K_r	T	ξ	Run-up	Run-down
m	m	-	s	-	cm	cm
0.100	0.062	0.63	0.66	1.3	3.2	0.3
0.140	0.056	0.40	0.73	1.2	4.9	1.4
0.166	0.015	0.09	0.94	1.4	8.2	3.7
0.239	0.014	0.06	1.13	1.4	12.2	5.5
0.250	0.038	0.15	1.55	1.9	20.9	6.7

D.2.27 Experiment S31 - Run 8

Test Parameters S31 - Run 8					
α	1:2	-			
ξ	2.5	-	L1	85	cm
D_n	30	mm	L2	85	cm
Δ_m	1.00	-			
ρ_s	2667	kg/m ³			
Fill Material	Small Angular				
Compaction	Increased				
Filter	Granular + Geotex				
Remark					

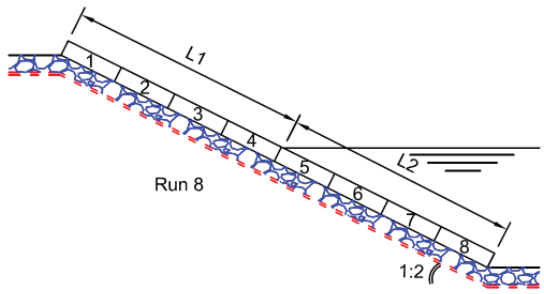


Mattress Information						
Compartment	Width	Volume	Mass	ρ_b	n^*	Grid
-	cm	cm ³	kg	kg/m ³	-	-
1	22.0	3135	7.10	2265	0.15	Normal
2	23.0	3174	7.20	2268	0.15	Normal
3	22.0	3102	7.10	2289	0.14	Normal
4	22.5	3172.5	7.20	2270	0.15	Normal
5	23.0	3105	7.10	2287	0.14	Normal
6	22.0	2970	6.80	2290	0.14	Normal
7	23.0	3105	7.10	2287	0.14	Normal
8	21.0	2835	6.50	2293	0.14	Normal

Wave Results						
H_i	H_r	K_r	T	ξ	Run-up	Run-down
m	m	-	s	-	cm	cm
0.082	0.024	0.29	1.49	3.2	5.8	3.1
0.136	0.049	0.36	1.72	2.9	10.9	8.4
0.221	0.025	0.12	1.92	2.6	18.8	10.2

D.2.28 Experiment S32 - Run 8

Test Parameters S32 - Run 8						
α	1:2	-				
ξ	3	-	L1	85	cm	
D_n	30	mm	L2	85	cm	
Δ_m	1.00	-				
ρ_s	2667	kg/m ³				
Fill Material	Small Angular					
Compaction	Increased					
Filter	Granular + Geotex					
Remark						

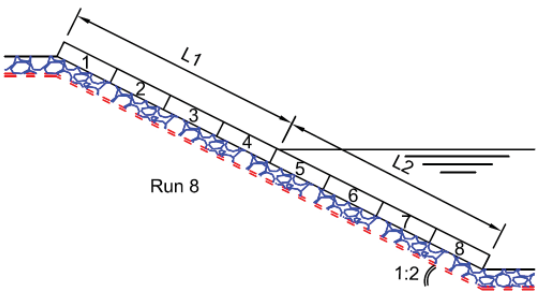


Mattress Information						
Compartment	Width	Volume	Mass	ρ_b	n^*	Grid
-	cm	cm ³	kg	kg/m ³	-	-
1	22.0	3135	7.10	2265	0.15	Normal
2	23.0	3174	7.20	2268	0.15	Normal
3	22.0	3102	7.10	2289	0.14	Normal
4	22.5	3172.5	7.20	2270	0.15	Normal
5	23.0	3105	7.10	2287	0.14	Normal
6	22.0	2970	6.80	2290	0.14	Normal
7	23.0	3105	7.10	2287	0.14	Normal
8	21.0	2835	6.50	2293	0.14	Normal

Wave Results						
H_i	H_r	K_r	T	ξ	Run-up	Run-down
m	m	-	s	-	cm	cm
0.135	0.051	0.38	1.84	3.1	10.0	9.6
0.169	0.067	0.39	2.12	3.2	15.6	12.0
0.180	0.023	0.13	2.18	3.2	18.2	12.8

D.2.29 Experiment S33 - Run 8

Test Parameters S33 - Run 8				
α	1:2	-		
ξ	4.5	-	L1	100 cm
D_n	30	mm	L2	100 cm
Δ_m	1.00	-		
ρ_s	2667	kg/m ³		
Fill Material	Small Angular			
Compaction	Increased			
Filter	Granular + Geotex			
Remark				



Mattress Information						
Compartment	Width	Volume	Mass	ρ_b	n^*	Grid
-	cm	cm ³	kg	kg/m ³	-	-
1	22.0	3135	7.10	2265	0.15	Normal
2	23.0	3174	7.20	2268	0.15	Normal
3	22.0	3102	7.10	2289	0.14	Normal
4	22.5	3172.5	7.20	2270	0.15	Normal
5	23.0	3105	7.10	2287	0.14	Normal
6	22.0	2970	6.80	2290	0.14	Normal
7	23.0	3105	7.10	2287	0.14	Normal
8	21.0	2835	6.50	2293	0.14	Normal

Wave Results						
H_i	H_r	K_r	T	ξ	Run-up	Run-down
m	m	-	s	-	cm	cm
0.131	0.055	0.42	2.22	3.8	11.8	11.4
0.134	0.071	0.53	2.47	4.2	16.0	12.5
0.146	0.080	0.55	2.61	4.3	22.9	12.8
0.155	0.101	0.65	2.86	4.5	27.1	14.3